UNIVERSITY OF STRATHCLYDE

DIVISION OF MECHANICS OF MATERIALS
DEPARTMENT OF MECHANICAL ENGINEERING
GLASGOW

WEB CRIPPLING

OF

COLD-FORMED PLAIN CHANNEL

STEEL SECTION BEAMS

This thesis is submitted for

the degree of Doctor of Philosophy

By

Ir. Harkali Setiyono, MSc

August 1994

CONTENTS

ABSTRACT

The web crippling strength of cold-formed plain channel steel section beams was investigated theoretically and experimentally in this research program. The web crippling strength in this thesis is termed the ultimate web crippling load and this was theoretically analysed using two different design specifications and a plastic mechanism approach. The two design specifications used in this research program were BS 5950 Part 5:1987 and European Recommendations For The Design of Light Gauge Steel Members,1987. In the plastic mechanism approach, a plastic mechanism model of web crippling failure was developed and analysed using a method of yield line analysis. This approach has resulted in analytical expressions and these are specially used to analyse the ultimate web crippling load of the plain channel section beams subjected to combined actions of web crippling and bending.

Besides the theoretical investigations, experimental investigations were also carried out for many plain channel section beam specimens of various dimensions. In the experimental investigations, test loads applied to the specimens were varied according to the loading conditions specified by AISI 1986 and they were transfered onto the specimens through various load bearing lengths. The experimental results were used to study the influence of various factors on the ultimate web crippling loads and to verify the theoretical results. The accuracy of theoretical results was statistically analysed and their deviations from the experimental results were limited within the acceptable scatter values ± 20%. Some examples of the web crippling behaviour of

the specimens characterized by their experimental load-deflection curves were also presented and, especially for the specimens under combined actions of web crippling and bending, their experimental load-deflection curves were compared to the theoretical collapse curves obtained from the plastic mechanism approach. Finally, the results of the experiments and the verification of each theory used in this research program are discussed and concluded in the last three chapters of this thesis.

NOTATION

The symbols defined in the following lists are the most important ones which are frequently used only and definitions of the other symbols can be found in the text where they exist.

B : Flange width

b : Yield arc depth

b_{ef} : Reduced effective width of compression elements in European Recommendations 1987

b_{eu} : effective width of the top flange according to BS 5950 Part 5 1987

D : Overall web depth in BS 5950 Part 5 1987

E : Modulus of elasticity

EOF : End one-flange loading

ETF : End two-flange loading

f_{ty} : Design value of yield stress in European Recommendations 1987

F_c : Theoretical ultimate web crippling load of a specimen subjected to web crippling only

F_{CB} : Theoretical ultimate web crippling load of a specimen subjected to combined actions of web crippling and bending

$F_{CB}1$: F_{CB} obtained from the first procedure of the plastic mechanism approach

$F_{CB}2$: F_{CB} obtained from the second procedure of the plastic mechanism approach

F_e : Experimental ultimate web crippling load

hw : Web depth or web height

hw/t : Web slenderness ratio

I_x : The second moment of effective cross section about the neutral axis

IOF : Interior one-flange loading

ITF : Interior two-flange loading

K : Coefficient of buckling

l : Span length

L : The whole length of specimen

M : Applied bending moment

M_c : Moment capacity of the section according to BS 5950 Part 5 1987

M_d : Design strength with respect to bending moment according to

European Recommendations 1987

M_{max} : Maximum applied bending moment = $F_{CB}(l-n)/4$

M_p : Fully plastic moment = $\sigma_y b t^2/4$

M_p' : Reduced plastic moment or moment capacity of a plastic hinge whose

direction is perpendicular to the direction of applied load = $M_p[1 -$

$\{P/(\sigma_y bt)\}^2]$

M_p'' : Moment capacity of a plastic hinge whose direction inclines at an angle of

β to the direction of applied load = $M_p [1 - \{P/(\sigma_y bt)\}^2] \sec^2\beta$

M_o : Out of plane bending moment accounting for the effect of round

corner between the top flange and the web in the analysis using plastic

mechanism approach

n : Load bearing length

n/t : Bearing length ratio

P : Applied concentrated load $= F_c$ or F_{CB}

P_o : Limiting compressive stress in the web according to BS 5950 Part 5 1987

P_{cr} : Local buckling stress

p_y : The design strength in BS 5950 Part 5 1987

r : Inside bend radius

r/t : Inside bend radius ratio

R_d : Design strength with respect to web crippling in European Recommendations 1987

R : Support reaction or concentrated load in European Recommendations 1987

t : Web thickness or flange thickness

W_1 : Energy dissipation at plastic hinge lines 2, 5 and 8

W_2 : Energy dissipation at plastic hinge lines 1, 3 and 6

W_3 : Energy dissipation at plastic hinge lines 4 and 7

W_{efc} : Elastic section modulus in compression region according to European Recommendations 1987

W_{eft} : Elastic section modulus in tension region according to European Recommendations 1987

W_{ext} : External energy due to virtual displacement of applied load P

W_{fl} : Energy dissipation at top flange mechanisms

W_w : Energy dissipation at web mechanisms

Y_c : Distance from the neutral axis to the top flange (compression region)

Y_t : Distance from the neutral axis to the bottom flange (tension region)

z_c : Elastic section modulus in compression region according to BS 5950

Part 5 1987 $= I_x/Y_c$

z_t : Elastic section modulus in tension region according to BS 5950 Part 5

1987 $= I_x/Y_t$

Θ : Web inclination

Δ : Overall maximum lateral deflection of web

Δh : Web crippling deformation, i.e. the decrease of web height due to the

action of applied load

σ_c : Compressive stress carried by the top flange

σ_{cr} : Buckling stress

σ_{max} : Maximum compressive stress

σ_y : Yield strength of the basic material

v : Poisson's ratio

Ψ_s : Reduction coefficient accounting for shear lag in European

Recommendations 1987

ρ : Reduction coefficient accounting for local buckling in European

Recommendations 1987

λ_p : Slenderness parameter

CHAPTER 1

INTRODUCTION

1.1. GENERAL.

A cold-formed plain channel steel section is one of various types of cold-formed steel sections generally used in structural framing. Examples of these types of sections can be seen in Figure 1.1 and they are formed in the cold state from steel sheets, strips, plates, or flat bars in roll-forming machines or by press brake or bending brake operations. The thickness of steel sheets or strips normally used in cold-formed steel structures ranges from 0.3 mm to about 6 mm. Cold-formed sections are not necessarily formed from thin steel sheets, steel plates as thick as 18 mm can be successfully cold-formed into structural shapes.

The cold-formed steel sections have a wide range of applications such as in automobiles, ships, railway coaches, bridge and building construction, storage racks etc. They are called cold-formed sections to distinguish them from the familiar group of hot-rolled shapes and members built up of plates. The application of cold-formed steel sections compared with that of hot-rolled steel sections in building construction provides the following advantages :

- More economical design can be achieved for relatively light loads and/or short span.

- Reducing weight and consequently high strength to weight ratio can be obtained.

- In the case of panels and decks, they can be used for floor, roof, wall

1

construction and they can also be used as shear diaphragms, enclosed cells for

electrical and other conduits.
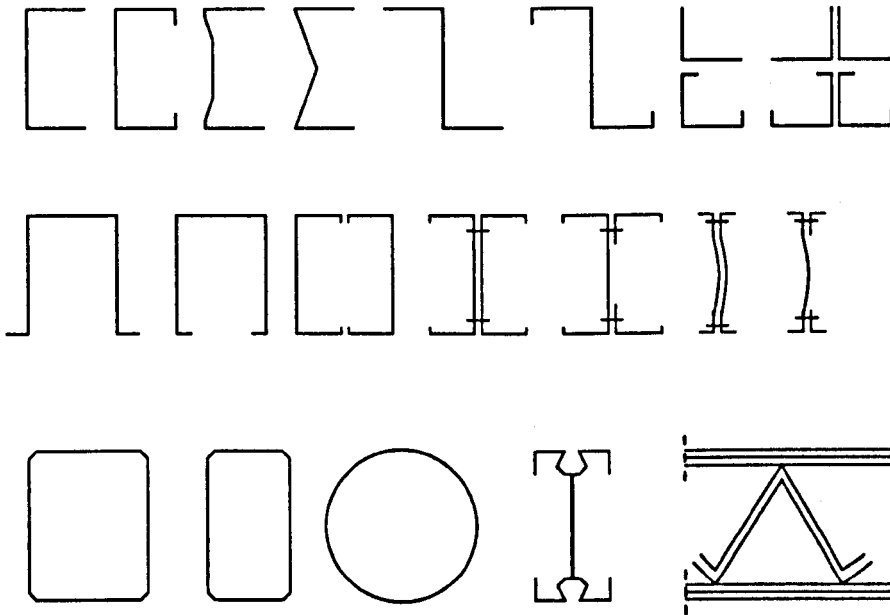
Figure 1.1. Cold-formed sections used in
structural framing. [1]

In cold-formed steel design, individual elements of cold-formed structural members

are usually thin with relatively large width-to-thickness ratios. These thin elements

may buckle locally at a stress level lower than the yield strength when they are

subjected to compression in flexural bending, axial compression, shear, or bearing.

However, the members do not normally fail at the buckling stress and they are still

able to carry loads larger than the loads at which local buckling has been initiated.

This condition is called the post-buckling strength of the members. Since one of the

major design criteria on cold-formed steel sections is often based on the local buckling of individual elements, the design load should be so determined that adequate safety is provided against failure by local buckling with due consideration given to the post-buckling strength.

Cold-formed steel sections such as I-sections, channels, Z-shapes, T-sections, hat sections and tubular members shown in Figure 1.1 can be used as beams which support transverse loads and/or applied moments and they are usually called cold-formed flexural members. There are two considerations which must be taken into account in designing cold-formed flexural members. The first is the moment-resisting capacity and the stiffness of the members. The second consideration is that the webs of beams must be capable of resisting shear, bending, combined bending and shear, and web crippling. There is also another factor, i.e. lateral-torsional instability, which must be taken into consideration but in this research program it is assumed that the members investigated are laterally stable.

From the above various aspects of the design considerations on cold-formed flexural members, only the strength of the members against web crippling was investigated in this research program. Web crippling is a failure mode of thin-walled webs of structures caused by concentrated loads or at reactions. This type of failure is shown in Figure 1.2 and must be avoided, because it signifies the limit of the load capacity of a beam. The web crippling strength can be predicted by using empirical formulae

available in the present design specifications for cold-formed steel sections. The study of the development of empirical formulae for predicting the web crippling strength has been already carried out by many researchers and these empirical formulae often have a limited range of applicability. It has also been reported in reference [24] that each empirical formula correlates well with the test results on which it is based, but the correlation is much worse for tests from other sources. On the basis of these reasons, it has been attempted to use another method for predicting the web crippling strength of cold-formed plain channel steel section beams in this research program. The method was developed by using an analytical model of web crippling failure.

Web crushing or web crippling at support
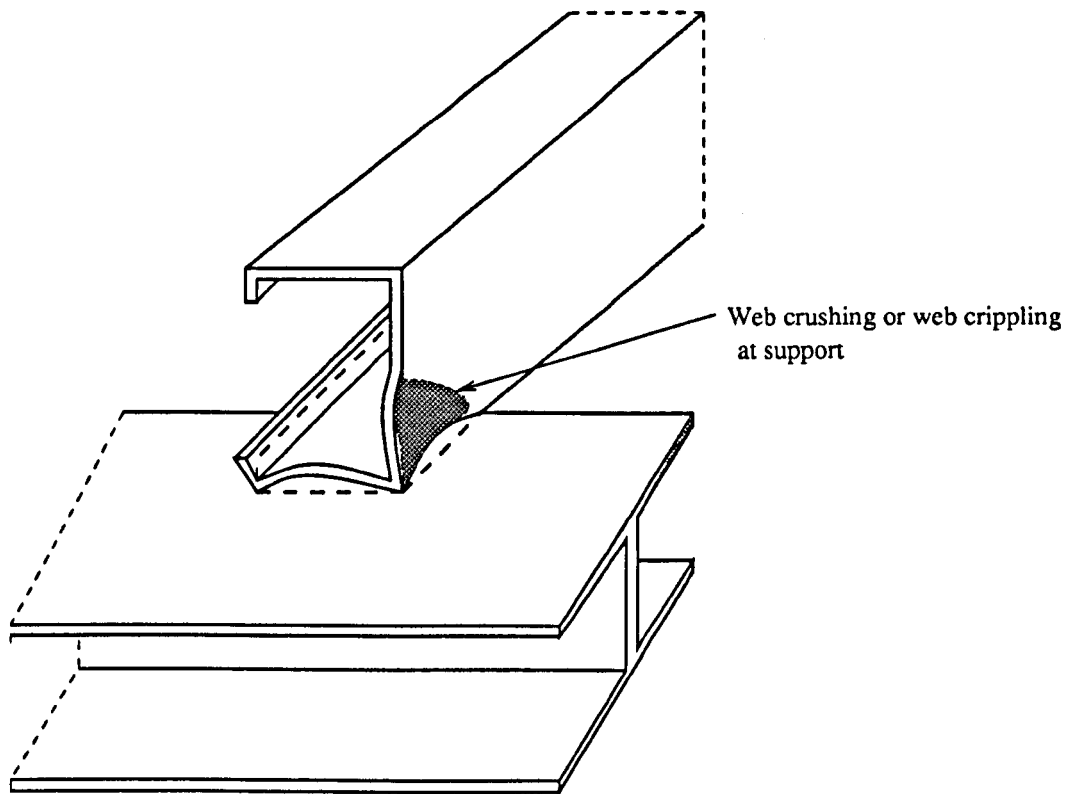
Figure 1.2. Web crippling failure. [41]

1.2. OBJECTIVE OF THE RESEARCH.

This research program was mainly aimed at investigating the strength of cold-formed plain channel steel section beams subjected to web crippling. The main objective was approached theoretically and experimentally. In the initial theoretical investigation, two different design specifications for cold-formed steel sections were used to predict the failure load of the sections under web crippling. Besides using the available design specifications of cold-formed steel sections, this research program was also aimed at developing another method for analysing the web crippling strength of the sections which was based on a purely theoretical analysis. The target of developing this analytical method was to obtain analytical expressions for analysing the web crippling strength of cold-formed plain channel steel section beams. In the experimental investigations, many cold-formed plain channel steel section beam specimens of various dimensions were tested to failure and their results were used to assess the relative accuracy of each theoretical analysis used in this research program.

1.3. SCOPE OF THE RESEARCH.

Subchapter 1.1 has shown many types of cold-formed sections which can be used as flexural members. One of the failure modes which may occur in these members is web crippling. According to the information given in numerous publications corresponding to the study of web crippling, the strength of cold-formed steel

sections under web crippling is affected by various parameters such as the bearing length ratio (n/t), the inside bend radius ratio (r/t), the web slenderness ratio (hw/t), the web inclination (Θ), the material yield strength etc. From these parameters, only three of them were considered in this research program, i.e. :

- The bearing length ratio (n/t)

- The web slenderness ratio (hw/t)

- The inside bend radius ratio (r/t)

where :

n   : Length of the load bearing plate or bearing length.

hw   : Height of the web or height of the section.

t   : Web thickness

r   : inside bend radius.

In order to study the influence of the above three parameters on the web crippling behaviour, experimental investigations were performed on many specimens with various web heights (hw) and inside bend radii (r). Test loads were applied on the specimens through the loading blocks of various widths (n). The specimens used in this research program were in the form of cold-formed plain channel steel section beams. According to the American Design Specification for cold-formed steel sections (AISI 1986), the loading conditions which can result in the web crippling failure are categorized as follows :

- End one-flange loading (EOF).

- Interior one-flange loading (IOF).

- End two-flange loading (ETF).

- Interior two-flange loading (ITF).

Illustrations of these above loading conditions can be seen in Figure 1.3. In investigating the strength of the specimens under web crippling, experiments were carried out using the above four loading conditions. In the case of IOF loading condition, the specimens would be subjected to combined actions of web crippling and bending while the EOF, ETF and ITF loading conditions would cause the specimens to be subjected mainly to web crippling only.

The theoretical investigations were carried out in two phases, in which the first phase was to analyse the specimens empirically using two different design specifications, i.e. BS 5950 Part 5 1987 and The European Recommendations for the Design of light Gauge Steel members 1987. These analyses were also intended to assess the relative accuracy of these design specifications in estimating the web crippling strength of the specimens. The relative accuracy was shown in the form of diagrams of experimental and theoretical load ratios with respect to the three parameters studied. The second phase was to analyse the specimens by using an analytical theory which is termed " *Plastic mechanism analysis* ".

In the plastic mechanism analysis, the mode of web crippling failure was simulated

by a plastic mechanism model which was composed of some yield lines or plastic hinges. The analysis of the model was based on the application of a rigid plastic theory. This research program was concentrated on the development of the plastic mechanism analysis for the specimens which failed under the IOF loading condition. The accuracy of the application of the analytical expressions obtained from the plastic mechanism analysis was also assessed by comparing their results with experimental ones.
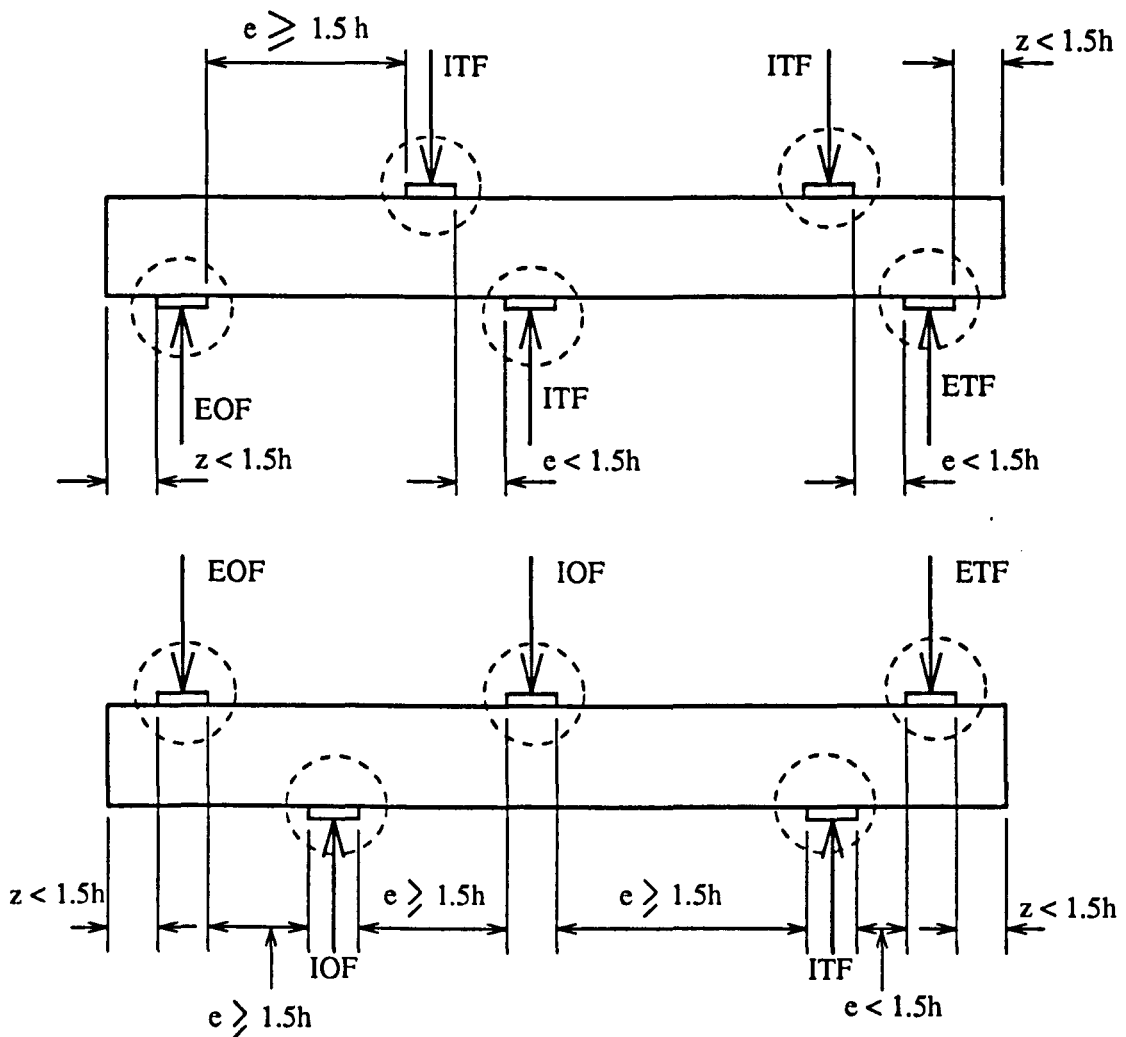
Figure 1.3. Loading conditions according to AISI 1986. [28]

8

CHAPTER 2

LITERATURE REVIEW

2.1. GENERAL.

In the initial phase of this research program, numerous publications and research reports have been carefully studied. Some of these cover theoretical and experimental investigations on the behaviour of cold-formed steel beams subjected to web crippling and combined actions of web crippling and bending. There are also publications which discuss theoretical and experimental studies on the buckling and post buckling behaviour of plates under various conditions of loading. In addition, the available design criteria for preventing web crippling of cold-formed steel sections which are normally used in the UK, the USA and EUROPE have also been carefully studied.

This chapter reviews the most relevant publications used in this research program. Some of these publications will be reviewed very briefly, whereas the others will be reviewed in more detail. The presentations are divided as in the following subchapters :

2.1. General.

2.2. Web crippling.

2.3. Buckling and plastic mechanisms.

2.4. Current design criteria :

    2.4.1. BS 5950 Part 5 1987.

    2.4.2. A.I.S.I.

    2.4.3. European Recommendations 1987.

2.5. Author's conclusions.

2.2. WEB CRIPPLING.

The study of web crippling of cold-formed steel beams has been going on since the 1940s. Most of the studies of this behaviour were carried out experimentally and their results were used to develop the design formulae. The theoretical analysis of web crippling is extremely complicated because it involves the following factors [1] :

- Non-uniform stress distribution under the applied load.

- Elastic and inelastic instability of the web element.

- Local yielding in the immediate region of load application.

- Bending produced by eccentric load when it is applied on the bearing flange at a distance beyond the curved transition of the web.

- Initial out-of-plane imperfection of plate elements.

- Various edge restraints provided by beam flanges and interaction between flange and web elements.

During 1940s and 1950s, the behaviour of web crippling was experimentally investigated by Winter, Pian and Zetlin [2,3,4] at Cornell University. Their investigations were carried out in two phases,i.e. the first phase was the study of web crippling of I-beams which provide a high degree of restraint against rotation. The I-beams were tested under various loading conditions and the test results indicated

10

that the ultimate web crippling loads of I-beams depend primarily on the actual bearing length ratio (n/t) and the yield strength of material (σ_y). The second phase was the study of web crippling of cold-formed steel beams having single unreinforced webs such as hat sections, channels, Z-sections and rectangular tubes. It was found from this second study that the web crippling behaviour for these types of section was mainly affected by the following parameters :

- The actual bearing length ratio (n/t).

- The inside bend radius ratio (r/t).

- The web depth ratio (h/t).

- The yield strength of material (σ_y).

On the basis of the research findings of Cornell University, empirical expressions for predicting the ultimate web crippling load were derived and proposed for design criteria in early editions of the American Iron and Steel Institute (AISI 1968).[5] The specifications contain the empirical expressions for each type of sections as mentioned above. The web crippling behaviour of channel sections was also studied by George D. Ratliff [6] in 1975. This research was to investigate the interaction of crippling and bending for C-shaped joists cold-formed from steel sheets. The results of Ratliff's investigation were proposed as interaction formulae of crippling and bending for C-shaped beams with web stiffener or without web stiffener.

Three years later,i.e. in 1978, similarly experimental investigations were also

performed by Hetrakul and Yu [7,8] at University of Missouri-Rolla. In their research, Hetrakul and Yu investigated the structural strength of cold-formed steel I-beams subjected to combined crippling and bending. A number of I-beam specimens were tested and the results were used to develop the interaction formulae for the bending and crippling of I-beams having a high degree of restraint against the rotation of webs. The test specimens were fabricated from channel sections connected back to back with self-tapping screws (# 12x14x3/4 Tek screws) which were placed at a distance of 12.7 mm from top and bottom flanges. The specimens used in the research of University of Missouri-Rolla (UMR) are shown in Figure 2.1.

Each of the specimen in this research was also tested as a simply supported beam where the test load was applied at the mid-span of the specimen through a bearing plate and supporting plates with rollers were placed at both ends. The test load was applied in increments of 10% of the predicted ultimate load throughout the test. Lateral displacements of the web were measured at the initial load, then at approximately one-half of the predicted ultimate load, and finally at the failure load.

The values of ultimate loads obtained from the experiment (P_t) were used to calculate actual bending moments (M_t). Ultimate web crippling loads in the absence of bending $(P_u')_c$ were calculated by using the following equation :

$$(P_u')_c = t^2 \, \sigma_y \, [1.49 - 0.53(\sigma_y/33)] \, [0.88 + 0.12(t/0.075)]$$
$$\times \, [15 + 3.23\sqrt{N/t}] \quad \ldots\ldots\ldots\ldots\ldots \quad (2.2.1)$$

Where :

t   : Thickness of the individual web element in inches.

σ_y : Yield point of steel in kips per square inch.

N   : Length of the bearing plate in inches.

The computed ultimate moments $(M_u)_c$ were determined according to the strength of flanges and the bending strength of webs. The smallest values obtained from these methods were used for $(M_u)_c$ in the analysis.

Two interaction formulae for combined crippling and bending moments were resulted from this research. The first one is applicable only for I-beams having $(h/t) \leq 400/\sqrt{(\sigma_y)}$ and $(W/t) \leq (W/t)_{lim}$ while the second one is applicable for I-beams having other combinations of the h/t and W/t.

The first formula :

$$0.56 \frac{P_t}{(P'_u)_c} + \frac{M_t}{(M_u)_c} = 1.38 \ldots \ldots \ldots (2.2.2)$$

The second formula :

$$0.61 \frac{P_t}{(P'_u)_c} + \frac{M_t}{(M_u)_c} = 1.18 \ldots \ldots \ldots \ldots \ldots (2.2.3)$$

Where :

h/t   : The depth to thickness ratio of the web element.

W/t   : The flat width ratio of the compression element.

$(W/t)_{lim}$: The limiting flat-width ratio according to the load determination

specified by AISI 1968.
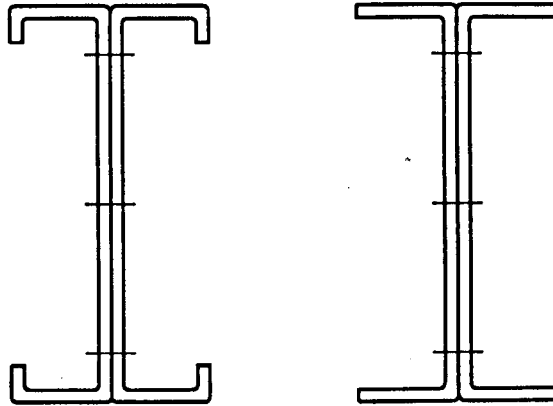
Figure 2.1. Specimens of UMR.

During 1982-1986, B.A. Wing and R.M. Schuster[9,10] investigated web crippling expressions for multi-web deck sections subjected to interior one-flange loading (IOF), interior two-flange loading (ITF) and exterior two-flange loading (ETF) experimentally. The objective of their investigations was mainly aimed at determining the load resistance of multi-web deck sections under IOF (Figure 2.2.) and under ITF as well as ETF (Figure 2.3.).

This type of section is extensively used in building construction. In the case of interior one-flange loadings, failure of the deck section can occur by combined crippling and bending, but when the ratio of bending moment to the ultimate bending moment < 0.3, the primary mode of failure can be considered by web crippling only. In two-flange loading, the deck section fails by web crippling and ultimate load carrying capacities of the above three loading conditions are functions of a number

14

of parameters, namely, the web slenderness ratio, the inside bend radius ratio, the bearing length ratio, the angle of web inclination and the yield strength of the steel.

In their research program, only three of these above parameters were studied and they were as follows :

- inside bend radius to web thickness ratio (r/t).

- bearing length to web thickness ratio (n/t).

- angle of inclination (Θ).

Experimental ultimate loads obtained from the tests of IOF, ITF and ETF were compared with ultimate loads computed using the AISI-1980. The new expressions for estimating the test loads have also been developed and formulated as follows : Interior one flange loading (IOF) [10] :

$$P_{W2} = 16.6\ t^2\ \sigma_y\ (sine\ \theta)(1 - 0.000985H)(1 + 0.00526N)$$
$$x\ (1 - 0.0740\sqrt{R})(1 - 0.221k)\ \dots\dots\ (2.2.4)$$

Interior two flange loading (ITF) [9]

$$P_{W4} = 18.0\ t^2\ \sigma_y\ (sine\ \theta)(1 - 0.00139H)(1 + 0.00948N)$$
$$x\ (1 - 0.0306\sqrt{R})(1 - 0.221k)\ \dots\dots\ (2.2.5)$$

Exterior two flange loading (ETF) [9] :

$$P_{W6} = 10.9\ t^2\ \sigma_y\ (sine\ \theta)(1 - 0.00206H)(1 + 0.00887N)$$
$$x\ (1 - 0.111\sqrt{R})(1 - 0.0777k)\ \dots\dots\ (2.2.6)$$

Where   :

t   : Web thickness   ; σ_y : Yield strength

Θ : Angle of web inclination, $\leq 90^\circ$

H   : Web slenderness ratio, h/t

N   : Bearing length to web thickness ratio, n/t

R   : Inside bend radius to web thickness ratio, r/t

k   : σ_y (ksi)/33 or σ_y (N/mm2)/228

Results of using the new expressions to predict ultimate web crippling loads were presented in the form of diagrams of load ratios vs. $\sqrt{R}$ or N. Some of the presented diagrams for each loading condition can be seen in Figures 2.5 - 2.7.
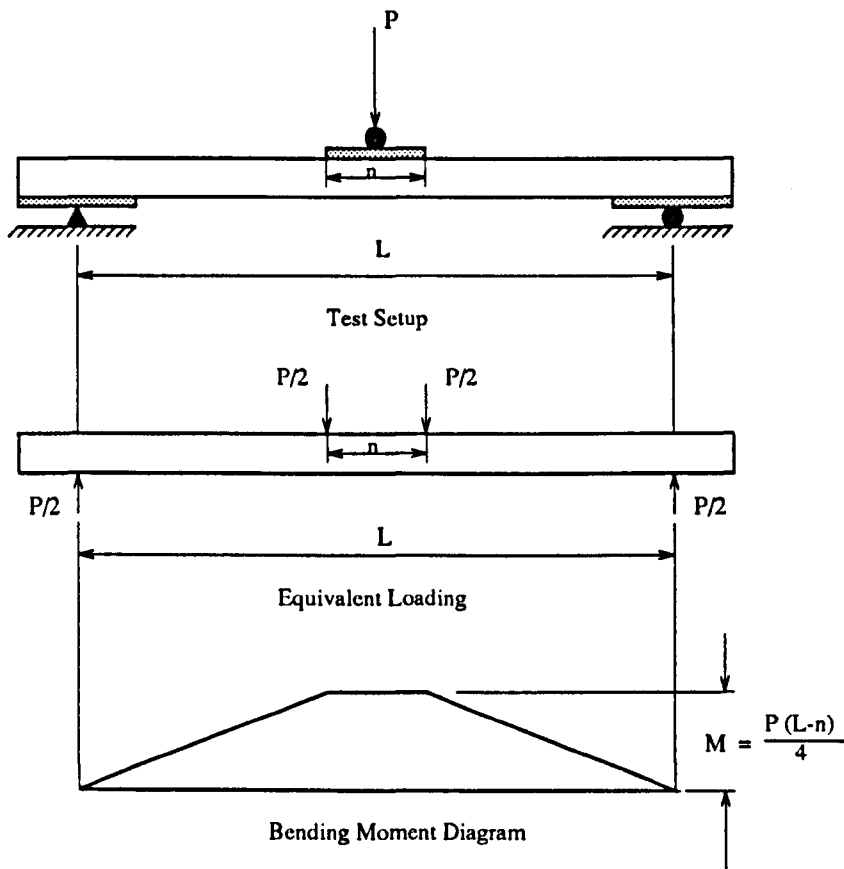
Figure 2.2. Interior one-flange loadings and moment diagrams.[10]

16
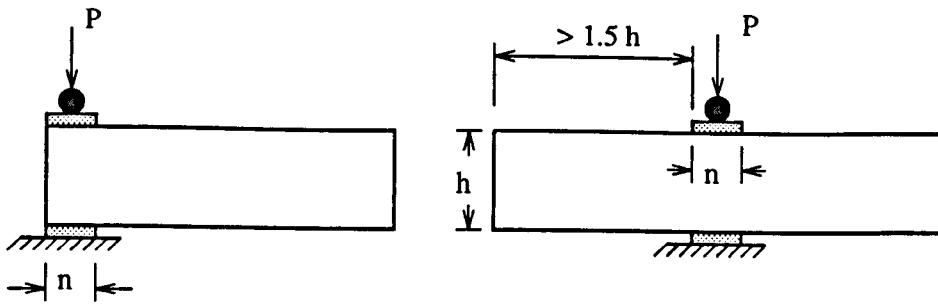
Figure 2.3. Interior and exterior two-flange loadings.[9]
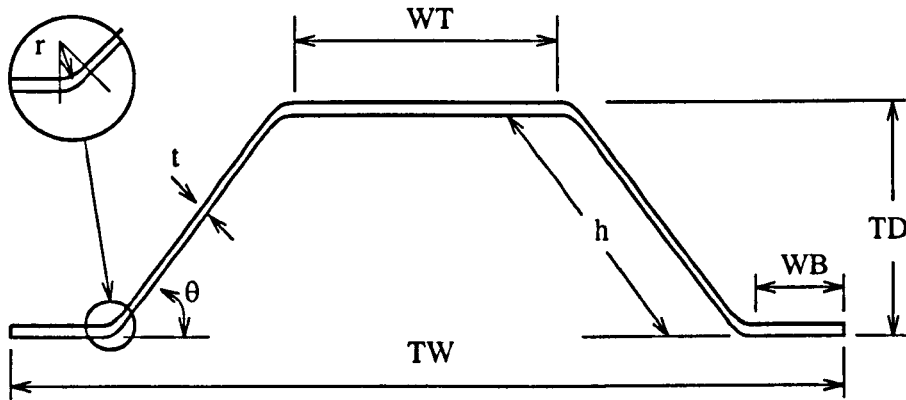
Figure 2.4. Specimens of Wing and Schuster.[9,10]
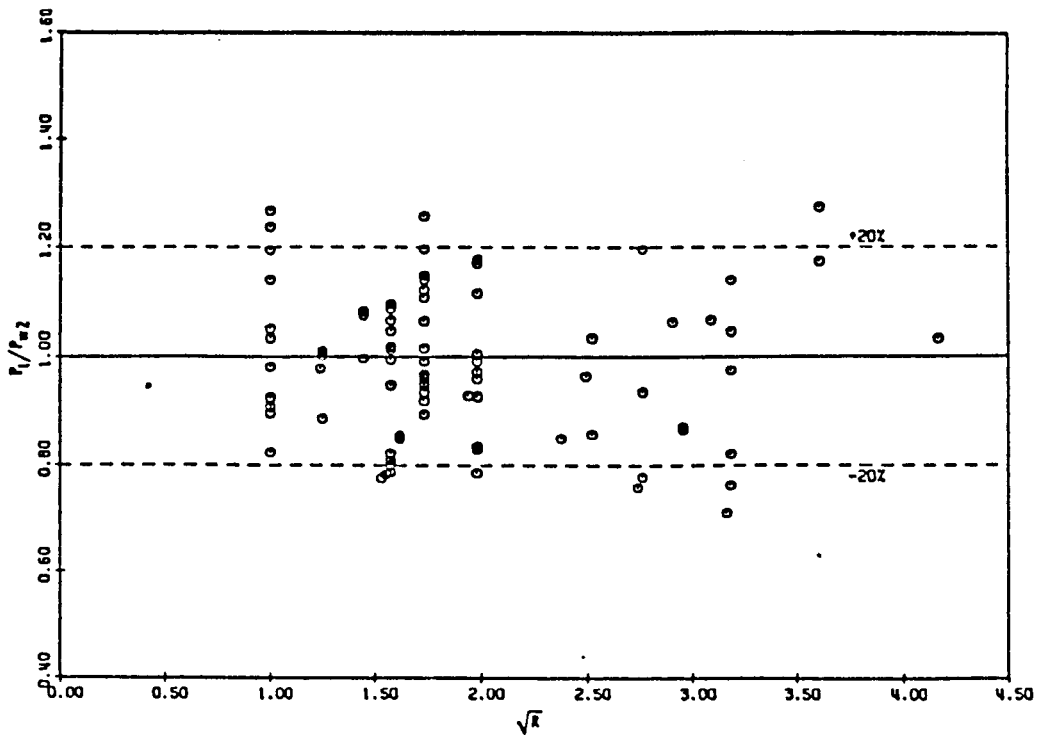
Figure 2.5. Load ratio (P_t/P_{w2}) vs. $\sqrt{R}$ for interior one-flange loadings.[10]

17
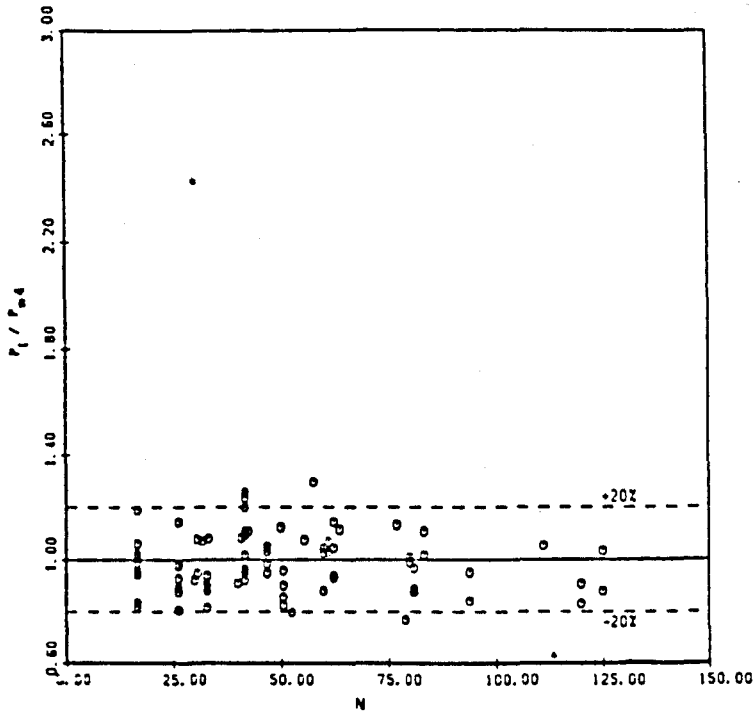
Figure 2.6. Load ratio (P_t/P_{w4}) vs. N for interior two-flange loadings.[9]
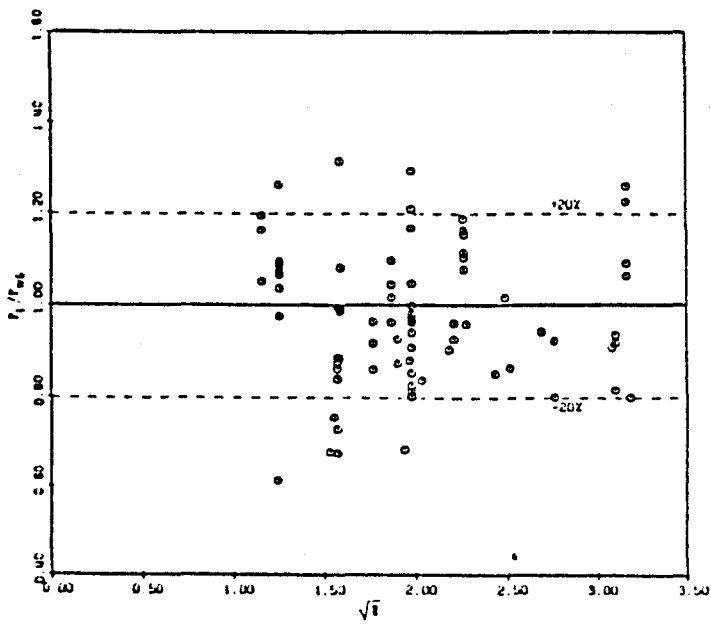
Figure 2.7. Load ratio (P_t/P_{w6}) vs. $\sqrt{R}$ for exterior two-flange
loading.[9]

18

In 1986, C.Santaputra, M.B.Parks and W.W.Yu[11] also studied the web crippling behaviour of high strength steels. The purpose of their investigations was to develop additional design criteria that can be used for a wide range of high strength steels. This material is widely used in automotive structural components and it was intended to achieve weight reduction of the components while complying with federal safety standards. Because many of the existing design criteria for web crippling were only applicable for steels with yield strengths up to 80 ksi (552 MPa) it was therefore desirable to develop a comprehensive design guide which is suitable for high strength steels with yield strengths up to 190 ksi (1310 MPa).

An experimental investigation was performed on cold-formed steel beams fabricated from high strength sheet steels commonly used in the automobile industry. Two types of specimens were used in the experiment,i.e. hat sections (Figure 2.8a) and I-beams (Figure 2.8b). The materials used for the specimens had yield strengths of 60 to 165 ksi (414 to 1138 MPa). The experiments were carried out for the following loading conditions :

- Interior one-flange loading (IOF)

- End one-flange loading (EOF)

- Interior two-flange loading (ITF)

- End two-flange loading (ETF)

In order to avoid the problem of discontinuity between the web crippling equations for the above basic loading conditions, additional tests were performed for the

transition ranges.

Figure 2.9 shows the test arrangements in which the test loads were applied on the specimens through bearing plates. All specimens in one-flange loading test were simply supported and loaded at their mid-spans. The IOF tests were carried out by placing a bearing plate of 50.8 mm width under the test load whereas bearing plates of 101.6 mm width were used at both ends. Web crippling failure of EOF tests was expected to occur at the end of the specimen and this could be obtained by placing a bearing plate of 101.6 mm width under the test load while bearing plates of 50.8 mm width were placed at both ends of the specimen. Tests of ITF were carried out by placing two bearing plates of 50.8 mm width at the middle of the specimen for both top and bottom flanges. The plates of the same width were still used for the tests of ETF and they were placed at one end of the specimens while the other end was elastically supported to keep the specimens in a horizontal position throughout the tests.

The transition ranges which were examined in additional tests are as follows :

- Transition between Interior one-flange loading and Interior two-flange loading.

- Transition between Interior one-flange loading and End one-flange loading.

- Transition between End one-flange loading and End two-flange loading.

The test setup of the first transition was the same as that of the IOF test except that

one end bearing plate was moved in order to vary the clear distance between the opposite bearing plates from 0.1h to 0.75h. The expected failure was under the applied concentrated load. The second transition test was carried out by moving one end bearing plate closer to the bearing plate under the applied concentrated load such as shown in Figure 2.9f and failure was expected at the reaction. The test arrangement of the third transition was also the same as that of the EOF test but the bearing plate under the applied concentrated load was moved closer to the end bearing plate. Failure of this test was expected at reaction closer to the applied load.

Failure modes of the test specimens were also carefully inspected and it has been found that the failure modes of web crippling can be classified into two types of failure,i.e. over stressing (bearing) failure and buckling failure. The former occured just under the bearing plate with relatively small lateral displacement of the web. The applied load increased steadily up to the ultimate load and remained at that level for a long period of time while the bearing plate gradually penetrated into the web. The latter indicated that the applied load also increased steadily up to the ultimate load but after that the load suddenly dropped. The lateral displacement of the web was relatively large even before failure.

In this research, new prediction equations which cover a wide range of steel strengths were developed and proposed as design recommendations. The recommendations can be used to estimate the ultimate load of a component subjected to crippling only or

a combination of crippling and bending moment. The application is also divided into two parts,namely, for beams having single webs and for I-beams with flanges connected to bearing plates. Full information of the design recommendations will be discussed in more detail in subchapter 2.4. Current design criteria. The ultimate web crippling loads predicted by the newly developed equations give good agreement with the experimental ultimate loads for all cases. The diagram in figure 2.10 is one of the results which indicates the accuracy of the proposed design recommendations.
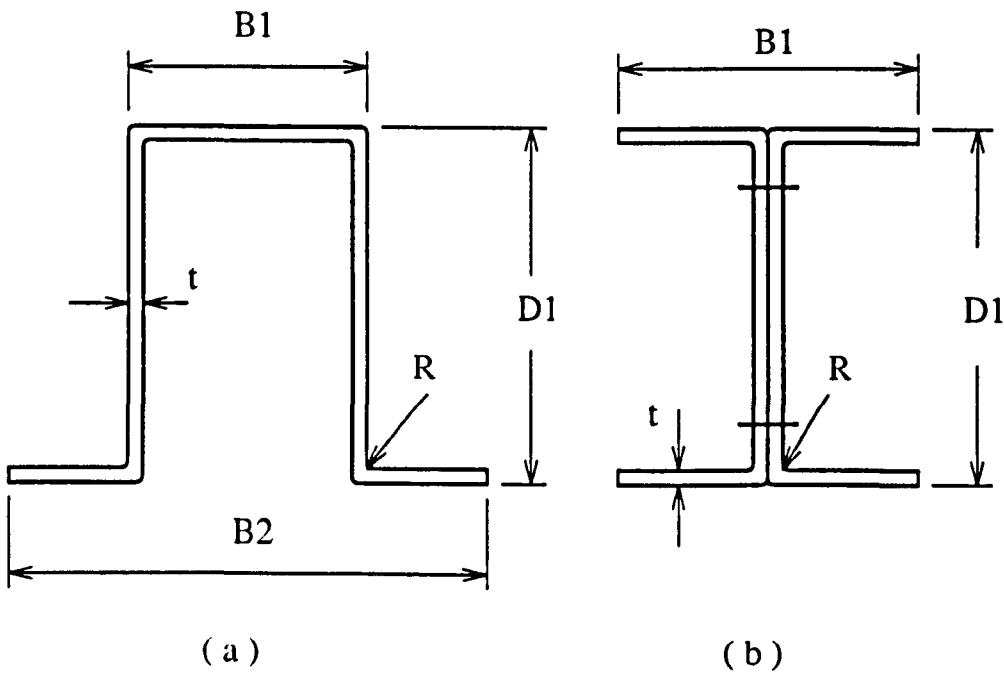
Figure 2.8. Hat sections and I-beams

a) Interior One-Flange Loading (IOF)

b) End One-Flange Loading (EOF)

c) Interior Two-Flange Loading (ITF)

d) End Two-Flange Loading (ETF)

e) Transition between IOF and ITF

f) Transition between IOF and EOF

g) Transition between EOF and ETF
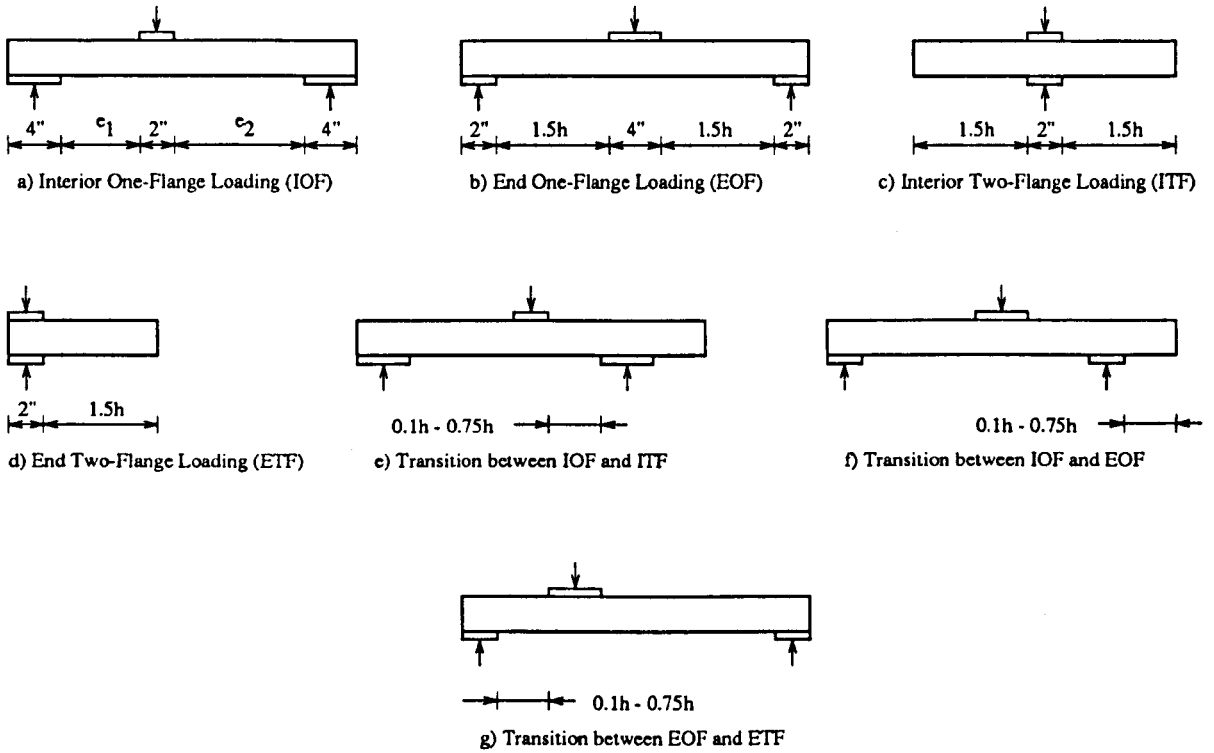
Figure 2.9. Test arrangements of Santaputra et.al
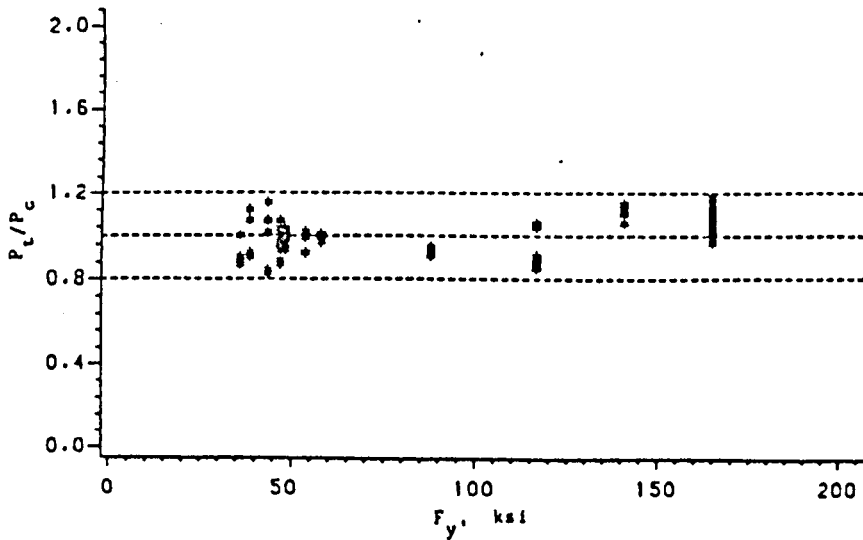
Figure 2.10. Load ratio P_t/P_c vs. Yield strength F_y for hat sections subjected to IOF.

23

Another investigation carried out by J.Studnička[12] in 1989 was also aimed at predicting the web crippling resistance of multi-web deck sections subjected to end one-flange loading, end two-flange loading and interior one-flange loading. The investigation was carried out experimentally and the results were compared with the theoretical ones calculated using the AISI Specification, 1986, and the Canadian code CAN 3-S136-M84 1984. Two types of specimen were used in the experiment and these are shown in Figure 2.11. The specimens were simply supported at both ends and test loads were applied at the centre of the specimens as shown in Figure 2.12. The distance m was varied to obtain the conditions of one-flange loading and two-flange loading. Transverse tie rods were bolted to the bottom flanges of the sections to prevent the spread of webs during loading and the test were performed in both positions of N and R (Figure 2.13).

Some comments have been made by the investigator concerning the test results obtained by using Interior and End loads. The comments are as follows :

-   Test loads are not substantially different for the N and R positions of the web deck.

-   Test results are almost linearly influenced by the bearing width n.

-   Test loads for specimens with ties are greater than those of specimens without ties.

Additional comments have also been made for the End loading tests in which the influence of m and k on the test loads is not too significant.

Results of comparing the test loads and the theoretical ones for Interior loading tests are presented in Figures 2.14 and 2.15. It can be seen that using the Canadian Standard almost all data are within the acceptable scatter limits ± 20%. In the case of End loading, a new, slightly modified, expression has been developed to improve the Canadian Standard. This new expression is

$$P = 10 \ t^2 \ \sigma_y \ (sine\theta) \ (1 - 0.1\frac{\sigma_y}{230}) \ (1 - 0.1\sqrt{R})$$
$$x \ (1 - \frac{H}{500}) \ (1 + \frac{K}{1.5H}) \ (1 + 0.005N) \ \ldots\ldots\ldots\ldots (2.2.7)$$

Where :

P : Web crippling capacity for End one-flange loading or End two-flange loading.

t : Web thickness.

σ_y : Yield strength.

Θ : Angle between plane of web and plane of bearing surface $45° \le \Theta \le 90°$.

k : Distance between end of deck and end of bearing plate.

R : r/t ; r : inside bend radius.

H : hw/t ; hw : clear distance between the flats of flanges measured in the plane of webs

K : k/t

N : n/t ; n : Bearing length

Figure 2.16 shows the comparison between the web crippling capacity calculated using the formula 2.2.7 and the experimental values.
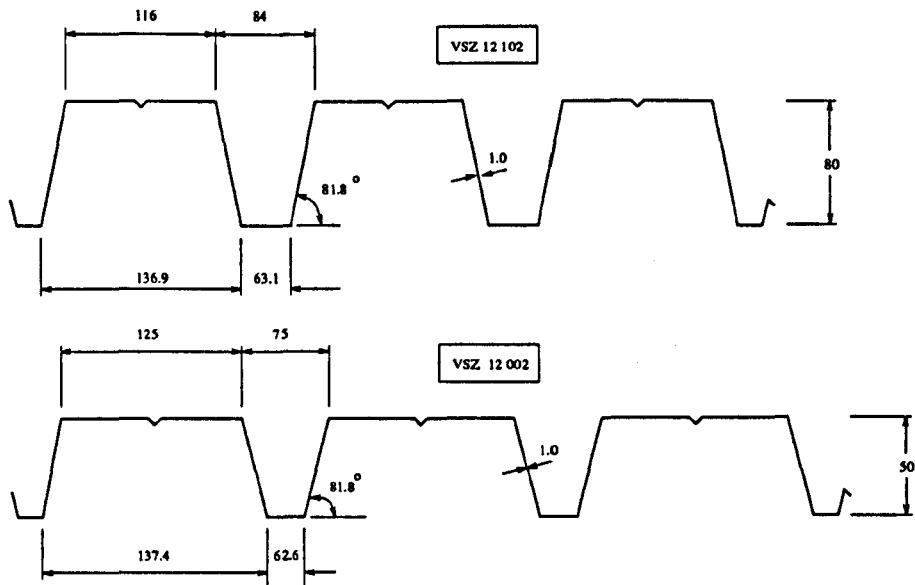
Figure 2.11. Specimens of Studnička.

(i)

(ii)
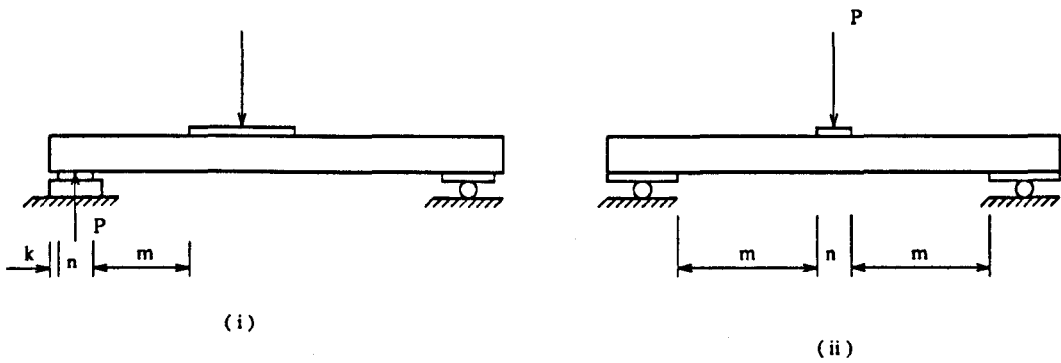
Figure 2.12. Test setup of End loading (i) and Interior loading (ii).

Position N
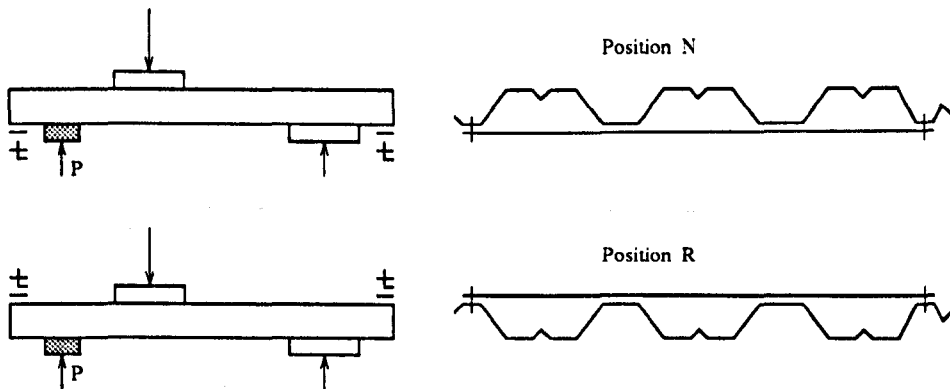
Position R

Figure 2.13. Positions of N and R.
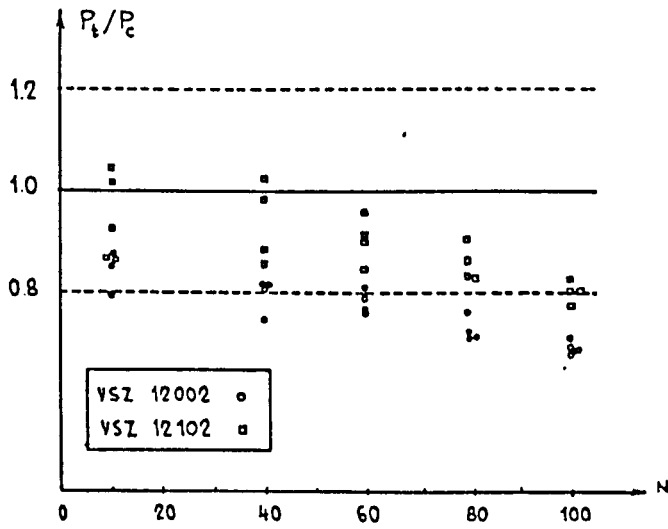
Figure 2.14. Test load P_t vs. Theoretical load P_c obtained from
AISI specification (Interior loading).
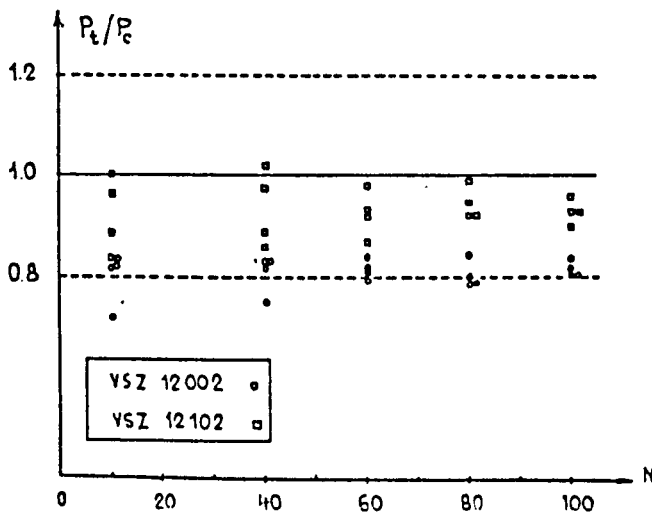
Figure 2.15. Test load P_t vs. Theoretical load P_c obtained from
CAN 3 - S136 (Interior loading).

27
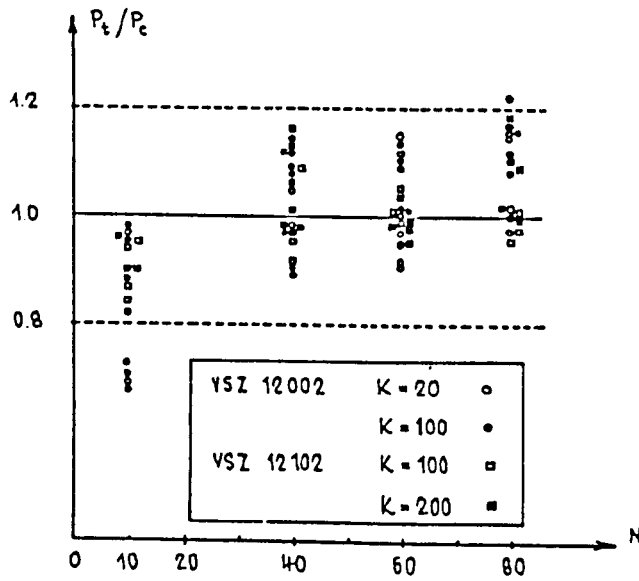
Figure 2.16. Test load P_t vs. Theoretical load P_c obtained from the formula 2.2.7 (End loading).

The previous research reviews always deal with the web crippling strength of cold-formed steel sections without web perforations. According to the research findings of K.S. Sivakumaran and K.M. Zielonka[13] in 1989 the existence of web opening has a significant effect on the web crippling strength of the cold-formed steel sections. The influence of the web opening was studied by K.S. Sivakumaran and K.M. Zielonka through experimental research. Parameters considered in their investigation covered web depth to thickness ratio, opening height to web depth ratio and opening width to bearing length ratio.

The main objective of their research was to generate an empirical formula for the ultimate load on a thin-walled cold-formed steel section by taking into account the

28

size of its web opening. Specimens used in their experiments were C-shaped lipped

channel sections such as shown in Figure 2.17 and they were made of galvanized

steels with different yield strengths. Rectangular holes were chosen for the web

opening and they were located at the mid-span of the specimens. The height of the

holes varied from 3 mm to 75% of the web depth and their widths varied from 3 mm

to 152 mm.

Test loads were applied on the specimen through two loading blocks of 51 mm width

and the specimen was supported at its mid-span by a reaction bearing block of 51

mm width. The complete arrangement of the test can be seen in Figure 2.18. The

tests were first carried out for specimens without web perforations and the subsequent

tests were for specimens with perforations. The loading arrangement such as shown

in Figure 2.18 satisfies the conditions of interior one-flange loading. A hydraulic jack

which could produce an axial force of about 250 N was used to maintain the

specimen always in a horizontal position during the test. Vertical deflection of the top

flange and horizontal or lateral deflection of the web were also measured by using

displacement transducers (LVDT). As the test load reached its maximum value the

test was then stopped.

Modes of failure observed from the test results indicate that in the specimen without

a perforated web, the failure occurs by formation of a local yield zone under the

bearing block. In the case of specimens with perforated webs, the yield zones also

occur under the bearing block and around the corners of the web opening. On the basis of lateral deflection of the web obtained from the tests, the types of failure can be characterized as web crippling (bearing) and web crippling (buckling) failures. The first type of failure occurs right under the bearing plate with relatively small lateral deflection of the web while the second one exhibits large lateral deflection of the web prior to reaching the ultimate loads. The diagram in Figure 2.19 is an example of a load-deflection diagram resulted from the experiment.

The types of failure are generally influenced by the web slenderness ratio and the size of web opening. The specimens with high slenderness ratios and small web openings tend to fail by web crippling (buckling). The web crippling (bearing) failure occurs in the perforated or unperforated-web specimens with low slenderness ratios or in the specimens with high slenderness ratios and large web openings. The test results also indicate that the existance of the web opening tend to reduce the ultimate web crippling load. The authors also proposed a reduction factor (R) for the web crippling strength of the section with a web opening as stated in the following formula.

$$\textit{The reduction factor } R = \frac{P \textit{ (with opening)}}{P \textit{ (without opening)}} \dots\dots\dots (2.2.8)$$

$$R = [1 - 0.197 \left(\frac{a}{h}\right)^2] [1 - 0.127 \left(\frac{b}{n_1}\right)^2] \dots\dots (2.2.9)$$

Where :

P : Ultimate failure load ; a : Opening height

h : Web depth ; b : Opening width

n_1 : $n + k(h - a)$; k : 1 for the load dispersion angle of 45°

The results of using the above formula are presented in Figure 2.20.
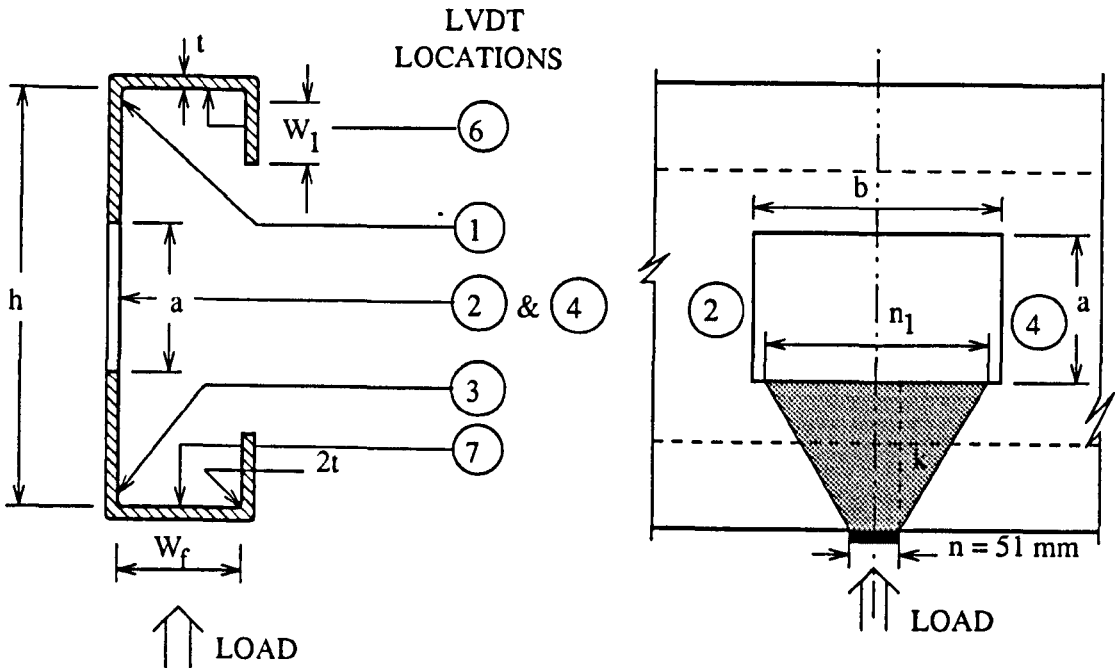
Figure 2.17. The cross section of the specimen and the web opening.
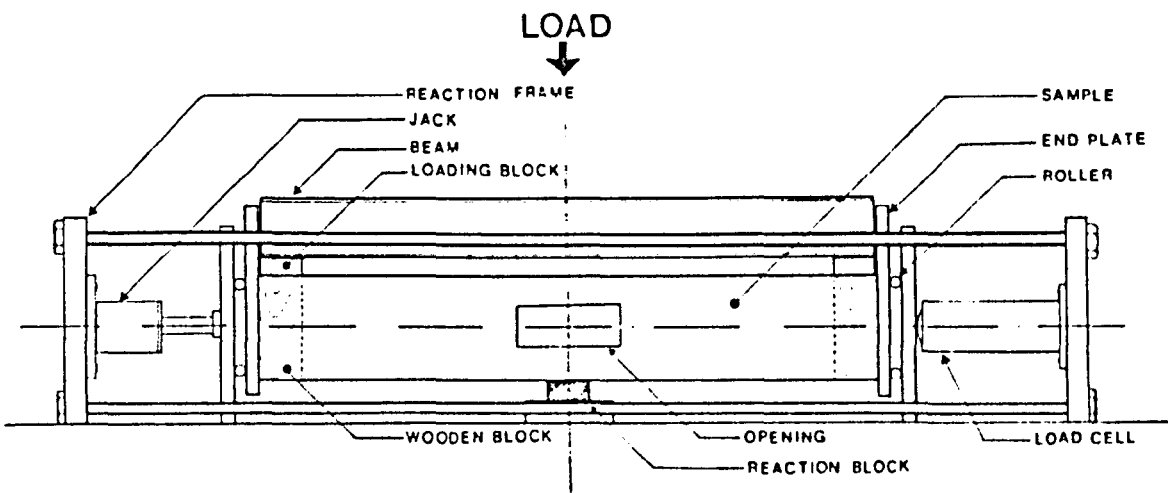
Figure 2.18. The test arrangement.
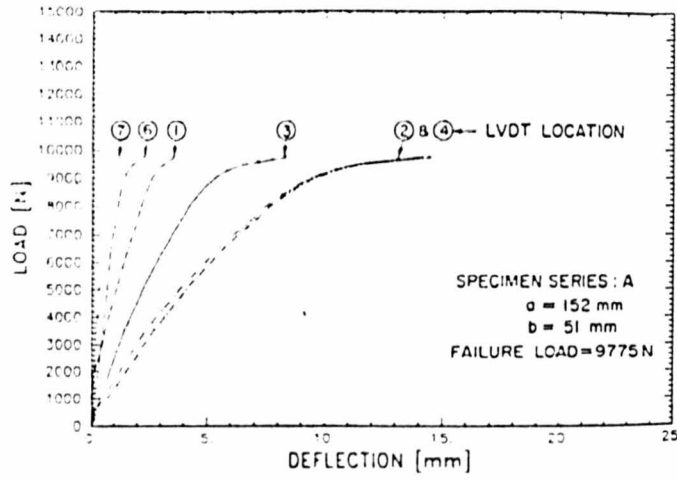
Figure 2.19. Load-deflection behaviour of the specimens.
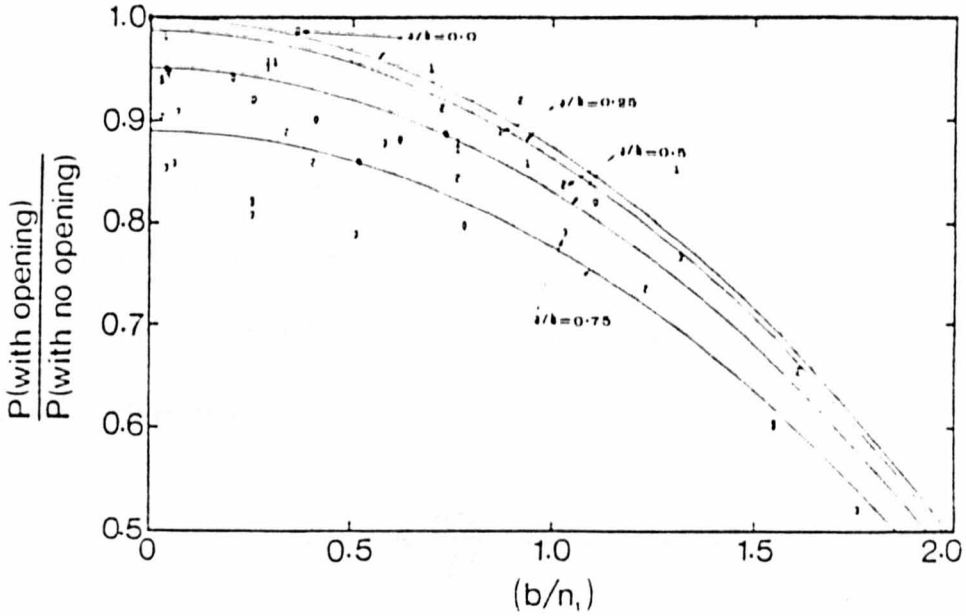
Figure 2.20. Effect of the opening size on web crippling strength.

32

2.3. BUCKLING AND PLASTIC MECHANISMS.

As discussed in the previous subchapter, all experimental studies on web crippling behaviour dealt with sections subjected to locally applied loads. Although webs and flanges of the sections are interactive, it is also useful to study the behaviour of idealized separate rectangular flat plates loaded by localized in-plane edge forces. There are many investigators who have studied this behaviour since the 1950s and their studies generally relate to the analysis of critical elastic buckling loads of the plates under this type of loading.

For example, in 1955, Zetlin[3] studied the behaviour of the rectangular plate which was simply supported along its four edges. The load was applied on one edge of the plate and symmetrically distributed about the centre of the longitudinal edges of the plate (Figure 2.21). The energy method was used to analyse the plate and the buckling load was found to have the same form as that of simply supported rectangular plates uniformly compressed in one direction[14]. Zetlin formulated the buckling load as follows:

$$P_{cr} = K \frac{\pi^2 D}{L^2} \quad \dots \dots \dots \dots (2.3.1)$$

Where :

P_{cr} : Critical buckling load.

D   : Flexural rigidity.

33

K : Constant depending on the ratios of h/L and 2B/L.
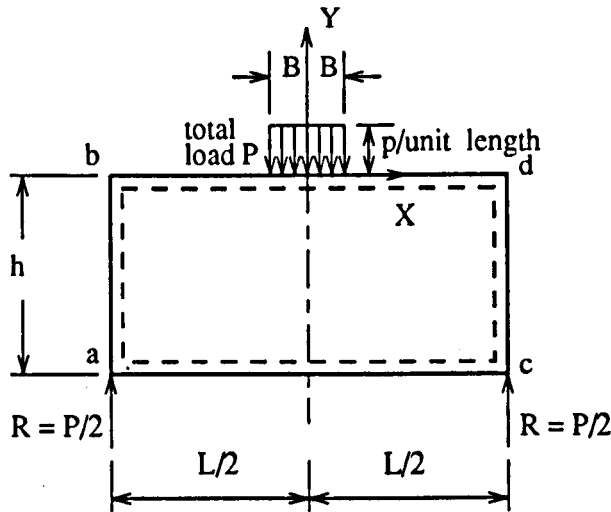
Figure 2.21. Loading arrangement in Zetlin's research.

In 1972, M.Z. Khan And A.C. Walker[15,16] also investigated the similar problem of plate buckling as studied by Zetlin. They approximated the deflected shapes of the plate by using finite element solution and used them to solve the potential energy of the plate. The buckling load given by Khan and Walker was in the form :

$$P_{cr} = K \frac{\pi^2 D}{2B} \quad\text{............ (2.3.2)}$$

Where :

P_{cr} : Critical elastic buckling load.

K : Buckling coefficient depending on the ratios of L/B and C/B.

B : Half depth of the plate.

C : Half width of loading.

Relations between K and L/B or C/B can be seen in Figure 2.22. The plates supported by shear forces in the figure are identical with the plates supported by end reactions as shown in Figure 2.23. Experimental investigations were also performed to obtain the maximum loads at which the plates collapse. Figure 2.24 shows the comparison between the experimental ultimate loads and the critical elastic buckling loads and it can be seen that the collapse loads are larger than the elastic buckling loads. Thus it can be concluded that the plates often have reserves of strength beyond the critical buckling loads.
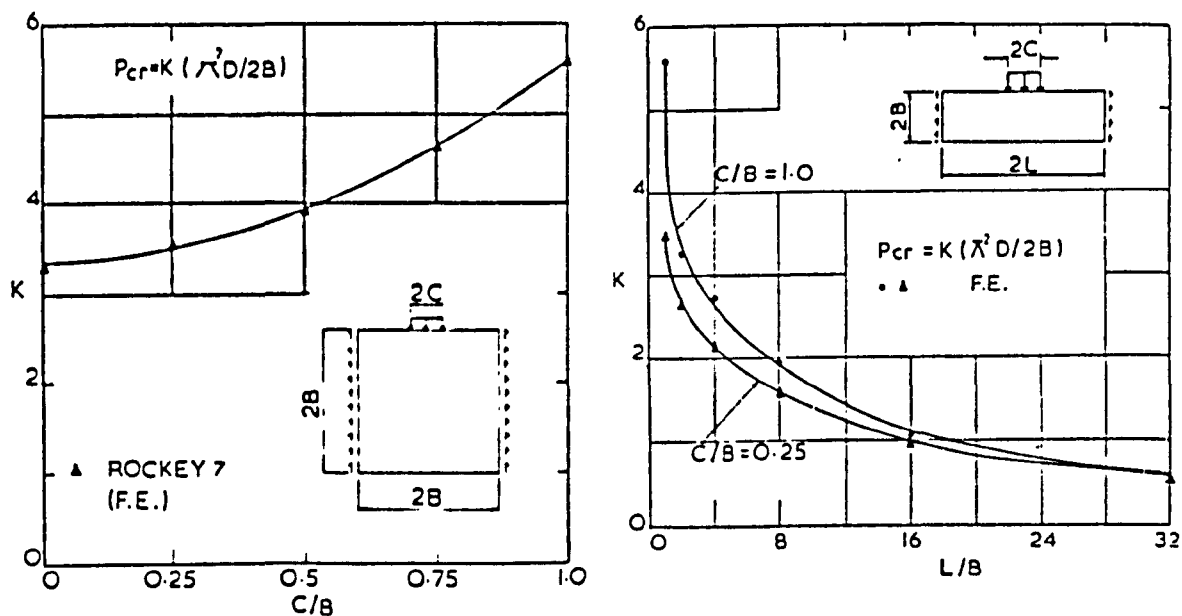
Figure 2.22. Variations of buckling coefficient (K).
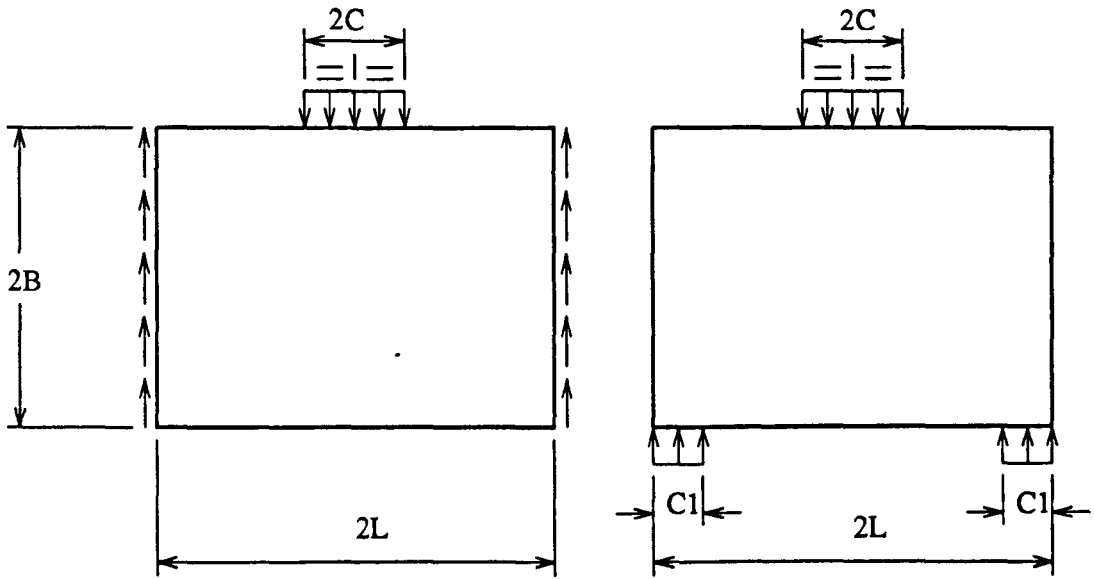
Figure 2.23. Loading geometries.
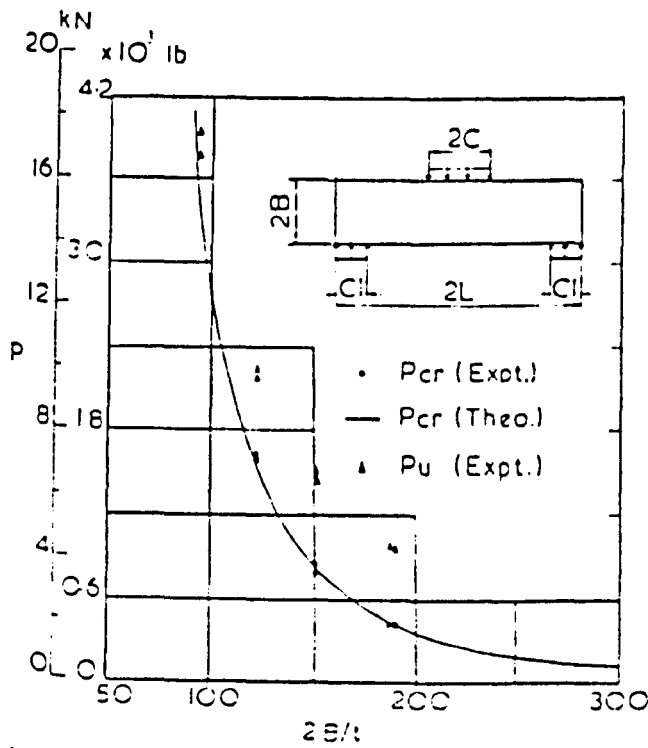
Figure 2.24. Variations of critical buckling and collapse loads for
L/B = 4.0, C/B = 1.0.

36

A similar study was also carried out by Kenneth, El-gaaly and Bagchi[17] in 1972, but this study also considered the effect of shear stresses (τ) and in-plane bending moments (M) upon the edge loads necessary to cause buckling. According to their results the shear stresses or the in-plane bending moments will reduce the applied edge loads which can cause buckling. The effects of shear stresses and in-plane bending moments upon the buckling loads can be seen in Figure 2.25.
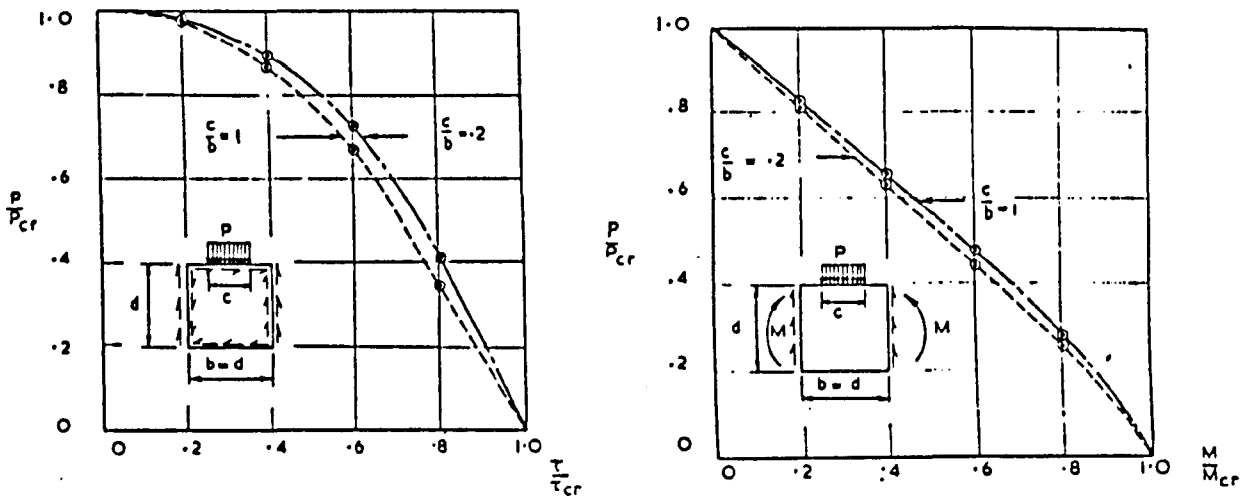
Figure 2.25. Effects of τ and M upon the applied edge loads.

The behaviour of plates under compression loads was also studied by R.M. Korol and A.N. Sherbourne[18,19] using a plastic mechanism approach. The plates were subjected to uniaxially compressed loads which were uniformly distributed along the edges of

the plates. According to their studies, the collapse loads of the plates can be obtained from the intersection of postbuckling loading paths and rigid-plastic unloading lines. The elastic postbuckling loading path can be obtained by using an energy method while the rigid-plastic unloading or plastic mechanism line can be obtained by considering the change in the plastic collapse load with geometry changes in the bent plate. In this study, Korol and Sherbourne introduced a model of plastic mechanism called " *A pitch roof type of mechanism* " to analyse the behaviour of plates after collapse. The model of plastic mechanism can be seen in Figure 2.26.
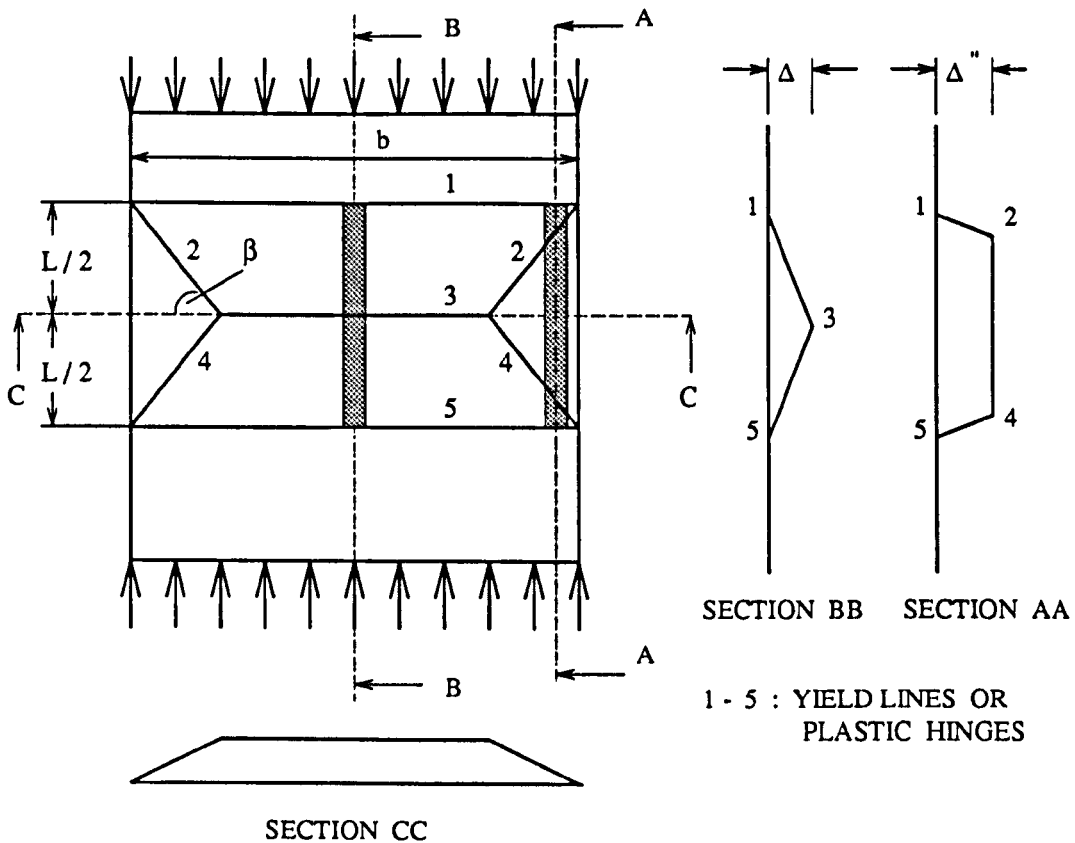
Figure 2.26. Pitch roof type of mechanism.

In 1973, N.W. Murray[20] investigated buckling mechanisms of stiffened panels under the combination of axial compression loads and pure bending moments. There are two types of buckling mechanism that can occur in the stiffened plate under the combined bending and compression, namely, Mode I and Mode II mechanisms. In the case of mode I, a buckling mechanism occurs in the plate and the stiffener is in tension and remains straight (Figure 2.27) while in mode II, a buckling mechanism takes place in the stiffener and the plate is partially or entirely in tension (Figure 2.28).

(a) Mode I mechanism :

Figure 2.29 shows the mode I mechanism and its equilibrium conditions can be expressed by considering cross section x_1-x_1 and cross section x_2-x_2 of the mechanisms. From Figure 2.31, the axial equilibrium will be :

$$P = F_{PL} + F_{sc} - F_{st} \dots\dots\dots (2.3.3)$$

$$F_{PL} = \sigma_y \, t_1 \, a + \sigma_y \, t_1 \, (s - 2a) \, [\, \sqrt{(\frac{2\Delta}{t_1})^2 + 1} - \frac{2\Delta}{t_1} \,] \dots\dots (2.3.4)$$

$$F_{sc} = \sigma_y \, t_2 \, (h_2 - c) \dots\dots\dots (2.3.5)$$

$$F_{st} = \sigma_y \, t_2 \, c \dots\dots\dots (2.3.6)$$

In these above formulae :

σ_y : Yield strength.   ; t_1 : Plate thickness.
t_2 : Stiffener thickness.   ; h_2 : Stiffener depth.

c : Depth of tension yield zone in the stiffener.

a : Dimension of mode I plastic mechanism.

s : Spacing of stiffeners.

Rotational equilibrium about o :

$$P (\delta + h_2 - e - c) + M = F_{PL} (t_1 + h_2 - c) + \frac{F_{sc} (h_2 - c)}{2} + \frac{F_{st} c}{2}$$

.... (2.3.7)

Where :

$$\delta = \frac{t_1 (\frac{\Delta}{t_1})^2}{a (\frac{t_1}{2} + h_2 - c)}$$ .... (2.3.8)

(b) Mode II mechanism :

In the mode II, failure mechanisms take place on the stiffener. This type of failure can occur when one of the stiffener has buckled and Figure 2.32 illustrates a part of the stiffened panel at which failure has taken place. Deflection and forces acting on the stiffened panel after buckling can be seen from a half portion of the stiffened panel as shown in Figure 2.33. The axial force of the stiffener is

$$F_s = \frac{\sigma_y\, t_2\, h_2}{2} \left[\sqrt{(\frac{2\Delta}{K\, t_2})^2 + 1} - \frac{2\Delta}{K\, t_2} + \frac{K\, t_2}{2\Delta} \ln\left[\sqrt{(\frac{2\Delta}{K\, t_2})^2 + 1} + \frac{2\Delta}{K\, t_2} \right] \right]$$

.... (2.3.9)

Where : $K = 1 + \sec^2 \beta$

The moment on the stiffener is as follows :

$$M_s = \frac{\sigma_y \, t_2^3 \, h_2^2 \, K^2}{12 \, \Delta^2} \left[\left[\left(\frac{2\Delta}{K \, t_2}\right)^2 + 1\right]^{\frac{3}{2}} - 1 - \left(\frac{2\Delta}{K \, t_2}\right)^3 \right] \quad \text{....... (2.3.10)}$$

The axial force on the plate is

$$F_{PL} = \sigma_y \, s \, (t_1 - 2d_1) \quad \text{......... (2.3.11)}$$

and the moment carried by it is

$$M_{PL} = \sigma_y \, s \, d_1 \, (t_1 - d_1) \quad \text{....... (2.3.12)}$$

d_1 : Depth of tension yield zone of the plate

The applied load P for a given moment M is obtained from the following formulae.

$$P = \frac{\delta + e - AD - B - \sqrt{(\delta + e - AD - B)^2 - 4 \, A^2 \, C \, (CB^2 + DB + F')}}{2 \, A^2 \, C}$$

$$\text{.................................... (2.3.13)}$$

Where :

$$\delta = \frac{\Delta^2}{2 \, h_2^2 \, \tan\beta} \qquad\qquad A = -\frac{1}{2 \, \sigma_y \, s}$$

$$B = \frac{t_1}{2} + \frac{F_s}{2 \, \sigma_y \, s} \qquad\qquad C = -\sigma_y \, s$$

$$D = 2 \, \sigma_y \, t_1 \, s \qquad\qquad F' = M_s - M - \frac{\sigma_y \, t_1^2 \, s}{2}$$

41

If the load P is given, then the moment M can be explicitly expressed as follows :

$$M = C \, d_1^2 + D \, d_1^2 + F'' \, \dots\dots\dots\dots (2.3.14)$$

Where :

$$d_1 = \frac{t_1}{2} - \frac{P - F_s}{2 \, \sigma_y \, s}$$

$$F'' = M_s - P \, (\delta + e) - \frac{\sigma_y \, t_1^2 \, s}{2}$$
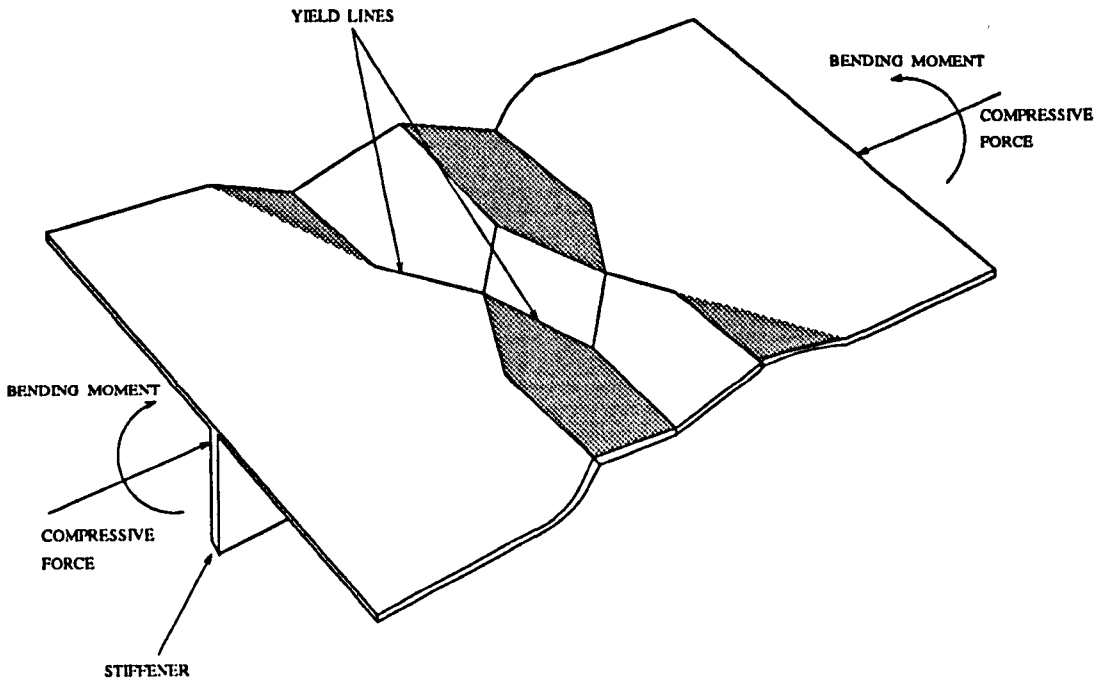
Figure 2.27. Buckling mechanism of mode I.

42
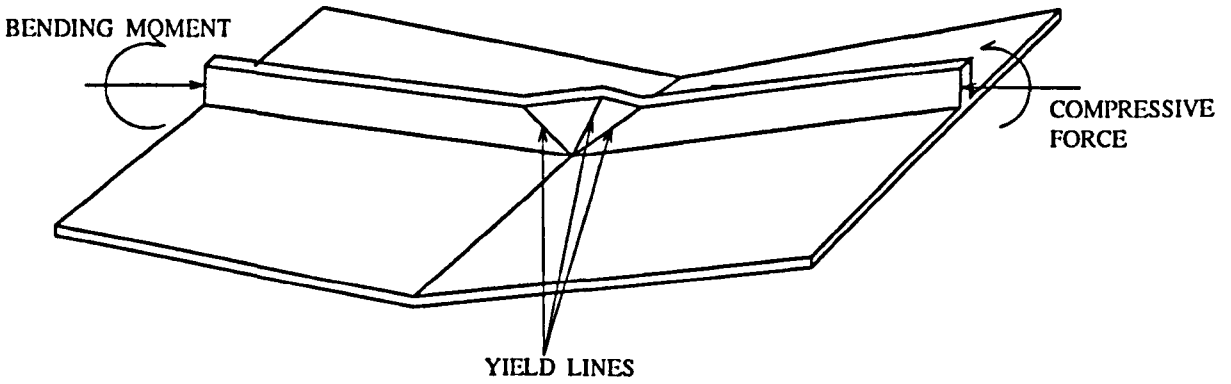
Figure 2.28. Buckling mechanism of mode II.
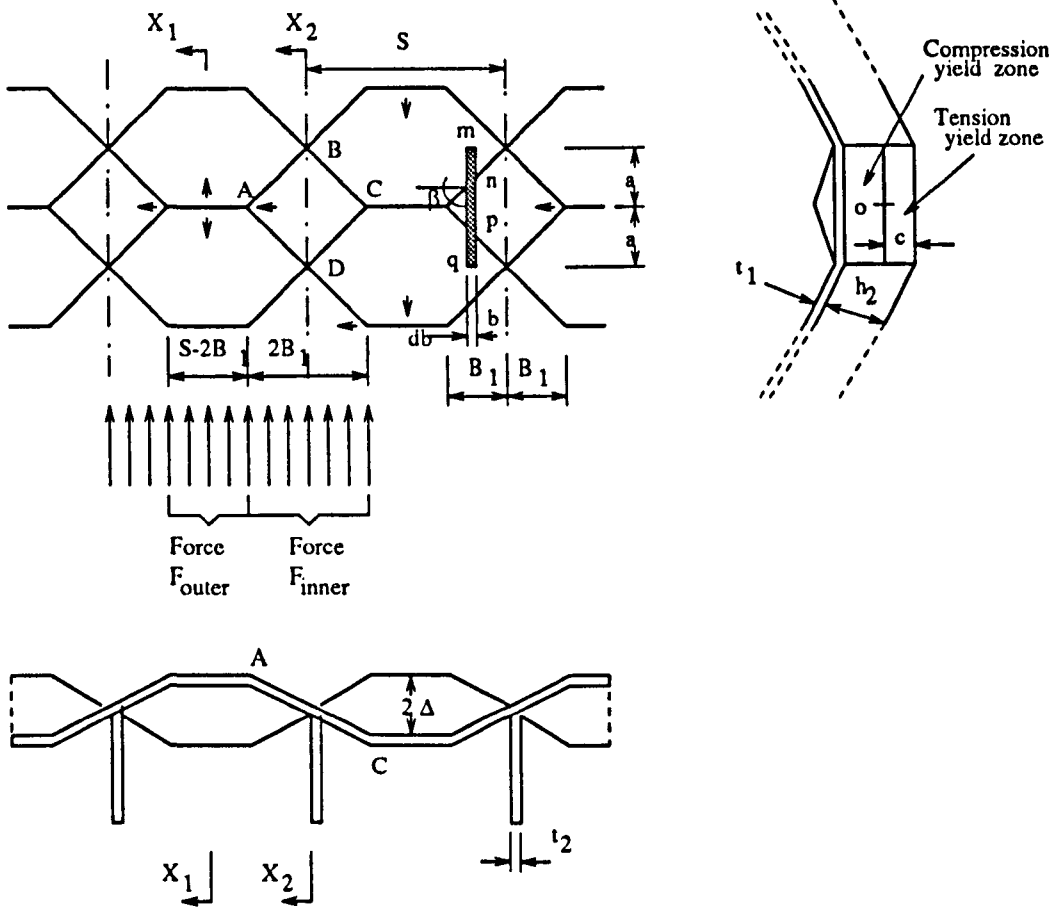
Figure 2.29. Mode I mechanism of with $\beta = 45°$ and $B_1 = a$.

43
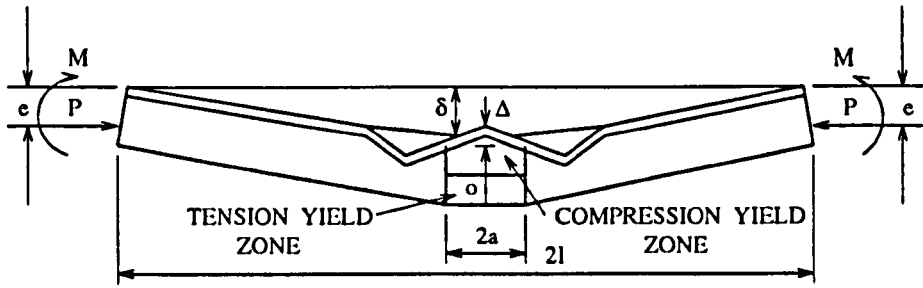
Figure 2.30. Cross section x_1-x_1 of the above mechanism.
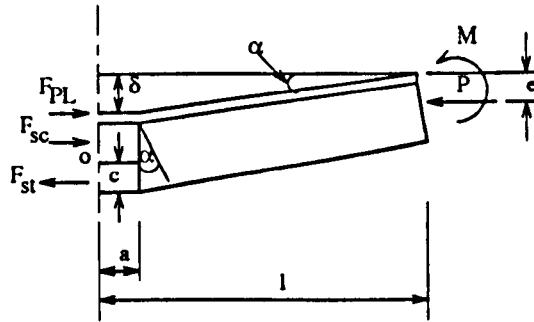
Figure 2.31. Cross section x_2-x_2 of the above mechanism.
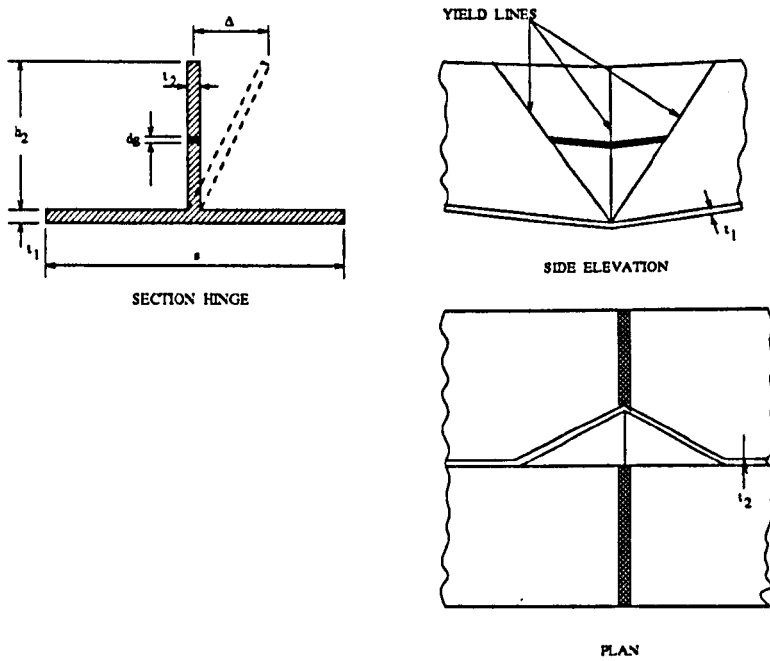
Figure 2.32. Failure of the stiffened panel in mode II mechanism.

44
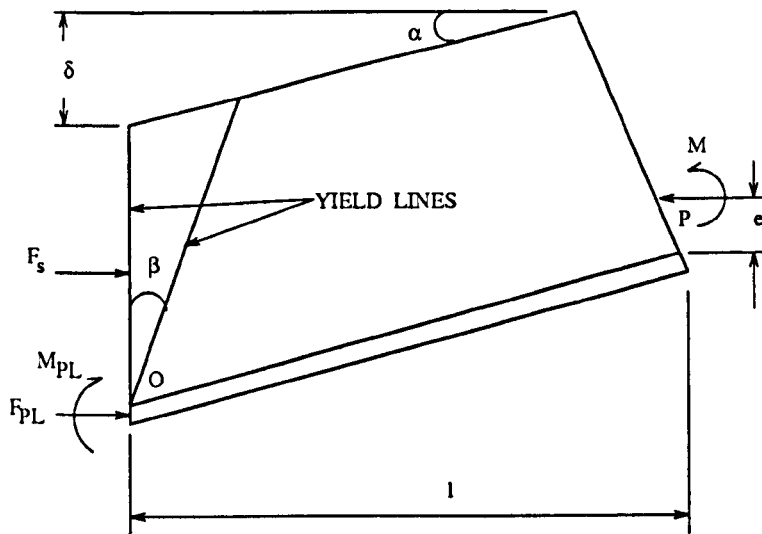
Figure 2.33. Deflection and forces on the postbuckled panel.

In 1975, A.C. Walker and N.W. Murray[21] studied the collapse behaviour of rectangular plates subjected to uniform compression along two opposite edges. A pitch roof type of mechanism which was similar to that shown in Figure 2.26, but with the aspect ratio L/b = 0.5 was used by Walker and Murray to predict the behaviour of the plate at collapse. It can be seen in the Figure that the mechanism consists of two typical regions. The first region contains strips BB and it is composed of three yield lines which are perpendicular to the direction of loading. The second one contains strips AA and it is composed of four yield lines where two of them are perpendicular to the load directions and the other ones incline at an angle of β.

Analyses of the mechanisms were carried out on the basis of equilibrium equations at strips AA and BB. The equilibrium equations were then solved for the whole portion of the plate. From this solution, the average stress σ for the whole plate width

45

can be expressed as follows:

$$\frac{\sigma}{\sigma_y} = \frac{1}{4} \left[\cot\beta \left(\sqrt{(\frac{2\Delta}{Kt})^2 + 1} - \frac{2\Delta}{Kt} \right) - 2 \cot\beta \left(\sqrt{(\frac{\Delta}{t})^2 + 1} - \frac{\Delta}{t} \right) \right.$$

$$\left. + \frac{Kt\cot\beta}{2\Delta} \ln(\sqrt{(\frac{2\Delta}{Kt})^2 + 1} + \frac{2\Delta}{Kt}) \right] + \sqrt{(\frac{\Delta}{t})^2 + 1} - \frac{\Delta}{t}$$

.... (2.3.15)

Where : $K = 1 + \sec^2\beta$ and σ_y : Yield strength.

The pitch-roof type of mechanism as shown in Figure 2.26 was also used by P. Davies, K.O. Kemp and A.C. Walker[22] to study the failure mechanism of a plate under the similar loads. They assumed that plastic hinges or yield lines are formed under the influence of a bending moment M, a compressive axial (membrane) force N acting at the mid-plane of the plate and a shearing force S acting uniformly over the thickness of the plate t (Figure 2.34). The behaviour of the mechanisms was analysed by considering that the plate can be divided into a number of strips which are free to slide in relation to each other. The analysis of the mechanism was also performed using an equilibrium approach and the total force P acting on the plate is

$$P = \sigma_y t (N_1 + 2 N_2) \dots\dots\dots\dots (2.3.16)$$

Where : σ_y : Yield strength.

$$N_1 = (b - L \tan\beta) \left(\sqrt{(\frac{\Delta}{t})^2 + 1} - \frac{\Delta}{t} \right) \quad .... \quad (2.3.17)$$

$$N_2 = \frac{1}{2} \tan\beta \left[\sqrt{\frac{1 + \cosec^2\beta}{2 + 3 \cos^2\beta}} \right] \left[\sqrt{1 + \frac{4 (\frac{\Delta}{t})^2}{(2 + 3 \cos^2\beta) (1 + \cosec^2\beta)}} \right]$$

$$+ \frac{L \tan\beta (1 + \cosec^2\beta)}{4 (\frac{\Delta}{t})} \ln\left[\frac{2 (\frac{\Delta}{t})}{\sqrt{(2 + 3 \cos^2\beta) (1 + \cosec^2\beta)}} \right.$$

$$+ \left. \sqrt{1 + \frac{4 (\frac{\Delta}{t})^2}{(2 + 3 \cos^2\beta) (1 + \cosec^2\beta)}} \right] - \frac{L \Delta \tan\beta}{t (2 + 3 \cos^2\beta)}$$

$$..................................... \quad (2.3.18)$$

d : depth of neutral axis below
mid-plane

Figure 2.34. Cross section of plastic hinge

In 1981, N.W. Murray and P.S. Khoo[23] studied the post-collapse behaviour of thin-walled structures and postulated that behaviour can be approximated using a rigid plastic theory. When the rigid plastic theory is plotted together with an elastic theory, the failure load of the structure can be roughly evaluated. Figure 2.35 shows such a combination of curves for a simple pin-ended column and a simply supported plate. It can be seen from the curves that P_F or σ_F is the load or stress corresponding to the failure of the strut or the plate. According to their investigations, the failure modes of thin-walled structures are by means of spatial plastic mechanisms. It has been found that these mechanisms actually consist of an assembly of basic mechanisms which are compatible to each other.

There are eight basic mechanisms and their characteristic equations have been developed and presented in table 2.1. The equations can be used to analyse the mechanisms of collapse of structural members as shown in Figure 2.36. The analysis of plastic mechanism can be carried out using the following formulae. The fully plastic moment (M_p) for a rectangular plate of width b and thickness t is

$$M_p = \frac{\sigma_y \, b \, t^2}{4} \quad \text{............. (2.3.19)}$$

σ_y : Yield strength

When the plate carries an axial compression load P, its moment capacity will be reduced and formulated as in equation (2.3.20). In this equation, P_y represents the squash load and it is equal to σ_y multiplied by the cross section area.

48

$$M_p' = M_p \left[1 - \left(\frac{P}{P_y}\right)^2 \right] = \frac{\sigma_y \, b \, t^2}{4} \left[1 - \left(\frac{P}{\sigma_y \, b \, t}\right)^2 \right] \quad \text{........ (2.3.20)}$$

In these above two cases, the direction of plastic hinge is at right angles to the long direction of the plate or the direction of axial load P. If the direction of the plastic hinge inclines at an angle β to the direction of axial load P, the moment capacity of the plastic hinge becomes

$$M_p'' = M_p' \sec^2 \beta = \frac{\sigma_y \, b \, t^2}{4} \left[1 - \left(\frac{P}{\sigma_y \, b \, t}\right)^2 \right] \sec^2 \beta \quad \text{........ (2.3.21)}$$

There are two main categories of plastic mechanisms, namely, true mechanisms and quasi-mechanisms. The former can be developed from flat sheets which form the cross section of the strut or beam while the latter can not be developed simply by bending along the hinge lines. The difference of these two mechanisms can be explained using mechanisms in Figure 2.37. The mechanism shown in Figure 2.37(a) is a true mechanism because it can be made by simply folding along the hinge lines. Figure 2.37(b) is an example of a quasi mechanism because it can not be achieved without membrane deformation within parts of the cross section.

An example of using these above basic mechanisms is the analysis of plastic mechanisms of the collapsed structure CW1 in Figure 2.36(a). The mechanism is in

49

the form of a type 8 basic mechanism (flip-disc) and each flange is divided into a compression yield zone and a tension yield zone (Figure 2.38). The depth of the tension yield zone (d_1) varies during the collapse process. The fibres at point O do not change length so that the point O can be taken as a pivot point. From the geometry of the mechanism in its deformed position, the values of α and δ can be written as follows :

$$\alpha = \frac{\Delta^2}{2 a (b_2 - d_1)} \quad ; \quad \delta = \frac{\Delta^2 L}{2 a (b_2 - d_1)} \quad \ldots\ldots\ldots\ldots (2.3.22)$$

For equilibrium conditions only a half portion of the channel is considered. Axial equilibrium :

$$P = P_1 + P_2 - P_3 \quad \ldots\ldots\ldots\ldots (2.3.23)$$

Rotational equilibrium about the point O :

$$P (\delta + b_2 - d_1 - e) = P_1 (b_2 - d_1) + \frac{P_2 (b_2 - d_1)}{2} + \frac{P_3 d_1}{2} \quad \ldots. (2.3.24)$$

$$P_2 = 2 \sigma_y (b_2 - d_1) t \quad ; \quad P_3 = 2 \sigma_y d_1 t \quad \ldots\ldots\ldots (2.3.25)$$

P_1 is obtained from equation 8 of table 1.

Subtituting equations (2.3.22) and (2.3.25) into equation (2.3.24) the following non-dimensional equation is obtained.

$$\left[\frac{P_1}{\sigma_y\,b_2\,t} - 1 + \frac{2\,d_1}{b_2}\right]\left[\frac{\Delta L}{2\,a\,b_2^2\,(1 - \frac{d_1}{b_2})} + 1 - \frac{d_1}{b_2} + \frac{e}{b_2}\right]$$

$$- \frac{P_1}{\sigma_y\,b_2\,t}\,(1 - \frac{d_1}{b_2}) - 1 + 2\,\frac{d_1}{b_2} = 0 \ \dots\dots\ (2.3.26)$$

A comparison between the foregoing analysis and experimental results is shown in Figure 2.39. The simple plastic hinge line as seen in the figure is based on the assumption that the cross section does not deform during collapse. Its application has extremely overestimated the experimental load carrying capacity of thin-walled structures.
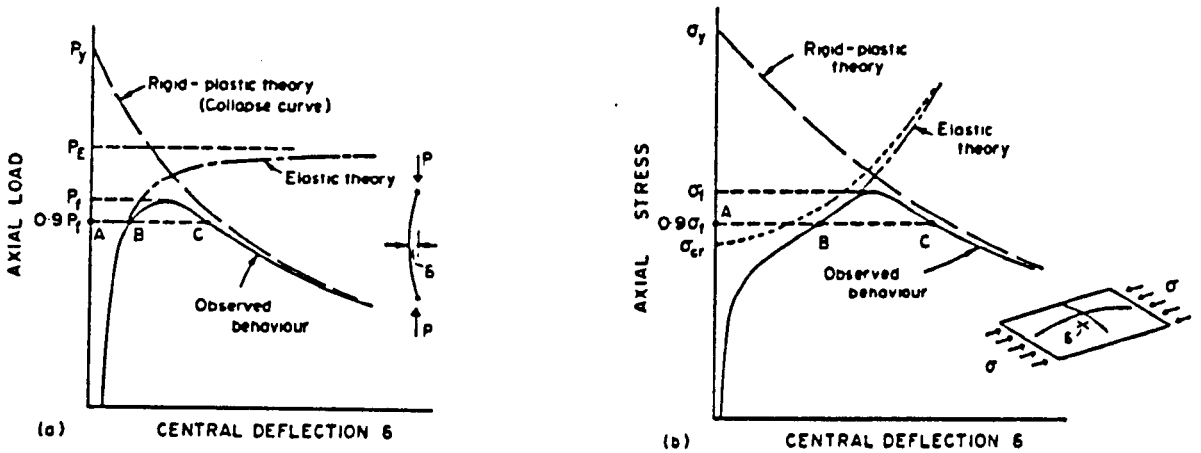
Figure 2.35. The behaviour of an imperfect strut (a) and an imperfect plate (b).

51

(a) CW1   (b) CW2

(c) CF1   (d) CF2   (e) CF3
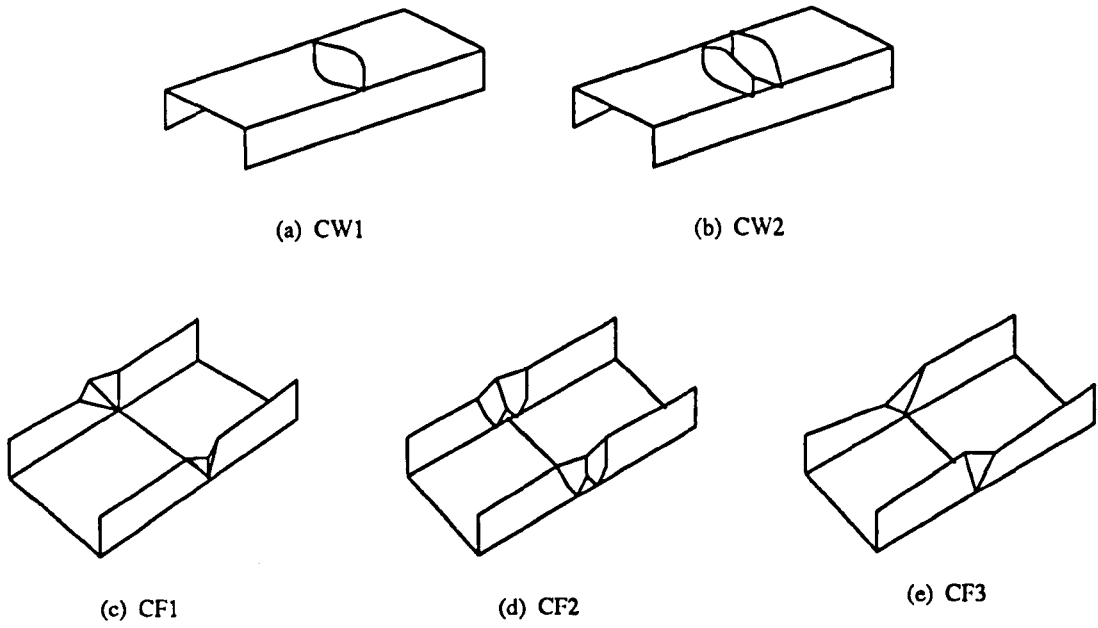
Figure 2.36. Plastic mechanisms of channel column obtained from tests.
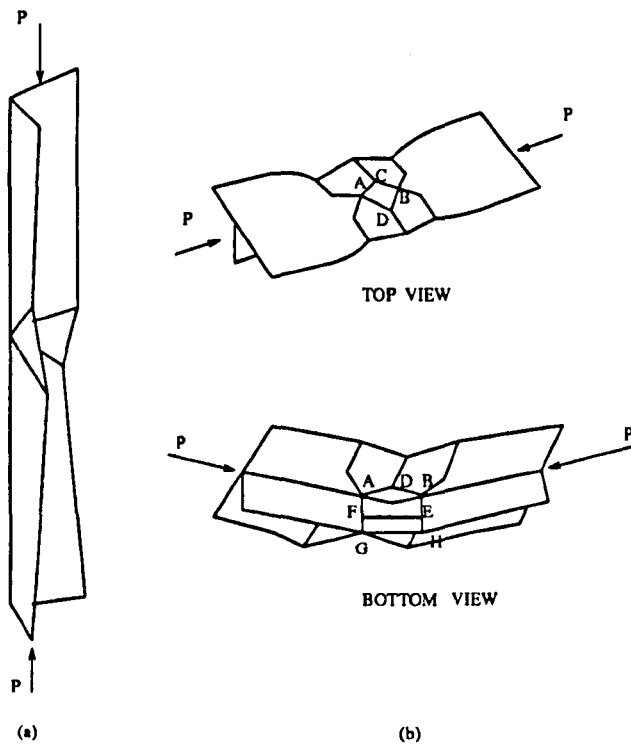
Figure 2.37. (a) true mechanism and (b) quasi-mechanism.
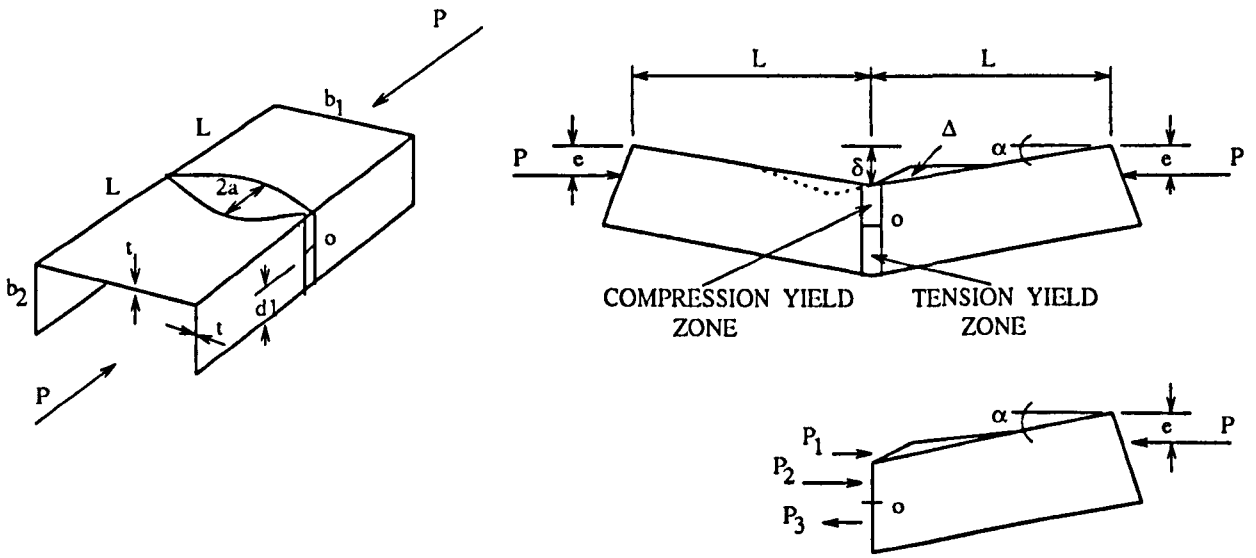
Figure 2.38. Analysis of a plate mechanism of CW1 with the web in compression.
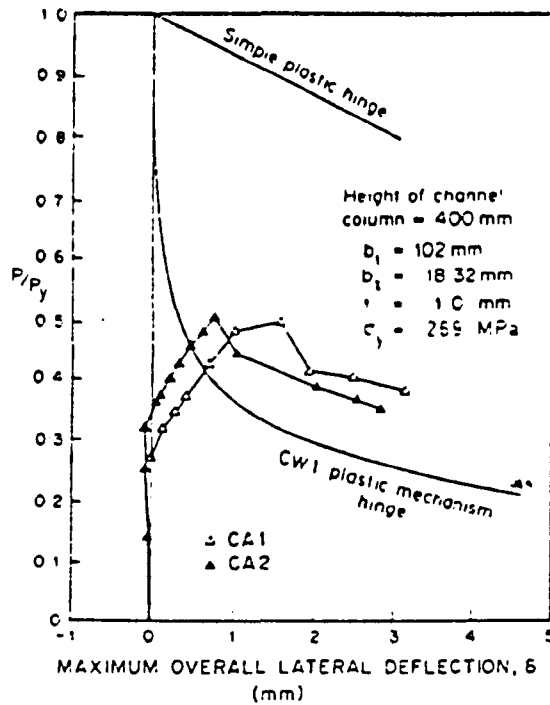
Figure 2.39. Comparison of rigid-plastic curves based on simple and local mechanisms and experimental results.

53

Table 2.1. True basic mechanisms [30]

$$\kappa_1 = 1 + \sec^2 \beta; \ \kappa_2 = \sec^2 \beta; \ \kappa_3 = 2\sec^2 \beta$$

#	Mechanism		Equations
1			$P = \sigma_y tb \left\{ \sqrt{\left[\left(\dfrac{2\Delta}{t}\right)^2 + 1\right]} - \dfrac{2\Delta}{t} \right\}$ $e = b/2$
2			$P = \sigma_y tb \left\{ \sqrt{\left[\left(\dfrac{\Delta}{t}\right)^2 + 1\right]} - \dfrac{\Delta}{t} \right\}$ $e = b/2$
3			$P = \dfrac{\sigma_y tb}{2} \left\langle \sqrt{\left[\left(\dfrac{2\Delta}{\kappa_1 t}\right)^2 + 1\right]} - \dfrac{2\Delta}{\kappa_1 t} + \dfrac{\kappa_1 t}{2\Delta} \right.$ $\left. \ln\left\{ \sqrt{\left[\left(\dfrac{2\Delta}{\kappa_1 t}\right)^2 + 1\right]} + \dfrac{2\Delta}{\kappa_1 t} \right\} \right\rangle$ $Pe = \dfrac{\sigma_y t^3 b^2 \kappa_1^2}{12\Delta^2} \left\{ \left[\left(\dfrac{2\Delta}{\kappa_1 t}\right)^2 + 1\right]^{3/2} - 1 - \left(\dfrac{2\Delta}{\kappa_1 t}\right)^3 \right\}$
4			Obtain solution by using the difference of two Type 3 mechanisms $P = P_1 - P_2$ $Pe = P_1 e_1 - P_2 e_2$
5	 End panels twist freely		Same equations as for Type 3 but replace κ_1 by κ_2
6	 All hinges inclined at β		Same equations as for Type 3 but replace κ_1 by κ_3
7			Same equations as for Type 5 but with $\beta = 45°$
8	 End panels twist and bend freely		$P = \dfrac{\sigma_y tb}{6} \left\langle 1 - \dfrac{2\Delta}{t} + \sqrt{\left[\left(\dfrac{2\Delta}{t}\right)^2 + 1\right]} - \dfrac{6\Delta}{t(1+4a^2/b^2)} \right.$ $\left. + 4 \cdot \sqrt{\left\{ \left[\dfrac{3\Delta}{2t(1+4a^2/b^2)}\right]^2 + 1 \right\}} \right\rangle$ $e = b/2$

------ Positive plastic hinge
······ Negative plastic hinge

54

M.C.M. Bakker[24] studied failure mechanisms of web crippling in 1992 and the mechanisms can be determined according to the mode of web deformation. One of the important parameters which describes the web deformation is the web crippling deformation Δh_w, that is, the decrease of the web height (Figure 2.40). By examining the mode of web deformation, the mechanisms can be distinguished into rolling mechanisms and yield arc mechanisms. In the experiments, these two types of mechanism can be recognized from their web deformation modes as well as from their typical load-deformation diagrams.

The rolling mechanism occurs in members with a large corner radius in which the web crippling deformation is caused by a rolling process of the corner radius through the web. Figure 2.41 shows a model of rolling mechanism and it can be seen that the yield line 1 tends to bend the web while the yield line 2 tends to straighten the flange. An example of the load-deformation diagram corresponding to the rolling mechanism is shown in Figure 2.42. The diagram also shows that after an initial bend, the load steadily increases up to the ultimate load and then the load gradually decreases.

In the case of the yield arc mechanism, a yield curve is formed in the web underneath the load bearing plate (Figure 2.43) and this type of mechanism occurs in members with a small corner radius. An example of the load-deformation diagram can be seen in Figure 2.44 and this indicates that the load steadily increases up to the

55

ultimate load and afterwards the load suddenly drops. This failure mechanism also exhibits relatively large lateral deformations of the web and small web crippling deformations.

The both mechanisms of web crippling can result in the formation of a local plastic hinge mechanism. As the local plastic hinge mechanism has started to develop, the rotation will take place in this hinge. The rotation caused by the plastic hinge mechanism in this study is termed as mechanism rotation and denoted by ϕ_{mec}. It has also been found from experiments that the hinge mechanism is initiated only after some elastic web crippling deformations and this is shown in Figure 2.45. $\Delta h_{w;imec}$ is the web crippling deformation at which the plastic mechanism starts to develop. The figure also indicates that the mechanism rotation does not happen ($\phi_{mec} = 0$) for $\Delta h_w \leq \Delta h_{w;imec}$.

In the above figure, the distance between the yield lines 8 and 10 (L_{yt}), the distance between the yield lines 9 (L_{yb}) and the web crippling deformation $\Delta h_{w;imec}$ indicate the character of the plastic hinge mechanism. A useful idealization which can be used to analyse the web crippling behaviour is a mechanism initiation load, i.e. the load at which the plastic mechanism is initially formed. In a load-deformation diagram, the mechanism initiation load can be determined as the point of intersection between elastic and rigid plastic curves. There are two different types of load-deformation curves as shown in Figure 2.46. The first curve (Figure 2.46A) shows the case when

the mechanism initiation load is equal to the ultimate load and at the first yield the

actual curve (indicated by the dotted curve) starts to deviate from the elastic curve

and coincide with the rigid plastic curve only after the formation of the plastic hinge

mechanism. This type of load-deformation curve occurs in members failing by yield

arc mechanisms. The second curve (Figure 2.46B) is the load-deformation curve for

members failing by rolling mechanisms in which the mechanism initiation load is

lower than the ultimate load and the rigid-plastic curve is not an unloading curve.
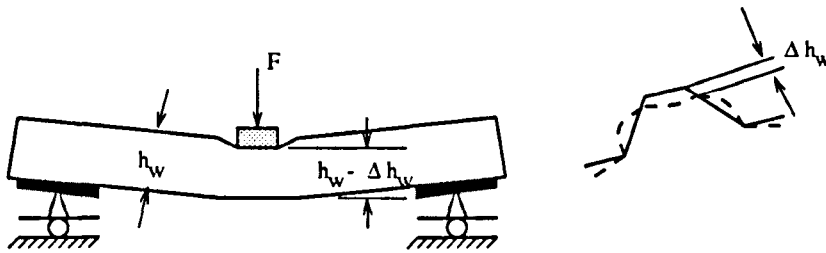
Figure 2.40. Web crippling deformation.
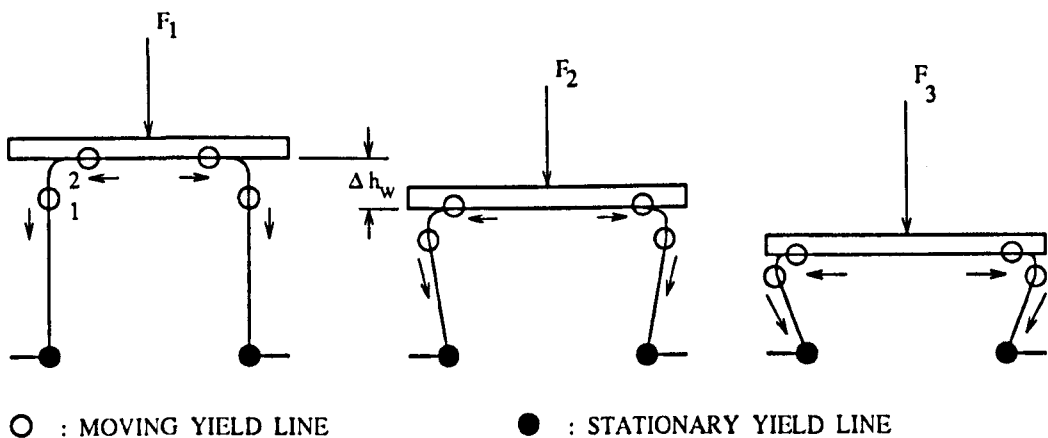
Figure 2.41. Web deformations of rolling mechanism.

O : MOVING YIELD LINE ● : STATIONARY YIELD LINE
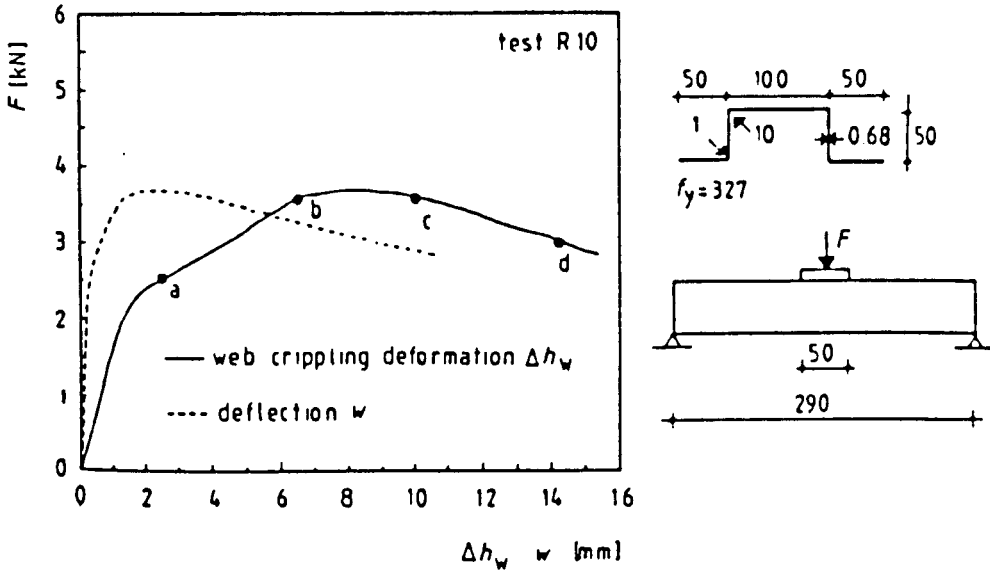
Figure 2.42. Load-deformation behaviour of rolling mechanism.

● : STATIONARY YIELD LINE
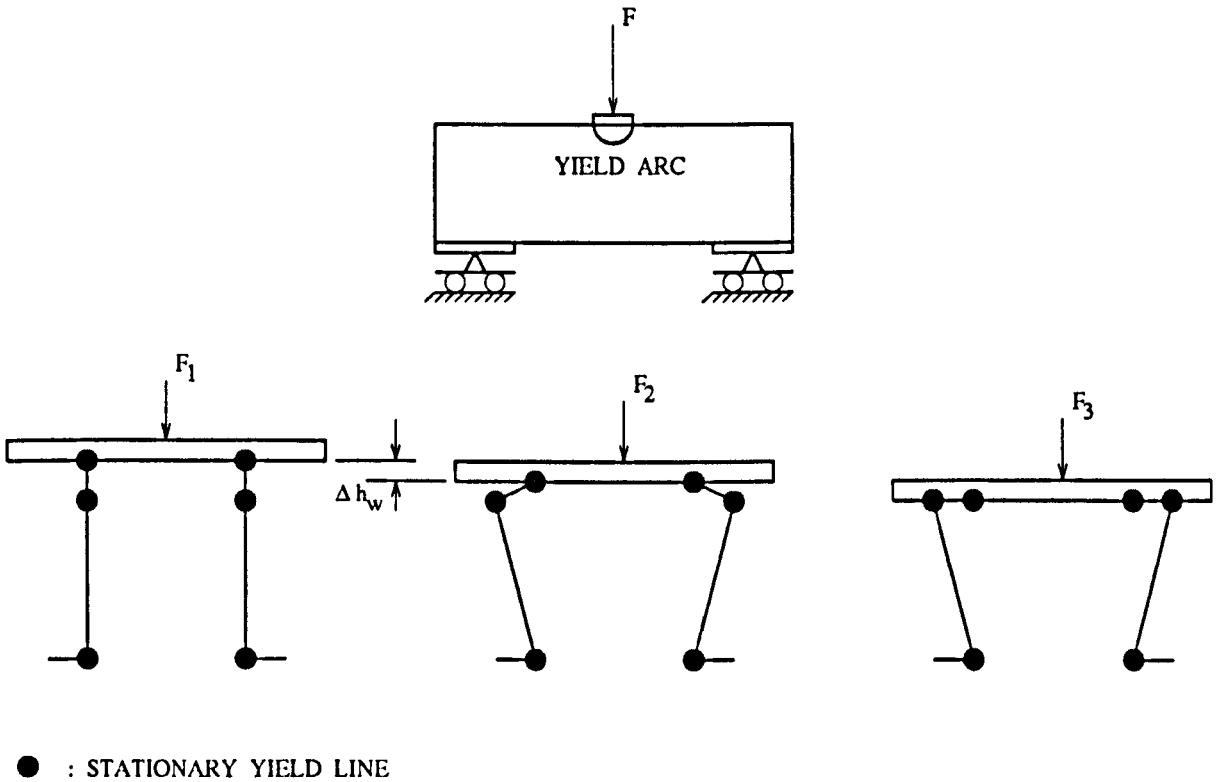
Figure 2.43. Web deformations of yield arc mechanism.

58
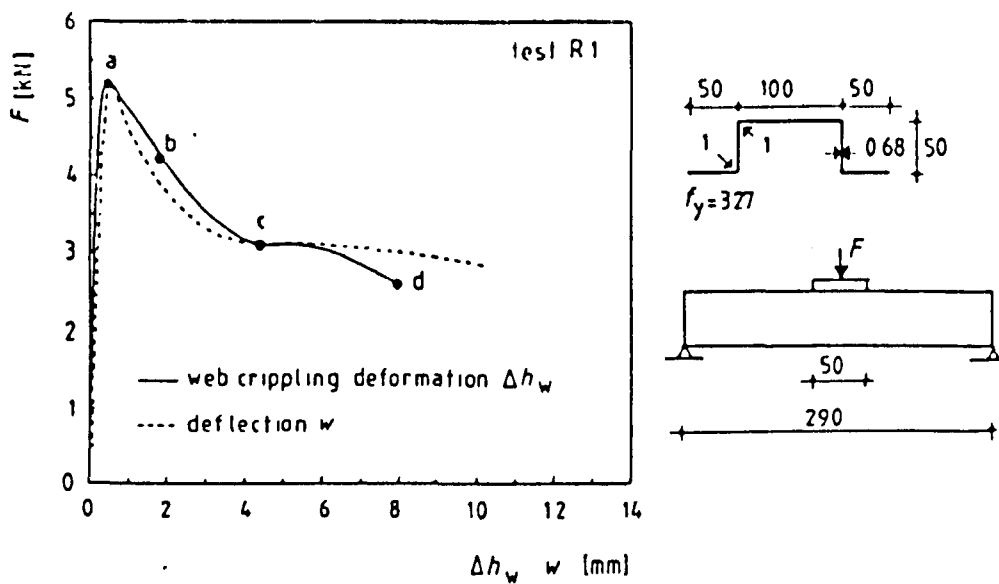
Figure 2.44. Load-deformation behaviour of yield arc mechanism.

8, 9 AND 10 : YIELD LINE IN FLANGES

: UNDEFORMED PART OF MEMBER
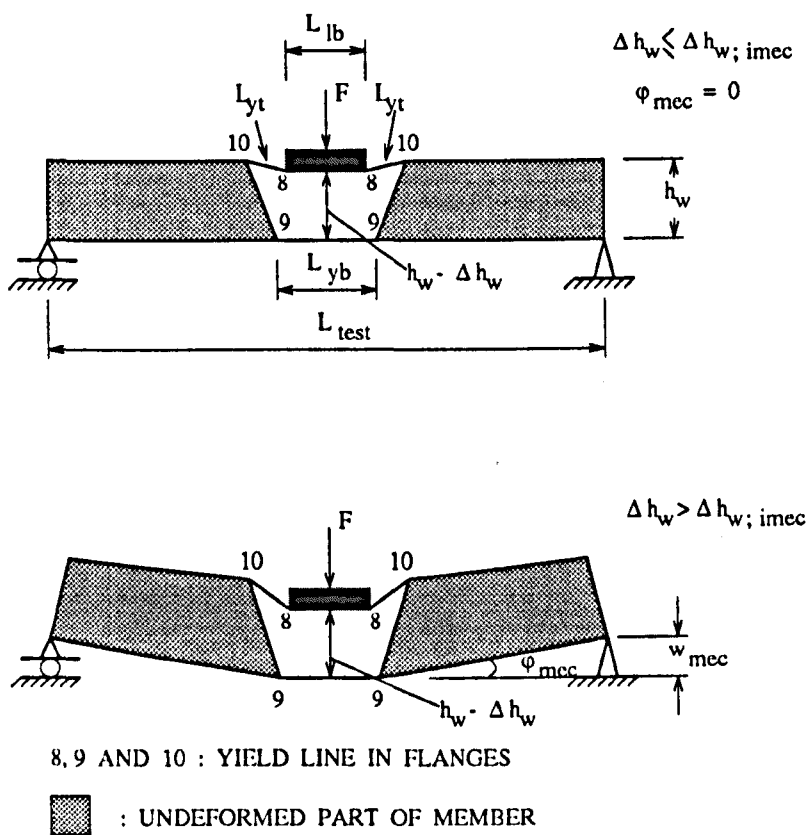
Figure 2.45. Plastic hinge mechanism.

A) rigid plastic curve = unloading curve   B) rigid plastic curve ≠ unloading curve
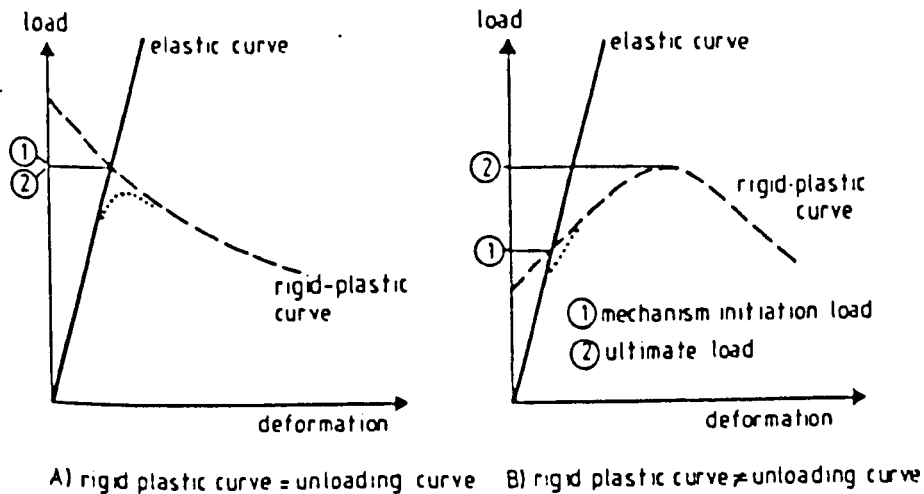
Figure 2.46. Load-deformation behaviour of rolling and yield arc mechanisms.

2.4. CURRENT DESIGN CRITERIA.

Design specifications for predicting web crippling loads of cold-formed steel beams discussed here are based on the empirical formulations. The specifications reviewed in this subchapter are as follows :

1. BS 5950 Part 5 1987.

2. AISI specification for the design of cold-formed steel structural members.

3. European recommendations for the design of light gauge steel members 1987.

2.4.1. BS 5950 Part 5 1987. [25]

The above British Standard contains the design specifications for Structural Steelwork

in building. The specifications for web crippling of cold-formed steel sections are discussed in section five of this standard in which the web crippling is termed as web crushing. The Standard categorizes the specifications of web crushing according to the types of beam and loading position. The categories are :

a. Types of beam :

- Beams or shapes having single thickness webs.

- I-beams and beams with restraint against web rotation.

b. Types and position of loadings :

- Single load or reaction near or at free end

- Single load or reaction far from free end

- Two opposite loads or reactions near or at free end

- Two opposite loads or reactions far from free end

The loads to cause local crushing of the beam webs at support points or points of concentrated load should be evaluated using the equations given in table 2.2 and 2.3. The equations in the tables are applicable for the following conditions,i.e. Beams with : $D/t \leq 200$; $r/t \leq 6$ and Decking with : $r/t \leq 7$; $N/t \leq 210$; $N/D \leq 3.5$.

Where :

D : The overall web depth (in mm).

t : The web thickness (in mm).

r : The inside bend radius (in mm).

N : The actual length of bearing (in mm); in the case of two equal and opposite concentrated loads distributed over unequal bearing lengths, the smaller

value of N should be taken.

P_w : The concentrated load resistance of a single web (in N).

c : The distance from the end of the beam to the load or the reaction

(in mm).

The constants C of the equations in table 2 and 3 represent the following values.

C_1 : 1.22 - 0.22 k   ; C_2 : 1.06 - 0.06 (r/t) ≤ 1.0

C_3 : 1.33 - 0.33 k   ; C_4 : 1.15 - 0.15 (r/t) ≤ 1.0

but not less than 0.50

C_5 : 1.49 - 0.53 k ≥ 0.6 ; C_6 : 0.88 - 0.12 m

C_7 : 1 + D/t/750 when D/t < 150 and C_7 : 1.20 when D/t > 150

C_8 : 1/k when D/t < 66.5 and C_8 : (1.10 - D/t/665)/k when D/t > 66.5

C_9 : 0.82 + 0.15 m   ; C_{10} : (0.98 - D/t/865)/k

C_{11} : 0.64 + 0.31 m   ; C_{12} : 0.7 + 0.3 $(\Theta/90)^2$

Where :

k : p_y/228 and p_y is the design strength (in N/mm2).

m : t/1.9

Θ : The angle (in degrees) between plane of web and plane of bearing surface

(45° ≤ Θ ≤ 90°).

The concentrated loads (P_w) calculated from the equations in tables 2.2 and 2.3 are

for beams under web crushing only, but if the beams are subjected to combined

62

actions of bending and web crushing, the effect of bending moment should be taken into account. In order to consider the bending effect, the following relationships should be used in designing the beams under combined bending and web crushing.

a. Sections having single-thickness webs :

$$\frac{1.2\ F_w}{P_w} + \frac{M}{M_c} \leq 1.5 \qquad ; \qquad \frac{F_w}{P_w} \leq 1 \qquad \frac{M}{M_c} \leq 1 \ .... \ (2.4.1)$$

b. I-beams made from two channels connected back-to-back or similar sections which provide a high degree of restraint against rotation of the web :

$$\frac{1.1\ F_w}{P_w} + \frac{M}{M_c} \leq 1.5 \qquad ; \qquad \frac{F_w}{P_w} \leq 1 \qquad \frac{M}{M_c} \leq 1 \ .... \ (2.4.2)$$

Where :

F_w : The concentrated web load or reaction.

P_w : The concentrated load resistance determined from tables 2.2 and 2.3.

M : The applied bending moment at the point of application of F_w.

M_c : Moment capacity determined on the basis of a limiting compressive

stress in the webs and effective widths of compression elements.

Table 2.2. Shape having single thickness webs
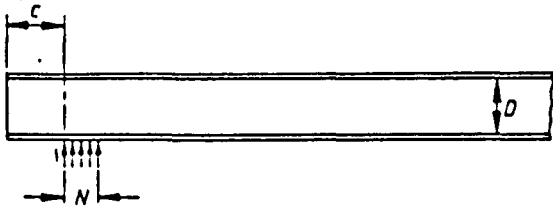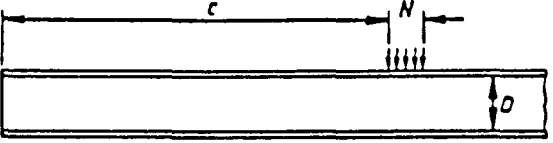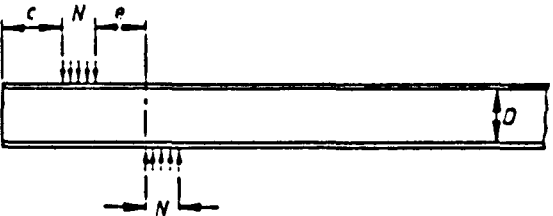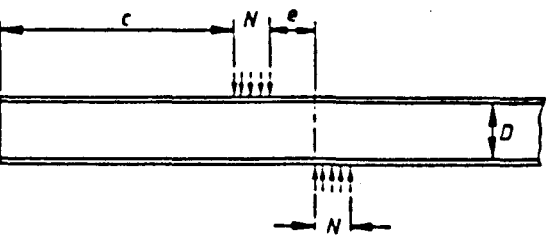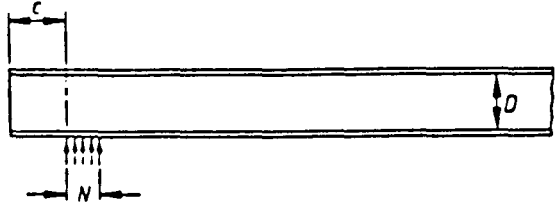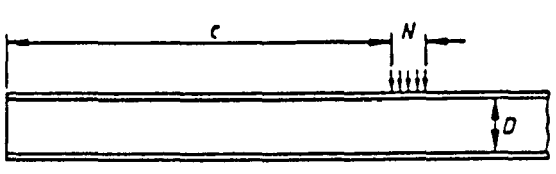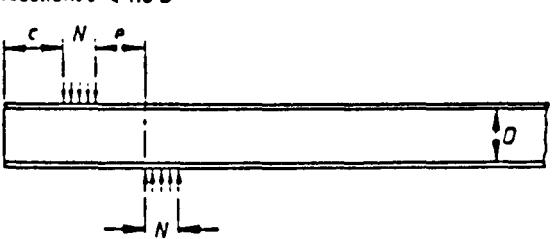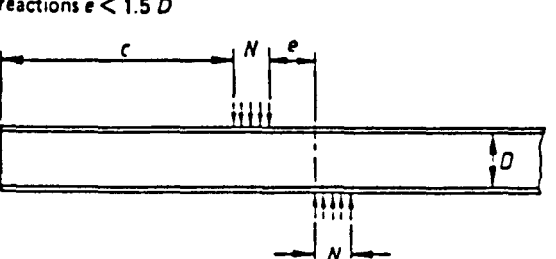
Type and position of loadings	Total web resistance, P_w

Single load or reaction
 	
$c < 1.5\,D$ Load or reaction near or at free end
	Stiffened flanges
	
	$P_w = t^2 k\, C_3\, C_4\, C_{12} \{2060 - 3.8\,(D/t)\} \times$
	     $\times \{1 + 0.01\,(N/t)\}$
	
	Unstiffened flanges
	
	$P_w = t^2 k\, C_3\, C_4\, C_{12} \{1350 - 1.73\,(D/t)\} \times$
	     $\times \{1 + 0.01/(N/t)\}^*$

Single load or reaction $c > 1.5\,D$ Load or reaction far from free end	Stiffened and unstiffened flanges $P_w = t^2 k\, C_1\, C_2\, C_{13} \{3350 - 4.6\,(D/t)\} \times$ $\times \{1 + 0.007\,(N/t)\}\dagger$
Two opposite loads or reactions $e < 1.5\,D$ $c < 1.5\,D$ Loads or reactions near or at free end	Stiffened and unstiffened flanges $P_w = t^2 k\, C_3\, C_4\, C_{12} \{1520 - 3.57\,(D/t)\} \times$ $\times \{1 + 0.01\,(N/t)\}$
Two opposite loads or reactions $e < 1.5\,D$ $c > 1.5\,D$ Loads or reactions far from free end	Stiffened and unstiffened flanges $P_w = t^2 k\, C_1\, C_2\, C_{12} \{4800 - 14\,(D/t)\} \times$ $\times \{1 + 0.0013\,(N/t)\}$

*When $N/t > 60$, the factor $\{1 + 0.01\,(N/t)\}$ may be increased to $(0.71 + 0.015\,(N/t))$.

†When $N/t > 60$, the factor $\{1 + 0.007\,(N/t)\}$ may be increased to $(0.75 + 0.011\,(N/t))$.

NOTE. In this table P_w represents the total load or reaction for one solid web connecting top and bottom flanges. For beams with two or more such adjacent webs P_w should be determined for each individual web and the results added to obtain the total crushing load.

Table 2.3. I-beams and beams with restraint against web rotation

Type and position of loadings	Total web resistance, P_w
Single load $c \leqslant 1.5\,D$ Load or reaction near or at free end	Stiffened and unstiffened flanges $P_w = t^2\,C_7\,p_y\,\{8.8 + 1.11\,(N/t)^{1/2}\}$
Single load or reaction $c > 1.5\,D$ Load or reaction far from free end	Stiffened and unstiffened flanges $P_w = t^2\,C_5\,C_6\,p_y\,\{13.2 + 1.63\,(N/t)^{1/2}\}$
Two opposite loads or reactions $e < 1.5\,D$ $c \leqslant 1.5\,D$ Loads or reactions near or at free end	Stiffened and unstiffened flanges $P_w = t^2\,C_{10}\,C_{11}\,p_y\,\{8.8 + 1.11\,(N/t)^{1/2}\}$
Two opposite loads or reactions $e < 1.5\,D$ $c > 1.5\,D$ Loads or reactions far from free end	Stiffened and unstiffened flanges $P_w = t^2\,C_8\,C_9\,p_y\,\{13.2 + 1.63\,(N/t)^{1/2}\}$

NOTE. In this table P_w represents the total load or reaction for one solid web connecting top and bottom flanges. For beams with two or more such adjacent webs P_w should be determined for each individual web and the results added to obtain the total crushing load.

65

2.4.2. A.I.S.I. [11,26,27,28]

AISI (American Iron and Steel Institute) design specifications reviewed in this subchapter are based on the AISI Specification for the design of cold-formed steel structural members 1980, 1986 and proposed design recommendations as stated in references 11 and 26. The AISI research and design rules also formed the basis of the BS 5950 Part 5 1987 design rules for web crushing. The specifications are also applied for two categories of beam, that is, beam having single unreinforced webs and I-beam having unreinforced webs with a high degree of restraint against rotation of webs. The loading conditions are also divided into four categories and they are illustrated in Figure 2.47. According to the figure, the four categories of loading conditions can be explained as follows :

- End one-flange loading (EOF) : e > 1.5 h and z < 1.5 h

- Interior one-flange loading (IOF) : e > 1.5 h and z ≥ 1.5 h

- End two-flange loading (ETF) : e ≤ 1.5 h and z < 1.5 h

- Interior two-flange loading (ITF) : e ≤ 1.5 h and z ≥ 1.5 h

Where h : Clear distance between flanges measured along the plane of the web (in).

It has been reported in reference 11 and 26 that the present available design criteria are not suitable for high strength materials with yield strengths exceeding 80 ksi. In fact many types of high strength steels with yield strengths from 80 to 190 ksi are

now used for automotive structural components, so that it is necessary to develop additional design criteria for the use of a broader range of high strength steels in automotive structures. Results of developing the new design criteria have been reported in reference 11 and 26 and they can be briefly explained as follows :

1. Concentrated loads or reactions.

The ultimate strengths of unreinforced beam webs subjected to concentrated loads or reactions can be estimated by using the equations in table 2.4 for beams having single unreinforced webs and in table 2.5 for I-beams with flanges connected to bearing plates. The equations are applicable for beams with $F_y \le$ 190 ksi; $h/t \le$ 200; $N/t \le$ 100; $N/h \le 2.5$ and $R/t \le 10$. The design equations for web crippling listed in tables 2.4 and 2.5 are categorized into nine classes depending on the values of e and z (Figures 2.48 and 2.49). The Symbols used in tables 4 and 5 have the following definitions.

e : Clear distance between edges of the adjacent opposite bearing plates

  (in). In the case of interior concentrated load shown in Figure 2.49, e

  should be taken as the smaller value of e_1 and e_2.

z : Distance between the edge of the bearing plate to the near end of the

  beam (in).

z_1 : Distance between the edge of the bearing plate to the far end of the

  beam (in).

F_y : Yield strength of the web (ksi).

67

h : Clear distance between flanges measured along the plane of web (in).

N : Actual length of bearing (in).

P_c : Governing ultimate web crippling load per web (kips).

P_{cb} : Web crippling load caused by buckling per web (kips).

P_{cy} : Web crippling load caused by bearing per web (kips).

R : Inside bend radius (in).

t : Web thickness (in).

Θ : Angle between the plane of web and the plane of bearing surface $\geq 45^\circ$ but

    no more than 90°.

C_{11} : $1 + 0.0122(N/t) \leq 2.22$; C_{12} : $1 + 0.217(N/t)^{0.5} \leq 3.17$

C_{21} : $1 - 0.247(R/t) \geq 0.32$; C_{22} : $1 - 0.0814(R/t) \geq 0.43$

C_{32} : $1 + 2.4(N/h) \leq 1.96$; C_{33} : $1 + 0.54(N/h) \leq 1.41$

C_{34} : $1 + 0.729(N/h) \leq 1.30$; C_{36} : $1 + 1.318(N/h) \leq 1.53$

C_{37} : $1 + 1.262(N/h)^{1.5} \leq 1.82$; C_{38} : $1 + 4(N/h)^3 \leq 2.69$

C_{41} : $1 - 0.00348(h/t) \geq 0.32$; C_{42} : $1 - 0.00170(h/t) \leq 0.81$

C_{43} : $1 - 0.00245(h/t) \geq 0.51$; C_{44} : $1 - 0.0000141(h/t)^2 \geq 0.44$

C_{45} : $1 - 0.00118(h/t) \leq 0.82$; C_{46} : $1 - 0.000471(h/t) \leq 0.95$

C_{47} : $1 - 0.0017(h/t) \geq 0.66$; C_{48} : $1 - 0.0060(h/t) \geq 0.46$

C_{51} : $1 - 0.298(e/h) \geq 0.52$; C_{52} : $1 - 0.120(e/h) \geq 0.40$

C_{55} : $1 - 0.233(e/h) \geq 0.58$; C_{64} : $1 + 4.547(z/h) \leq 7.82$

C_{68} : $1 + 0.109(z/h) \leq 1.22$; C_{73} : $1 + 0.56(z_1/h) \leq 1.98$

2. Combined bending and web crippling.

Unreinforced flat webs of shapes subjected to a combination of bending and reaction or concentrated load shall be designed to meet the following requirements.

a. Shapes having single webs :

$$\frac{M}{M_u} + 1.10 \frac{P_{mc}}{P_{cy}} \leq 1.42 \quad \ldots\ldots\ldots\ldots \quad (2.4.3)$$

Where :

M : Applied bending moment at or immediately adjacent to the point of application of the concentrated load or reaction P_{mc} (kip-in).

M_u : Ultimate bending moment permitted if bending moment only exists (kip-in).

P_{mc} : Concentrated load or reaction in the presence of bending moment (kips).

P_{cy} : Concentrated load or reaction in the absence of bending moment (kips) determined from table 2.4 for $e \geq 0.5h$ case 2.

The value of P_{mc} determined from equation 2.4.3 should not be greater than P_{cb} calculated from table 2.4 for $e \geq 0.5h$ case 2.

b. I-beams :

$$\frac{M}{M_u} + 1.07 \frac{P_{mc}}{P_{cy}} \leq 1.28 \quad \ldots\ldots\ldots \quad (2.4.4)$$

P_{cy} should be determined from table 2.5 for $e \geq 0.5h$ case 2. P_{mc} obtained from

69

equation 2.4.4 should not be greater than P_{cb} calculated from table 2.5 for $e \geq 0.5h$

case 2. M and M_u have the same definitions as those of shapes having single webs.

Table 2.4. (Shapes having single unreinforced webs)

e ≥ 0.5 h	1. $z = 0$; $(P_c)_1$ is the smaller of P_{cy} or P_{cb} where : $P_{cy} = 9.9 \ t^2 \ F_y \ C_{11} \ C_{21} \ (\sin \Theta)$ $P_{cb} = 0.047 \ E \ t^2 \ C_{41} \ C_{51} \ (\sin \Theta)$
	2. $z \geq 0.5h$; $(P_c)_2$ is the smaller of P_{cy} or P_{cb} where : $P_{cy} = 7.80 \ t^2 \ F_y \ C_{12} \ C_{22} \ (\sin \Theta)$ $P_{cb} = 0.028 \ E \ t^2 \ C_{32} \ C_{42} \ C_{52} \ (\sin \Theta)$
	3. $0 < z < 0.5h$; $(P_c)_3 = (P_c)_1 + \{(P_c)_2 - (P_c)_1\} \ (z/0.5h)$
e = 0	4. $z = 0$; $(P_c)_4 = P_{cb}$ where : $P_{cb} = 0.011 \ E \ t^2 \ C_{33} \ C_{43} \ C_{73} \ (\sin \Theta)$
	5. $z \geq 0.5h$; $(P_c)_5$ is the smaller of P_{cy} or P_{cb} where : $P_{cy} = 7.8 \ t^2 \ F_y \ C_{12} \ C_{22} \ (\sin \Theta)$ $P_{cb} = 0.0041 \ E \ t^2 \ C_{34} \ C_{44} \ C_{64} \ (\sin \Theta)$

Table 2.4. (Shapes having single unreinforced webs)

0 < e <0.5h	6. $0 < z < 0.5h$; $(P_c)_6 = (P_c)_4 + \{(P_c)_5 - (P_c)_4\}$ $(z/0.5h)$
	7. $z = 0$; $(P_c)_7 = (P_c)_4 + \{(P_c)_1 - (P_c)_4\}$ $(e/0.5h)$
	8. $z \geq 0.5h$; $(P_c)_8 = (P_c)_5 + \{(P_c)_2 - (P_c)_5\}$ $(e/0.5h)$
	9. $0 < z < 0.5h$; $(P_c)_9 = (P_c)_6 + \{(P_c)_3 - (P_c)_6\}$ $(e/0.5h)$

Table 2.5. (I-Beams with unreinforced webs)

e $\geq$ 0.5 h	1. $z = 0$; $(P_c)_1 = P_{cb}$ where : $P_{cb} = 0.063\ E\ t^2\ C_{45}\ C_{55}$
	2. $z \geq 0.5h$; $(P_c)_2$ is the smaller of P_{cy} or P_{cb} where : $P_{cy} = 15\ t^2\ F_y\ C_{12}$ $P_{cb} = 0.032\ E\ t^2\ C_{36}\ C_{46}$
	3. $0 < z < 0.5h$; $(P_c)_3 = (P_c)_1 + \{(P_c)_2 - (P_c)_1\}$ $(z/0.5h)$

71

Table 2.5. (I-Beams with unreinforced webs)

$e = 0$	4. $z = 0$; $(P_c)_4 = P_{cb}$ where : $$P_{cb} = 0.015 \, E \, t^2 \, C_{37} \, C_{47}$$
	5. $z \geq 0.5h$; $(P_c)_5$ is the smaller of P_{cy} or P_{cb} where : $$P_{cy} = 15 \, t^2 \, F_y \, C_{12}$$ $$P_{cb} = 0.051 \, E \, t^2 \, C_{38} \, C_{48} \, C_{68}$$
$0 < e < 0.5h$	6. $0 < z < 0.5h$; $(P_c)_6 = (P_c)_4 + \{(P_c)_5 - (P_c)_4\} \, (z/0.5h)$
	7. $z = 0$; $(P_c)_7 = (P_c)_4 + \{(P_c)_1 - (P_c)_4\} \, (e/0.5h)$
	8. $z \geq 0.5h$; $(P_c)_8 = (P_c)_5 + \{(P_c)_2 - (P_c)_5\} \, (e/0.5h)$
	9. $0 < z < 0.5h$; $(P_c)_9 = (P_c)_6 + \{(P_c)_3 - (P_c)_6\} \, (e/0.5h)$

Figure 2.47. Categories of loading conditions for web crippling
in AISI 1980 and 1986.
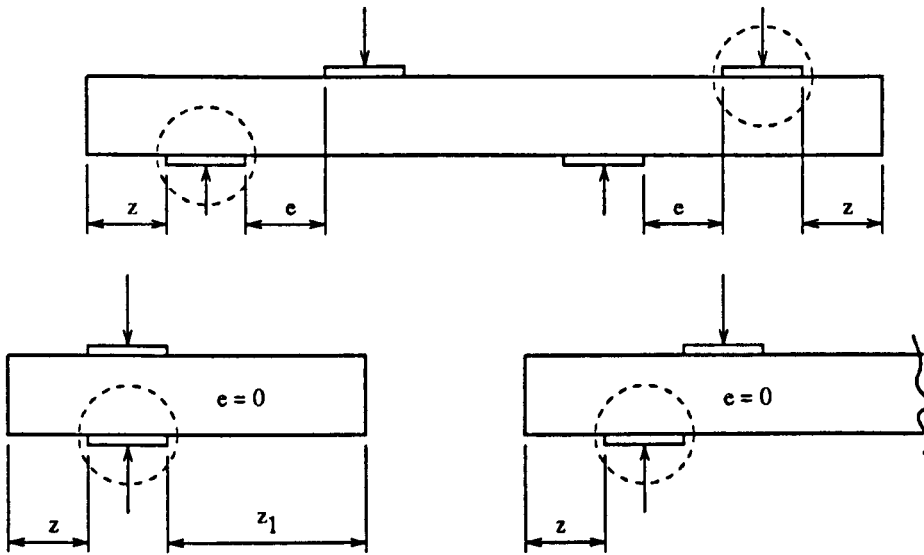
Figure 2.48. Definitions of e and z for reactions and concentrated loads.
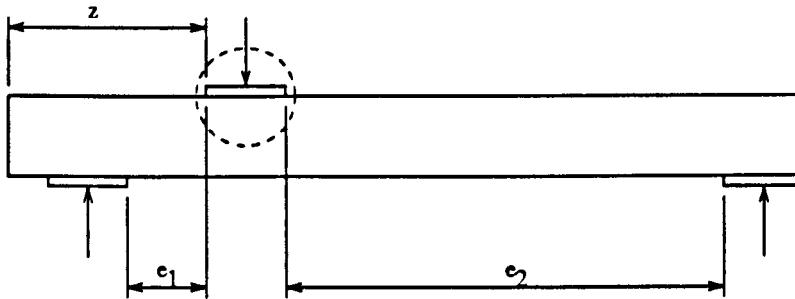
Figure 2.49. Definitions of e and z for Interior Concentrated Loads.

2.4.3. European Recommendations 1987. [29]

This recommendation is concerned with structural elements and frames for building and civil engineering and related structures which are cold-formed by processes such as cold-forming or press-braking. Design specifications for web crippling are discussed in R.4.4.2 of the European Recommendations. According to R.4.4.2 the conditions of loading are divided into the following categories :

74

- The first category is for the loads such as end supports of beams, loads near the end of a cantilever and loads applied so close to a support so that the distance from the support to the nearest edges of the loads, measured parallel to the beam axis, is less than 1.5 h_w .

- The second category is for intermediate supports and loads situated more than 1.5 h_w from a support or an end of a cantilever.

The recommendation classifies the beams according to the position of webs with regard to the load direction, namely, webs eccentric to the load direction (such as hat sections and channels) and webs concentric to the load direction (such as I-beams and similar). In order to avoid local buckling and crippling of a flat web under a concentrated load or a support reaction, the design value of the load transmitted locally must not exceed the value of design strength with respect to web crippling. This value can be calculated by using the following formulae which are valid only for $h_w/t \leq 200$.

1. Webs eccentric to the direction (Hat sections and channels).

   a. The first category :

$$R_d = 0.057 \, t^2 \, \sqrt{f_{ty} E} \, (1 - 0.1\sqrt{\frac{r}{t}}) \, (0.5 + \sqrt{\frac{0.02 \, l_a}{t}})$$
$$x \, (2.4 + (\frac{\theta}{90})^2) \, \text{..........} \, (2.4.5)$$

   b. The second category :

$$R_d = 0.114 \, t^2 \, \sqrt{f_{ty} \, E} \, (1 - 0.1\sqrt{\frac{r}{t}}) \, (0.5 + \sqrt{\frac{0.02 \, l_a}{t}})$$

$$x \, (2.4 + (\frac{\theta}{90})^2) \, \text{..............} \, (2.4.6)$$

2. Webs concentric to the load direction (I-beams and similar).

a. The first category :

$$R_d = t^2 \, f_{ty} \, (7.4 + 0.93 \, \sqrt{\frac{l_a}{t}}) \, \text{.............} \, (2.4.7)$$

b. The second category :

$$R_d = t^2 \, f_{ty} \, (11.1 + 2.41 \, \sqrt{\frac{l_a}{t}}) \, \text{...............} \, (2.4.8)$$

Where :

r   : Inner radius < 7 x the sheet thickness t.

l_a : Bearing length ; $l_a/h_w \leq 3.5$; $l_a/t \leq 210$.

Θ : Web inclination.

f_{ty} : The design yield stress which is equal to the yield stress of the basic

material (f_{yb}).

If the web is subjected to combined bending moment and concentrated load or

support reaction, the following condition should be satisfied :

76

$$\frac{M}{M_d} \leq 1 \qquad \text{when} \quad \frac{R}{R_d} \leq 0.25 \quad \dots\dots\dots (2.4.9)$$

$$\frac{M}{M_d} + \frac{R}{R_d} \leq 1.25 \qquad \text{when} \quad 0.25 < \frac{R}{R_d} \leq 1 \quad \dots\dots\dots (2.4.10)$$

Where :

M and R : Bending moment and support reaction or concentrated load.

R_d : Design strength with respect to crippling calculated from the

     formulae 2.4.5 - 2.4.8.

M_d : Design strength with respect to bending moment determined

     according to R 4.2.

In R 4.2, the design strength with respect to bending moment M_d can be obtained

from the following relationship.

$$M_d = f_{ty} \ W_{ef} \quad \dots\dots\dots\dots (2.4.11)$$

Where :

f_{ty} : Design value of yield stress in which according to R 2.5.1, f_{ty} may be

   taken from the lowest value between the yield stress of basic

   material (f_{tb}) and (1/1.1) x ultimate tensile stress.

W_{ef} : Section modulus of the effective cross section.

The effective web portion of flexural members may be determined on the basis of the

ratio of edge stresses (ψ) obtained by assuming the compression flange reduced but

the web being effective. Figure 2.50 is an example of determining the effective cross

section of a thin-walled flexural member. In determining the effective cross section of flexural members, effects of shear lag should be taken into account when the ratio of the span length L to width of compression element b is less than 20.
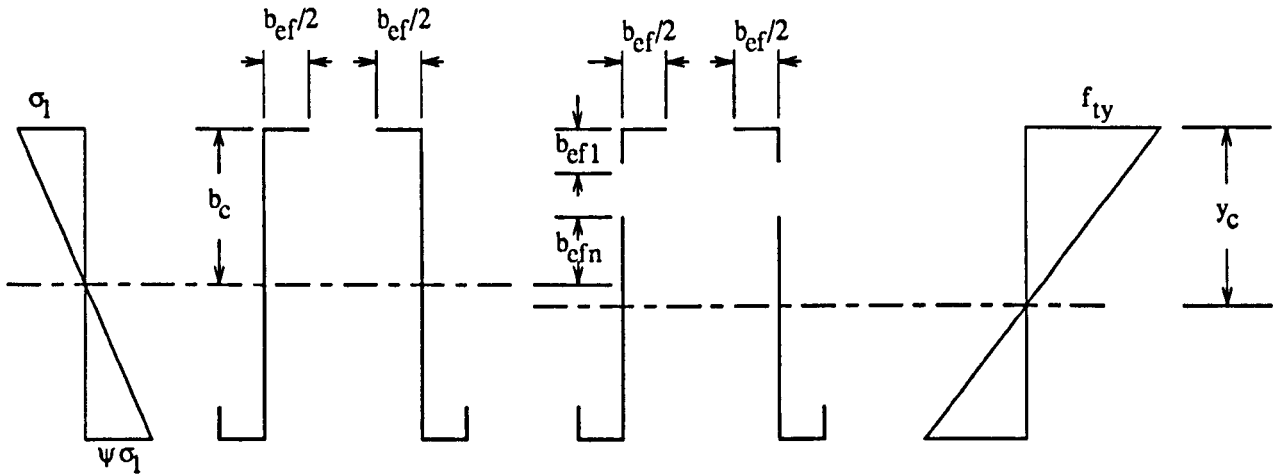
Figure 2.50. Example of determining the effective cross-section of thin-walled flexural members.

2.5. AUTHOR'S CONCLUSIONS.

On the basis of the literature of web crippling reviewed herein, the author believes that it is still complicated to obtain the expression of web crippling resistance from a purely theoretical analysis. Most of the ultimate web crippling loads are estimated using the formulae which are derived from experimental results. The web crippling is actually a kind of structural failure which is caused by a concentrated load and this

78

failure takes place locally at the point of loading. The investigations carried out by

M.Z. Khan and A.C. Walker have indicated that a structure under localized edge

loading does not collapse at the critical buckling load. Thus it can be concluded that

evaluation of the failure load requires examination of behaviour after buckling.

The field of investigation performed by Murray, Walker, Khoo, Davies and Kemp

provides the basic analysis for predicting the failure load of a structure using plastic

mechanisms. The analysis of the plastic mechanisms is based on the approximate

yield line theory. Failure mechanisms of web crippling have also been studied by

Bakker so that it will be possible to use the theory of plastic mechanisms for

analysing the ultimate web crippling load. The results presented in Figure 2.39

indicate that for plain channel sections subjected to compression loads, the analysis

of plastic mechanisms tends to underestimate the experimental ultimate loads for a

given deflection at failure. The failure mechanisms of these channel sections are

located far from the point of loading. Because web crippling failure occurs right

under the point of applied loads, it is therefore necessary to develop a plastic-

mechanism model for analysing the ultimate web crippling load. This will be

attempted by the author through this research program.

BS 5950, AISI and European recommendations have similar definitions concerning

the loading conditions,i.e. loads or reactions applied far from free end and loads or

reactions applied near or at free end. The only difference in defining the loading

conditions is that European recommendations do not distinguish between one-flange loading and two-flange loading. All loading conditions in the European recommendations are categorized only into the first category (End loading) and the second category (Intermediate loading). These above three design specifications are only applicable to analyse the web crippling resistance of sections without web perforations. Almost all parameters influencing web crippling resistance as stated in the research findings of Cornell University are taken into account by BS 5950 and European recommendations except the web slenderness which is not considered by European recommendations. In the case of proposed design recommendations as expressed in references 11 and 26, the web slenderness has significant effects on the ultimate load caused by buckling failure rather than on the one caused by bearing failure.

CHAPTER 3

EXPERIMENTAL INVESTIGATIONS

3.1. GENERAL.

The experimental investigations were carried out to study the influence of various loading conditions and parameters such as the bearing length ratio (n/t), the web slenderness ratio (hw/t) and the inside bend radius ratio (r/t) on the web crippling strength of cold-formed plain channel steel section beams. The loading conditions used in testing the specimens were similar to those specified by AISI 1986 in Figure 1.3 (Chapter 1) and in particular the tests under interior one-flange loading (IOF) were carried out for many specimens with various dimensions and bearing lengths. The prime reason for performing the IOF tests for many specimens was to obtain the necessary information for developing and verifying the plastic mechanism theory used to analyse the web crippling strength of the specimens under the IOF loading condition in this research program.

All of the loading conditions were applied statically to the specimens and deformed parts of the specimens under the applied loads were measured in the tests. The experiments were designed in such a way that the load-deformation behaviour of each specimen could be recorded directly during the tests. The web crippling strength of the specimens obtained from experiments was determined on the basis of maximum value of test loads which could be carried by the specimens and this value was measured from experimental load-deformation diagrams as well as from the test machine.

In the tests, reactions of the test loads were not transfered through bearing plates such as is indicated in the most publications on web crippling tests, but the reactions were transfered through pin supports. Test loads were transfered from the test machine to the specimens through a loading block. Besides transfering loads, the loading block and the supports were also designed to protect the specimens from being twisted due to the off-set position of the test loads with respect to the shear centre of the specimens.

In this chapter, experimental results are presented in the form of tables as well as diagrams of experimental load versus parameters studied. Typical examples of experimental load-deformation diagrams are also presented in order to know the characteristics of the specimens tested under each loading condition. Before carrying out the web crippling tests, tensile tests of the basic materials used to manufacture plain channel section beam specimens were also performed to identify necessary mechanical properties of the basic materials. These properties were needed to analyse theoretically the strength of the specimens under web crippling before performing the web crippling tests.

3.2. TEST PROGRAMS.

The test programs were divided into two steps, where the first step was material tests and the second one was the web crippling tests. The material tests were to carry out

tensile tests of basic materials which were in the form of steel sheets. The procedure

of carrying out the tensile tests followed BS 18 Part 3, 1971. The web crippling tests

were designed to study the strength of plain channel steel section beam specimens

subjected to combined actions of web crippling and bending as well as web crippling

only.

The first goal of the web crippling tests was achieved by testing the specimens under

the Interior one-flange loading (IOF). The second goal was accomplished by testing

the specimens under the End one-flange loading (EOF), End two-flange loading

(ETF) and Interior two-flange loading (ITF). In the case of the IOF loading, the tests

were carried out for specimens with various span lengths. The purpose of varying the

span lengths was to study the influence of various bending moments on the ultimate

web crippling loads of the specimens under the mid-span loading.

The specimens for web crippling tests were designed and manufactured according to

the loading conditions which would be applied to them. Their quantities were more

than 200 test specimens and most of them were specimens for the tests under the

mid-span loading. In order to study the influence of bearing length on the ultimate

web crippling loads, five loading blocks of different widths were used to transfer

applied loads onto the specimens. The web crippling tests were first carried out for

the mid-span or IOF loading and followed by EOF, ETF and ITF loading conditions.

All web crippling tests were employed on the same testing machine and two different

directions of web deformation with their corresponding test loads were continuously

measured during the tests.

3.3. MATERIAL TESTS.

The material tests were aimed at testing the mechanical properties of each group of

steel sheets used to manufacture specimens for web crippling tests. The sheets were

made of galvanized steels and the size of each sheet was 1250 mm x 1250 mm with

two different thickness, i.e. t = 1 mm and t = 1.1 mm. The tensile tests were carried

out according to BS 18 Part 3, 1971 where the design of tensile test specimens is as

follows :
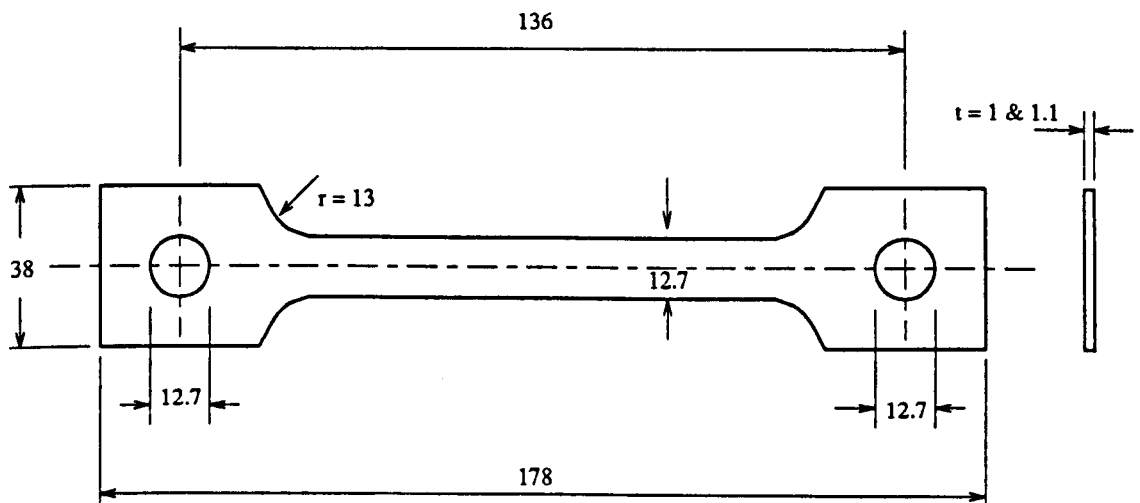
Figure 3.1. Tensile test specimen.

The above tensile test specimens were made from a small part of the sheets which was cut from along side of the galvanized steel sheet. Ten tensile test specimens were made for each series of tensile tests, in which these tests were divided into four series. The first and the fourth series were for specimens of 1.1 mm thick while the second and the third series were for specimens of 1 mm thick. The tensile tests were performed in two different machines, that is, a Universal fatigue testing machine Zwick rel 2061 and a Servohydraulic testing machine Avery Denison. The former machine was used for the first series and the latter one was for the other three series.

The tensile tests were carried out in the ambient temperature and load-extension curves were directly recorded during the tests. The extension of the specimen was measured using an electric extensometer which was affixed on the specimen at a gauge length of 50 mm. The increase of this extension was continuously measured up to the end of yielding process. The extensometer was no longer affixed on the specimen when the test load started to increase towards the maximum load until the specimen completely fractured. Load-extension curves were automatically plotted on a X-Y plotter during the tests. Figure 3.2 shows a typical load-extension curve obtained from the tensile test where it can be seen that during the strain hardening process the corresponding extension is not measured. From four series of the tensile tests, the average values of elastic modulus (E) are 196850 MPa (series 1), 195492 MPa (series 2), 212980 MPa (series 3) and 217302 MPa (series 4). The other mechanical properties are presented in the following table.

85
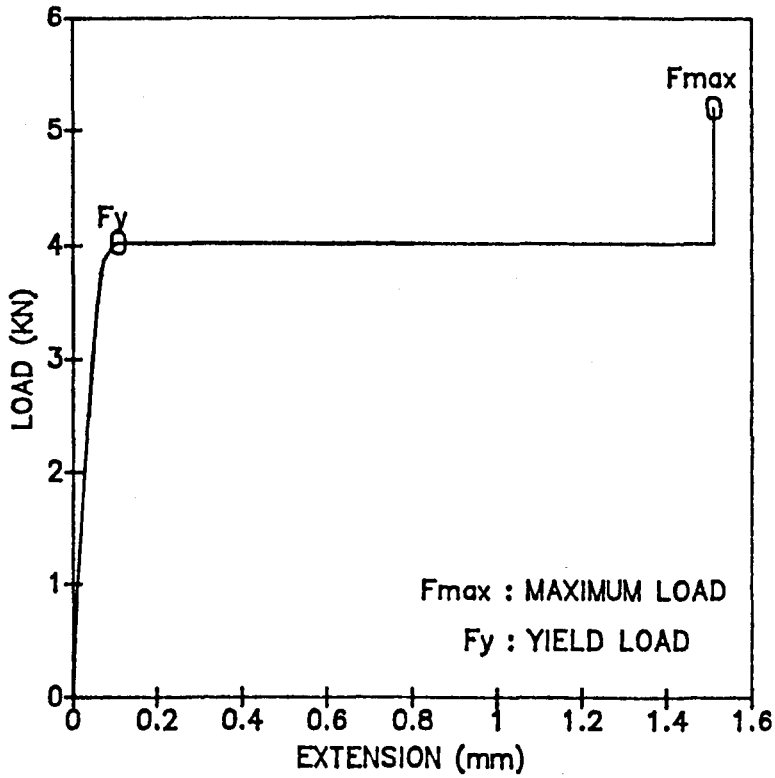
Figure 3.2. Load-extension curve.

The average values of mechanical properties obtained from four series of the tensile

tests are as follows :

SERIES	σ_y (MPa)	σ_{UTS} (MPa)	A (%)
1	$_{-18}\,303\,^{+26}$	$_{-20}\,387\,^{+19}$	$_{-2}\,30\,^{+3}$
2	$_{-14}\,307\,^{+7}$	$_{-5}\,374\,^{+9}$	$_{-4}\,29\,^{+1}$
3	$_{-14}\,320\,^{+13}$	$_{-12}\,388\,^{+7}$	$_{-1}\,31\,^{+1}$
4	$_{-10}\,328\,^{+8}$	$_{-3}\,398\,^{+3}$	$_{-1}\,33\,^{+1}$

± values indicate maximum and minimum deviations from the average value.

Where :

σ_y : Yield strength.

σ_{UTS} : Ultimate tensile strength.

A (%) : Percentage of elongation = $(l_1 - l_o)/l_o$ x 100%.

l_1 : Gauge length after fracture.

l_o : Initial gauge length (= 50 mm).

On the basis of the above properties, the thickness which is less than 3 mm and the

British Standard for galvanized steels BS 2989 : 1982, the material can be designated

by BS 2989 Sheet Z 28. This Standard also indicates that from a cast analysis, the

chemical compositions of this type of material are as follows :

GRADE	C_{max} (%)	Mn_{max} (%)	S_{max} (%)
28	0.20	0.80	0.04

3.4. TEST SPECIMEN.

Specimens used for web crippling tests in this research program were in the form of

plain channel section beams and they were fabricated from the galvanized steel BS

2989 Sheet Z 28 in the cold state. The quantity of the specimens was 220 specimens and they were fabricated with different dimensions. All measured dimensions of the specimens were properly documented and they can be seen in appendix A. Of 220 specimens tested, 158 specimens were designed for the tests of combined web crippling and bending moment while the rest of them were designed for the tests of web crippling only.

Figure 3.3 shows the design of specimens for web crippling tests with their pin holes of 15 mm in diameter. The first type of specimen (a) was used for the tests of combined web crippling and bending, whereas the second (b) and the third (c) types of specimen were used for the tests of web crippling only. In the case of the latter tests, the specimen (b) was for the EOF tests and the specimen (c) was for the ETF as well as ITF tests. In order to identify and distinguish them, they were therefore designated in different groups. Their designations were initiated with a capital letter H or S and followed by their individual numbers which were based on their nominal web depths.

In fabricating the specimens, the galvanized steel sheets were first cut to the required dimensions by using BESCO 'TRUECUT' GUILLIOTINE MODEL 4/08.MK.2. The cut sheets were marked with lines and points as shown in Figure 3.4. The lines demarcated the positions to be folded and the points were the centres of pin hole. In cutting and marking the sheets, the edges of the cut sheets were made as square as

possible and the demarcation lines were drawn perpendicular to the edges of the cut sheets and parallel to each other.

The dimensions of B and D in Figure 3.4 were determined according to the nominal dimensions of flange width and distance between top and bottom flanges. The dimensions of B were equal to 30 and 40 mm, while the dimensions of D were equal to 60, 70, 80, 90 and 100 mm. The distance of two centres of pin hole (l) shown in the first cut sheet was dependent on variations of bending moment applied on the specimens in the IOF tests and it was chosen to be equal to 175, 230, 300, 350, 400, 450 and 500 mm.

Before folding the cut sheets into the shapes of specimen, the cut sheets were exactly drilled at the centres of pin hole using DRILLING MACHINE ARBOGA COLUMN TYPE. Afterwards the cut sheets were folded by using a CHICAGO BOX AND PAN BENDING MACHINE at their demarcation lines into the final shapes of the specimens. The straightness of web and flanges of each specimen was carefully inspected using a square angle in order to ensure that the angle between the web and the flanges was at right angle.
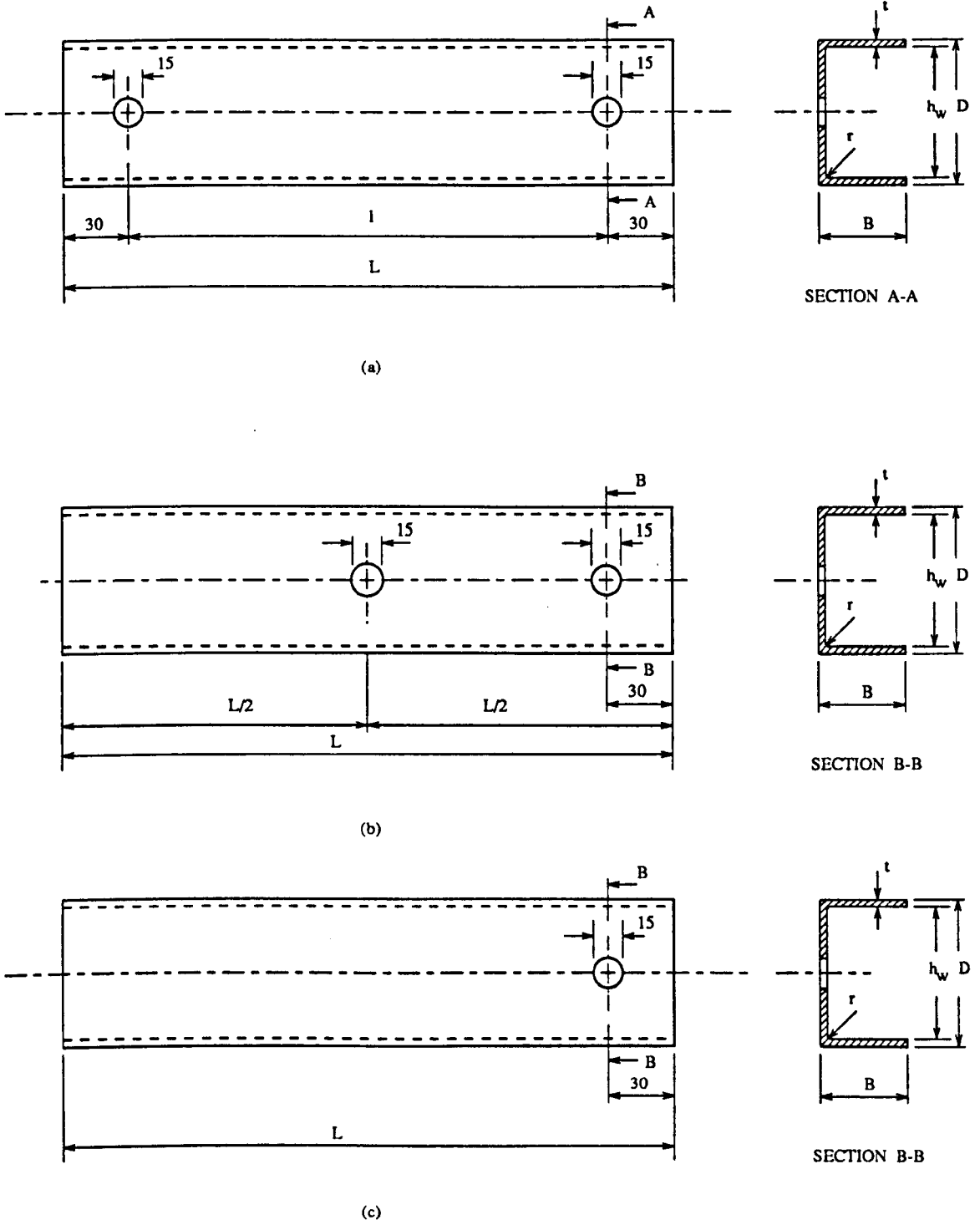
Figure 3.3. Design of test specimen.

90

FOR SPECIMEN UNDER IOF   FOR SPECIMEN UNDER EOF

FOR SPECIMEN UNDER ETF AND ITF

——— : DEMARCATION LINES   ● : CENTRES OF PIN HOLE
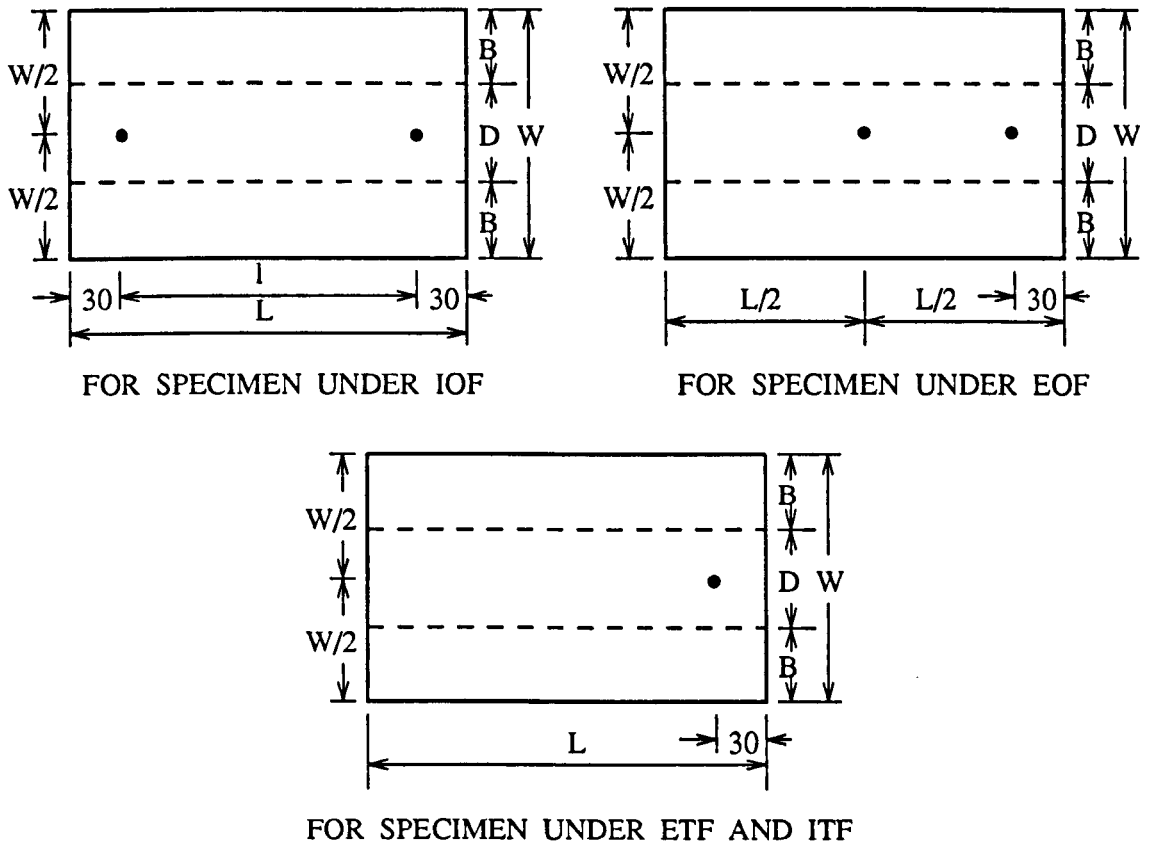
Figure 3.4. Cut sheets for fabricating test specimen.

3.5. TEST EQUIPMENT.

The equipment used in the web crippling test was as in the following lists.

1. TINIUS-OLSEN Electro Mechanical Testing Machine.

2. Test attachments which cover a test rig, supports and loading blocks.

3. Displacement transducers.

4. X - Y Plotters.

3.5.1. TINIUS-OLSEN ELECTRO MECHANICAL TESTING MACHINE.

In this investigation, the web crippling tests of the specimens were employed in a

TINIUS-OLSEN Electro Mechanical Testing Machine. It is annually calibrated by

Namas Test House (Bayliss Brown Limited) to BS 1610 : 11 : 85 and its maximum

capacity is 200000 lbs. This machine has four load ranges, so that it will be possible

to select appropriate test loads prior to the test execution. The test load is applied on

the specimens by lowering the crosshead of the machine and this movement is

activated by four electrically controlled power screws.

A photograph of the TINIUS-OLSEN machine used in this research program can be

seen in Figure 3.5. The test loads can be read from the load indicator scale shown in

the photograph where the scale is equipped by two load pointers. As the test is

running, the first pointer pushes the second one round clockwise the scale up to a

point at which the maximum load is attained. After that the first pointer moves

counter clockwise towards a scale corresponding to a zero load and the maximum

load can be easily read from the value indicated by the second pointer.

The rate of loading can be selected from the speed control dial and it is infinitely

variable within the speed range of the testing machine. In experiments, the testing

machine was normally run at low and constant speed except in the case of setting the

specimens or test rigs, the machine crosshead was lowered and raised at high speed.

This testing machine is also equipped with a graphic recorder which is able to plot load-deflection curves automatically during the tests. But this recorder was not used in this investigation and experimental load-deflection curves were plotted using X-Y plotters.
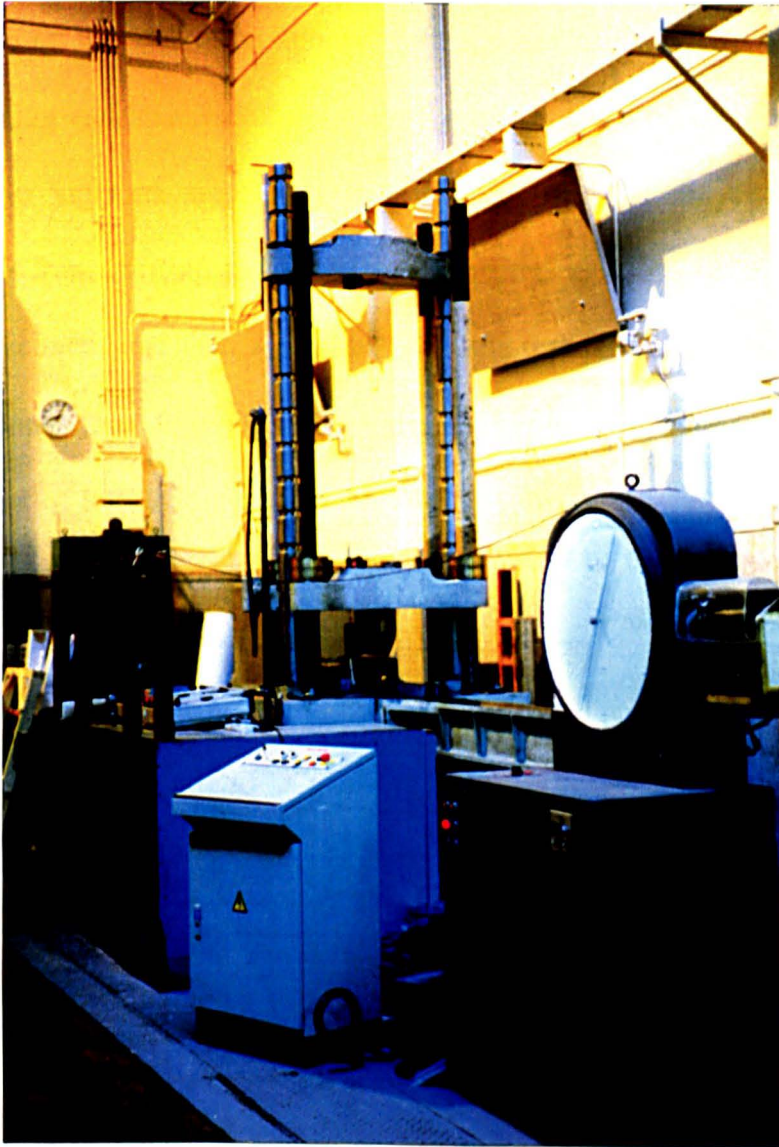
Figure 3.5. TINIUS-OLSEN testing machine.

93

3.5.2. TEST ATTACHMENTS.

Because the length of specimens was relatively short, it was therefore impossible to clamp the specimens direct to T-slots of the TINIUS-OLSEN machine. In order to be able to carry out the tests, it was necessary to make an attachment which could be used to fix the specimens onto the testing machine. The problem was then solved by designing and manufacturing a test rig which could be clamped direct to the T-slots. Two supports were also manufactured for the purpose of resisting the specimens from twisting and holding them on the test rig. The supports were pinned to the specimens and then assembled with the test rig through base plates by using bolted connections. Figure 3.6 illustrates the set-up of the specimens on the test rig for the test of IOF loading condition.
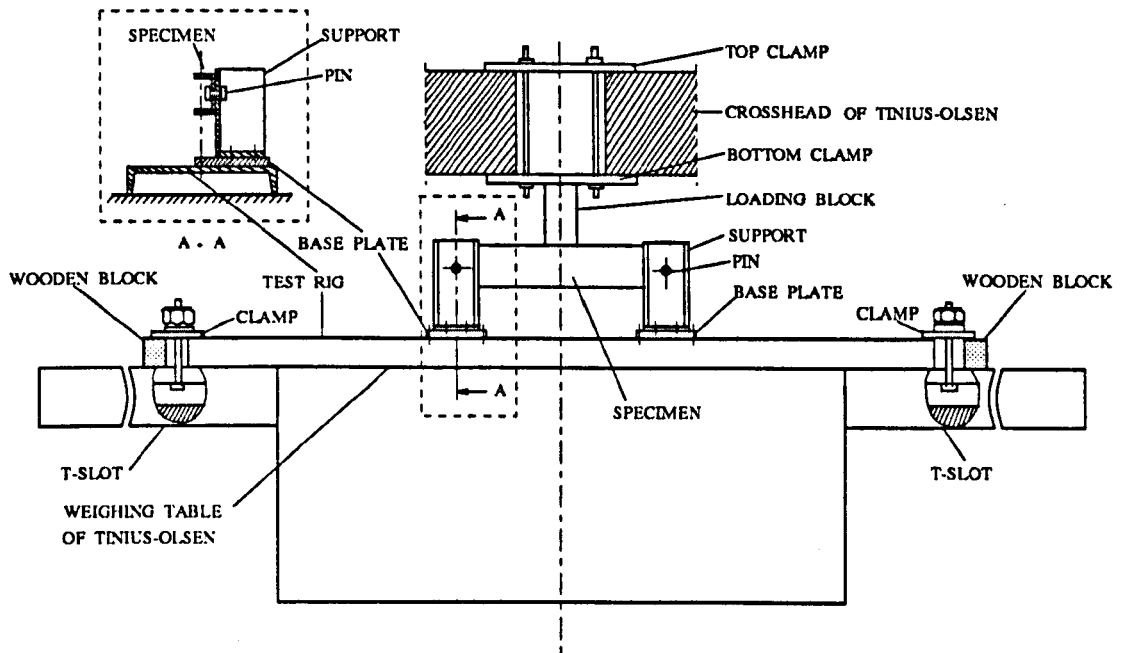
Figure 3.6. Set-up of specimen on the test rig.

94

Another set of attachments which was also manufactured was the loading blocks. These blocks were made of mild steel and basically designed to transfer test loads from the testing machine onto the specimens as well as to protect them from twisting. The loading blocks were bolted to the bottom clamp and fixed on the machine crosshead as shown in Figure 3.6. The design of the loading blocks can be seen in Figure 3.7, in which their dimensions of width (W) and thickness (B) are varied and the variations of W are intended to provide different load bearing lengths on the specimens in the experiments. The loading block (a) was used to transfer test loads from the Tinius-Olsen testing machine onto the specimens and the loading block (b) was used to carry reactions of the test loads in the tests of ETF as well as ITF.

W = 30, 35, 40, 45 and 50 mm
B = 50, 55, 60, 65 and 70 mm

(a)

W = 30, 40 and 50 mm

(b)
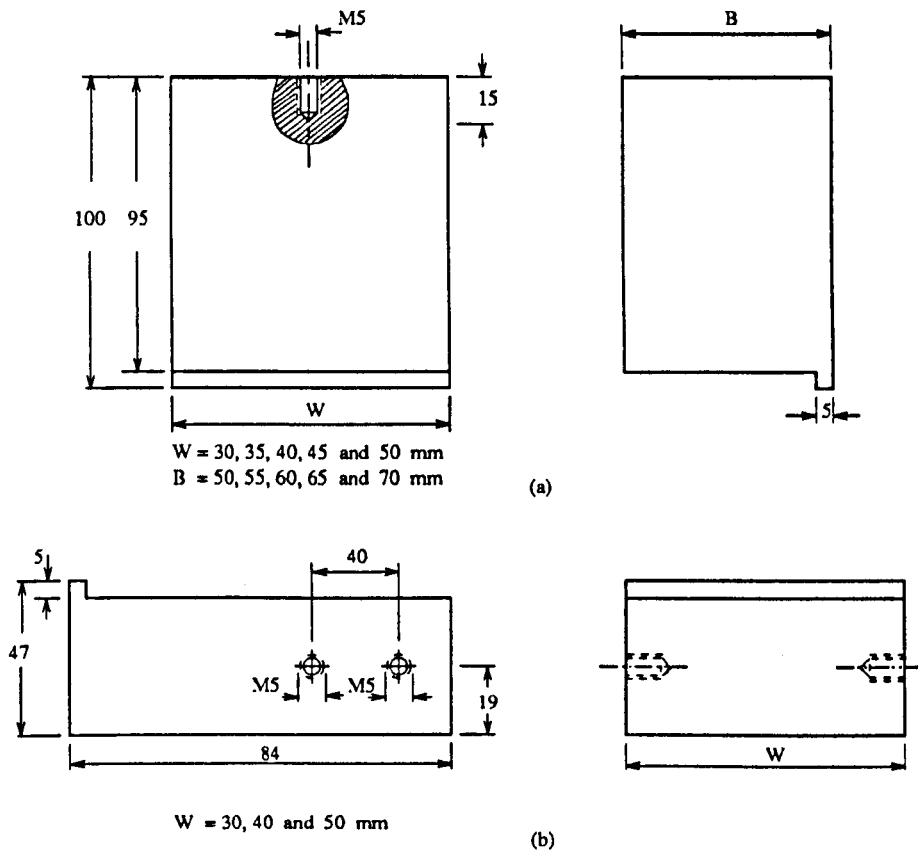
Figure 3.7. Design of loading blocks.

3.5.3. DISPLACEMENT TRANSDUCER.

Two transducers were used to measure the deflection of web of the specimens in the experiments. Each of the transducers has a stroke of 0 - 150 mm and its signal output was recorded by X-Y plotters. In order to ensure the accuracy of measuring the deflection of web, each of the transducers was carefully calibrated before using them in the experiments. One of the transducers was used to measure the vertical deflection of the web and the other was used to measure the lateral deflection of the web. The transducers were set up in such a way that as the web of the specimens deformed due to the action of test loads, the probe of each transducer was compressed towards its main housing. The changes of the probe displacement governed the signal output from the transducers and this signal was linearly proportional to the probe displacement.

3.5.4. X-Y PLOTTER.

Two X-Y plotters were used to plot load vs. deflection curves of the tested specimens, i.e. one plotter was to plot load vs. vertical deflection of web and the other one was to plot load vs. lateral deflection of web. Each of the plotters was connected to the displacement transducer and the load cell of the TINIUS-OLSEN testing machine, so that simultaneous signals of displacement and load could be received and recorded by the X-Y plotters throughout the experiments. Both of the

X-Y plotters have the following specifications.

Model Number   : Gould Series 60000

Recording area   : A3 size

Supply voltage   : 240 Volts A.C

Manufacturer   : Bryans Recorders Ltd.

3.6. WEB CRIPPLING TESTS.

In order to verify the results of the theoretical analyses presented in the following chapters, it was necessary to carry out web crippling tests of all designated specimens. These tests were accomplished in the TINIUS-OLSEN Electro Mechanical Testing Machine and they were divided into 5 test series. The first two series were the tests of combined web crippling and bending, while the last three series were the tests of web crippling only. More than 50% of the total number of specimen were tested under combined web crippling and bending (IOF), in which the first test series consisted of 132 specimens and the second test series consisted of 27 specimens. In the last three series of web crippling tests only, the rest of all specimens were tested under different loading conditions. The third series were the tests of 26 specimens under the EOF loading condition, while the fourth and the fifth series were the tests under the ETF and ITF loading conditions with 18 specimens for each of these series.

During the tests, vertical and horizontal (lateral) displacements of the web in all test

97

series were measured using displacement transducers. The transducer for measuring the vertical displacement of web was not directly affixed onto the web, but it was vertically affixed onto the crosshead of the TINIUS-OLSEN testing machine and the tip of its probe contacted a spacer block. As the crosshead moved downwards, the probe of the transducer was compressed by the spacer block towards its main housing and its displacement would be the same as the vertical displacement of the web under the loading point. In the case of lateral displacements of web, the transducer was horizontally affixed onto the weighing table of the TINIUS-OLSEN testing machine using a portable magnetic device and the tip of its probe touched the web at a point at which the maximum lateral deflection of web occured. The position of the maximum lateral deflection of the web could be approximately determined by testing a few samples of the specimen and observing their modes of web deformation at failure.

3.6.1. INTERIOR ONE-FLANGE LOADING (IOF) TESTS.

The IOF tests were performed by testing the specimens under three-point loading conditions where test loads were applied to the top flange of the specimens at their mid-spans and reactions of the test loads were carried by end pin supports. An illustration of this test arrangement can be seen in Figure 3.8 and this test arrangement causes the specimens to be subjected to combined actions of web crippling and bending moment. The ratio of maximum applied bending moment (M)

to the moment capacity (M_c) of the specimens was varied where the first test series were carried out with $M/M_c \geq 0.3$ and the second test series were for $M/M_c < 0.3$.

On the basis of nominal web depths (hw), the specimens were divided into 5 groups for the first test series and 3 groups for the second test series. The groups of specimen in the first test series consisted of specimens with hw = 60, 70, 80, 90, 100 mm and the second test series consisted of specimens with hw = 60, 80 and 100 mm. Each group of specimen were tested under different load bearing lengths (n), where the first test series used bearing lengths of 30, 35, 40, 45, 50 mm and the second test series used bearing lengths of 30, 40 and 50 mm.

Variations of applied bending moment were obtained by varying the distance between two end pin supports or the span lengths (l) of the specimens. In the first test series, the span lengths of specimen were 300, 350, 400, 450, 500 mm while in the second test series, the span lengths were 175, 230 and 300 mm. In order to know the consistency of results obtained from the tests, three to five specimens of the same web depth (hw) were tested under the same load bearing length (n). The maximum lateral deflection of the web was measured by fixing the tip of transducer probe at a point on the web which was located 15 mm (for test series 1) or 25 mm (for test series 2) underneath the load bearing length. The test loads were continuously applied to the specimens at a constant and low speed. As the test loads already decreased further from their maximum values attained, the tests were then stopped.
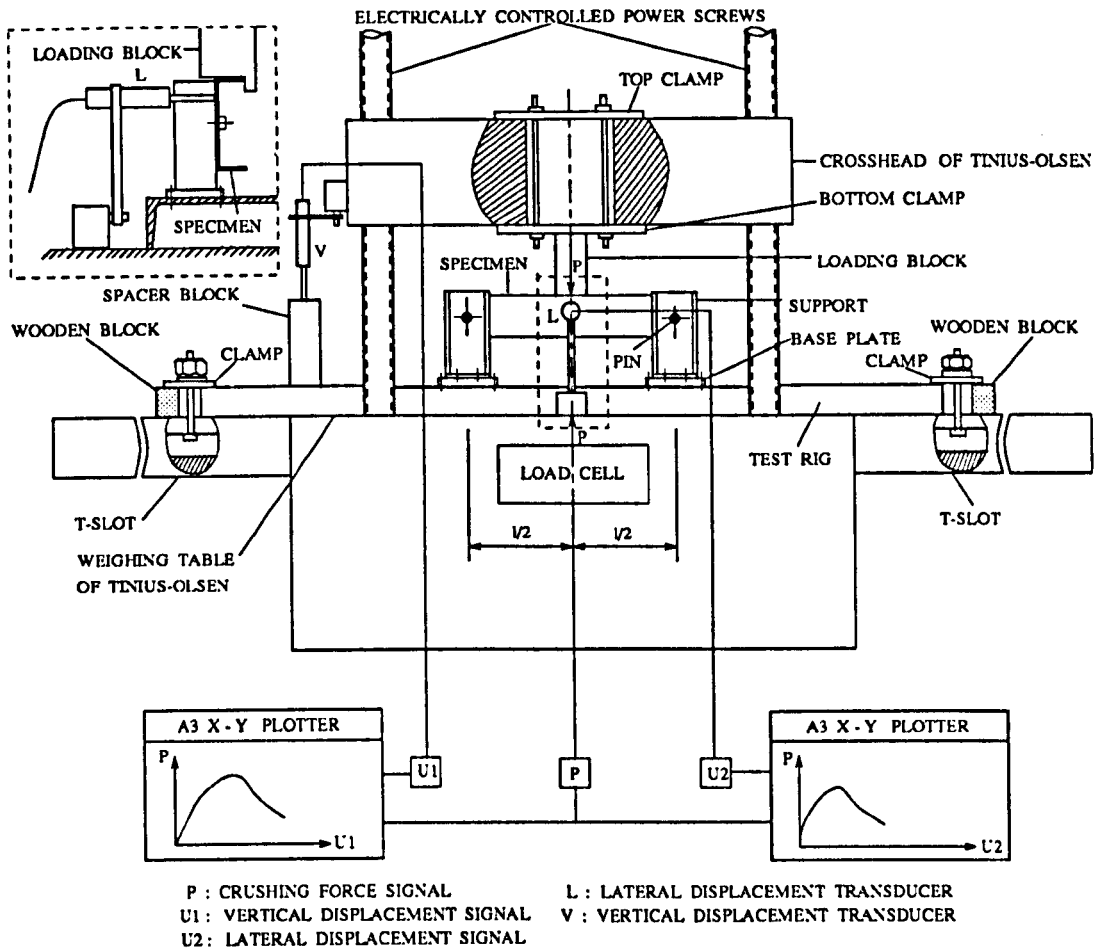
Figure 3.8. Test set-up of IOF loading condition.

3.6.2. END ONE-FLANGE LOADING (EOF) TESTS.

In the EOF tests, the specimens were still treated as three-point loading beams, but with a different test arrangement. One of end pin supports was shifted to the mid-span of the specimens and the other pin support was still located at the other end of

100

the specimen. Test loads were still applied to the top flange and exactly located at the free end of the specimens. Figure 3.9 indicates the test arrangement where this arrangement causes the bending moment at the point of loading to be negligible so that there is no interaction between concentrated load and bending moment. Thus, it is believed that the cause of failure of the specimens in this test arrangement is web crippling only.
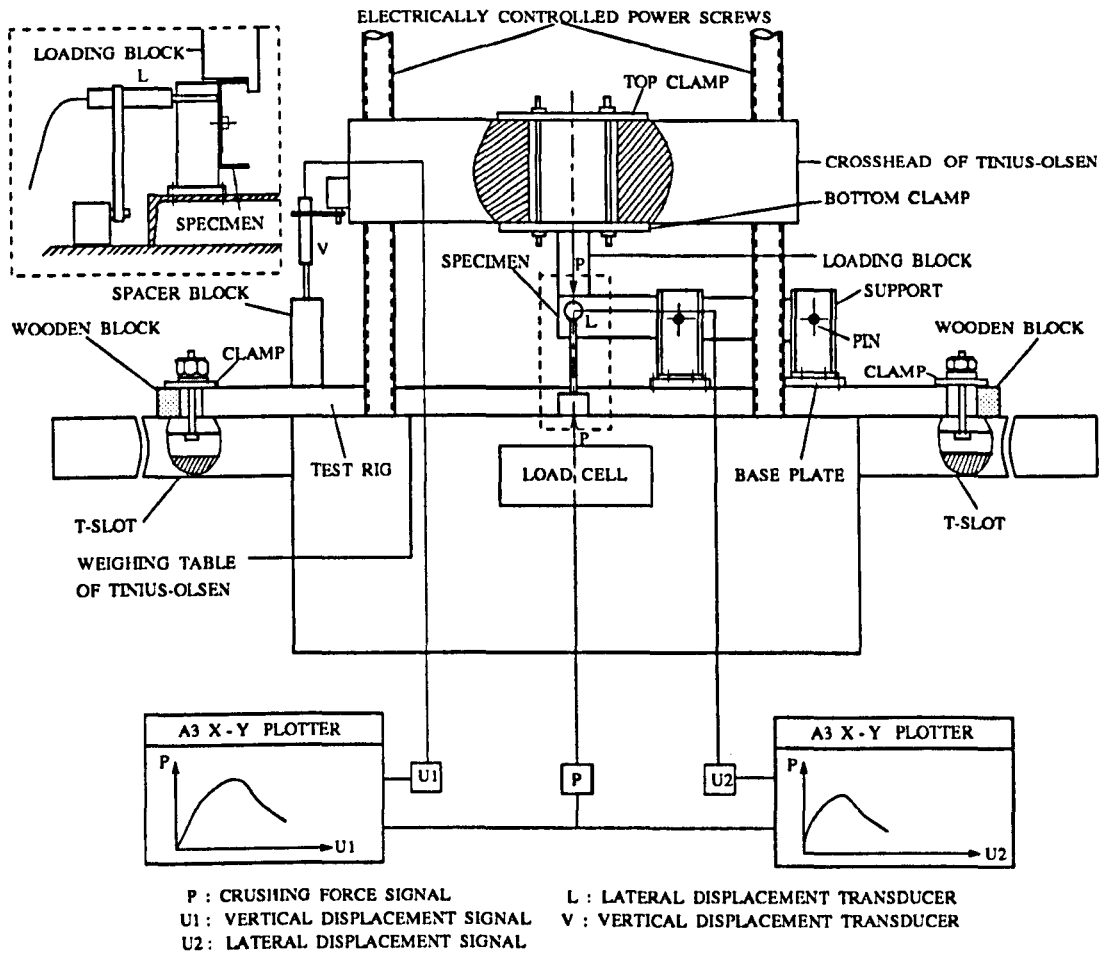
Figure 3.9. Test set-up of EOF loading condition.

The 26 specimens for the EOF tests were divided into 3 groups where each of the groups consisted of the specimens with the nominal web depths of 60, 80 and 100 mm. Each group of specimen were tested under the load bearing lengths (n) of 30, 40, 50 mm and the number of specimen from the same group tested under the same load bearing length was 3 specimens. The vertical and lateral deflections of the web were also measured using the same procedures as in the case of IOF tests. In measuring the lateral deflection of the web, the lateral displacement transducer was located about 30 mm underneath the load bearing length and at a distance of half load bearing length (n/2) from the free end of the specimens.

3.6.3. END TWO-FLANGE LOADING (ETF) TESTS.

The other tests of web crippling performed in this research program were the tests of End Two-Flange Loading. In these tests, the specimens were loaded on either side of their flanges and the test loads were located at one free end of the specimens. In order to maintain the specimens always in horizontal conditions, the other end of the specimens was connected to the pin support. As can be seen in Figure 3.10 that the top flange is subjected to the test load which is transfered through the loading block from the testing machine, while the bottom flange is subjected to the reaction of test load carried by the loading support. With reference to Figure 3.7, the loading block which transfers the test load onto the top flange is the loading block of type a and the loading support which carries the reaction of test load is the loading block of

102

type b. Thus, this test arrangement will cause the web of specimen to be crushed

from two opposite directions.
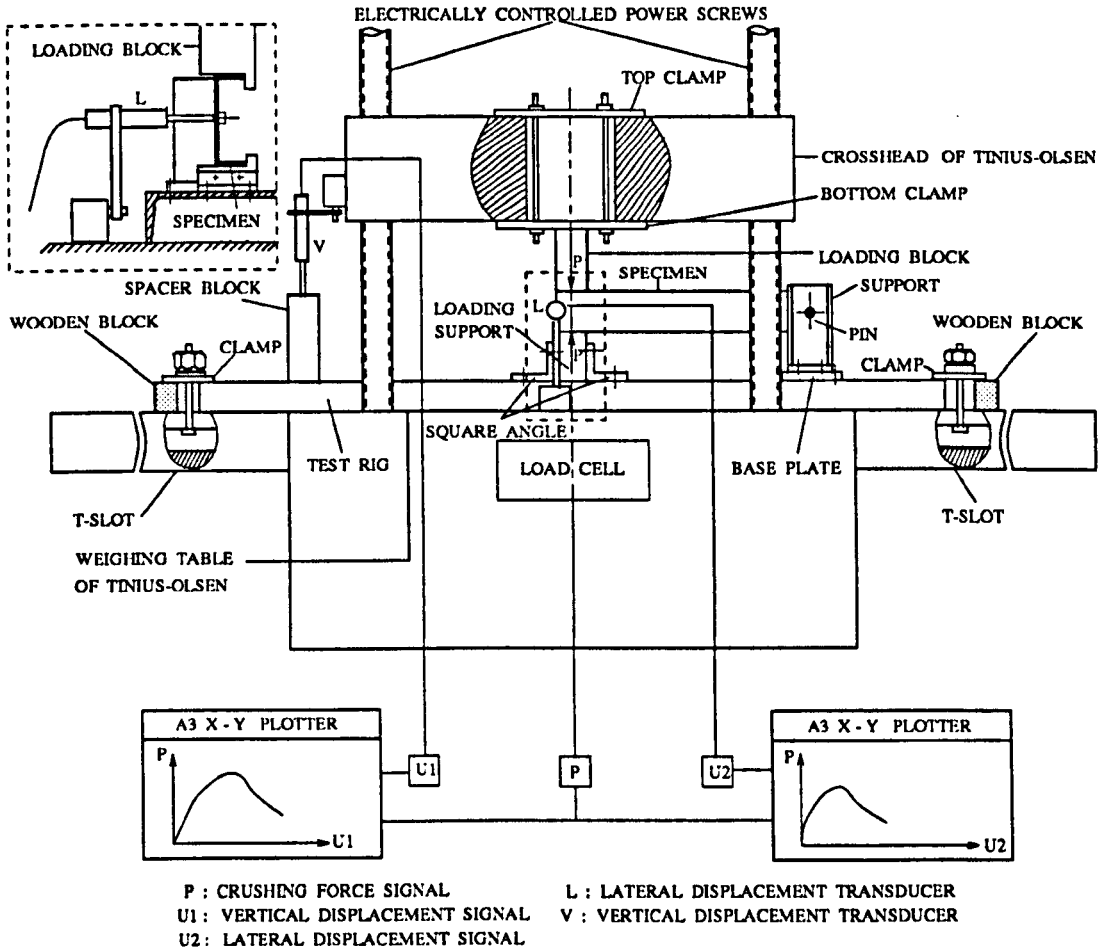
Figure 3.10. Test set-up of ETF loading condition.

The 18 specimen for the ETF tests were divided into 2 groups, in which each group consisted of the specimens with nominal web depths of 70 and 100 mm. The load bearing lengths applied to the top and bottom flanges in the experiments were 30, 40, 50 mm and they were used in testing each group of the specimens. The consistency of experimental results was also expected and for this purpose, at least three specimens of the same nominal web depths were tested under the same load bearing lengths. The measurement of vertical and lateral deflections of web was also carried out by the same procedures as those in the previous web crippling tests, only the position of lateral displacement transducer was approximately a half web depth underneath the load bearing length and exactly at the end of the specimens.

3.6.4. INTERIOR TWO-FLANGE LOADING (ITF) TESTS.

The tests of web crippling only were also carried out using an Interior Two-Flange Loading arrangement. Test loads were still applied on the top and bottom flanges using the same loading blocks, only their positions were shifted to the middle of the specimens. In order to keep the specimens in horizontal positions during the tests, one pin support was still used to support one free end of the specimens. Basically, the procedures of carrying out these tests were similar to those of ETF tests and the test set-up was as in the following figure.
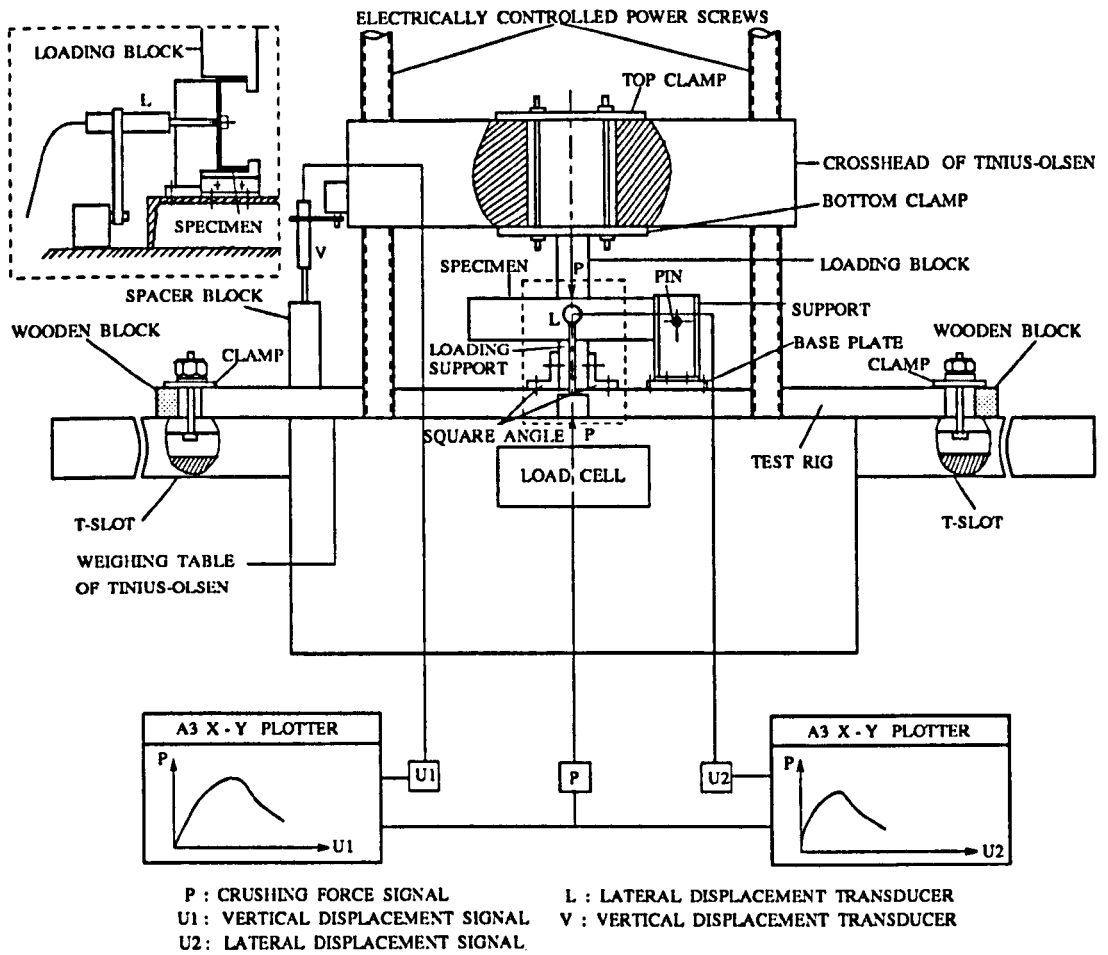
Figure 3.11. Test set-up of ITF loading condition.

3.7. RESULTS AND DISCUSSIONS.

All experimental results are presented in the following tables and diagrams of

experimental load (F_e) versus applied bending moment (M) and parameters studied

in this research program such as the bearing length ratio (n/t), the web slenderness

105

ratio (hw/t) and the inside bend radius ratio (r/t). Some typical examples of load-deflection diagram obtained from experiments are also shown to represent actual load-deflection behaviour of all specimens tested under each of the loading conditions. Finally, all factors influencing the web crippling strength of the specimens as indicated by the experimental results will be discussed in more detail.

3.7.1. INTERIOR ONE-FLANGE LOADING (IOF).

Table 3.1. $(M/M_c \geq 0.3)$

No.	Specimen	n/t	hw/t	r/t	l (mm)	M (KNmm)	F_c (KN)
1	H60-2	27.27	53.42	2.05	300	276.25	4.09
2	H60-4	27.27	53.42	2.05	300	279.25	4.14
3	H60-7	27.27	54.25	2.05	300	282.25	4.18
4	H60-9	27.27	54.23	2.05	300	279.25	4.14
5	H60-10	27.27	54.00	2.05	300	276.25	4.09
6	H60-18	31.53	54.86	2.03	300	289.40	4.37

Table 3.1. $(M/M_c \geq 0.3)$

No.	Specimen	n/t	hw/t	r/t	l (mm)	M (KNmm)	F_e (KN)
7	H60-19	31.53	54.06	2.03	300	289.40	4.37
8	H60-20	31.53	54.52	2.03	300	288.52	4.35
9	H60-21	31.53	53.65	2.03	300	290.88	4.39
10	H60-22	31.53	53.95	2.03	300	292.35	4.41
11	H60-23	36.04	54.06	2.03	300	296.95	4.57
12	H60-24	36.04	54.06	2.03	300	299.84	4.61
13	H60-25	36.04	54.41	2.03	300	294.35	4.53
14	H60-26	36.04	54.77	2.03	300	295.22	4.54
15	H60-27	36.04	54.06	2.03	300	297.24	4.57
16	H60-28	40.54	55.09	2.03	300	303.44	4.76
17	H60-29	40.54	54.54	2.03	300	309.68	4.86
18	H60-30	40.54	54.64	2.03	300	304.85	4.78
19	H60-31	40.54	54.36	2.03	300	306.84	4.81

Table 3.1. ($M/M_c \geq 0.3$)

No.	Specimen	n/t	hw/t	r/t	l (mm)	M (KNmm)	F_e (KN)
20	H60-32	40.54	53.74	2.03	300	309.11	4.85
21	H60-33	44.64	54.71	2.01	304	310.72	4.89
22	H60-34	45.05	53.26	2.03	302	312.76	4.96
23	H60-35	45.05	55.71	2.03	302	307.43	4.88
24	H60-36	45.05	55.67	2.03	300	306.66	4.91
25	H60-37	45.05	55.21	2.03	300	306.66	4.91
26	H70-6	27.03	62.35	2.03	350	317.44	3.97
27	H70-7	27.27	62.46	2.05	350	304.98	3.81
28	H70-8	27.27	62.46	2.05	350	312.81	3.91
29	H70-11	31.53	63.42	2.03	351	335.96	4.25
30	H70-12	31.53	63.22	2.03	351	337.37	4.27
31	H70-13	31.53	63.14	2.03	351	353.18	4.47
32	H70-14	31.53	63.79	2.03	350	346.11	4.40

Table 3.1. $(M/M_c \geq 0.3)$

No.	Specimen	n/t	hw/t	r/t	l (mm)	M (KNmm)	F_e (KN)
33	H70-15	31.53	62.95	2.03	351	349.32	4.42
34	H70-18	36.04	63.68	2.03	352	342.46	4.39
35	H70-19	36.04	63.33	2.03	352	349.75	4.48
36	H70-20	36.04	63.47	2.03	351	341.71	4.40
37	H70-21	40.54	63.51	2.03	350	359.54	4.72
38	H70-23	40.54	63.90	2.03	350	354.45	4.65
39	H70-24	40.54	63.51	2.03	350	366.66	4.81
40	H70-30	40.54	63.22	2.03	350	363.95	4.77
41	H70-25	45.05	63.13	2.03	350	373.33	4.98
42	H70-26	45.05	63.22	2.03	350	361.32	4.82
43	H70-27	45.05	62.76	2.03	350	363.66	4.85
44	H70-28	45.05	63.13	2.03	350	366.99	4.89
45	H70-29	45.05	63.56	2.03	350	361.99	4.83

Table 3.1. $(M/M_c \geq 0.3)$

No.	Specimen	n/t	hw/t	r/t	l (mm)	M (KNmm)	F_e (KN)
46	H80-9	27.27	72.30	2.05	398	374.47	4.07
47	H80-10	27.27	72.51	2.05	398	377.74	4.11
48	H80-11	27.03	72.55	2.03	402	394.26	4.24
49	H80-12	27.03	72.67	2.03	402	401.29	4.31
50	H80-13	27.03	73.26	2.03	402	390.95	4.20
51	H80-14	31.53	72.00	2.03	402	404.88	4.41
52	H80-15	31.53	72.12	2.03	402	421.20	4.59
53	H80-16	31.53	71.94	2.03	402	408.96	4.46
54	H80-17	36.04	72.23	2.03	402	412.64	4.56
55	H80-18	36.04	71.82	2.03	402	420.70	4.65
56	H80-19	36.04	72.44	2.03	402	416.27	4.60
57	H80-30	36.04	72.28	2.03	402	406.61	4.49
58	H80-31	36.04	71.89	2.03	402	412.24	4.56

Table 3.1. (M/M$_c$ ≥ 0.3)

No.	Specimen	n/t	hw/t	r/t	l (mm)	M (KNmm)	F$_e$ (KN)
59	H80-20	40.54	72.16	2.03	402	425.60	4.77
60	H80-21	40.54	73.04	2.03	402	417.67	4.68
61	H80-22	40.54	71.68	2.03	402	440.69	4.94
62	H80-23	40.54	72.96	2.03	403	431.18	4.82
63	H80-24	40.54	72.71	2.03	402	427.19	4.79
64	H80-25	45.05	72.85	2.03	402	454.48	5.16
65	H80-26	44.64	71.82	2.01	402	429.43	4.88
66	H80-27	45.05	72.10	2.03	402	446.26	5.07
67	H80-28	45.05	71.00	2.03	402	443.13	5.04
68	H80-29	45.05	72.59	2.03	402	443.91	5.04
69	H90-10	27.27	80.78	2.05	453	439.37	4.15
70	H90-11	27.27	80.69	2.05	453	437.02	4.13
71	H90-12	27.27	81.59	2.05	450	442.54	4.21

Table 3.1. $(M/M_c \geq 0.3)$

No.	Specimen	n/t	hw/t	r/t	l (mm)	M (KNmm)	F_e (KN)
72	H90-13	27.03	81.64	2.03	450	437.19	4.16
73	H90-14	30.00	88.98	2.25	451	341.78	3.25
74	H90-15	35.00	88.98	2.25	451	347.90	3.35
75	H90-16	31.53	82.25	2.03	451	442.28	4.25
76	H90-17	31.53	81.00	2.03	451	456.16	4.39
77	H90-18	36.04	81.52	2.03	451	463.02	4.51
78	H90-19	35.71	80.10	2.01	451	465.30	4.53
79	H90-20	36.36	81.82	2.05	451	482.21	4.69
80	H90-21	40.54	81.32	2.03	451	471.38	4.64
81	H90-22	40.18	80.09	2.01	451	473.64	4.67
82	H90-23	40.54	81.32	2.03	450	468.42	4.63
83	H90-24	45.45	89.57	2.27	451	359.86	3.55
84	H90-25	40.54	81.18	2.03	451	489.89	4.83

Table 3.1. $(M/M_c \geq 0.3)$

No.	Specimen	n/t	hw/t	r/t	l (mm)	M (KNmm)	F_e (KN)
85	H90-26	45.45	81.77	2.05	451	483.61	4.82
86	H90-27	45.05	81.45	2.03	451	508.38	5.07
87	H90-28	45.05	81.27	2.03	451	478.70	4.78
88	H90-29	44.64	79.96	2.01	451	513.74	5.12
89	H90-30	45.05	81.43	2.03	451	474.94	4.74
90	H100-1	30.00	99.35	2.25	500	400.90	3.41
91	H100-2	30.00	99.96	2.25	501	401.75	3.41
92	H100-3	30.00	98.97	2.25	502	403.13	3.42
93	H100-4	30.30	102.09	2.27	501	387.09	3.29
94	H100-5	30.30	101.29	2.27	502	387.91	3.29
95	H100-6	35.35	101.53	2.27	501	380.39	3.27
96	H100-7	35.71	102.58	2.30	501	385.57	3.31
97	H100-8	35.00	99.90	2.25	501	410.96	3.53

Table 3.1. $(M/M_c \geq 0.3)$

No.	Specimen	n/t	hw/t	r/t	l (mm)	Md (KNmm)	F_e (KN)
98	H100-9	35.00	99.60	2.25	502	405.61	3.47
99	H100-10	35.00	99.90	2.25	501	399.04	3.43
100	H100-11	40.00	99.60	2.25	502	431.58	3.74
101	H100-12	40.00	98.51	2.25	502	403.32	3.49
102	H100-13	40.00	99.75	2.25	502	423.88	3.67
103	H100-14	40.00	99.60	2.25	502	404.87	3.51
104	H100-15	40.82	101.81	2.30	502	407.95	3.53
105	H100-16	45.00	98.77	2.25	502	425.39	3.72
106	H100-17	45.00	100.08	2.25	502	435.55	3.81
107	H100-18	45.00	100.26	2.25	502	436.06	3.82
108	H100-19	45.45	102.32	2.27	501	415.33	3.64
109	H100-20	45.45	100.39	2.27	503	418.68	3.66
110	H100-21	50.00	99.52	2.25	503	439.30	3.88

Table 3.1. (M/M$_c$ ≥ 0.3)

No.	Specimen	n/t	hw/t	r/t	l (mm)	M (KNmm)	F$_e$ (KN)
111	H100-22	50.51	101.39	2.27	502	430.79	3.81
112	H100-23	50.00	100.11	2.25	502	433.80	3.84
113	H100-24	51.02	102.48	2.30	502	436.82	3.87
114	H100-25	50.00	100.24	2.25	502	440.34	3.90
115	H100-52	30.00	101.33	2.25	500	381.53	3.25
116	H100-53	30.61	104.89	2.30	500	371.07	3.16
117	H100-54	30.00	100.52	3.25	500	365.85	3.11
118	H100-55	30.00	99.39	3.25	500	365.85	3.11
119	H100-56	30.61	100.82	4.34	500	344.94	2.94
120	H100-57	30.93	101.87	4.38	500	344.94	2.94
121	H100-58	40.40	103.56	2.27	500	471.62	4.10
122	H100-59	40.82	105.44	2.30	500	467.53	4.07
123	H100-60	40.40	100.61	3.28	500	452.70	3.94

Table 3.1. $(M/M_c \geq 0.3)$

No.	Specimen	n/t	hw/t	r/t	l (mm)	M (KNmm)	F_e (KN)
124	H100-61	41.67	104.04	3.39	500	445.02	3.87
125	H100-62	40.00	99.36	4.25	500	455.25	3.96
126	H100-63	40.40	99.01	4.29	500	439.91	3.83
127	H100-64	50.51	103.29	2.27	500	460.37	4.09
128	H100-65	51.55	106.25	2.32	500	477.88	4.25
129	H100-66	49.50	98.95	2.23	500	467.87	4.16
130	H100-67	50.51	100.42	3.28	500	442.85	3.94
131	H100-68	49.50	97.40	4.21	500	445.36	3.96
132	H100-69	50.00	98.00	4.25	500	450.36	4.00

Table 3.2. ($M/M_c < 0.3$)

No.	Specimen	n/t	hw/t	r/t	l (mm)	M (KNmm)	F_e (KN)
1	H60-6	40.40	60.59	3.79	175	147.15	4.36
2	H60-8	40.00	59.62	3.50	176	145.18	4.27
3	H60-11	40.00	60.26	3.25	176	124.10	4.45
4	H60-12	51.02	60.33	3.32	177	148.27	4.67
5	H60-38	50.00	61.12	3.75	177	151.59	4.89
6	H60-39	50.00	59.40	3.50	175	148.75	4.76
7	H80-35	40.40	80.61	3.79	230	208.05	4.38
8	H80-36	40.40	80.20	3.75	230	207.10	4.36
9	H80-37	40.00	79.48	3.75	230	207.10	4.36
10	H80-32	30.00	80.52	3.50	230	215.00	4.30
11	H80-33	30.00	79.00	3.75	230	223.50	4.47
12	H80-34	30.00	80.00	3.75	230	223.50	4.47
13	H100-28	30.30	101.01	4.04	300	253.80	3.76

117

Table 3.2. $(M/M_c < 0.3)$

No.	Specimen	n/t	hw/t	r/t	l (mm)	M (KNmm)	F_e (KN)
14	H100-29	40.00	99.58	4.00	300	289.25	4.45
15	H100-30	40.00	99.98	4.00	300	289.25	4.45
16	H100-31	40.00	101.94	4.00	300	290.55	4.47
17	H100-32	50.51	101.94	4.04	300	283.13	4.53
18	H100-33	50.00	99.78	4.00	300	294.38	4.71
19	H100-34	50.00	99.80	4.00	300	283.13	4.53
20	H100-36	30.00	101.88	2.25	300	288.23	4.27
21	H100-37	30.30	99.41	3.28	300	288.23	4.27
22	H100-41	39.60	100.97	2.23	300	297.79	4.58
23	H100-42	40.40	103.05	2.27	300	306.47	4.71
24	H100-44	39.60	98.63	3.22	300	318.03	4.89
25	H100-47	50.51	102.40	2.27	300	325.26	5.20
26	H100-49	50.50	100.83	3.28	300	323.75	5.18
27	H100-50	50.00	98.00	4.25	300	323.59	5.18
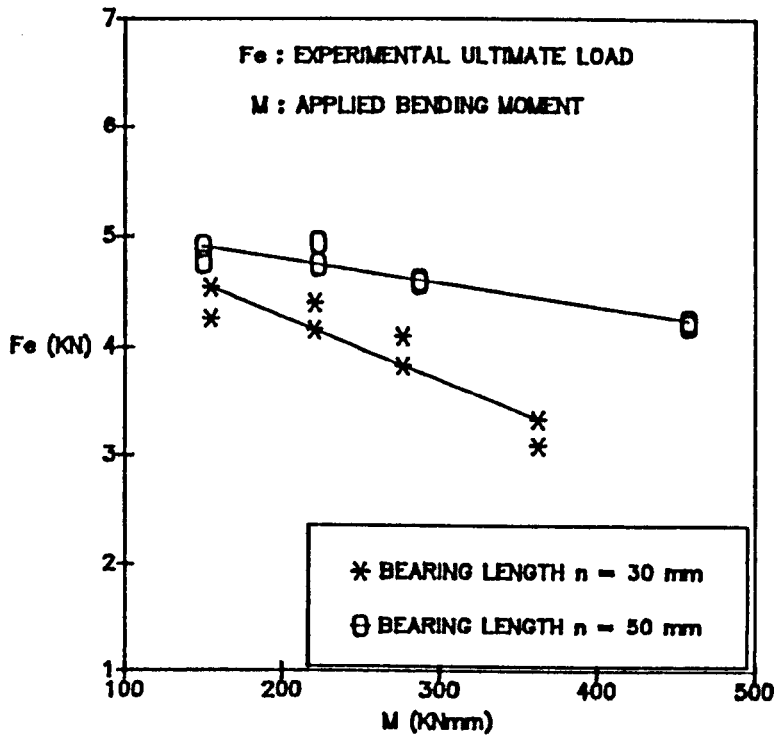
Figure 3.12. Load vs. applied bending moment of IOF tests.
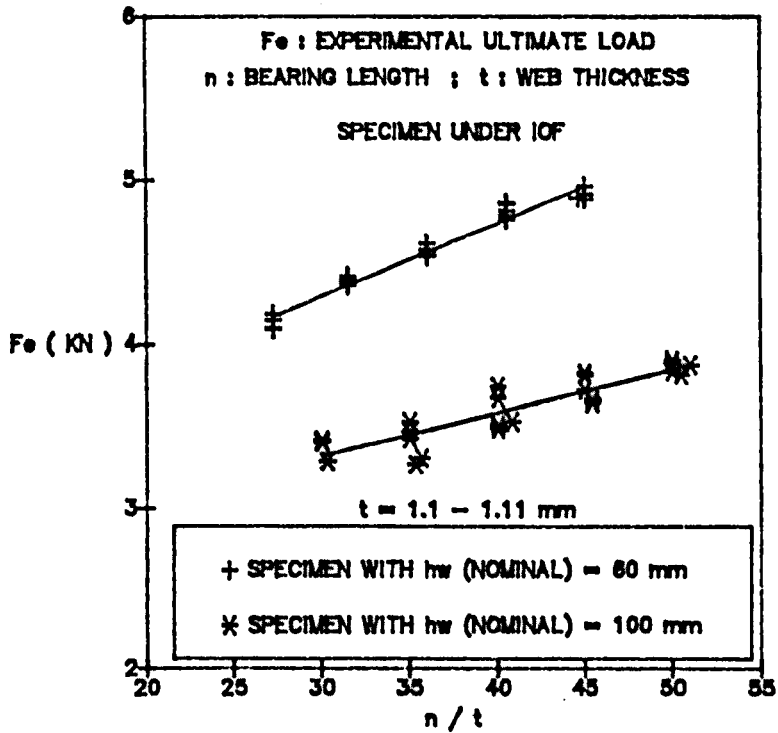
Figure 3.13. Load vs. bearing length ratio of IOF tests.

119
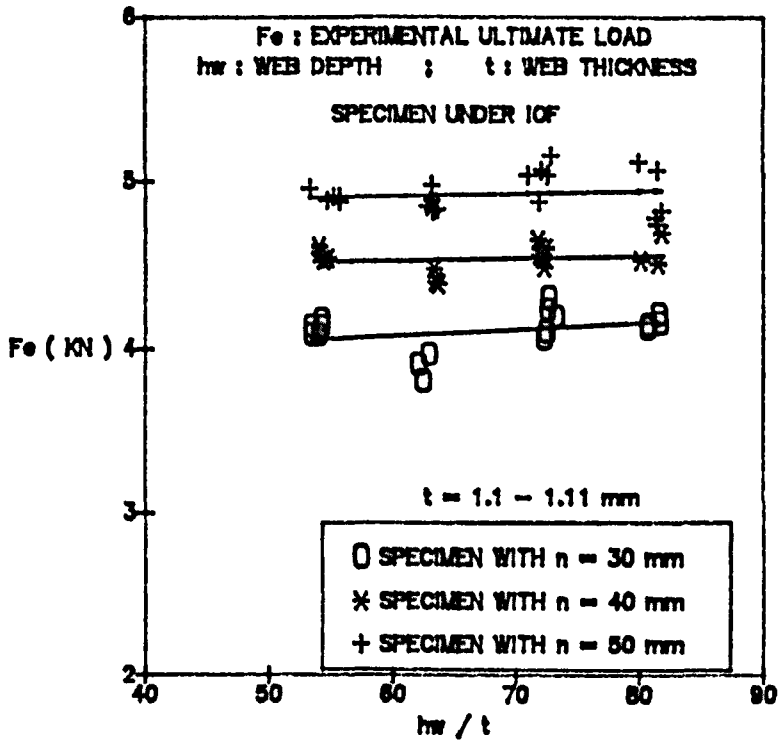
Figure 3.14. Load vs. web slenderness ratio of IOF tests.
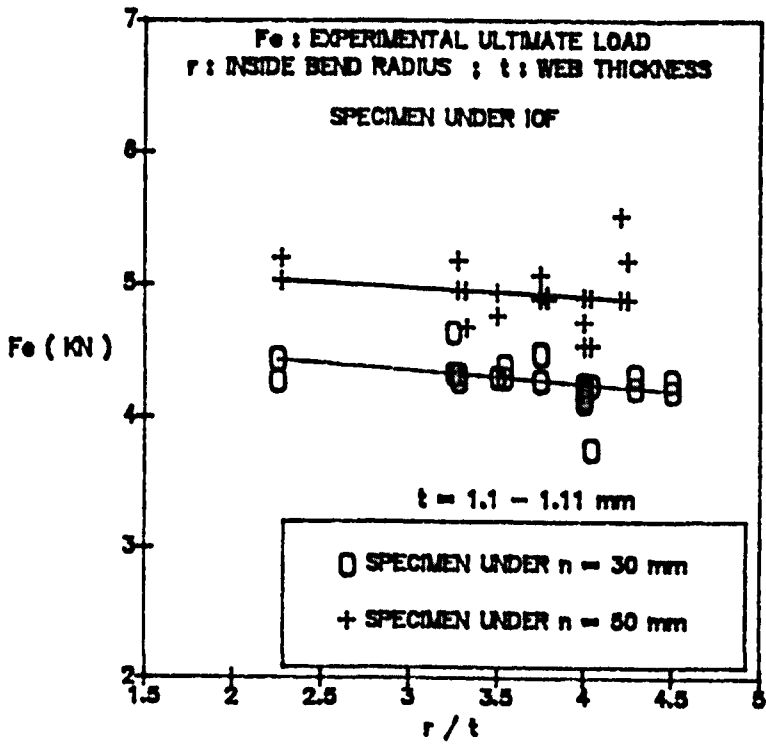
Figure 3.15. Load vs. inside bend radius ratio of IOF tests.

3.7.2. END ONE-FLANGE LOADING (EOF).

Table 3.3.

No.	Specimen	n/t	hw/t	r/t	F_e (KN)
1	S100-1	30.00	99.36	4.00	1.73
2	S100-2	30.30	100.93	4.04	1.65
3	S100-3	30.30	101.03	4.04	1.68
4	S100-4	40.40	101.84	4.04	1.88
5	S100-5	40.40	101.93	4.04	1.86
6	S100-6	40.00	101.14	4.00	1.85
7	S100-7	50.00	100.00	4.00	2.10
8	S100-8	50.00	100.16	4.00	2.21
9	S100-9	50.00	99.28	4.00	2.14
10	S80-1	30.00	79.68	3.75	1.86
11	S80-2	30.00	80.00	3.75	1.81
12	S80-3	30.00	80.20	3.75	1.86

Table 3.3

No.	Specimen	n/t	hw/t	r/t	F_e (KN)
13	S80-4	40.00	79.58	3.75	2.14
14	S80-5	40.00	80.00	3.75	2.09
15	S80-6	40.82	83.65	3.83	1.93
16	S80-7	50.00	79.00	3.75	2.38
17	S80-8	50.00	79.50	3.75	2.60
18	S80-9	50.00	79.50	3.75	2.37
19	S60-1	30.30	60.40	3.54	2.15
20	S60-2	30.30	60.00	3.54	2.08
21	S60-3	30.00	59.68	3.50	2.08
22	S60-4	40.00	59.78	3.50	2.54
23	S60-5	40.00	59.70	3.50	2.59
24	S60-6	40.00	59.38	3.50	2.58
25	S60-7	50.00	60.00	3.50	3.11
26	S60-8	50.00	59.50	3.50	2.94
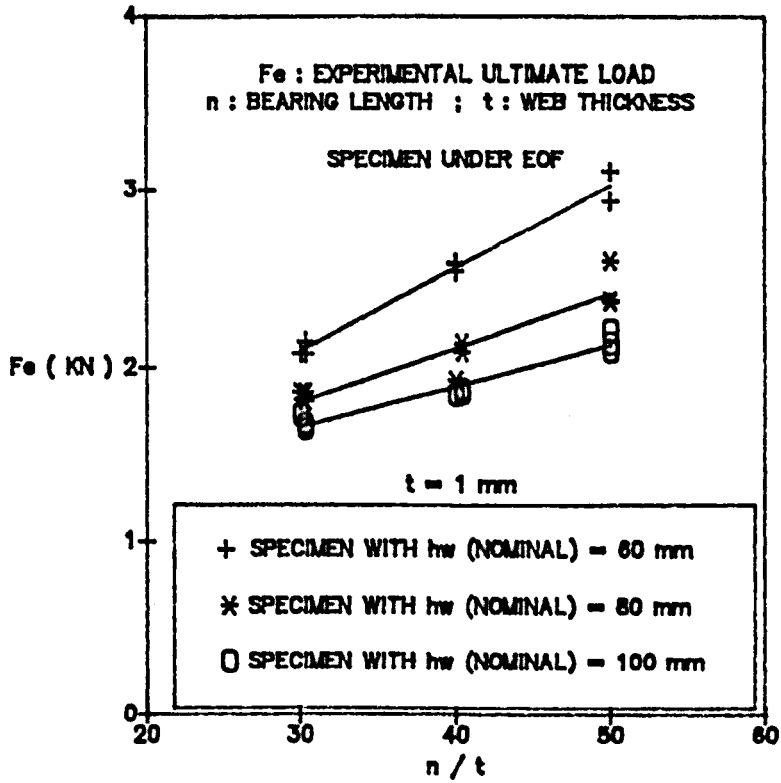
Figure 3.16. Load vs. bearing length ratio of EOF tests.
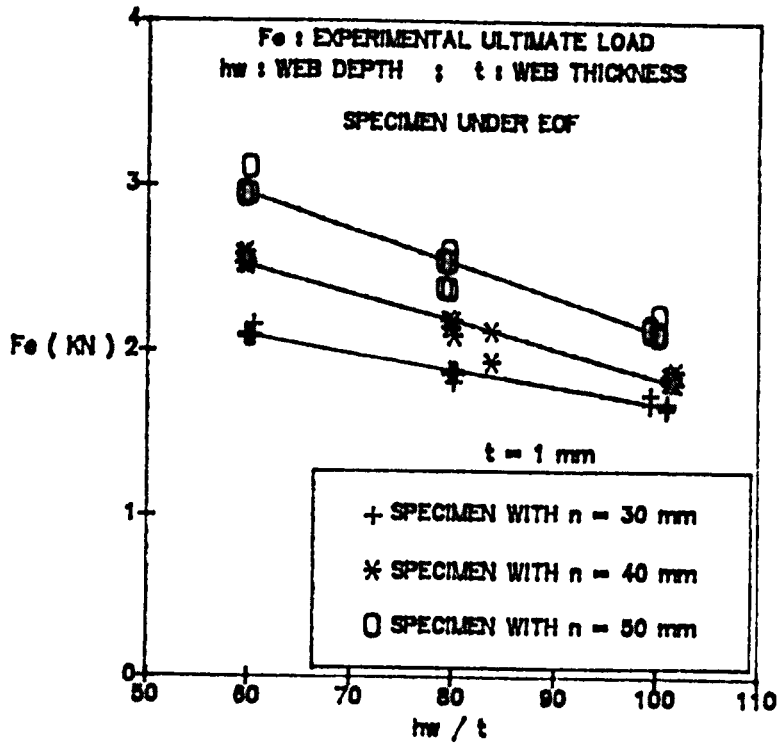
Figure 3.17. Load vs. web slenderness ratio of EOF tests.
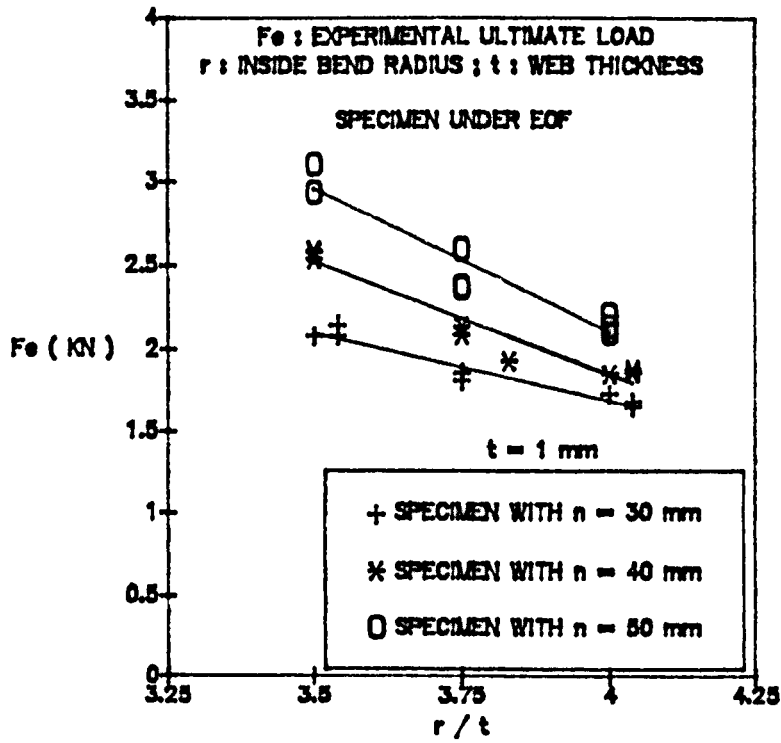
Figure 3.18. Load vs. inside bend radius ratio of EOF tests.

3.7.3. END TWO-FLANGE LOADING (ETF).

Table 3.4.

No.	Specimen	n/t	hw/t	r/t	F_e (KN)
1	H4-1	27.03	64.29	1.80	1.89
2	H4-2	27.27	65.09	2.05	1.78
3	H4-3	27.03	64.94	1.80	1.81
4	H4-4	36.36	65.56	1.82	2.00

Table 3.4.

No.	Specimen	n/t	hw/t	r/t	F_e (KN)
5	H4-5	36.04	65.21	1.80	2.03
6	H4-6	36.70	66.29	1.83	1.87
7	H4-7	45.87	66.09	2.06	2.16
8	H4-8	45.87	66.26	2.06	2.20
9	H4-9	45.87	65.39	2.06	2.25
10	H5-1	27.27	93.64	2.05	1.64
11	H5-2	27.27	92.62	2.05	1.84
12	H5-3	27.03	91.73	2.03	1.64
13	H5-4	36.04	91.50	2.03	2.05
14	H5-5	36.04	91.68	2.03	1.98
15	H5-6	36.36	92.56	2.05	1.99
16	H5-7	45.45	93.55	2.05	2.19
17	H5-8	45.45	93.18	2.05	2.32
18	H5-9	45.05	92.07	2.03	2.22
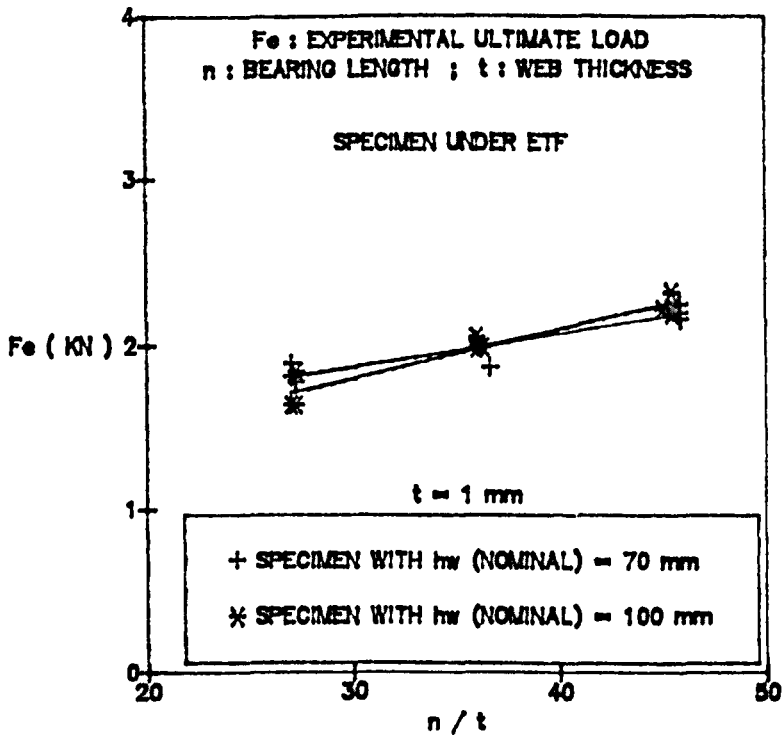
Figure 3.19. Load vs. bearing length ratio of ETF tests.
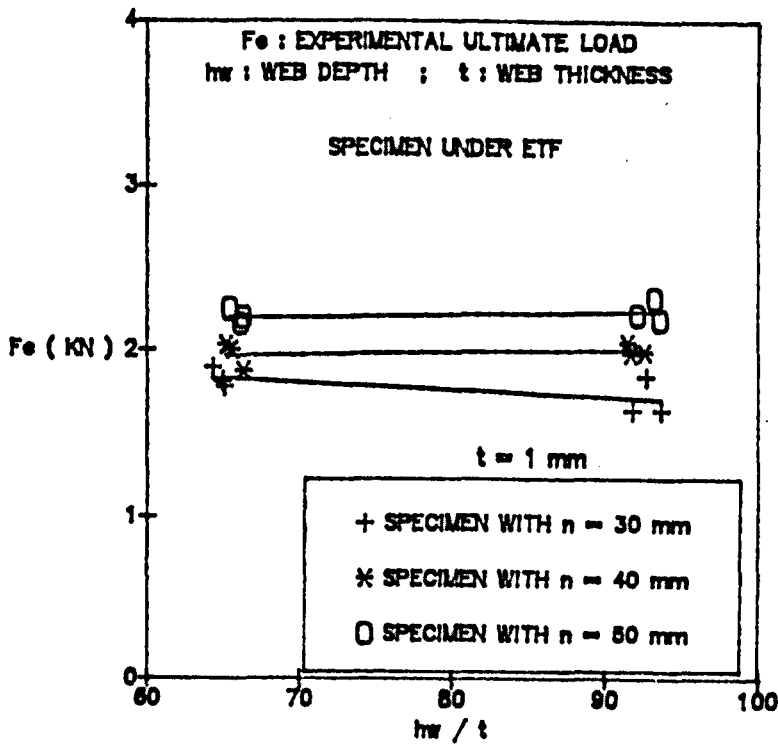
Figure 3.20. Load vs. web slenderness ratio of ETF tests.

126

3.7.4. INTERIOR TWO-FLANGE LOADING (ITF).

Table 3.5.

No.	Specimen	n/t	hw/t	r/t	F_e (KN)
1	H6-1	27.03	64.34	1.80	4.53
2	H6-2	27.03	64.14	1.80	4.75
3	H6-3	26.79	63.02	1.79	4.53
4	H6-4	36.04	64.07	1.80	4.87
5	H6-5	36.04	64.16	1.80	5.14
6	H6-6	36.04	63.68	1.80	5.05
7	H6-7	44.64	63.48	1.79	5.26
8	H6-8	45.05	64.25	1.80	5.17
9	H6-9	45.05	65.93	1.80	5.18
10	H7-1	27.27	92.40	1.82	4.58
11	H7-2	27.03	91.82	1.79	4.56
12	H7-3	27.03	92.41	1.80	4.63
13	H7-4	35.71	90.63	1.79	4.85

Table 3.5.

No.	Specimen	n/t	hw/t	r/t	F_e (KN)
14	H7-5	36.04	91.51	1.80	4.88
15	H7-6	36.36	92.24	1.82	4.88
16	H7-7	45.05	91.98	1.80	4.88
17	H7-8	45.45	92.75	1.82	5.28
18	H7-9	45.45	92.58	1.82	4.68
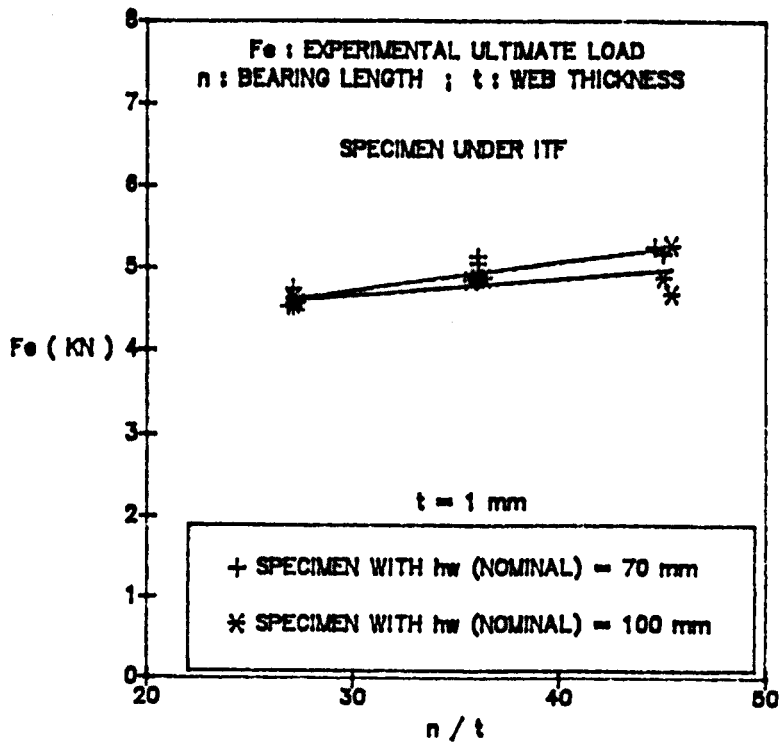
Figure 3.21. Load vs. bearing length ratio of ITF tests.
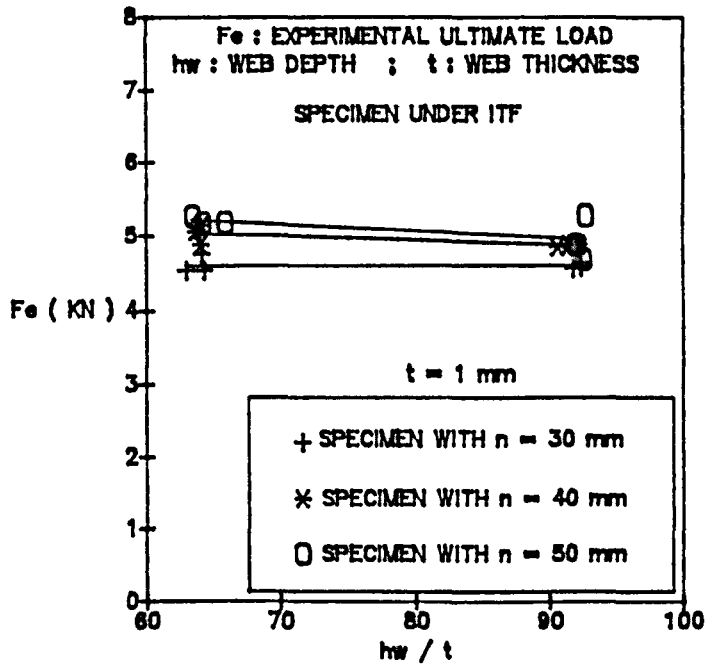
Figure 3.22. Load vs. web slenderness ratio of ITF tests.

3.7.5. LOAD-DEFLECTION CURVES.
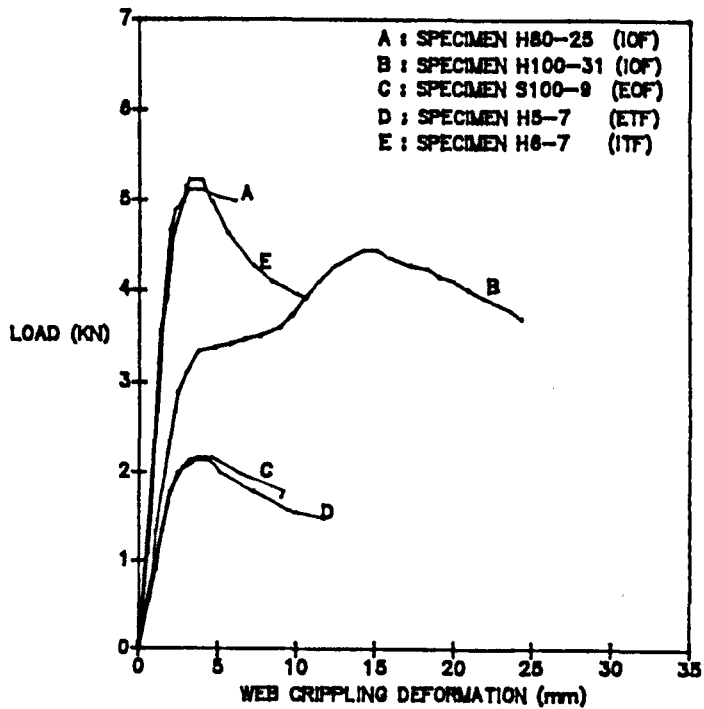
Figure 3.23. Load vs. web crippling deformation.

129
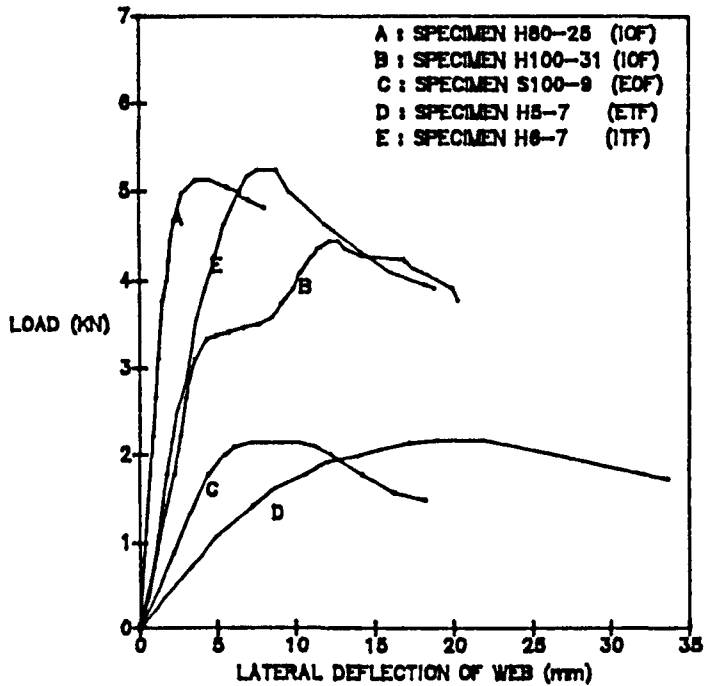
Figure 3.24. Load vs. lateral deflection of web.

3.7.6. DISCUSSION.

The experimental results presented in the tables and the diagrams of load vs.

parameters studied in this research program have shown that the values of ultimate

web crippling load are affected by various factors. In the case of the specimens tested

under combined actions of web crippling and bending (IOF tests), the ultimate web

crippling loads are severely affected by the magnitude of bending moment acting on

the specimens. This can be seen in Figure 3.12 where as the value of bending

moment (M) increases, the value of experimental ultimate web crippling load (F_e)

130

decreases. The similar effect on the ultimate web crippling loads in the IOF test is also shown in Figure 3.15, where the larger values of inside bend radius ratio (r/t) tend to decrease the values of F_e. In contrast to the parameter of bearing length ratio (n/t) as indicated in Figure 3.13 that the larger the values of n/t, the higher the values of F_e. Regarding to the influence of web slenderness ratio (hw/t) in the IOF test, Figure 3.14 shows that the variations of hw/t almost have no significant effects on the values of F_e. Thus, it can be concluded that the web crippling strength of the specimens tested under the IOF loading condition is more affected by the applied bending moment and parameters such as n/t and r/t than by the web slenderness ratio (hw/t).

If the specimens are tested under the EOF or ETF as well as ITF loading conditions, the web crippling strength of the specimens is no longer affected by the bending moment and only the influence of the three parameters studied is necessary to be found out. In the case of EOF tests, all of the three parameters studied have significant effects on the values of web crippling load and this is clearly shown in Figures 3.16-3.18. The influence of bearing length ratio (n/t) on the values of F_e is quite similar to that shown in the IOF tests, that is, the larger values of n/t tend to increase the ultimate web crippling loads. The parameters of hw/t and r/t in this type of test seem to have a similar effect on the ultimate web crippling loads where it can be seen in Figures 3.17 and 3.18, the ultimate web crippling loads will reduce due to the increase of the values of hw/t and r/t.

The results of ETF and ITF tests plotted in Figures 3.19-3.22 indicate that the web

crippling strength of the specimens tested under these types of loading is influenced

by the parameter of n/t only, whereas the effect of the web slenderness ratio (hw/t)

is also the same as that in the IOF tests. The influence of r/t in these tests is not

plotted because all specimens tested under these loading conditions had the same

inside bend radii. Thus, it can be found out from all of the experimental results that

only two of the three parameters studied in this research program, namely the bearing

length ratio (n/t) and the inside bend radius ratio (r/t) have significant roles in

influencing the strength of the specimens subjected to combined actions of web

crippling and bending as well as web crippling only. The influence of web

slenderness ratio (hw/t) on the web crippling strength of the specimens depends on

the loading conditions applied to them, where this parameter will extremely affect the

web crippling strength of the specimens if they are subjected to the EOF loading

condition.

Another important feature of web crippling behaviour also presented in this chapter

is experimental load-deflection curves, where these curves will show the different

behaviour of the specimens tested under each loading condition. Typical examples

of load-deflection curve for some specimens obtained from experiments are plotted

in Figures 3.23-3.24. It can be seen in the curves that the maximum values of test

load attained for specimens tested under the IOF and ITF loading conditions are

much higher than those for the specimens tested under the EOF and ETF loading

conditions. Thus, on the basis of these figures and all of the experimental results presented in the tables, it can be concluded that the specimens will be stronger to carry the concentrated loads applied far from their free ends instead of carrying the concentrated loads applied exactly at their free ends.

CHAPTER 4

APPLICATION OF

BS 5950 PART 5 1987

4.1. GENERAL.

BS 5950 Part 5 1987 gives recommendations for the design of structural steelwork in buildings and allied structures using cold-formed sections. This design code is primarily intended for sections of thickness up to 8 mm. The sections may be either open or closed and should be made up of flat elements bounded either by free edges or by bends with included angles not exceeding 135° and internal radii not exceeding 5t where t is the material thickness. The closed sections may be made by means of

- joining together two previously formed open sections by continuous welding or

- forming a single flat strip to be a box and continuously welding the longitudinal joint.

This chapter dicusses the application of BS 5950 Part 5 1987 in analysing the strength of the specimens under combined web crippling and bending as well as under web crippling only. The analysis followed the procedures described in section five of BS 5950 Part 5 1987. In order to analyse the strength of the specimens under combined web crippling and bending, the specimens were treated as three-point loading beams where they were loaded at their mid-spans and supported at both ends. The strength of the specimens under web crippling only was predicted using formulae given in table 2.2 for *single load or reaction near or at free end as well as two opposite loads near or at free end and far from free end.*

In the case of specimens under combined web crippling and bending, the moment capacity of the specimens should also be calculated in the analysis. According to this design code that the determination of moment capacity of the sections should be based on a limiting compressive stress in the webs and the effective width of the compression elements. The thickness of the specimens was also considered in the calculation of the section properties. In BS 5950 Part 5 1987, if the material thickness is up to 3.2 mm, the material can be assumed to be concentrated at the mid-line of the section and round corners are replaced by intersections of the flat elements. Because the thickness of the specimens was less than 3.2 mm, the idealized cross section of the specimens used in the analysis was therefore as shown in Figure 4.1 (b).
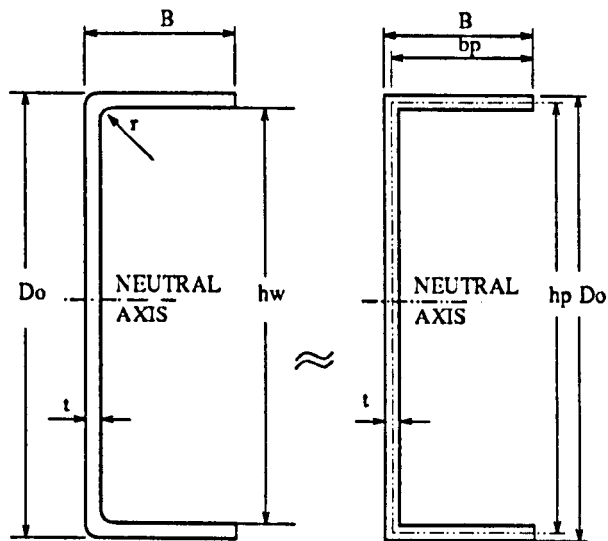
(a) Actual cross section.   (b) Idealized cross section.

Figure 4.1. Cross section of the specimen.

In the above figure :

       B   : Flange width.

    hw   : Web height or web depth.

     r   : Bend radius.

     t   : Web thickness (= flange thickness).

bp = B - 0.5t   :   hp = hw + t

4.2. DETERMINATION OF MOMENT CAPACITY.

In order to satisfy the procedures of analysis required by BS 5950 Part 5 1987, prior to the determination of moment capacity of the sections, the analysis was carried out to calculate the limiting stress in the webs and the effective widths of the compression elements. If the specimen is subjected to the mid-span loading, the top flange will be subjected to a compressive stress while the web and bottom flange will be subjected to stress gradient and a tensile stress respectively. By considering the effective width of the top flange, the stress distribution carried by the specimen is therefore as shown in Figure 4.2. The limiting compressive stress in the web was calculated using the following formula :

$$p_o = [\ 1.13 - 0.0019\ \frac{D}{t}\ (\ \frac{Y_s}{280}\ )^{0.5}\ ]\ p_y \quad \ldots \ldots \ldots \quad (4.2.1)$$

where :

p_o : The limiting compressive stress in the web (in N/mm^2 or MPa).

136

D : The overall web depth (in mm) or in Figure 4.1 $D = hw$.

Y_s : The material yield strength (in N/mm^2 or MPa).

t : The web thickness (in mm).

p_y : The design strength (in N/mm^2 or MPa) and in this analysis p_y was

the same as the yield strength (Y_s).
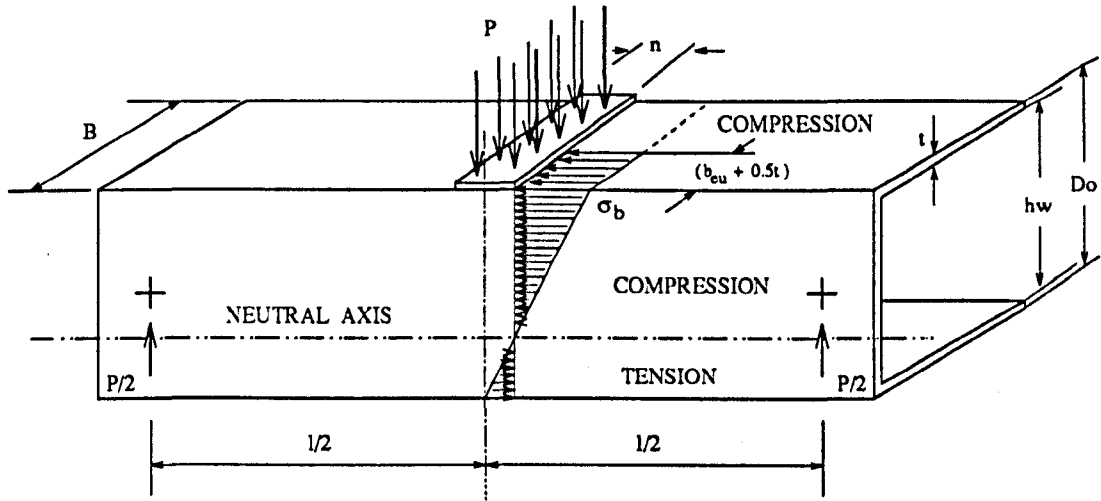
Figure 4.2. Stress distribution on the specimen
under mid-span loading.

It can be seen in the above figure that the top and bottom flanges are unstiffened

elements, because they are supported only along one side of their longitudinal edges

by the web. From the above figure, the web can be considered as a stiffened element

because it is longitudinally supported along its both edges by the top and bottom

flanges. In this analysis, the web and the bottom flanges were assumed to be fully

effective and the calculation of effective widths was employed for the top flange

only. The effective width calculation of the top flange followed the procedures

137

described in section four of BS 5950 Part 5 1987. The following figure indicates the effective cross section of the specimen used in analysing the moment capacity.
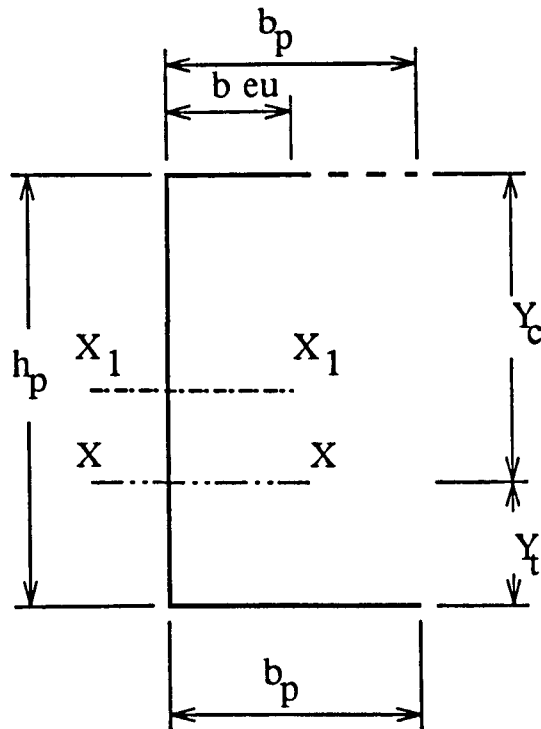
Figure 4.3. Effective cross section of the specimen.

b_{eu} : Effective width of the top flange.

$X1 - X1$: Neutral axis of the full cross section.

$X - X$: Neutral axis of the effective cross section.

The effective width calculation of the top flange was carried out by using the procedure of calculating the effective width of an unstiffened element under uniform compression, where its effective width (b_{eu}) was calculated from :

138

$$b_{eu} = 0.89 \; b_{eff} + 0.11 \; b_p \; \ldots\ldots\ldots\ldots\ldots \; (4.2.2)$$

The compressive stress acting on the effective element (f_c) was equal to the limiting compressive stress in the web (p_o).

$$For \; \frac{f_c}{p_{cr}} < 0.123 \quad ; \quad \frac{b_{eff}}{b_p} = 1 \; \ldots\ldots\ldots \; (4.2.3)$$

$$For \; \frac{f_c}{p_{cr}} \geq 0.123 \quad ; \quad \frac{b_{eff}}{b_p} = [1 + 14 \, [\, (\frac{f_c}{p_{cr}})^{0.5} - 0.35]^4 \,]^{-0.2}$$

$$\ldots\ldots\ldots\ldots\ldots\ldots\ldots\ldots\ldots\ldots\ldots \; (4.2.4)$$

$f_c = p_o$, p_o was calculated using equation 4.2.1

p_{cr} : the local buckling stress of the element given by :

$$p_{cr} = 185000 \; K \; (\; \frac{t}{b} \;)^2 \; \ldots\ldots\ldots\ldots \; (4.2.5)$$

where :

t   : The top flange thickness = the web thickness.

b   : The full width of the top flange = b_p.

K   : The local buckling coefficient of the top flange and it was obtained

from

$$K = K_1 = 1.28 - \frac{0.8 \; h}{2 + h} - 0.0025 \; h^2 \; \ldots\ldots\ldots\ldots \; (4.2.6)$$

In equation (4.2.6) h is defined as follows :

$$h = \frac{b_p}{h_p} \quad \ldots \ldots \ldots \ldots \ldots \ldots (4.2.7)$$

The value of p_{cr} was calculated by using equations (4.2.5), (4.2.6) and (4.2.7). This value was then used to calculate the ratio of f_c / p_{cr} and the value of b_{eff} in equation (4.2.3) or (4.2.4). Substitution of b_{eff} obtained from this calculation into equation (4.2.2) gaves the effective width of the top flange (b_{eu}).

The position of the neutral axis X-X in Figure 4.2 was calculated from :

$$Y_t = \frac{\sum_{i=1}^{n} A_i \cdot Y_i}{\sum_{i=1}^{n} A_i} \quad \ldots \ldots \ldots \ldots \ldots (4.2.8)$$

All moments in this above formula were taken about the bottom flange, so that :

$$Y_t = \frac{t \, (\, b_{eu} \cdot h_p + 0.5 \, h_p^2 + b_p \cdot 0 \,)}{t \, (b_{eu} + h_p + b_p)}$$

$$Y_t = \frac{b_{eu} \cdot h_p + 0.5 \, h_p^2}{b_{eu} + h_p + b_p} \quad \ldots \ldots \ldots \ldots \ldots (4.2.9)$$

$$Y_c = h_p - Y_t \quad \ldots \ldots \ldots \ldots \ldots (4.2.10)$$

The second moment of the effective cross section about the neutral axis X-X (I_x) was obtained from :

$$I_x = t \, [\, b_{eu} \cdot Y_c^2 + \frac{1}{3} \, (\, Y_c^3 + Y_t^3 \,) + b_p \cdot Y_t^2 \,] \quad \ldots \ldots (4.2.11)$$

The complete derivation of this formula can be seen in appendix B-1.

The elastic section modulus in :

- *Compression region :* $\quad z_c = \dfrac{I_x}{Y_c}$ . . . . (4.2.12)

- *Tension region :* $\quad z_t = \dfrac{I_x}{Y_t}$ . . . . (4.2.13)

On the basis of Figure 4.3 and the above formulae, the value of z_c would be less than

the value of z_t so that Yielding first occured in the compression region. The moment

capacity of the section (M_c) was therefore calculated using the following expression.

$$M_c = p_o \cdot z_c \quad . . . . (4.2.14)$$

4.3. CALCULATION OF ULTIMATE WEB CRIPPLING LOAD.

The ultimate web crippling load which is meant in this thesis is a maximum

concentrated load acting on the specimen under combined web crippling and bending

and under web crippling only. In the case of combined web crippling and bending,

it is denoted by F_{CB} and this load was calculated using the interaction formula of

combined bending and web crushing (or web crippling) available in BS 5950 Part

5 1987. The formula used in the analysis was equation (2.4.1) in subchapter 2.4,

where P_w was calculated by using equation in table 2.2 of subchapter 2.4 for the case

of load or reaction far from free end. In the case of the loading condition as shown

in Figure 4.4, the value of applied moment M was therefore equal to M_{max} where the

maximum moment can be expressed as in the following formula.

$$M_{max} = \frac{F_{CB} \ (1 - n)}{4} \quad \ldots \ldots \ldots \ldots \quad (4.3.1)$$

F_w was equated to F_{CB} and M_c was obtained from equation (4.2.14). Hence, equation (2.4.1) can be rewritten as follows :

$$\frac{1.2 \ F_{CB}}{P_w} + \frac{F_{CB} \ (1 - n)}{4 \ M_c} \leq 1.5$$

$$\frac{F_{CB} \ [\ 4.8 \ M_c + P_w \ (1 - n) \ ]}{4 \ P_w \ M_c} \leq 1.5$$

OR

$$F_{CB} = \frac{6 \ P_w \ M_c}{4.8 \ M_c + P_w \ (1 - n)} \quad \ldots \ldots \ldots \ldots \ldots \quad (4.3.2)$$
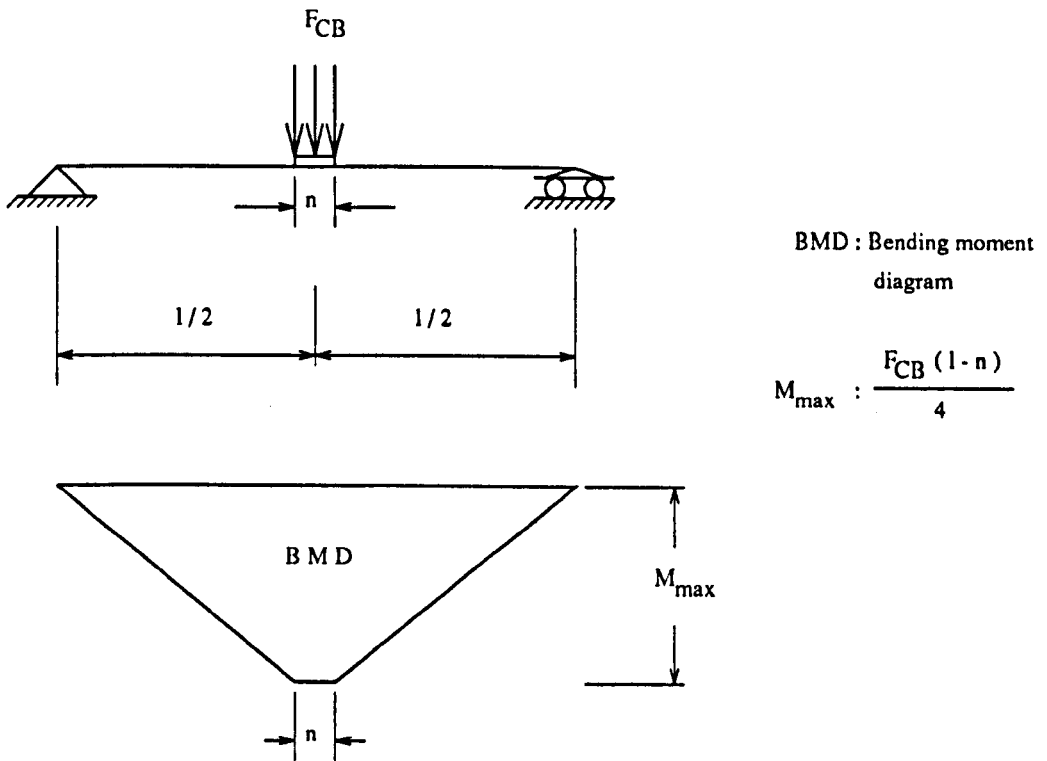
Figure 4.4. Three-point loading beam.

The following analysis is an example of using BS 5950 Part 5 1987 in predicting the ultimate load F_{CB} of the specimen H90-26. Dimensions of the specimen were as follows :

- Web depth h_w = 89.95 mm   ;   Web thickness = Flange thickness t = 1.10 mm.

- Flange width B = 42.14 mm ;   Inside bend radius r = 2.25 mm.

- Web inclination Θ = 90°.

A concentrated load was applied at the middle of the specimen through a loading block of width n = 50 mm and its both ends were supported at a distance of l = 451 mm. The yield strength of the material used to manufacture the specimen was equal to 303 MPa.

The first step of performing the analysis is to calculate the limiting compressive stress (p_o) in the web, i.e. :

$$p_o = [\ 1.13 - 0.0019 \ . \ \frac{89.95}{1.10} \ . \ (\frac{303}{280})^{0.5} \ ] \ 303 \ \ MPa$$

$$p_o = 293.42 \ \ MPa$$

The second step is to determine the effective width of the top flange.

$$b_p = (\ 42.14 - 0.5 \ x \ 1.10 \ ) \ \ mm = 41.59 \ \ mm$$

$$h_p = (\ 89.95 + 1.10 \ ) \ \ mm = 91.05 \ \ mm$$

$$h = \frac{b_p}{h_p} = \frac{41.59}{91.05} = 0.46$$

The local buckling coefficient of the top flange :

143

$$K = 1.28 - \frac{0.8 \ x \ 0.46}{2 + 0.46} - 0.0025 \ x \ 0.46^2 = 1.13$$

Substitution of K into equation (4.2.5) gives the local buckling stress of the top flange (p_{cr}).

$$p_{cr} = 185000 \ x \ 1.13 \ x \ (\frac{1.10}{41.59})^2 \ MPa$$

$$p_{cr} = 146.24 \ MPa$$

The compressive stress acting on the top flange :

$$f_c = p_o = 293.42 \ MPa$$

$$\frac{f_c}{p_{cr}} = \frac{293.42}{146.24} = 2.01 > 0.123$$

On the basis of this above value, equation (4.2.4) is therefore used to calculate b_{eff}.

$$\frac{b_{eff}}{41.59} = [\ 1 + 14 \ (\ 2.01^{0.5} - 0.35 \ )^4 \ ]^{-0.2} = 0.55$$

$$b_{eff} = 41.59 \ x \ 0.55 \ mm = 22.87 \ mm$$

Thus the effective width of the top flange :

$$b_{eu} = (\ 0.89 \ x \ 22.87 + 0.11 \ x \ 41.59 \ ) \ mm = 24.93 \ mm$$

Refer to Figure 4.3 the position of neutral axis X-X was calculated by using equations (4.2.10) and (4.2.11).

144

$$Y_t = \frac{24.93 \times 91.05 + 0.5 \times 91.05^2}{24.93 + 91.05 + 41.59} \ mm = \frac{6414.93}{157.57} \ mm$$

$$Y_t = 40.71 \ mm \quad ; \quad Y_c = (91.05 - 40.71) \ mm = 50.34 \ mm$$

The second moment of the effective cross section about the neutral axis X-X :

$$I_x = 1.10 \left[24.93 \times 50.34^2 + \frac{1}{3}(50.34^3 + 40.71^3) + 41.59 \times 40.71^2\right] \ mm^4$$

$$I_x = 216826.34 \ mm^4$$

The elastic section modulus in :

$$Compression \ region : z_c = \frac{216826.34}{50.34} \ mm^3 = 4307.24 \ mm^3$$

$$Tension \ region : z_t = \frac{216826.34}{40.71} \ mm^3 = 5326.12 \ mm^3$$

$z_c < z_t$, Yielding first occured in the compression region and the moment capacity of the section (M_c) :

$$M_c = 293.42 \times 4307.24 \ Nmm = 1263830.36 \ Nmm = 1263.83 \ KNmm$$

The concentrated load resistance (P_w) in the absence of a bending moment as stated in equation (4.3.2) is calculated by using the formula in table 2.2 of subchapter 2.4 for the case of load or reaction far from free end, i.e. :

145

$$P_w = t^2 \, K \, C_1 \, C_2 \, C_{12} \, [3350 - 4.6 \, (\tfrac{D}{t})] \, [1 + 0.007 \, (\tfrac{N}{t})]$$

$$\frac{N}{t} = \frac{n}{t} = \frac{50}{1.10} = 45.45 < 60 \quad ; \quad K = \frac{P_y}{228} = \frac{303}{228} = 1.33$$

$$\frac{D}{t} = \frac{h_w}{t} = \frac{89.95}{1.10} = 81.77 \quad ; \quad C_1 = 1.22 - 0.22 x 1.33 = 0.93$$

$$C_2 = 1.06 - 0.06 x \frac{2.25}{1.10} = 0.94 \quad ; \quad C_{12} = 0.7 + 0.3 \, x (\frac{90}{90})^2 = 1$$

$$P_w = 1.10^2 \, x \, 1.33 \, x \, 0.93 \, x \, 0.94 \, x \, 1 \, x$$

$$(3350 - 4.6 x 81.77) (1 + 0.007 x 45.45) \, N$$

$$P_w = 5514.21 \quad N = 5.51 \; KN$$

Substitution of M_c and P_w into equation (4.3.2) :

$$F_{CB} = \frac{6 \; x \; 5514.21 \; x \; 1263830.36}{4.8 \; x \; 1263830.36 + 5514.21 \; (\; 451 - 50 \;)} \quad N$$

$$F_{CB} = \frac{33085.26 \; x \; 1263830.36}{8277583.94} \quad N$$

$$F_{CB} = \underline{5051.49} \; N = \underline{5.05} \; KN$$

The specimens under combined web crippling and bending were divided into 5 groups according to their nominal web depths. Their designations were initiated with the capital letter (H) and followed by their nominal web depths and numbers. The ultimate web crippling load of the specimens under web crippling only is denoted by F_c and it was predicted using the formulae obtained from table 2.2, i.e. :

146

- Single load or reaction near or at free end (EOF) :

$$n/t \leq 60 :$$

$$F_C = t^2 \, k \, C_3 \, C_4 \, C_{12} \, [1350 - 1.73\,(h_w/t)\,] \, [1 + 0.01\,(n/t)\,]$$

$$n/t > 60 :$$

$$F_C = t^2 \, k \, C_3 \, C_4 \, C_{12} \, [1350 - 1.73\,(h_w/t)\,] \, [0.71 + 0.015\,(n/t)\,]$$

- Two opposite loads near or at free end (ETF) :

$$F_C = t^2 \, k \, C_3 \, C_4 \, C_{12} \, [1520 - 3.57\,(hw/t)\,] \, [1 + 0.01\,(n/t)\,]$$

- Two opposite loads far from free end (ITF) :

$$F_C = t^2 \, k \, C_1 \, C_2 \, C_{12} \, [4800 - 14\,(hw/t)\,] \, [1 + 0.0013\,(n/t)\,]$$

A computer program was also written for the purpose of using BS 5950 Part 5 1987 in predicting F_{CB} and F_C of all specimens in this investigation and the program can be seen in appendix C. The results of using BS 5950 Part 5 1987 are presented in the following tables, where the results for specimens under combined web crippling and bending (IOF) consist of 2 series of analysis. The first series are for the analysis of web crippling strength of the specimens with the ratio of applied bending moment to moment capacity $M/M_c \geq 0.3$, while the second series are for the analysis with $M/M_c < 0.3$.

147

4.4. RESULTS.

4.4.1. SPECIMENS UNDER COMBINED WEB CRIPPLING AND BENDING (IOF).

Table 4.1. SERIES 1

No.	Specimen	n/t	hw/t	r/t	l (mm)	M_c (KNmm)	F_{CB} (KN)
1	H60-2	27.27	53.42	2.05	300	705.85	4.58
2	H60-4	27.27	53.42	2.05	300	712.27	4.59
3	H60-7	27.27	54.25	2.05	300	728.62	4.61
4	H60-9	27.27	54.22	2.05	300	720.71	4.60
5	H60-10	27.27	54.00	2.05	300	724.63	4.61
6	H60-18	31.53	54.86	2.03	300	746.00	4.82
7	H60-19	31.53	54.06	2.03	300	733.82	4.80
8	H60-20	31.53	54.52	2.03	300	741.27	4.81
9	H60-21	31.53	53.65	2.03	300	726.90	4.79
10	H60-22	31.53	53.95	2.03	300	735.47	4.80

Table 4.1. SERIES 1

No.	Specimen	n/t	hw/t	r/t	l (mm)	M_c (KNmm)	F_{CB} (KN)
11	H60-23	36.04	54.06	2.03	300	733.82	4.91
12	H60-24	36.04	54.06	2.03	300	733.82	4.91
13	H60-25	36.04	54.41	2.03	300	739.55	4.92
14	H60-26	36.04	54.77	2.03	300	745.75	4.93
15	H60-27	36.04	54.06	2.03	300	735.42	4.92
16	H60-28	40.54	55.09	2.03	300	749.78	5.05
17	H60-29	40.54	54.54	2.03	300	741.82	5.04
18	H60-30	40.54	54.64	2.03	300	743.48	5.04
19	H60-31	40.54	54.36	2.03	300	738.15	5.03
20	H60-32	40.54	53.74	2.03	300	729.60	5.02
21	H60-33	44.64	54.69	2.01	304	763.27	5.24
22	H60-34	45.05	53.26	2.03	302	723.98	5.12
23	H60-35	45.05	55.71	2.03	302	760.22	5.18

Table 4.1.   SERIES 1

No.	Specimen	n/t	hw/t	r/t	l (mm)	M_c (KNmm)	F_{CB} (KN)
24	H60-36	45.05	55.85	2.03	300	761.82	5.19
25	H60-37	45.05	55.21	2.03	300	751.07	5.17
26	H70-6	27.27	62.88	2.05	350	868.39	4.58
27	H70-7	27.27	62.43	2.05	350	860.16	4.57
28	H70-8	27.27	62.03	2.05	350	853.81	4.56
29	H70-11	31.53	63.42	2.03	351	895.30	4.78
30	H70-12	31.53	63.22	2.03	351	890.27	4.77
31	H70-13	31.53	63.14	2.03	351	888.58	4.77
32	H70-14	31.53	63.79	2.03	350	901.35	4.79
33	H70-15	31.53	62.95	2.03	351	888.78	4.77
34	H70-18	36.04	63.68	2.03	352	897.87	4.89
35	H70-19	36.04	63.33	2.03	352	893.42	4.88
36	H70-20	36.04	63.47	2.03	351	891.98	4.89

Table 4.1. SERIES 1

No.	Specimen	n/t	hw/t	r/t	l (mm)	M_c (KNmm)	F_{CB} (KN)
37	H70-21	40.54	63.51	2.03	350	894.09	5.00
38	H70-23	40.54	63.90	2.03	350	900.17	5.01
39	H70-24	40.54	63.51	2.03	350	895.34	5.01
40	H70-30	40.54	63.22	2.03	350	890.45	5.00
41	H70-25	45.05	63.13	2.03	350	888.88	5.11
42	H70-26	45.05	63.22	2.03	350	893.53	5.12
43	H70-27	45.05	62.76	2.03	350	884.41	5.10
44	H70-28	45.05	63.13	2.03	350	890.87	5.11
45	H70-29	45.05	63.56	2.03	350	896.44	5.12
46	H80-9	27.27	72.26	2.05	398	1086.95	4.64
47	H80-10	27.27	72.47	2.05	398	1092.60	4.64
48	H80-11	27.03	72.55	2.03	402	1118.33	4.72
49	H80-12	27.03	72.67	2.03	402	1118.98	4.72

Table 4.1. SERIES 1

No.	Specimen	n/t	hw/t	r/t	l (mm)	M_c (KNmm)	F_{CB} (KN)
50	H80-13	27.03	73.26	2.03	402	1127.53	4.73
51	H80-14	31.53	72.00	2.03	402	1109.73	4.82
52	H80-15	31.53	72.11	2.03	402	1108.92	4.82
53	H80-16	31.53	71.94	2.03	402	1107.20	4.82
54	H80-17	36.04	72.23	2.03	. 402	1112.93	4.93
55	H80-18	36.04	71.82	2.03	402	1103.99	4.92
56	H80-30	36.04	72.28	2.03	402	1112.85	4.93
57	H80-19	35.71	71.79	2.01	402	1131.57	5.02
58	H80-31	36.04	71.89	2.03	402	1106.59	4.93
59	H80-20	40.54	72.16	2.03	402	1110.43	5.04
60	H80-21	40.54	73.04	2.03	402	1126.76	5.05
61	H80-22	40.54	71.68	2.03	402	1100.70	5.03
62	H80-23	40.54	72.96	2.03	403	1122.50	5.05

Table 4.1. SERIES 1

No.	Specimen	n/t	hw/t	r/t	l (mm)	M_c (KNmm)	F_{CB} (KN)
63	H80-24	40.54	72.71	2.03	402	1120.12	5.05
64	H80-25	45.05	72.85	2.03	402	1119.43	5.16
65	H80-26	44.64	71.82	2.01	402	1132.10	5.24
66	H80-27	45.05	72.10	2.03	402	1107.78	5.15
67	H80-28	45.05	71.00	2.03	402	1086.77	5.12
68	H80-29	45.05	72.59	2.03	402	1118.50	5.16
69	H90-10	27.27	80.78	2.05	453	1252.66	4.60
70	H90-11	27.27	80.69	2.05	453	1248.16	4.59
71	H90-12	27.27	81.59	2.05	450	1264.55	4.61
72	H90-13	27.03	81.64	2.03	450	1296.08	4.70
73	H90-14	30.00	88.98	2.25	451	1079.53	3.81
74	H90-15	35.00	88.98	2.25	451	1079.53	3.91
75	H90-16	31.53	82.25	2.03	451	1311.30	4.82

153

Table 4.1. SERIES 1

No.	Specimen	n/t	hw/t	r/t	l (mm)	M_c (KNmm)	F_{CB} (KN)
76	H90-17	31.53	81.00	2.03	451	1283.18	4.80
77	H90-18	36.04	81.52	2.03	451	1289.95	4.91
78	H90-19	35.71	80.10	2.01	451	1299.07	4.99
79	H90-20	36.36	81.82	2.05	451	1268.84	4.82
80	H90-21	40.54	81.32	2.03	451	1287.40	5.01
81	H90-22	40.18	80.09	2.01	451	1300.75	5.10
82	H90-23	40.54	81.32	2.03	450	1288.20	5.02
83	H90-24	45.45	89.57	2.27	451	1059.14	4.02
84	H90-25	40.54	81.18	2.03	451	1288.67	5.02
85	H90-26	45.45	81.77	2.05	451	1267.96	5.03
86	H90-27	45.05	81.45	2.03	451	1294.67	5.13
87	H90-28	45.05	81.27	2.03	451	1290.16	5.12
88	H90-29	44.64	79.96	2.01	451	1295.36	5.20

Table 4.1. SERIES 1

No.	Specimen	n/t	hw/t	r/t	l (mm)	M_c (KNmm)	F_{CB} (KN)
89	H90-30	45.05	81.43	2.03	451	1290.84	5.12
90	H100-1	30.00	99.35	2.25	500	1250.27	3.83
91	H100-2	30.00	99.96	2.25	501	1259.86	3.83
92	H100-3	30.00	98.97	2.25	502	1244.93	3.82
93	H100-4	30.30	102.09	2.27	501	1253.67	3.76
94	H100-5	30.30	101.29	2.27	502	1245.42	3.75
95	H100-6	35.35	101.53	2.27	501	1244.20	3.85
96	H100-7	35.71	102.58	2.30	501	1225.14	3.77
97	H100-8	35.00	99.90	2.25	501	1258.91	3.92
98	H100-9	35.00	99.60	2.25	502	1254.20	3.92
99	H100-10	35.00	99.90	2.25	501	1258.91	3.92
100	H100-11	40.00	99.60	2.25	502	1255.64	4.01
101	H100-12	40.00	98.51	2.25	502	1238.52	4.00

Table 4.1. SERIES 1

No.	Specimen	n/t	hw/t	r/t	l (mm)	M_c (KNmm)	F_{CB} (KN)
102	H100-13	40.00	99.75	2.25	502	1258.63	4.02
103	H100-14	40.00	99.60	2.25	502	1256.27	4.01
104	H100-15	40.82	101.81	2.30	502	1218.48	3.86
105	H100-16	45.00	98.77	2.25	502	1244.34	4.10
106	H100-17	45.00	100.08	2.25	502	1259.97	4.11
107	H100-18	45.00	100.26	2.25	502	1263.75	4.11
108	H100-19	45.45	102.32	2.27	501	1254.74	4.04
109	H100-20	45.45	100.39	2.27	503	1232.89	4.02
110	H100-21	50.00	99.52	2.25	503	1253.76	4.20
111	H100-22	50.51	101.39	2.27	502	1248.22	4.13
112	H100-23	50.00	100.11	2.25	502	1262.22	4.20
113	H100-24	51.02	102.48	2.30	502	1227.23	4.04
114	H100-25	50.00	100.24	2.25	502	1263.44	4.20

Table 4.1. SERIES 1

No.	Specimen	n/t	hw/t	r/t	l (mm)	M_c (KNmm)	F_{CB} (KN)
115	H100-52	30.00	101.33	2.25	500	1313.28	3.95
116	H100-53	30.61	104.89	2.30	500	1295.70	3.80
117	H100-54	30.00	100.52	3.25	500	1310.54	3.75
118	H100-55	30.00	99.39	3.25	500	1289.10	3.74
119	H100-56	30.61	100.82	4.34	500	1252.13	3.39
120	H100-57	30.93	101.87	4.38	500	1231.01	3.32
121	H100-58	40.40	103.56	2.27	500	1312.61	4.07
122	H100-59	40.82	105.44	2.30	500	1301.60	3.99
123	H100-60	40.40	100.61	3.28	500	1276.60	3.85
124	H100-61	41.67	104.04	3.39	500	1223.56	3.62
125	H100-62	40.00	99.36	4.25	500	1294.97	3.72
126	H100-63	40.40	99.01	4.29	500	1255.96	3.63
127	H100-64	50.51	103.29	2.27	500	1306.32	4.25

Table 4.1. SERIES 1

No.	Specimen	n/t	hw/t	r/t	l (mm)	M_c (KNmm)	F_{CB} (KN)
128	H100-65	51.55	106.25	2.32	500	1279.97	4.10
129	H100-66	49.50	98.95	2.23	500	1320.86	4.41
130	H100-67	50.51	100.42	3.28	500	1274.50	4.03
131	H100-68	49.50	97.40	4.21	500	1301.57	3.97
132	H100-69	50.00	98.00	4.25	500	1277.18	3.89

Table 4.2. SERIES 2

No.	Specimen	n/t	hw/t	r/t	l (mm)	M_c (KNmm)	F_{CB} (KN)
1	H60-6	40.40	60.59	3.79	175	621.24	4.23
2	H60-8	40.00	59.62	3.50	176	628.31	4.38
3	H60-11	40.00	60.26	3.25	176	631.41	4.45

Table 4.2. SERIES 2

No.	Specimen	n/t	hw/t	r/t	l (mm)	M_c (KNmm)	F_{CB} (KN)
4	H60-12	51.02	60.33	3.32	177	604.12	4.51
5	H60-38	50.00	61.12	3.75	177	644.93	4.57
6	H60-39	50.00	59.40	3.50	175	622.90	4.64
7	H80-35	40.40	80.61	3.79	230	886.10	4.13
8	H80-36	40.00	80.20	3.75	230	906.54	4.22
9	H80-37	40.00	79.48	3.75	230	898.25	4.22
10	H80-32	30.00	80.52	3.50	230	906.56	4.05
11	H80-33	30.00	79.00	3.75	230	891.24	3.99
12	H80-34	30.00	80.00	3.75	230	901.55	3.99
13	H100-28	30.30	101.01	4.04	300	1178.65	3.74
14	H100-29	40.00	99.58	4.00	300	1188.64	4.03
15	H100-30	40.00	99.98	4.00	300	1194.15	4.03
16	H100-31	40.00	101.94	4.00	300	1220.17	4.03

Table 4.2. SERIES 2

No.	Specimen	n/t	hw/t	r/t	l (mm)	M_c (KNmm)	F_{CB} (KN)
17	H100-32	50.51	101.94	4.04	300	1188.78	4.15
18	H100-33	50.00	99.78	4.00	300	1190.42	4.24
19	H100-34	50.00	99.80	4.00	300	1201.74	4.24
20	H100-36	30.00	101.88	2.25	300	1246.78	4.35
21	H100-37	30.30	99.41	3.28	300	1188.11	4.02
22	H100-41	39.60	100.97	2.23	300	1269.37	4.68
23	H100-42	40.40	103.05	2.27	300	1230.48	4.49
24	H100-44	39.60	98.63	3.22	300	1243.35	4.42
25	H100-47	50.51	102.40	2.27	300	1223.31	4.73
26	H100-49	50.50	100.83	3.28	300	1212.16	4.47
27	H100-50	50.00	98.00	4.25	300	1210.56	4.29

4.4.2. SPECIMENS UNDER WEB CRIPPLING ONLY (EOF, ETF AND ITF).

Table 4.3. SERIES 3 (EOF)

No.	Specimen	n/t	hw/t	r/t	F_C (KN)
1	S100-1	30.00	99.36	4.00	1.00
2	S100-2	30.30	100.93	4.04	0.97
3	S100-3	30.30	101.03	4.04	0.97
4	S100-4	40.40	101.84	4.04	1.05
5	S100-5	40.40	101.93	4.04	1.05
6	S100-6	40.00	101.14	4.00	1.08
7	S100-7	50.00	100.00	4.00	1.16
8	S100-8	50.00	100.16	4.00	1.16
9	S100-9	50.00	99.28	4.00	1.16
10	S80-1	30.00	79.68	3.75	1.10
11	S80-2	30.00	80.00	3.75	1.10
12	S80-3	30.00	80.20	3.75	1.10

Table 4.3. SERIES 3 (EOF)

No.	Specimen	n/t	hw/t	r/t	F_C (KN)
13	S80-4	40.00	79.58	3.75	1.19
14	S80-5	40.00	80.00	3.75	1.19
15	S80-6	40.82	83.65	3.83	1.12
16	S80-7	50.00	79.00	3.75	1.28
17	S80-8	50.00	79.50	3.75	1.27
18	S80-9	50.00	79.50	3.75	1.27
19	S60-1	30.30	60.40	3.54	1.18
20	S60-2	30.30	60.00	3.54	1.18
21	S60-3	30.00	59.68	3.50	1.21
22	S60-4	40.00	59.78	3.50	1.30
23	S60-5	40.00	59.70	3.50	1.30
24	S60-6	40.00	59.38	3.50	1.30
25	S60-7	50.00	60.00	3.50	1.39
26	S60-8	50.00	59.50	3.50	1.39

Table 4.4. SERIES 4 (ETF)

No.	Specimen	n/t	hw/t	r/t	F_C (KN)
1	H4-1	27.03	64.29	1.80	2.19
2	H4-2	27.27	65.09	2.05	2.06
3	H4-3	27.03	64.94	1.80	2.18
4	H4-4	36.36	65.56	1.82	2.29
5	H4-5	36.04	65.21	1.80	2.34
6	H4-6	36.70	66.29	1.83	2.24
7	H4-7	45.87	66.09	2.06	2.30
8	H4-8	45.87	66.26	2.06	2.30
9	H4-9	45.87	65.39	2.06	2.31
10	H5-1	27.27	93.64	2.05	1.89
11	H5-2	27.27	92.62	2.05	1.90
12	H5-3	27.03	91.73	2.03	1.94
13	H5-4	36.04	91.50	2.03	2.08
14	H5-5	36.04	91.68	2.03	2.08

Table 4.4. SERIES 4 (ETF)

No.	Specimen	n/t	hw/t	r/t	F_C (KN)
15	H5-6	36.36	92.56	2.05	2.04
16	H5-7	45.45	93.55	2.05	2.17
17	H5-8	45.45	93.18	2.05	2.17
18	H5-9	45.05	92.07	2.03	2.22

Table 4.5. SERIES 5 (ITF)

No.	Specimen	n/t	hw/t	r/t	F_C (KN)
1	H6-1	27.03	64.34	1.80	6.15
2	H6-2	27.03	64.14	1.80	6.16
3	H6-3	26.79	63.02	1.79	6.30
4	H6-4	36.04	64.07	1.80	6.23
5	H6-5	36.04	64.16	1.80	6.23
6	H6-6	36.04	63.68	1.80	6.24

Table 4.5. SERIES 5 (ITF)

No.	Specimen	n/t	hw/t	r/t	F_C (KN)
7	H6-7	44.64	63.48	1.79	6.43
8	H6-8	45.05	64.25	1.80	6.29
9	H6-9	45.05	65.93	1.80	6.30
10	H7-1	27.27	92.40	1.82	5.43
11	H7-2	27.03	91.82	1.79	5.55
12	H7-3	27.03	92.41	1.80	5.53
13	H7-4	35.71	90.63	1.79	5.74
14	H7-5	36.04	91.51	1.80	5.62
15	H7-6	36.36	92.24	1.82	5.50
16	H7-7	45.05	91.98	1.80	5.67
17	H7-8	45.45	92.75	1.82	5.55
18	H7-9	45.45	92.58	1.82	5.55

CHAPTER 5

APPLICATION OF

EUROPEAN RECOMMENDATIONS 1987

5.1. GENERAL.

This chapter discusses the application of the EUROPEAN RECOMMENDATIONS

for the design of light gauge steel members, 1987, in analysing the web crippling

strength of the specimens. These recommendations are also concerned with structural

members and frames for buildings and civil engineering and related structures which

are cold-formed by processes such as cold-rolling or press-braking. The

Recommendations give methods of design by calculation or testing for the load-

bearing capacity and service ability of elements and their connections under mainly

static loads. Methods of analysing the web crippling strength of the specimens are

explained in R4 of this Recommendation. The procedures involved in using the

European Recommendations for analysing the web crippling strength of the

specimens are generally similar to those of using BS 5950 Part 5 1987.

The calculation of the section properties of the specimens in the European

Recommendations is also based on the effective cross sections determined by rules

given in R3 of the Recommendations. The cross section of the specimen used in this

analysis was still in the form of an idealized cross section as shown in Figure 4.1,

because according to the European Recommendations the cross section may be

assumed to be concentrated at the centre line and the round corner may be ignored,

i.e. a cross section may be assumed to be made up of flat elements with sharp

corners. The Recomendations permit one to use this assumption when the inner

corner radius $r \leq 5t$ and $r/b_p < 0.15$, where t and b_p are as defined in Figure 4.1. The moment capacity in this Recommendation is termed the design strength with respect to bending moment and its determination should also be based on the effective cross section. M_d is used by The European Recommendations to represent the design strength with respect to bending moment.

5.2. DETERMINATION OF THE DESIGN STRENGTH WITH RESPECT TO BENDING MOMENT.

Before determining the design strength with respect to bending moment, the analysis was first carried out to calculate the effective width of compression elements. In The European Recommendations, the effect of shear lag should also be considered in calculating the effective width for flexural members with short spans and this can be carried out according to the clause in R4.3, i.e. :

" *In flexural members for which the ratio l/b is less than 20, the effective area of either tension or compression flange is to be reduced due to the effect of shear lag.* "

In this above clause l is the span length and b is the full width of the flange.

Methods of determining the effect of shear lag in R4.3 can be used for stiffened and unstiffened elements. In the case of unstiffened elements such as the top and bottom flanges of the specimens used in this research program, the reduced effective width

due to the effect of shear lag is formulated as follows :

- Unstiffened flange in compression :

$$b_{ef} = \psi_s' \, \rho \, b_p \quad \dots \dots \dots \dots \dots \quad (5.2.1)$$

- Unstiffened flange in tension :

$$b_{ef} = \psi_s' \, b_p \quad \dots \dots \dots \dots \dots \dots \quad (5.2.2)$$

Where :

b_{ef} : reduced effective width.

b_p : flat width of the top or bottom flange (see Figure 4.1).

ψ_s' : $0.85 \, \psi_s$

ψ_s : reduction coefficient accounting for shear lag and it is obtainable from

Figure 5.2, where curve 1 in this figure is to be used for midspan and curve

2 is to be used for support and in the region of a point load.

ρ : reduction coefficient accounting for local buckling.

According to R3 of this Recommendations, the value of ρ for stiffened and unstiffened flanges may be obtained from :

$$\rho = 1 \quad ; \quad \text{when } \lambda_p \leq 0.673 \quad \dots \dots \dots \dots \dots \quad (5.2.3)$$

$$\rho = \frac{(1 - \dfrac{0.22}{\lambda_p})}{\lambda_p} \quad ; \quad \text{when } \lambda_p > 0.673 \quad \dots \dots \dots \dots \dots \quad (5.2.4)$$

λ_p is a slenderness parameter and in the case of unstiffened elements under compression, the expression of λ_p can be derived by using the rules given in R3.3,

i.e. :

$$0 \leq \psi \leq 1$$
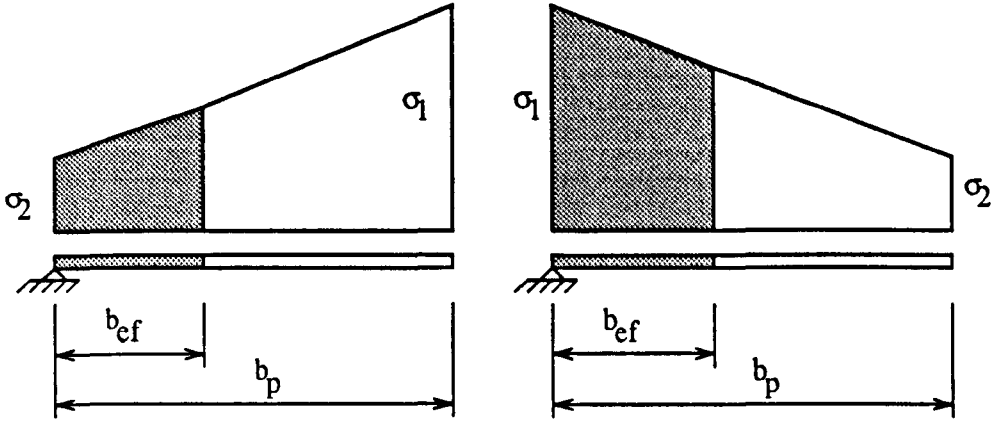
Case Ia : $\psi = \sigma_2/\sigma_1$ Case IIa : $\psi = \sigma_2/\sigma_1$

Figure 5.1. Unstiffened element under non uniform compression.

$$\text{Case Ia :} \quad \lambda_p = \frac{0.75 \ b_p}{t} \sqrt{\frac{(3 + \psi) \ f_{ty}}{E}} \ \ldots\ldots\ldots (5.2.5)$$

$$\text{Case IIa :} \quad \lambda_p = \frac{0.75 \ b_p}{t} \sqrt{\frac{(1 + 3\psi) \ f_{ty}}{E}} \ \ldots\ldots (5.2.6)$$

It can be seen in Figure 4.2 that the top flange of the specimen is subjected to uniform compression, so that the value of ψ used in this analysis must be equal to 1. Substitution of $\psi = 1$ into equations (5.2.5) and (5.2.6) gives :

$$\lambda_p = \frac{0.75 \ b_p}{t} \sqrt{\frac{4 \ f_{ty}}{E}} \ \ldots\ldots\ldots\ldots (5.2.7)$$

In order to account for the effect of shear lag, f_{ty} should be replaced by $\psi_s' \ f_{ty}$ so that equation (5.2.7) becomes :

169

$$\lambda_p = \frac{0.75\ b_p}{t} \sqrt{\frac{4\ x\ 0.85\ \psi_s\ f_{ty}}{E}}$$

or

$$\lambda_p = \frac{0.75\ b_p}{t} \sqrt{\frac{3.4\ \psi_s\ f_{ty}}{E}} \quad \dots \dots \dots \quad (5.2.8)$$

where :

E   : Modulus of elasticity.

f_{ty} : Design yield stress.

$f_{ty} = f_{yb}$ (tensile yield stress of the basic material).

Equation (5.2.8) should be used together with either equation (5.2.3) or (5.2.4) in analysing the effective width of unstiffened elements of flexural members with short spans (l/b < 20). If the ratio of l/b ≥ 20, the effective width of the unstiffened elements will be :

$$Compression\ elements\ :\ \ b_{ef} = \rho\ b_p \quad \dots \dots \quad (5.2.9)$$

$$Tension\ elements\ :\ \ b_{ef} = b_p\ (fully\ effective) \quad \dots \quad (5.2.10)$$

On the basis of an example of determining the effective cross section of a thin-walled flexural members as shown in Figure 2.50, the analysis of effective widths of the specimens used in this research program was therefore carried out only for their top flanges and compression portions of their webs (see Figure 5.4), whereas their bottom flanges were still fully effective.
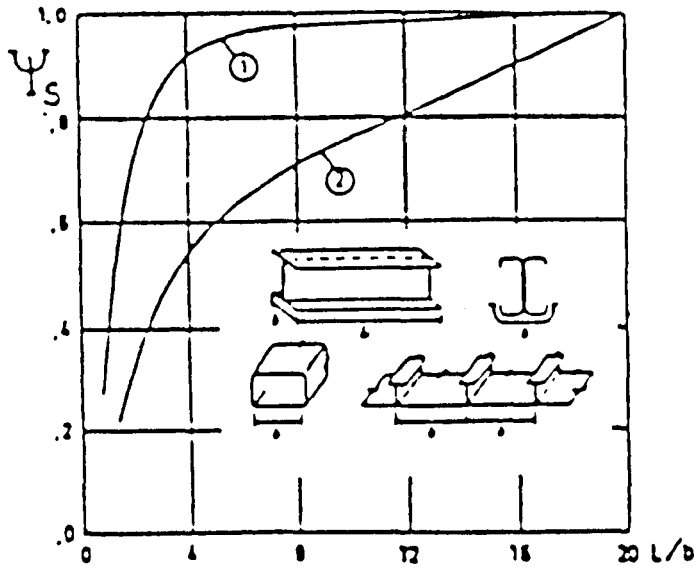
Figure 5.2. Reduction coefficient ψ_s.

Figure 4.2 also shows that the web of the specimen is a stiffened element and subjected to stress gradient. The analysis of the effective width of this element should still be based on the rules given in R3.2, i.e. :
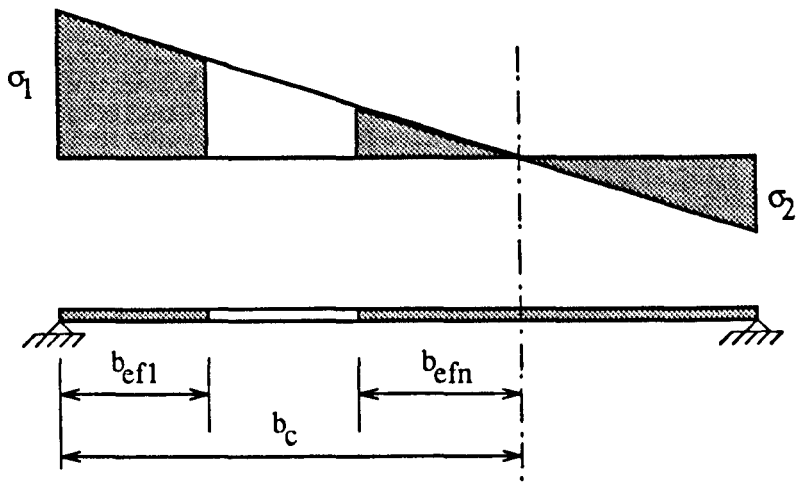
$$\sigma_2 < 0 < \sigma_1 \; ; \; \psi = \sigma_2 / \sigma_1$$

Figure 5.3. Stiffened element under stress gradient.

171

$$b_{ef1} = 0.4 \; \rho \; b_c \qquad ; \qquad b_{efn} = 1.5 \; b_{ef1} \; \ldots \ldots \; (5.2.11)$$

Reduction coefficient accounting for local buckling ρ is still determined from either

equation (5.2.3) or (5.2.4), but the slenderness parameter (λ_p) is calculated from :

$$\lambda_p = \frac{1.052 \; b_p}{t} \sqrt{\frac{f_{ty}}{E \; K_\sigma}} \; \ldots \ldots \ldots \; (5.2.12)$$

where :

$$K_\sigma = [\frac{(1 - \psi)}{(0.362 - 0.103 \; \psi)}]^2 \; ; \; when \; -0.5 < \psi < 0 \; \ldots \; (5.2.13)$$

or

$$K_\sigma = 5.85 \; (1 - \psi)^2 \; ; \quad when \quad \psi \leq -0.5 \; \ldots \ldots \ldots \; (5.2.14)$$

According to R4.2 that " *In order to avoid an iterative procedure, the*

effective portions of the web may be based on ψ *obtained by assuming*

the compression flange reduced but the web being fully effective " and on

the basis of Figure 2.50, the determination of the effective cross section of the

specimen was carried out by using Figure 5.4. From Figure 5.4 (a), the initial position

of the neutral axis X1-X1 :

$$h_2 = \frac{b_{ef} \times h_p + 0.5 \; h_p^2 + b_p \times 0}{b_{ef} + h_p + b_p} \; \ldots \ldots \ldots \ldots \; (5.2.15)$$

$$h_1 = h_p - h_2 \; \ldots \ldots \ldots \ldots \; (5.2.16)$$

172

where :

b_{ef} : effective width of the top flange.

h_p : height of the web.

$$For \ \frac{l}{b} < 20 \ , \quad b_{ef} = 0.85 \ \psi_s \ \rho \ b_p \ ; \quad For \ \frac{l}{b} \geq 20 \ , \quad b_{ef} = \rho \ b_p$$

(a)   (b)
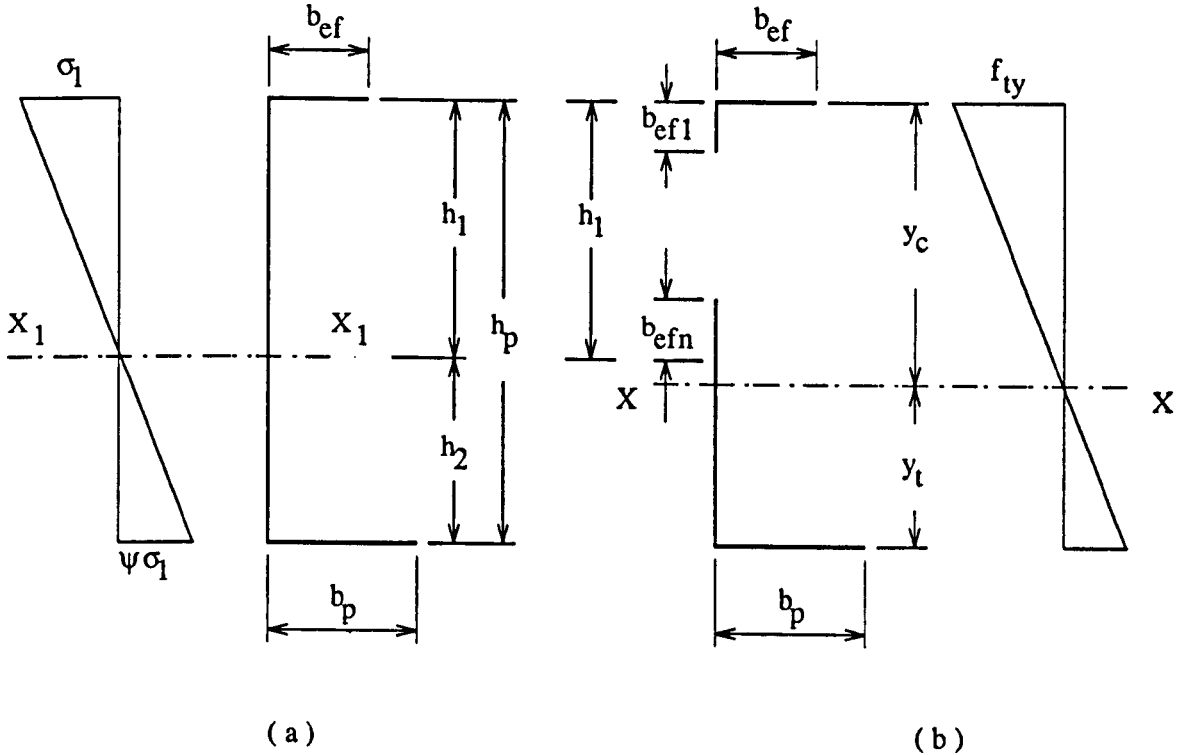
Figure 5.4. Determination of effective cross section of the specimen.

By examining the stress gradient in Figure 5.4 (a), the value of ψ was obtained from

the following relationship.

$$\frac{\sigma_1}{-\psi \ \sigma_1} = \frac{h_1}{h_2} \quad ; \quad \psi = -\frac{h_2}{h_1} \quad \ldots \ldots \ldots (5.2.17)$$

The value of ψ obtained from equation (5.2.17) was then used with equations (5.2.13)

or (5.2.14) and (5.2.12) for calculating b_{ef1} and b_{efn} from equation (5.2.11), where b_c

173

$= h_1$ so that the equation can be rewritten as follows :

$$b_{ef1} = 0.4 \; \rho \; h_1 \qquad ; \qquad b_{efn} = 0.6 \; \rho \; h_1$$

The final position of the neutral axis X-X :

$$Y_t = \frac{b_{ef} \; h_p + b_{ef1} \; h_p - 0.5 b_{ef1}^2 + b_{efn} \; h_2 + 0.5 b_{efn}^2 + 0.5 h_2^2}{b_{ef} + b_{ef1} + b_{efn} + h_2 + b_p}$$

$$\dots\dots\dots\dots\dots\dots (5.2.18)$$

$$Y_c = h_p - Y_t \dots\dots\dots\dots\dots (5.2.19)$$

The complete derivation of equation (5.2.18) can be seen in appendix B-2. The second moment of the effective cross section about the neutral axis X-X (I_X) :

$$I_X = t \; [\; Y_c^2 \; b_{ef} + \frac{b_{ef1}^3 + (b_{efn} + h_2 - Y_t)^3 + Y_t^3)}{3} + Y_t^2 \; b_p \;]$$

$$\dots\dots\dots\dots\dots\dots\dots\dots (5.2.20)$$

The derivation of the above formula is presented in appendix B-3. When yielding first occurs in the compression edge of the web, the section modulus in the compression region may be formulated as follows :

$$W_{efc} = \frac{I_X}{Y_c} \dots\dots\dots\dots\dots (5.2.21)$$

The design strength with respect to bending moment (M_d) can be calculated from:

$$M_d = f_{ty} \; W_{efc} \dots\dots\dots\dots\dots (5.2.22)$$

In equations (5.2.18) and (5.2.20), the value of $b_{ef} = 0.85 \; \psi_s \rho \; b_p$ for $l/b < 20$ and $b_{ef} = \rho \; b_p$ for $l/b \geq 20$.

174

5.3. CALCULATION OF ULTIMATE WEB CRIPPLING LOAD.

In these Recommendations, the calculation of the ultimate web crippling load of specimens under combined web crippling and bending (F_{CB}) can be carried out by using equation (2.4.9) or (2.4.10) in subchapter 2.4. It can also be concluded from these equations that the strength of web in equation (2.4.9) is more affected by bending moment M only while in equation (2.4.10) it is affected by interactions of bending moment M and concentrated load R. Because one of the main objectives of this research program was aimed at predicting the strength of beams under combined concentrated load and bending moment, the equation (2.4.10) was therefore used to calculate ultimate web crippling loads of all specimens under combined web crippling and bending and the symbol of concentrated load R in the equation was replaced by F_{CB}. By setting M in the equation (2.4.10) with M_{max} as indicated in Figure 4.4, the formula for predicting F_{CB} can be derived as follows :

$$\frac{F_{CB} \; (\; 1 \; - \; n \;)}{4 \; M_d} \; + \; \frac{F_{CB}}{R_d} \; \leq \; 1.25$$

$$\frac{F_{CB} \; [\; R_d \; (\; 1 \; - \; n \;) \; + \; 4 \; M_d \;]}{4 \; M_d \; R_d} \; \leq \; 1.25$$

$$F_{CB} \; = \; \frac{1.25 \; M_d \; R_d}{R_d \; (\; 1 \; - \; n \;) \; + \; M_d} \; \dots\dots\dots\dots\dots\dots\dots \; (5.3.1)$$

In using the above formula for predicting the ultimate web crippling load F_{CB}, the design strength with respect to web crippling only R_d was calculated from equation

175

(2.4.6).

An example of using The European Recommendations - 1987 is the analysis of the previous problem (specimen H90-26). In using this recommendation, the modulus of elasticity E should also be included in the analysis and for this specimen the value of E was equal to 196850 MPa. The ratio of l/b = 451/42.14 = 10.70 < 20, the specimen was therefore considered as a flexural member with a short span and according to R4.3, the effect of shear lag should be considered in calculating the effective width of either the top or bottom flange. In this analysis, the effective width of the top flange was chosen to be reduced due to the effect of shear lag.

* Calculation of the effective width of the top flange :

The top flange is an unstiffened element in compression and the calculation of its effective width is carried out as follows :

$$\psi_s' = 0.85 \ \psi_s$$

where $\psi_s = 0.956$ (*estimated using Figure* 5.2)

The slenderness parameter (λ_p) for the top flange is obtained from :

$$\lambda_p = \frac{0.75 \times 41.59}{1.10} \sqrt{\frac{3.4 \times 0.956 \times 303}{196850}}$$

$$\lambda_p = 2.01 > 0.673$$

On the basis of the above value, the reduction coefficient accounting for local

176

buckling is calculated by using equation (5.2.4), so that the coefficient of local

buckling for the top flange is :

$$\rho = \frac{(1 - \frac{0.22}{2.01})}{2.01} = 0.443$$

Substitution of ρ and ψ_s' into equation (5.2.1) gives the effective width of the top

flange (b_{ef}) :

$$b_{ef} = (0.850 \; x \; 0.956 \; x \; 0.443 \; x \; 41.59) \; mm = 14.97 \; mm$$

* Calculation of the effective width of the compressive portion of the web :

The web of the specimen was subjected to stress gradient and the effective width of

its compressive portion should be determined according to R4.2 and Figure 5.4. The

initial position of the neutral axis X1-X1 of the specimen H90-26 is calculated from

equations (5.2.15) and (5.2.16) :

$$h_2 = \frac{14.97 \; x \; 91.05 + \frac{91.05^2}{2}}{14.97 + 91.05 + 41.59} \; mm = \frac{5508.07}{147.61} \; mm = 37.32 \; mm$$

$$h_1 = (91.05 - 37.32) \; mm = 53.73 \; mm$$

$$\psi = - \frac{h_2}{h_1} = - \frac{37.32}{53.73} = - 0.69 < - 0.5$$

K_σ is calculated using equation (5.2.14) :

177

$$K_\sigma = 5.85 \ (1 + 0.69 \ )^2 = 16.71$$

$$\lambda_p = \frac{1.052 \ x \ 41.59}{1.10} \sqrt{\frac{303}{196850 \ x \ 16.71}} = 0.38 < 0.673$$

Thus the reduction coefficient accounting for local buckling in the web is obtained

from equation (5.2.3), i.e. :

$$\rho = 1$$

The effective width of the compressive portion of the web :

$$b_{ef1} = 0.4 \ x \ 1 \ x \ h_1 = 0.4 \ x \ 1 \ x \ 53.73 \ mm = 21.49 \ mm$$

$$b_{efn} = 0.6 \ x \ 1 \ x \ h_1 = 0.6 \ x \ 53.73 \ mm = 32.24 \ mm$$

The bottom flange is still fully effective and the final position of the neutral axis X-X

becomes :

$$Y_t = \frac{14.97x91.05 \ + \ 21.49x91.05}{14.97 \ + \ 21.49 \ + \ 32.24 \ + \ 37.32 \ + \ 41.59}$$

$$- \ \frac{0.5x21.49^2 \ + \ 32.24x37.32 \ + \ 0.5x(32.24^2 \ + \ 37.32^2)}{14.97 \ + \ 21.49 \ + \ 32.24 \ + \ 37.32 \ + \ 41.59}$$

$$Y_t = \frac{5508.07}{147.61} = 37.32 \ mm \ ; \ Y_c = (91.05-37.32) \ mm = 53.73 \ mn$$

The second moment of the effective cross section about the neutral axis X-X :

$$I_x = 1.10 \ x \ [53.73^2x14.97 \ + \ \frac{21.49^3+(32.24+37.32-37.32)^3}{3}$$

$$+ \ \frac{37.32^3}{3} \ + \ 37.32^2x41.59] = 146242.32 \ mm^4$$

The elastic section modulus in compression region :

$$W_{efc} = \frac{I_x}{Y_c} = \frac{146242.32}{53.73} \ mm^3 = 2721.80 \ mm^3$$

Hence, the design strength with respect to bending moment (M_d) :

$$M_d = 303 \ x \ 2721.80 \ Nmm = 824705.40 \ Nmm = 824.71 \ KNmm$$

The web crippling load of the specimen H90-26 is obtained from equation (5.3.1),

but before doing that the design strength with respect to crippling R_d is first

calculated using equation (2.4.6), i.e. :

$$R_d = 0.114 \ t^2 \ \sqrt{f_{ty} \ E} \ (1 - 0.1 \ \sqrt{\frac{r}{t}}) \ (0.5 + \sqrt{\frac{0.02 \ l_a}{t}})$$

$$x \ (2.4 + (\frac{\theta}{90})^2)$$

$$R_d = 0.114 \ x \ 1.10^2 \ \sqrt{303 \ x \ 196850} \ (1 - 0.1\sqrt{\frac{2.25}{1.10}})$$

$$x \ (0.5 + \sqrt{\frac{0.02 \ x \ 50}{1.10}}) \ (2.4 + 1)$$

$$R_d = 4150.29 \ N = 4.15 \ KN$$

The ultimate web crippling load F_{CB} :

$$F_{CB} = \frac{1.25 \ x \ 824705.40 \ x \ 4510.29 \ x \ 4}{4510.29 \ (451-50) \ + \ 4 \ x \ 824705.40} \ N$$

$$F_{CB} = \frac{4649575648 \ x \ 4}{5107447.89} \ N = \underline{3641.41} \ N = \underline{3.64} \ KN$$

In the case of specimens under web crippling only, the ultimate web crippling loads

(F_C) were predicted by using equation (2.4.5) for EOF and ETF loading conditions

and equation (2.4.6) for ITF loading condition.The application of The European Recommendations - 1987 for predicting the ultimate web crippling loads of all specimens was also performed using a computer program and the program can be seen in appendix D. Estimated results of F_{CB} and F_C for all specimens are presented in the following tables.

5.4. RESULTS.

5.4.1. SPECIMENS UNDER COMBINED WEB CRIPPLING AND BENDING (IOF).

Table 5.1. SERIES 1

No.	Specimen	n/t	hw/t	r/t	l (mm)	M_d (KNmm)	F_{CB} (KN)
1	H60-2	27.27	53.42	2.05	300	442.90	3.03
2	H60-4	27.27	53.42	2.05	300	446.40	3.04
3	H60-7	27.27	54.25	2.05	300	456.91	3.06
4	H60-9	27.27	54.23	2.05	300	452.58	3.05
5	H60-10	27.27	54.00	2.05	300	454.25	3.06

Table 5.1. SERIES 1

No.	Specimen	n/t	hw/t	r/t	l (mm)	M_d (KNmm)	F_{CB} (KN)
6	H60-18	31.53	54.86	2.03	300	469.32	3.24
7	H60-19	31.53	54.06	2.03	300	461.05	3.22
8	H60-20	31.53	54.52	2.03	300	466.04	3.23
9	H60-21	31.53	53.65	2.03	300	456.44	3.21
10	H60-22	31.53	53.95	2.03	300	461.70	3.22
11	H60-23	36.04	54.06	2.03	300	461.05	3.33
12	H60-24	36.04	54.06	2.03	300	461.05	3.33
13	H60-25	36.04	54.41	2.03	300	464.86	3.34
14	H60-26	36.04	54.77	2.03	300	468.99	3.35
15	H60-27	36.04	54.06	2.03	300	461.91	3.33
16	H60-28	40.54	55.09	2.03	300	471.85	3.46
17	H60-29	40.54	54.54	2.03	300	466.37	3.45
18	H60-30	40.54	54.64	2.03	300	467.48	3.45

Table 5.1. SERIES 1

No.	Specimen	n/t	hw/t	r/t	l (mm)	M_d (KNmm)	F_{CB} (KN)
19	H60-31	40.54	54.36	2.03	300	464.01	3.44
20	H60-32	40.54	53.74	2.03	300	458.09	3.43
21	H60-33	44.64	54.71	2.01	304	480.30	3.62
22	H60-34	45.05	53.26	2.03	302	454.08	3.51
23	H60-35	45.05	55.71	2.03	302	478.83	3.58
24	H60-36	45.05	55.67	2.03	300	477.96	3.58
25	H60-37	45.05	55.21	2.03	300	472.80	3.57
26	H70-6	27.03	62.35	2.03	350	562.22	3.14
27	H70-7	27.27	62.46	2.05	350	549.12	3.08
28	H70-8	27.27	62.46	2.05	350	549.12	3.08
29	H70-11	31.53	63.42	2.03	351	572.55	3.27
30	H70-12	31.53	63.22	2.03	351	569.31	3.26
31	H70-13	31.53	63.14	2.03	351	568.21	3.26

Table 5.1. SERIES 1

No.	Specimen	n/t	hw/t	r/t	l (mm)	M_d (KNmm)	F_{CB} (KN)
32	H70-14	31.53	63.79	2.03	350	576.79	3.28
33	H70-15	31.53	62.95	2.03	351	567.79	3.26
34	H70-18	36.04	63.68	2.03	352	574.61	3.38
35	H70-19	36.04	63.33	2.03	352	571.31	3.37
36	H70-20	36.04	63.47	2.03	351	570.91	3.37
37	H70-21	40.54	63.51	2.03	350	572.16	3.48
38	H70-23	40.54	63.90	2.03	350	576.46	3.49
39	H70-24	40.54	63.51	2.03	350	572.82	3.48
40	H70-30	40.54	63.22	2.03	350	569.41	3.48
41	H70-25	45.05	63.13	2.03	350	568.32	3.57
42	H70-26	45.05	63.22	2.03	350	571.05	3.58
43	H70-27	45.05	62.76	2.03	350	564.95	3.56
44	H70-28	45.05	63.13	2.03	350	569.39	3.57

Table 5.1. SERIES 1

No.	Specimen	n/t	hw/t	r/t	l (mm)	M_d (KNmm)	F_{CB} (KN)
45	H70-29	45.05	63.56	2.03	350	573.53	3.58
46	H80-9	27.27	72.30	2.05	398	693.64	3.18
47	H80-10	27.27	72.51	2.05	398	697.13	3.19
48	H80-11	27.03	72.55	2.03	402	714.30	3.24
49	H80-12	27.03	72.67	2.03	402	715.15	3.24
50	H80-13	27.03	73.26	2.03	402	721.83	3.25
51	H80-14	31.53	72.00	2.03	402	707.79	3.34
52	H80-15	31.53	72.12	2.03	402	708.00	3.34
53	H80-16	31.53	71.94	2.03	402	706.36	3.34
54	H80-17	36.04	72.23	2.03	402	710.36	3.46
55	H80-18	36.04	71.82	2.03	402	704.36	3.44
56	H80-19	36.04	72.44	2.03	402	712.72	3.46
57	H80-30	36.04	72.28	2.03	402	710.54	3.46

Table 5.1. SERIES 1

No.	Specimen	n/t	hw/t	r/t	l (mm)	M_d (KNmm)	F_{CB} (KN)
58	H80-31	36.04	71.89	2.03	402	705.87	3.45
59	H80-20	40.54	72.16	2.03	402	708.89	3.55
60	H80-21	40.54	73.04	2.03	402	720.43	3.58
61	H80-22	40.54	71.68	2.03	402	702.24	3.54
62	H80-23	40.54	72.96	2.03	403	718.15	3.57
63	H80-24	40.54	72.71	2.03	402	715.88	3.57
64	H80-25	45.05	72.85	2.03	402	716.19	3.67
65	H80-26	44.64	71.82	2.01	402	722.68	3.71
66	H80-27	45.05	72.10	2.03	402	707.39	3.65
67	H80-28	45.05	71.00	2.03	402	692.75	3.62
68	H80-29	45.05	72.59	2.03	402	714.59	3.66
69	H90-10	27.27	80.78	2.05	453	811.89	3.20
70	H90-11	27.27	80.69	2.05	453	809.39	3.20

Table 5.1. SERIES 1

No.	Specimen	n/t	hw/t	r/t	l (mm)	M_d (KNmm)	F_{CB} (KN)
71	H90-12	27.27	81.59	2.05	450	820.97	3.22
72	H90-13	27.03	81.64	2.03	450	842.32	3.28
73	H90-14	30.00	88.98	2.25	451	705.42	2.73
74	H90-15	35.00	88.98	2.25	451	705.42	2.83
75	H90-16	31.53	82.25	2.03	451	852.53	3.41
76	H90-17	31.53	81.00	2.03	451	833.06	3.39
77	H90-18	36.04	81.52	2.03	451	838.85	3.50
78	H90-19	35.71	80.10	2.01	451	842.24	3.54
79	H90-20	36.36	81.82	2.05	451	824.11	3.45
80	H90-21	40.54	81.32	2.03	451	836.62	3.60
81	H90-22	40.18	80.09	2.01	451	842.96	3.65
82	H90-23	40.54	81.32	2.03	450	837.00	3.61
83	H90-24	45.45	89.57	2.27	451	692.08	2.96

Table 5.1. SERIES 1

No.	Specimen	n/t	hw/t	r/t	l (mm)	M_d (KNmm)	F_{CB} (KN)
84	H90-25	40.54	81.18	2.03	451	836.53	3.60
85	H90-26	45.45	81.77	2.05	451	823.47	3.64
86	H90-27	45.05	81.45	2.03	451	840.69	3.70
87	H90-28	45.05	81.27	2.03	451	837.68	3.70
88	H90-29	44.64	79.96	2.01	451	839.78	3.74
89	H90-30	45.05	81.43	2.03	451	838.82	3.70
90	H100-1	30.00	99.35	2.25	500	833.74	2.79
91	H100-2	30.00	99.96	2.25	501	841.11	2.79
92	H100-3	30.00	98.97	2.25	502	829.43	2.78
93	H100-4	30.30	102.09	2.27	501	840.71	2.76
94	H100-5	30.30	101.29	2.27	502	832.95	2.75
95	H100-6	35.35	101.53	2.27	501	833.65	2.85
96	H100-7	35.71	102.58	2.30	501	821.93	2.81

187

Table 5.1. SERIES 1

No.	Specimen	n/t	hw/t	r/t	l (mm)	M_d (KNmm)	F_{CB} (KN)
97	H100-8	35.00	99.90	2.25	501	840.38	2.90
98	H100-9	35.00	99.60	2.25	502	836.76	2.89
99	H100-10	35.00	99.90	2.25	501	840.38	2.90
100	H100-11	40.00	99.60	2.25	502	837.37	2.98
101	H100-12	40.00	98.51	2.25	502	824.24	2.97
102	H100-13	40.00	99.75	2.25	502	839.45	2.99
103	H100-14	40.00	99.60	2.25	502	837.63	2.98
104	H100-15	40.82	101.81	2.30	502	815.05	2.89
105	H100-16	45.00	98.77	2.25	502	830.50	3.06
106	H100-17	45.00	100.08	2.25	502	841.80	3.08
107	H100-18	45.00	100.26	2.25	502	844.39	3.08
108	H100-19	45.45	102.32	2.27	501	842.38	3.04
109	H100-20	45.45	100.39	2.27	503	822.85	3.02

Table 5.1. SERIES 1

No.	Specimen	n/t	hw/t	r/t	l (mm)	M_d (KNmm)	F_{CB} (KN)
110	H100-21	50.00	99.52	2.25	503	836.14	3.15
111	H100-22	50.51	101.39	2.27	502	834.68	3.12
112	H100-23	50.00	100.11	2.25	502	842.92	3.16
113	H100-24	51.02	102.48	2.30	502	822.29	3.06
114	H100-25	50.00	100.24	2.25	502	844.14	3.16
115	H100-52	30.00	101.33	2.25	500	898.72	2.98
116	H100-53	30.61	104.89	2.30	500	891.42	2.90
117	H100-54	30.00	100.52	3.25	500	893.03	2.90
118	H100-55	30.00	99.39	3.25	500	877.32	2.89
119	H100-56	30.61	100.82	4.34	500	849.96	2.72
120	H100-57	30.93	101.87	4.38	500	837.01	2.68
121	H100-58	40.40	103.56	2.27	500	901.25	3.16
122	H100-59	40.82	105.44	2.30	500	897.02	3.11

Table 5.1. SERIES 1

No.	Specimen	n/t	hw/t	r/t	l (mm)	M_d (KNmm)	F_{CB} (KN)
123	H100-60	40.40	100.61	3.28	500	869.12	3.04
124	H100-61	41.67	104.04	3.39	500	835.86	2.90
125	H100-62	40.00	99.36	4.25	500	879.68	3.03
126	H100-63	40.40	99.01	4.29	500	851.32	2.96
127	H100-64	50.51	103.29	2.27	500	896.98	3.33
128	H100-65	51.55	106.25	2.32	500	882.12	3.24
129	H100-66	49.50	98.95	2.23	500	898.19	3.41
130	H100-67	50.51	100.42	3.28	500	867.20	3.22
131	H100-68	49.50	97.40	4.21	500	880.88	3.24
132	H100-69	50.00	98.00	4.25	500	864.27	3.18

Table 5.2. SERIES 2

No.	Specimen	n/t	hw/t	r/t	l (mm)	M_d (KNmm)	F_{CB} (KN)
1	H60-6	40.40	60.59	3.79	175	390.03	3.22
2	H60-8	40.00	59.62	3.50	176	393.83	3.29
3	H60-11	40.00	60.26	3.25	176	396.70	3.32
4	H60-12	51.02	60.33	3.32	177	378.56	3.43
5	H60-38	50.00	61.12	3.75	177	405.48	3.55
6	H60-39	50.00	59.40	3.50	175	390.59	3.54
7	H80-35	40.40	80.61	3.79	230	577.13	3.26
8	H80-36	40.00	80.20	3.75	230	590.14	3.32
9	H80-37	40.00	79.48	3.75	230	583.80	3.31
10	H80-32	30.00	80.52	3.50	230	591.00	3.08
11	H80-33	30.00	79.00	3.75	230	578.80	3.05
12	H80-34	30.00	80.00	3.75	230	586.94	3.05
13	H100-28	30.30	101.01	4.04	300	795.94	2.99

Table 5.2. SERIES 2

No.	Specimen	n/t	hw/t	r/t	l (mm)	M_d (KNmm)	F_{CB} (KN)
14	H100-29	40.00	99.58	4.00	300	801.12	3.29
15	H100-30	40.00	99.98	4.00	300	805.91	3.30
16	H100-31	40.00	101.94	4.00	300	826.49	3.31
17	H100-32	50.51	101.94	4.04	300	804.61	3.47
18	H100-33	50.00	99.78	4.00	300	802.77	3.52
19	H100-34	50.00	99.80	4.00	300	809.03	3.52
20	H100-36	30.00	101.88	2.25	300	862.19	3.41
21	H100-37	30.30	99.41	3.28	300	816.24	3.23
22	H100-41	39.60	100.97	2.23	300	876.44	3.75
23	H100-42	40.40	103.05	2.27	300	852.40	3.63
24	H100-44	39.60	98.63	3.22	300	853.63	3.63
25	H100-47	50.51	102.40	2.27	300	846.14	3.87
26	H100-49	50.50	100.83	3.28	300	834.59	3.75

Table 5.2. SERIES 2

No.	Specimen	n/t	hw/t	r/t	l (mm)	M_d (KNmm)	F_{CB} (KN)
27	H100-50	50.00	98.00	4.25	300	828.59	3.70

5.4.2. SPECIMENS UNDER WEB CRIPPLING ONLY (EOF, ETF AND ITF).

Table 5.3. SERIES 3 (EOF)

No.	Specimen	n/t	hw/t	r/t	F_C (KN)
1	S100-1	30.00	99.36	4.00	1.53
2	S100-2	30.30	100.93	4.04	1.50
3	S100-3	30.30	101.03	4.04	1.50
4	S100-4	40.40	101.84	4.04	1.64
5	S100-5	40.40	101.93	4.04	1.64
6	S100-6	40.00	101.14	4.00	1.67

Table 5.3. SERIES 3 (EOF)

No.	Specimen	n/t	hw/t	r/t	F_C (KN)
7	S100-7	50.00	100.00	4.00	1.80
8	S100-8	50.00	100.16	4.00	1.80
9	S100-9	50.00	99.28	4.00	1.80
10	S80-1	30.00	79.68	3.75	1.54
11	S80-2	30.00	80.00	3.75	1.54
12	S80-3	30.00	80.20	3.75	1.54
13	S80-4	40.00	79.58	3.75	1.69
14	S80-5	40.00	80.00	3.75	1.69
15	S80-6	40.82	83.65	3.83	1.63
16	S80-7	50.00	79.00	3.75	1.82
17	S80-8	50.00	79.50	3.75	1.82
18	S80-9	50.00	79.50	3.75	1.82
19	S60-1	30.30	60.40	3.54	1.53
20	S60-2	30.30	60.00	3.54	1.53

Table 5.3. SERIES 3 (EOF)

No.	Specimen	n/t	hw/t	r/t	F_C (KN)
21	S60-3	30.00	59.68	3.50	1.56
22	S60-4	40.00	59.78	3.50	1.70
23	S60-5	40.00	59.70	3.50	1.70
24	S60-6	40.00	59.38	3.50	1.70
25	S60-7	50.00	60.00	3.50	1.83
26	S60-8	50.00	59.50	3.50	1.83

Table 5.4. SERIES 4 (ETF)

No.	Specimen	n/t	hw/t	r/t	F_C (KN)
1	H4-1	27.03	64.29	1.80	2.16
2	H4-2	27.27	65.09	2.05	2.10
3	H4-3	27.03	64.94	1.80	2.16
4	H4-4	36.36	65.56	1.82	2.32

195

Table 5.4. SERIES 4 (ETF)

No.	Specimen	n/t	hw/t	r/t	F_c (KN)
5	H4-5	36.04	65.21	1.80	2.35
6	H4-6	36.70	66.29	1.83	2.28
7	H4-7	45.87	66.09	2.06	2.43
8	H4-8	45.87	66.26	2.06	2.43
9	H4-9	45.87	65.39	2.06	2.43
10	H5-1	27.27	93.64	2.05	2.10
11	H5-2	27.27	92.62	2.05	2.10
12	H5-3	27.03	91.73	2.03	2.14
13	H5-4	36.04	91.50	2.03	2.33
14	H5-5	36.04	91.68	2.03	2.33
15	H5-6	36.36	92.56	2.05	2.30
16	H5-7	45.45	93.55	2.05	2.47
17	H5-8	45.45	93.18	2.05	2.47
18	H5-9	45.05	92.07	2.03	2.51

Table 5.5. SERIES 5 (ITF)

No.	Specimen	n/t	hw/t	r/t	F_C (KN)
1	H6-1	27.03	64.34	1.80	4.31
2	H6-2	27.03	64.14	1.80	4.31
3	H6-3	26.79	63.02	1.79	4.38
4	H6-4	36.04	64.07	1.80	4.71
5	H6-5	36.04	64.16	1.80	4.71
6	H6-6	36.04	63.68	1.80	4.71
7	H6-7	44.64	63.48	1.79	5.14
8	H6-8	45.05	64.25	1.80	5.06
9	H6-9	45.05	65.93	1.80	5.06
10	H7-1	27.27	92.40	1.82	4.24
11	H7-2	27.03	91.82	1.79	4.31
12	H7-3	27.03	92.41	1.80	4.31
13	H7-4	35.71	90.63	1.79	4.78
14	H7-5	36.04	91.51	1.80	4.71

Table 5.5. SERIES 5 (ITF)

No.	Specimen	n/t	hw/t	r/t	F_C (KN)
15	H7-6	36.36	92.24	1.82	4.63
16	H7-7	45.05	91.98	1.80	5.06
17	H7-8	45.45	92.75	1.82	4.98
18	H7-9	45.45	92.58	1.82	4.98

CHAPTER 6

PLASTIC COLLAPSE MECHANISMS

OF

THIN-WALLED STEEL STRUCTURES

6.1. GENERAL.

Because the objective of this research program was also aimed at using plastic mechanisms for analysing the web crippling strength of the specimens, it is therefore very useful to discuss plastic collapse mechanisms of thin-walled steel structures in this chapter before carrying out the analysis. When thin-walled steel structures carry increasing loads, they will first develop local elastic buckling which involves a deformation of their cross sections and then change the local elastic buckling into local plastic mechanisms as they collapse. This is in contrast to thick-walled steel structures which under increasing loads, first tend to buckle globally without deformations of the cross section and subsequently develop a simple plastic hinge at the middle of their lengths as collapse occurs. The distinction between failure modes of thick and thin-walled steel structures can be illustrated by the failure modes of a conventional strut and a thin-walled channel strut as shown in Figure 6.1.

The local plastic mechanisms of thin-walled steel structures are composed of yield lines or plastic hinges which lie in all directions. A typical example shown in Figure 6.2 is local plastic mechanisms of a plain channel section beam subjected to pure bending with unstiffened components in compression. At first sight the local plastic mechanisms appear to be a confused conglomaration of plastic hinges and distorted plates. However, the studies carried out by N.W. Murray[50] have shown that the plastic hinges can often be treated in a systematic way because they are made up of

199

a number of so-called " *basic plastic mechanisms* " which are compatible with each other. These basic plastic mechanisms have already been discussed in subchapter 2.3 and their types are listed in table 2.1.
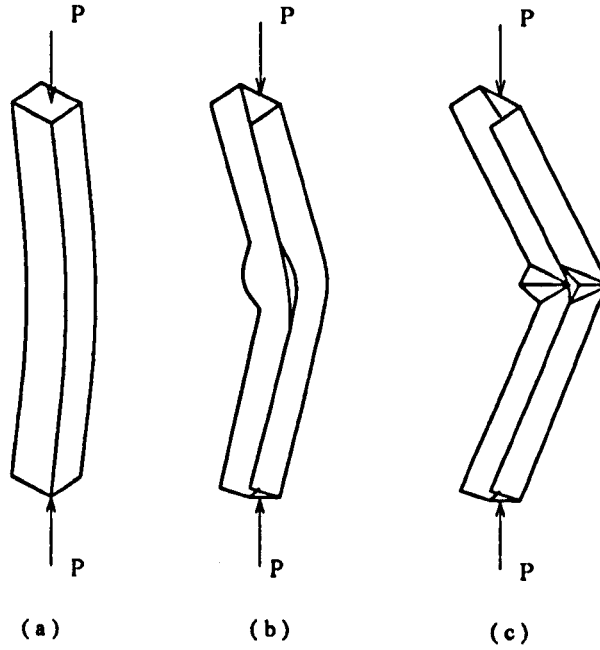
Figure 6.1. Failure of conventional and thin-walled channel strut. [55]

M : BENDING MOMENT
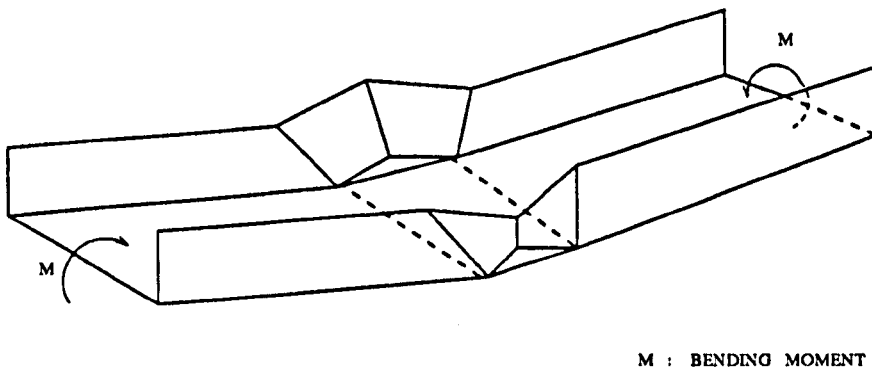
Figure 6.2. Local plastic mechanisms of a plain channel section beam under pure bending.

200

The plastic collapse mechanisms can be used to analyse the post-yield or post-collapse behaviour of thin-walled steel structures. This post-collapse behaviour is an important feature in the plastic mechanism analysis because it can be used to estimate the failure load of the structures. The complete behaviour of thin-walled steel structures can be described approximately by using two different models of theory, i.e. an ideal linear-elastic model which describes their elastic behaviour and an ideal rigid-plastic model which describes their post-collapse behaviour. Both of these theoretical models will form a theoretical load-deflection diagram of a thin-walled steel structure as shown in Figure 6.3. A failure (or ultimate) load of the structure may be estimated from the theoretical load-deflection diagram by means of determining the point of intersection of the elastic and the rigid plastic curves and this is called " **Cut-off strength** " [53].

The dotted curve as shown in Figure 6.3 represents the actual load-deflection curve of the structure. This curve starts to deviate from the elastic curve as the first yield occurs and then coincide with the rigid-plastic curve just after the development of plastic mechanisms. The load-deflection diagram also indicates three different limit loads which can be explained as follows :

- P_e : elastic limit load, i.e. the load which corresponds to the occurence of the first yield in the structure.

- P_f : ultimate limit load, i.e. the maximum load that can be carried by the structure.

201

- P_m : plastic limit load, i.e. the load at which plastic collapse

  mechanisms have already been developed in the structure.
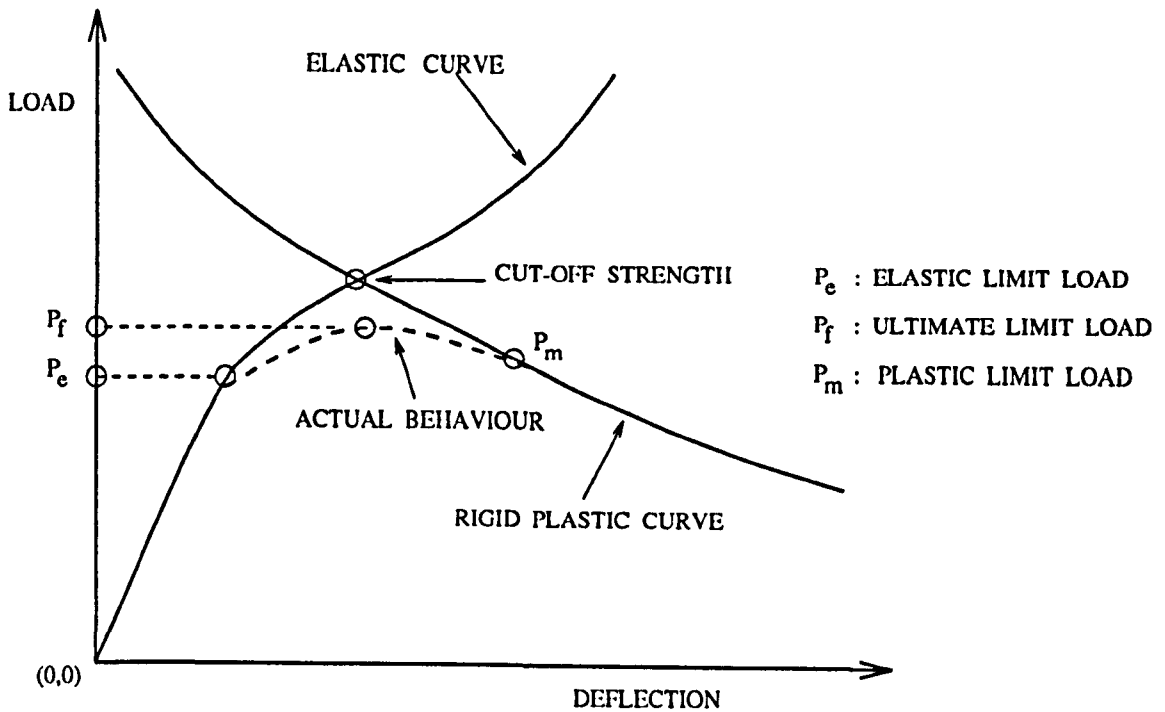
Figure 6.3. General load-deflection diagram of
thin-walled steel structures.

As mentioned before thin-walled steel structures at collapse will develop localized

plastic mechanisms. The study of collapse has generally been concentrated on trying

to understand what is hapenning when loads on the structure are in the vicinity of

their maximum value. The maximum load or in some literature it is called the

maximum load carrying capacity of a structure is often used as the sole basis for its

design [45]. This maximum load can be approximated using a rigid plastic theory and

the general idea of this theory will be discussed in the following subchapter.

202

6.2. RIGID-PLASTIC THEORY.

The rigid-plastic theory assumes a material behaves according to the elastic-perfectly-plastic stress-strain relationship and this behaviour can be seen in Figure 6.4. This assumption means that the effect of strain- hardening may be neglected because it tends to spread plastic hinges instead of allowing them to develop along a line as is assumed in the theory. As long as the spreading of the plastic hinges is not too large compared to the unyielded length of plate adjacent to the plastic hinges, the effect of strain-hardening is eventually not too significant. Moreover, interest usually focuses on the behaviour of the structure in the region of collapse and a little beyond it.

In the rigid plastic theory, the region between the plastic hinges is also assumed to remain flat. This assumption is reasonable once the plastic mechanism is well developed. For these reasons it can be anticipated that there will be discrepancies between calculated results obtained using the rigid-plastic theory and experimental results. Nevertheless, the application of the rigid plastic theory can provide some understanding of the way thin-walled structures behave in the vicinity of the ultimate loads and may determine whether a structure is brittle or ductile. The structure is called brittle when its load-deflection curve indicates a sharp peak, i.e. after the ultimate load is reached, the curve suddenly drops in a very steep manner. In the case of a ductile structure, its behaviour is not represented by a load-deflection curve with a sharp peak and this is desirable in a structure because it can give more warning

before the structure fails.
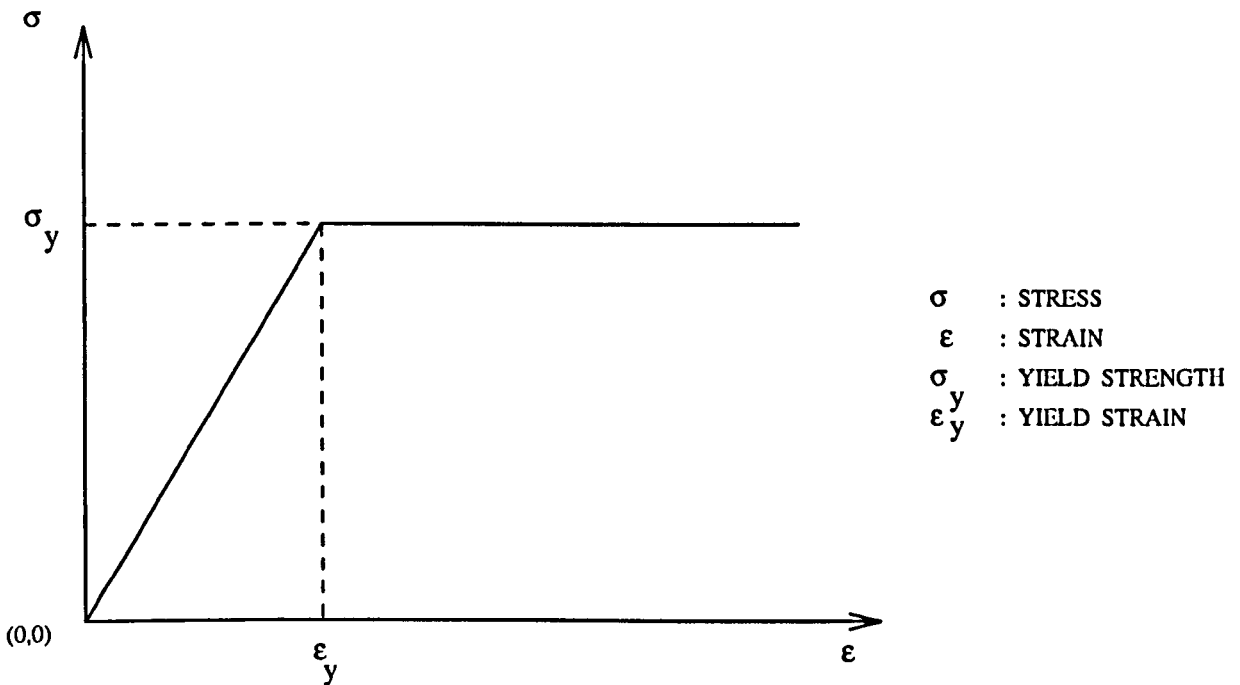
Figure 6.4. Elastic-perfectly-plastic behaviour.[61]

An exact rigid-plastic theory will satisfy all the following conditions, i.e. :

a. Equilibrium   :   each part of the structure and the structure as a whole is in equilibrium with the applied loads and the reactions at the support.

b. Mechanism   :   sufficient (in number) plastic hinges are developed so that the whole or part of the structure can deflect as a mechanism.

c. Yield   :   at no point in the structure can the bending exceed the plastic moment capacity of the cross section.

However, except in the case of the simplest of the structures it is not easy to satisfy

simultaneously all three conditions. It has been found expedient to resort to approximate methods which satisfy only two of the conditions, namely a method which satisfies the equilibrium and mechanism conditions and another method which satisfies the equilibrium and yield conditions.

A simple example of using the rigid-plastic theory is the analysis of a mild steel strut whose cross section is rectangular and the strut is pinned about its minor principal axis at each end. The dimensions of the strut are shown in Figure 6.5 where B >> H so that there is no doubt that if the strut is subjected to the axial load P, it will fail by bending about its minor axis. If the axial load P is not considered, the stress distribution in a fully plastic rectangular cross section of the strut is as shown in Figure 6.6(a), whereas if the axial load P is also carried by the cross section the stress distribution will be as shown in Figure 6.6(b).
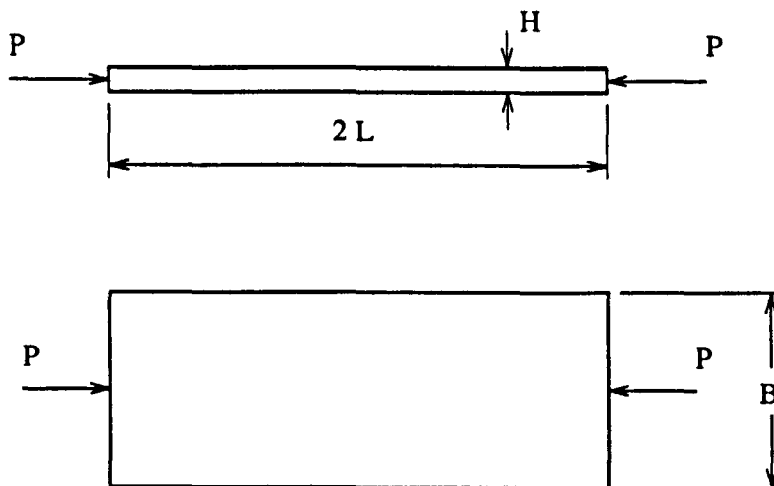
Figure 6.5. Dimension of a pin-ended strut.
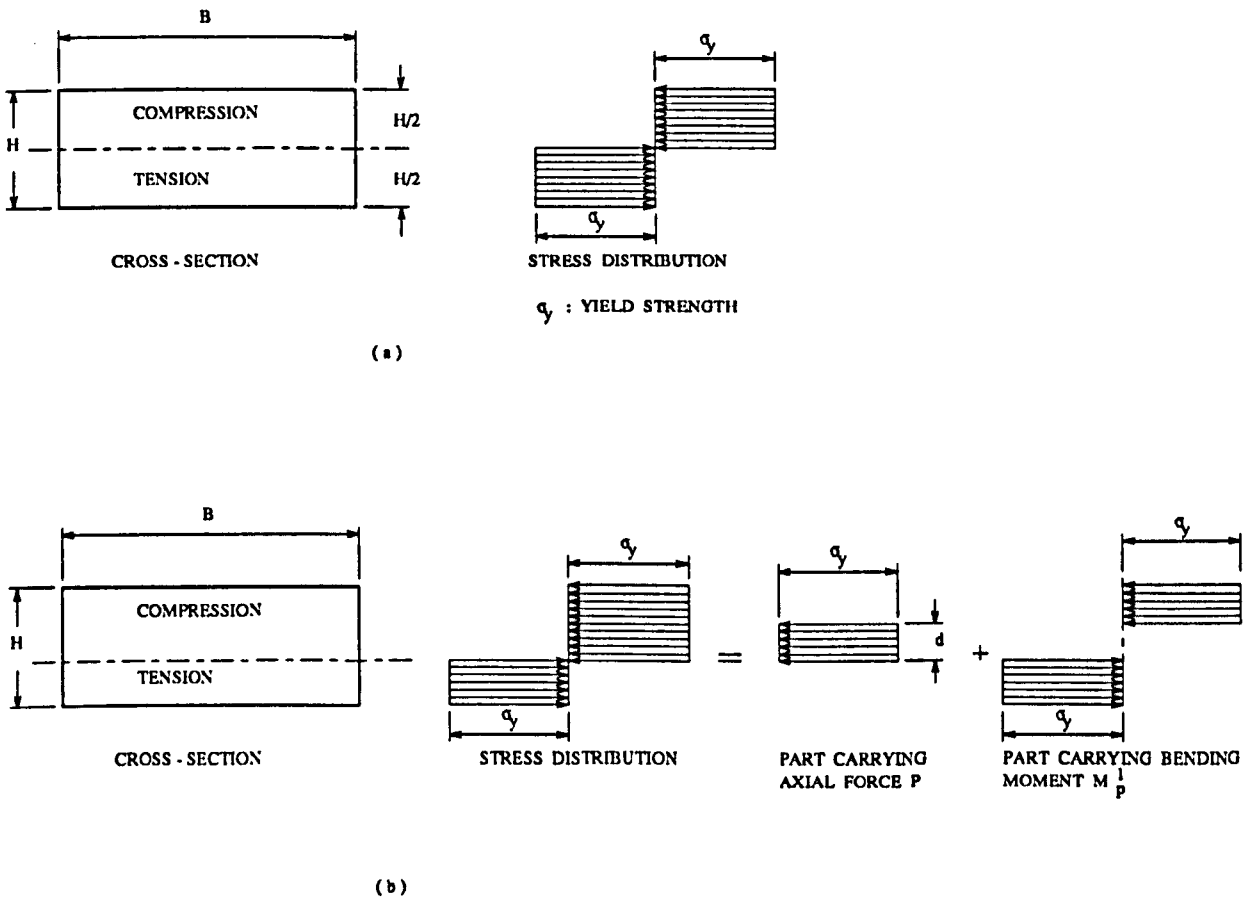
Figure 6.6. Stress distribution in a fully plastic
rectangular cross section.

On the basis of the stress distribution shown in Figure 6.6(a), a full plastic moment

of the cross section may be expressed as follows :

$$M_p = \frac{\sigma_y \, B \, H^2}{4} \quad \dots\dots\dots\dots\dots \quad (6.2.1)$$

If the axial load P must also be carried by the cross section, the plastic moment will

be reduced and it is designated by a symbol of M_p'. It can be seen in Figure 6.6(b)

that the central core of the strut of depth d carries the axial load P and this load can

be formulated as :

$$P = \sigma_y \, B \, d \quad \dotfill \quad (6.2.2)$$

The outer part carries the reduced plastic moment M_p' where :

$$M_P' = \frac{\sigma_y \, B \, (H^2 - d^2)}{4} \quad \dotfill \quad (6.2.3)$$

From equations (6.2.2) and (6.2.3) d can be eliminated to yield the following equation.

$$M_P' = \frac{\sigma_y \, B \, H^2}{4} \left[1 - \left(\frac{P}{P_s}\right)^2 \right] = M_p \left[1 - \left(\frac{P}{P_s}\right)^2 \right] \quad \dotfill \quad (6.2.4)$$

In this equation P_s is a squash load and equal to $\sigma_y BH$. The equation (6.2.4) is applied to the perfect pin-ended strut as shown in Figure 6.5. As the axial load P reaches the squash load P_s the strut becomes unstable and it deflects away from its initial position such as shown in Figure 6.7. A hinge is formed at the mid-span of the strut, i.e. at the location where the maximum deflection (Δ) takes place. The stress distribution has a pattern similar to that shown in Figure 6.6(b).
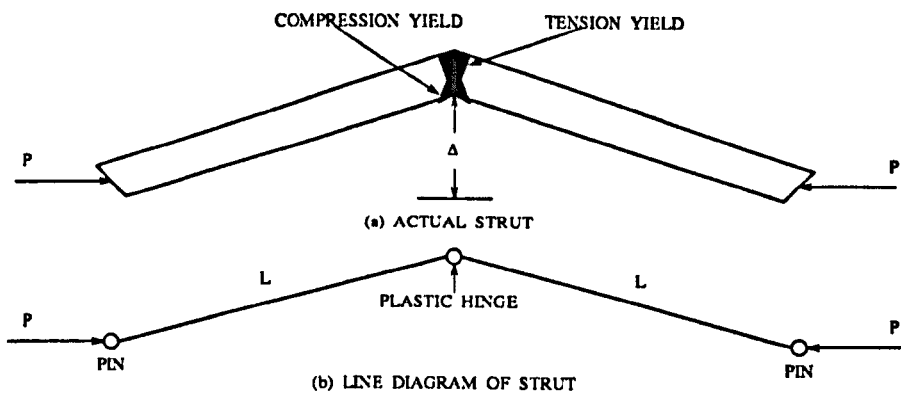
Figure 6.7. Pin-ended strut and its line diagram when collapsing.

In order to maintain an equilibrium condition of the strut after buckling laterally, a static moment on one half of the strut caused by the axial load P has to be the same as the reduced plastic moment M_p'. This can be expressed as in the following relationship.

$$P \Delta = M_p' = M_p [1 - (\frac{P}{P_s})^2] \quad \ldots\ldots\ldots\ldots\ldots\ldots \quad (6.2.5)$$

The above equation can be solved explicitly for P as follows :

$$\frac{M_p}{P_s^2} P^2 + P \Delta - M_p = 0 \quad ; \quad M_p P^2 + P_s^2 \Delta P - P_s^2 M_p = 0$$

$$P = \frac{- P_s^2 \Delta + \sqrt{P_s^4 \Delta^2 + 4 P_s^2 M_p^2}}{2 M_p} = \frac{- P_s^2 \Delta + 2 P_s M_p \sqrt{\dfrac{P_s^2 \Delta^2}{4 M_p^2} + 1}}{2 M_p}$$

Hence :

$$\frac{P}{P_s} = \frac{- P_s \Delta}{2 M_p} + \sqrt{(\frac{P_s \Delta}{2 M_p})^2 + 1} \quad \ldots\ldots\ldots\ldots\ldots \quad (6.2.6)$$

or substitution $P_s = \sigma_y B H$ and equation (6.2.1) into the right side of equation (6.2.6) gives :

$$\frac{P}{P_s} = - \frac{2 \Delta}{H} + \sqrt{(\frac{2 \Delta}{H})^2 + 1} \quad \ldots\ldots\ldots\ldots\ldots\ldots \quad (6.2.7)$$

According to equation (6.2.7), if P/P_s is plotted against Δ/H the graph will be an unloading curve, i.e. as the lateral deflection Δ increases the load carrying capacity of the strut decreases (Figure 6.8). This is incidentally the cause of the sudden

collapse of steel struts when they reach their ultimate loads. If the strut remains elastic its load carrying capacity does not decrease after buckling.
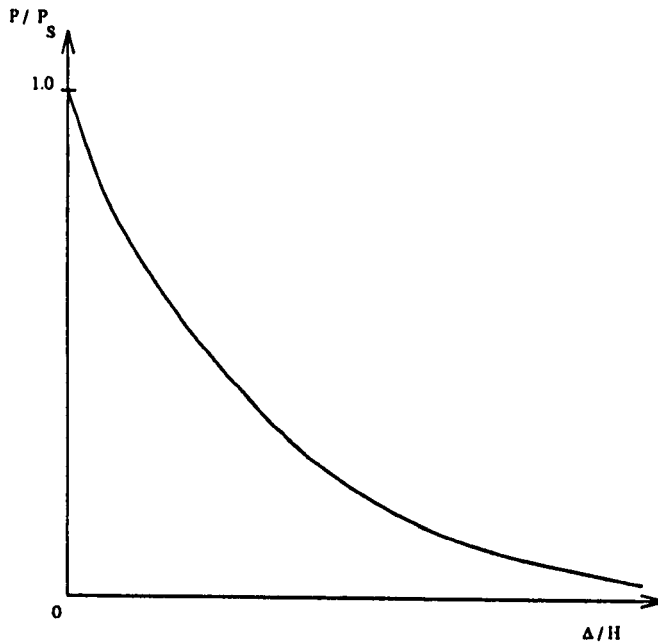
Figure 6.8. Collapse curve of a pin-ended strut.

6.3. MOMENT CAPACITY OF PLASTIC HINGES.

The yield line method has been widely used to study local collapse mechanisms of thin-walled steel structures. In the application of the yield line method, the determination of the moment capacity of a yield line or a plastic hinge is a fundamental requirement. As discussed in the previous subchapter, a plastic moment or a reduced plastic moment of a structure can be analysed using the rigid plastic theory. In the application of this theory on the analysis of a pin-ended strut such as

shown in Figure 6.7, as the strut collapse, it forms a plastic hinge at the middle of its length.

The moment capacity of the plastic hinge is the same as the reduced plastic moment as stated in equation (6.2.4). In this case, the position of plastic hinge is perpendicular to the direction of the axial load P. Thus, for a plastic hinge which is oriented at an angle of 90^0 to the direction of thrust P, its moment capacity can be generally expressed as follows :

$$M_p' = \frac{\sigma_y \, b \, t^2}{4} \left[1 - \left(\frac{P}{\sigma_y \, b \, t} \right)^2 \right] \dots\dots\dots\dots\dots (6.3.1)$$

Where :

M_p' : moment capacity of the plastic hinge.

σ_y : material yield strength.

b   : width of the plastic hinge.

t   : thickness of the plastic hinge.

The formula of moment capacity as indicated in equation (6.3.1) is determined according to the assumed stress distribution over the thickness of plastic hinge and this method is termed the statical approach [47]. In the plastic collapse mechanisms of thin-walled steel structures, not all plastic hinges lie at right angles to the direction of the thrust P but there are also plastic hinges whose directions incline to the direction of the thrust P. It is therefore necessary to derive an expression for the

210

moment capacity of a plastic hinge which is inclined at an angle β to the direction of the thrust P. This can also be derived using the statical approach.

A strip of flat plate of width b shown in Figure 6.9 is considered to be used for deriving the expression of moment capacity of an inclined plastic hinge. For convenience it is assumed there is a diagonal strip of material AB which has a yield stress σ_y while the remainder of the plate is infinitely rigid. As in Figure 6.6 the central core of the material of depth t_1 is assumed to carry the axial load P so that

$$P = \sigma_y \, b \, t_1 \quad \text{.............. (6.3.2)}$$

Across AB there is a moment M_p''' carried by the remaining area of the cross section and a twisting moment. M_p''' is calculated from stresses acting on the remaining area of the cross section, i.e. :

$$M_p''' = \sigma_y \, \frac{(t^2 - t_1^2)}{4} \, b \, \sec\beta \quad \text{................ (6.3.3)}$$

From equation (6.3.2) $t_1 = P/(\sigma_y \, b)$ and when t_1 is substituted into equation (6.3.3), the equation becomes :

$$M_p''' = \frac{\sigma_y \, b}{4} \, [\, t^2 - (\frac{P}{\sigma_y \, b})^2 \,] \, \sec\beta \; = \; \frac{\sigma_y \, b \, t^2}{4} \, [\, 1 - (\frac{P}{\sigma_y \, b \, t})^2 \,] \, \sec\beta$$

or

$$M_p''' = M_p' \, \sec\beta \quad \text{................ (6.3.4)}$$

M_p' is the moment capacity if the plastic hinge is perpendicular to the direction of

axial load P. The diagram of moment vectors in Figure 6.9(b) shows that

$$M_p'' = M_p''' \sec\beta \quad .... \quad (6.3.5)$$

From equations (6.3.4) and (6.3.5), the moment capacity along the plate width b of a plastic hinge which is oriented at an angle β to the direction of the thrust P may be written as follows :

$$M_p'' = M_p' \sec^2\beta = \frac{\sigma_y \, b \, t^2}{4} \left[1 - \left(\frac{P}{\sigma_y \, b \, t}\right)^2 \right] \sec^2\beta \quad .... \quad (6.3.6)$$

DIAGRAM OF MOMENT VECTORS
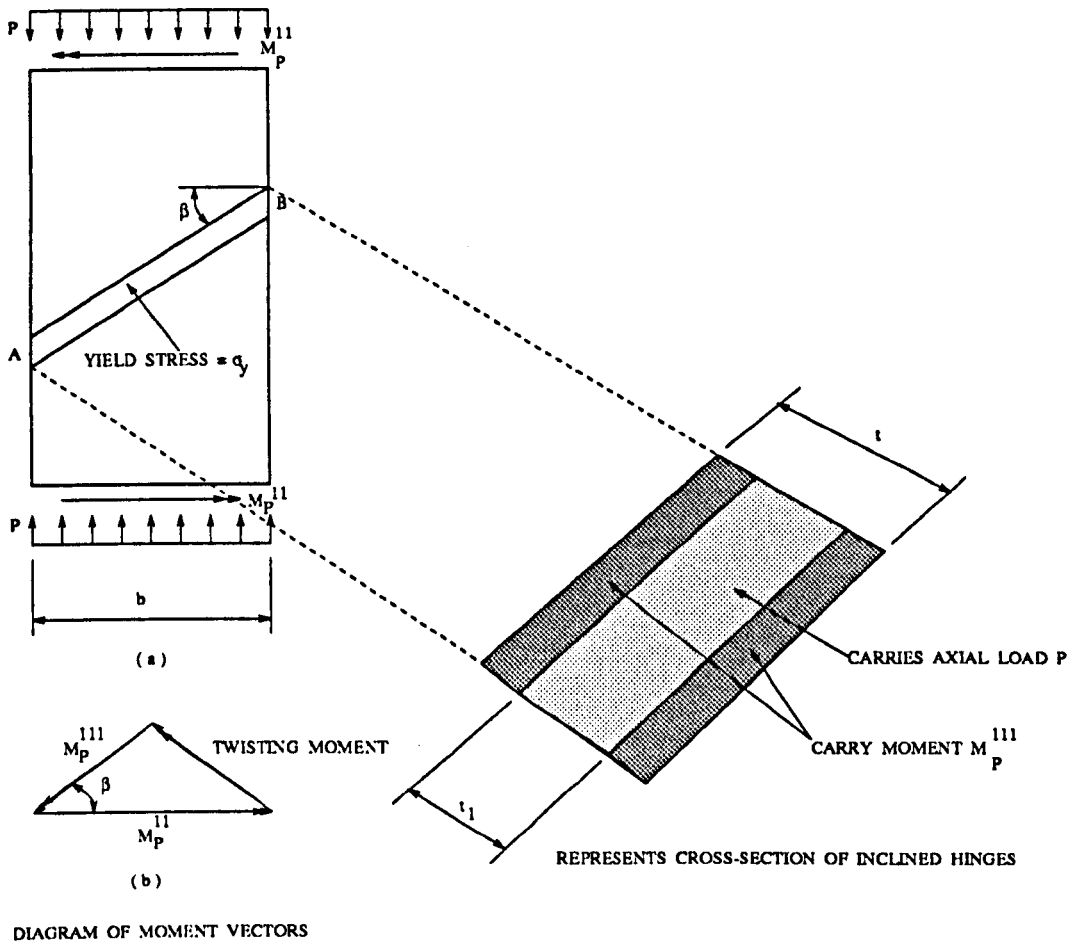
Figure 6.9. Moment capacity of inclined plastic hinge.

6.4. COLLAPSE LOAD ANALYSIS.

The previous subchapter has shown that the failure or collapse load of thin-walled steel structures can be roughly estimated from the intersection between the elastic and rigid plastic curves. The latter curve represents the post-yield or post-collapse behaviour of thin-walled steel structures. This behaviour is important in analysing plastic-collapse mechanisms of thin-walled steel structures because besides collapse loads, it can also provide insight into the ductility of the structures. The post-collapse load-deformation behaviour of thin-walled steel structures can be analysed using the yield line approach. There are two different methods in using the yield line approach for analysing collapse loads of thin-walled steel structures, i.e. a work method and an equilibrium method [53].

The work method is based on the principle of virtual work where the work performed by the external forces due to a virtual displcement is equated to the energy dissipated in the yield lines. A simple example of using the work method for calculating the collapse load is the analysis of a built-in beam shown in Figure 6.10. The beam is subjected to a central concentrated load W and the beam will collapse when the load W has increased up to its maximum value. At the collapse stage, the beam deflects and forms plastic hinges at points A, B and C such as shown in Figure 6.10 (b). It can be seen that as the beam collapses, the load W moves through a small distance. For a very small rotating angle Θ, the displacement of the load W is equal to $L\Theta/2$.

213
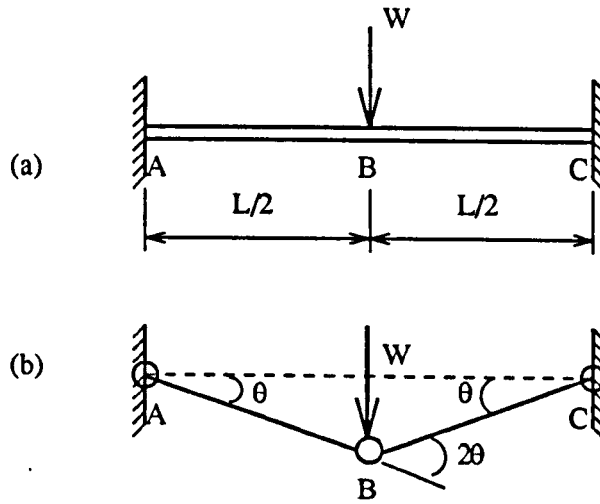
Figure 6.10. Collapse load analysis of built-in beam.

The total external energy (work) done by the load W is :

$$E_{ext} = \frac{W L \theta}{2}$$

This energy is absorbed by the plastic hinges at A, B and C so that the energy dissipated in the plastic hinges will be :

$$E_{dis} = M_p (\theta + \theta + 2\theta) = 4 M_p \theta$$

where :

E_{dis} : energy dissipated at plastic hinges. '

M_p : plastic moment of plastic hinges.

By equating E_{ext} to E_{dis}, the load W can be expressed in terms of plastic moment M_p and the span of the beam L.

214

$$\frac{W\,L\,\theta}{2} = 4\,M_p\,\theta \quad .... (6.4.1)$$

$$W = \frac{8\,M_p}{L} \quad .... (6.4.2)$$

Equation (6.4.1) may be regarded as a virtual work equation and the load W

expressed in equation (6.4.2) is considered as the failure or collapse load of the beam.

In the equilibrium method, plastic collapse mechanisms are thought to consist of

independent strips parallel to the direction of loading. The maximum load carrying

capacity of each strip is calculated from the static equilibrium of the strip. The

collapse load of the whole structure is determined by integrating the maximum load

carrying capacities of all strips. As an example of using the equilibrium method is

the analysis of collapse load of the plate shown in Figure 6.11.
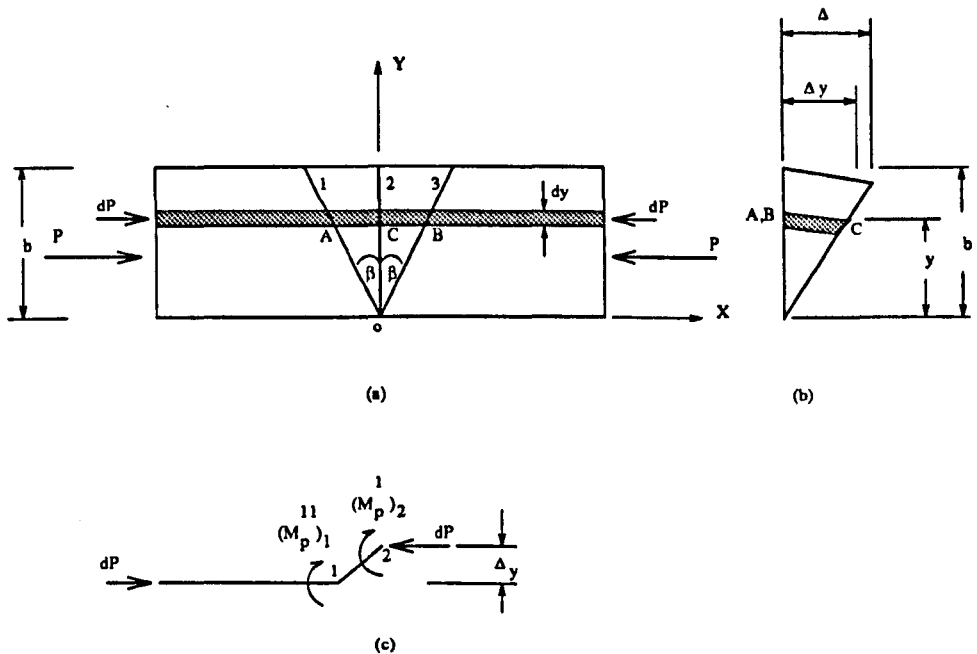
Figure 6.11. Analysis of collapse load using equilibrium method.

215

The above figure shows that the analysis of collapse load of the plate can be started by analysing the longitudinal strip of width dy. In order to obtain the elemental load dP, only a half portion of the strip shown in Figure 6.11 (c) is analysed and according to its static moment equilibrium the elemental load dP can be derived from the following relationship.

$$dP \, \Delta_y = d(M_p')_2 + d(M_p'')_1$$

$$dP \, \Delta_y = \frac{\sigma_y \, dy \, t^2}{4} \, [1 - (\frac{dP}{\sigma_y \, dy \, t})^2] + \frac{\sigma_y \, dy \, t^2}{4} \, [1 - (\frac{dP}{\sigma_y \, dy \, t})^2] \, \sec^2\beta$$

$$dP \, \Delta_y = (1 + \sec^2\beta) \, \frac{\sigma_y \, dy \, t^2}{4} \, \frac{[\, (\sigma_y \, dy \, t)^2 - dP^2 \,]}{(\, \sigma_y \, dy \, t \,)^2}$$

$$(1 + \sec^2\beta)dP^2 + 4 \, \Delta_y \, \sigma_y \, dy \, dP - (1 + \sec^2\beta)(\sigma_y \, dy \, t)^2 = 0 \, ... \, (6.4.3)$$

From Figure 6.11(b), Δ_y can be expressed in terms of Δ and plate width b, i.e. :

$$\frac{\Delta_y}{\Delta} = \frac{y}{b} \qquad ; \qquad \Delta_y = \frac{\Delta \, y}{b} \, ... \, (6.4.4)$$

substitutions of (6.4.4) into equation (6.4.3) and equating $(1 + \sec^2\beta)$ to K_1 :

$$b \, K_1 \, dP^2 + 4 \, \Delta \, \sigma_y \, ydy \, dP - b \, K_1 \, (\sigma_y \, dy \, t)^2 = 0$$

$$dP = \frac{- 4 \, \Delta \, \sigma_y \, ydy + \sqrt{(4 \, \Delta \, \sigma_y \, ydy)^2 + 4 \, b^2 \, K_1^2 \, (\sigma_y \, dy \, t)^2}}{2 \, b \, K_1}$$

$$dP = \frac{- 4 \, \Delta \, \sigma_y \, ydy + 2 \, b \, K_1 \, t \, \sigma_y \, ydy \, \sqrt{(\frac{2 \, \Delta}{b \, K_1})^2 + \frac{1}{y^2}}}{2 \, b \, K_1}$$

$$dP = \sigma_y \, t \, [\, \sqrt{(\frac{2 \, \Delta}{b \, K_1})^2 + \frac{1}{y^2}} - \frac{2 \, \Delta}{b \, K_1 \, t} \,] \, ydy \, ... \, (6.4.5)$$

By integrating this above elemental load dP from y = 0 to y = b, the collapse load of the plate can be expressed as follows :

$$P = \frac{\sigma_y \, t \, b}{2} \left[\sqrt{(\frac{2\Delta}{K_1 t})^2 + 1} - \frac{2\Delta}{K_1 t} + \frac{k_1 t}{2\Delta} \ln\left(\sqrt{(\frac{2\Delta}{K_1 t})^2 + 1} + \frac{2\Delta}{K_1 t}\right) \right] \quad \text{......} \quad (6.4.6)$$

CHAPTER 7

APPLICATION

OF

PLASTIC MECHANISM APPROACH

7.1. GENERAL.

This chapter discusses the analysis of ultimate web crippling loads using the plastic mechanism approach. In order to carry out the analysis, an idealized plastic mechanism model which simulates failure modes of web crippling of the specimens was developed and analysed using principles of yield line analysis. As discussed in the previous chapter, there are two basic methods in analysing yield line or plastic mechanisms of thin-walled steel structures, i.e. an energy (work) method and an equilibrium method. This chapter describes the development of an energy method for analysing the ultimate web crippling load of specimens subjected to combined actions of web crippling and bending (IOF).

Prior to the development of the idealized plastic mechanism model for analysing the ultimate web crippling load, some samples of failure modes of the specimens under IOF tests were observed in the laboratory. It could be seen from the observation that at failure the specimens formed yield curves underneath and in the vicinity of the loading point. Figure 7.1 indicates the observed yield line patterns of web crippling of the specimens failed under the IOF loading condition. The patterns form local collapse mechanisms of the specimens which are also termed as web crippling of the specimens and they consist of 15 yield lines. The area which is bounded by the yield lines 2 and 9 is the position of applied loads and the length of bearing load is exactly the same as that of the yield line 2.

218

In developing an idealized plastic mechanism model of web crippling, all yield lines in the local collapse mechanisms of the specimens as shown in Figure 7.1 are idealized in the form of straight yield lines. The application of an energy method for analysing the ultimate web crippling load is based on the virtual work equation. In this method, the external energy caused by the virtual displacement of the applied load is equated to the energy dissipation at plastic hinges. This energy equation is then used to derive the expression of ultimate web crippling load of the specimens. The energy dissipation at the plastic hinges was determined on the basis of bending energy and the effect of axial (membrane) force was not considered in the initial analysis, although this was later modified.
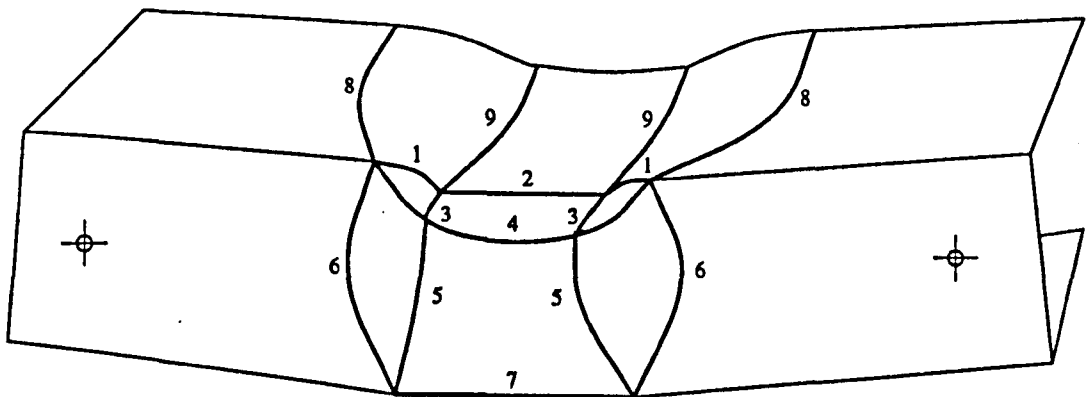
Figure 7.1. Observed plastic mechanisms of web crippling.

In determining the external energy, the virtual displacement of the applied load was not only taken from the local deflection of the web due to the crushing action, but

also took account of the deflection of the whole beam caused by the global bending effect. The deflection of the whole beam was also elastically analysed, where in this analysis, the effect of local buckling on the compression elements was considered by means of an effective width approach. The concept of determining the effective width of the compression elements was basically similar to that of BS 5950 Part 5 1987, i.e the calculation of effective width was employed for the top flange only. The elastic analysis of the beam deflection was intended to establish an elastic load-deflection equation, where this would be combined with the other equation of theoretical load-deflection obtained from the plastic mechanism approach in order to estimate the ultimate web crippling load.

7.2. IDEALIZED PLASTIC MECHANISM MODEL.

The development of the idealized plastic mechanism model of web crippling was performed by idealizing the actual mechanisms shown in Figure 7.1 and this can be seen in Figure 7.2. In the idealized mechanisms of web and top flange indicated by the dotted lines, all observed yield curves are replaced by straight yield lines and the lengths of yield lines 2, 5 and 8 are assumed to be identical. The yield curves 8 in the top flange are replaced by straight yield lines 10 which are parallel to the direction of yield lines 9. Figure 7.2 also shows 3 parameters which characterize the deformation of web and top flange. The local deflection of the top flange due to the action of applied load causes the decrease of web height and this is called web

220

crippling deformation (Δh). Another parameter which is represented by a symbol b is the yield arc depth, i.e. the maximum distance of the yield curve underneath the applied load measured from the original position of the deflected portion of the top flange where at this yield arc depth the maximum lateral deflection of the web (Δ) takes place.
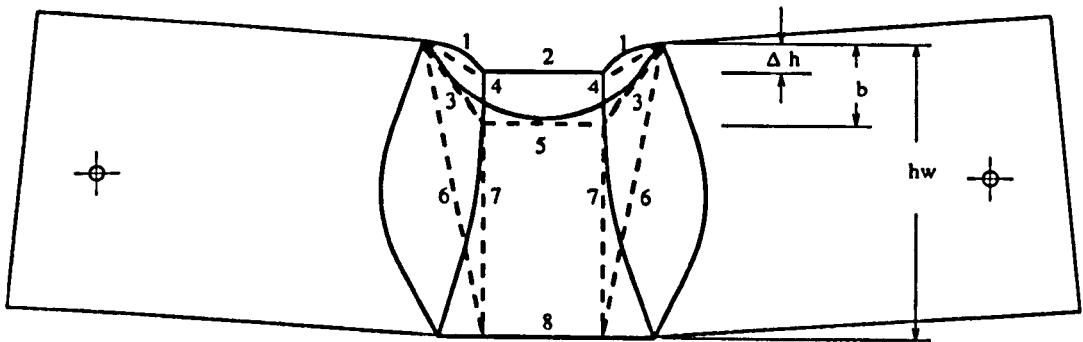
Δ h : WEB CRIPPLING DEFORMATION   b : YIELD ARC DEPTH   hw : WEB DEPTH

(a) Web mechanisms (Front view)
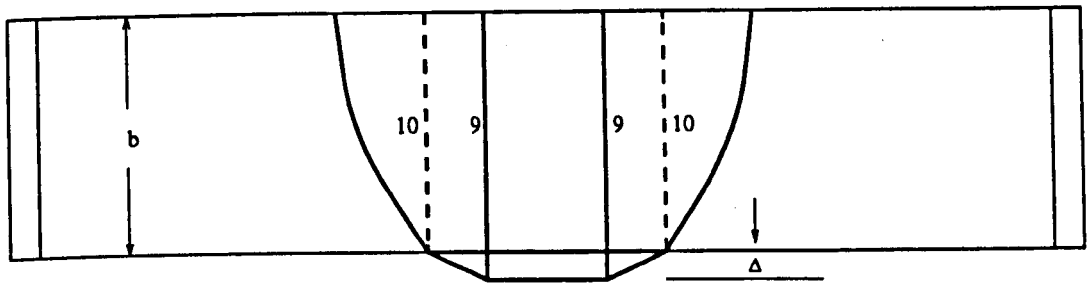
b : TOP FLANGE WIDTH Δ : MAXIMUM LATERAL DEFLECTION
OF WEB

(b) Top flange mechanisms (Top view)

Figure 7.2. Idealization of actual mechanisms.

221

Both idealized mechanisms in the top flange and the web form the idealized plastic mechanism model of web crippling (Figure 7.3) and it is used for analysing the ultimate web crippling loads for all specimens subjected to IOF loading condition in this research program.
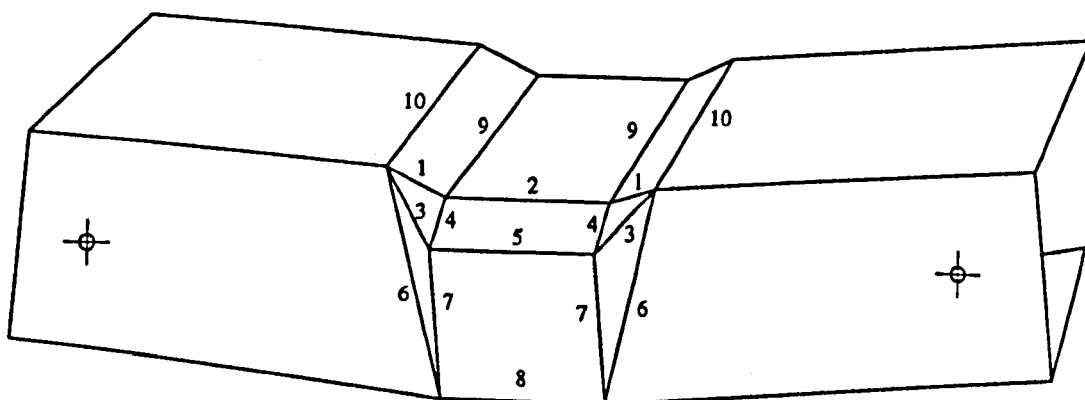
Figure 7.3. Idealized plastic mechanism model of web crippling.

The above idealized plastic mechanism model was analysed using the energy method and this was carried out according to the following assumptions.

- The effect of membrane force on the moment resisting capacity of the plastic hinge can be neglected, so that the fully plastic moment can be taken as the moment capacity of the plastic hinge. This assumption is subsequently modified to provide reduction in the hinge moment capacity.

- The plastic hinges are rotated through small angles, so that the hinge rotation may be predicted according to the small deflection theory.

- Flange curling can be neglected, so that the local deflection of the top flange may be considered to be equal to the web crippling deformation (Δh).

- All yield lines are assumed to be straight.

- The cross section of the plastic mechanism model may be represented by centre lines of the model and the round corner radius is replaced by the intersection of the centre lines of the web and the flanges.

- The effect of the corner radius is taken into account in the determination of external energy and it is assumed that the web loading acts at the edge of the radius between web and flange.

- All dimensions of the mechanisms are measured about the centre line.

7.3. PLASTIC MECHANISM ANALYSIS OF THE IDEALIZED MODEL.

In the application of the energy method for analysing the model, the external energy caused by the virtual displacement of the applied load is equated to the energy dissipated at the plastic hinges of the web and the top flange. The basic equation of the energy analysis used is as follows :

$$W_{ext} = \sum_{i=1}^{i=n} [(M_p)_i . \theta_i . l_i] \quad \dots \dots \dots \dots \dots \dots \quad (7.3.1)$$

Where :

W_{ext} : external energy caused by the virtual displacement of the applied load.

M_p : moment resisting capacity of the plastic hinge per unit length.

θ : rotation angle of the plastic hinge line.

l : length of the plastic hinge line.

223

The external energy (W_{ext}) is determined according to the displacement of applied load shown in Figure 7.4, i.e. :

$$W_{ext} = P(\Delta h + \eta) + M_o\theta_1 \dots\dots\dots\dots\dots (7.3.2)$$

Where :

P : applied load.

Δh : web crippling deformation.

η : deflection of the beam due to the global bending moment.

M_o : out of plane bending moment at the intersection of web and top flange and this is caused by the effect of round corner radius, $M_o = P(r+0.5t)$.

θ_1 : rotation angle of the hinge line 2.

In the above equation, η and θ_1 are analysed using plastic hinge mechanisms shown in Figure 7.4. This analysis is based on the small deflection theory.

$$\phi_{mec} = \frac{e_2}{\sqrt{(hw+t)^2+e^2}} \quad ; \quad e_1 = e\cos\theta = e(1 - \frac{\theta^2}{2})$$

$$\theta = \frac{\Delta h}{e} \quad ; \quad e_1 = e(1 - \frac{\Delta h^2}{2e^2}) = \frac{2e^2 - \Delta h^2}{2e}$$

$$e_2 = e - \frac{(2e^2 - 2\Delta h^2)}{2e} = \frac{\Delta h^2}{2e} \quad ; \quad \theta_1 = \frac{\Delta}{b}$$

$$\phi_{mec} = \frac{\Delta h^2}{2e\sqrt{(hw+t)^2+e^2}} \quad ; \quad \eta = \phi_{mec}\frac{(1-n)}{2} = \frac{\Delta h^2(1-n)}{4e\sqrt{(hw+t)^2+e^2}}$$

By using these above expressions and equation (7.3.2), the equation of external energy can be expanded as follows :

$$W_{ext} = P\Delta h + \frac{P\Delta h^2(1-n)}{4e\sqrt{(hw+t)^2+e^2}} + \frac{P(r+0.5t)\Delta}{b}$$

$$W_{ext} = \frac{P\left[4beC1\Delta h + bC2\Delta h^2 + 4C1(r+0.5t)\Delta\right]}{4beC1} \quad \ldots (7.3.3)$$

$$where : \quad C1 = \sqrt{(hw+t)^2+e^2} \quad ; \quad C2 = 1 - n$$

TOP VIEW

SECTION A-A
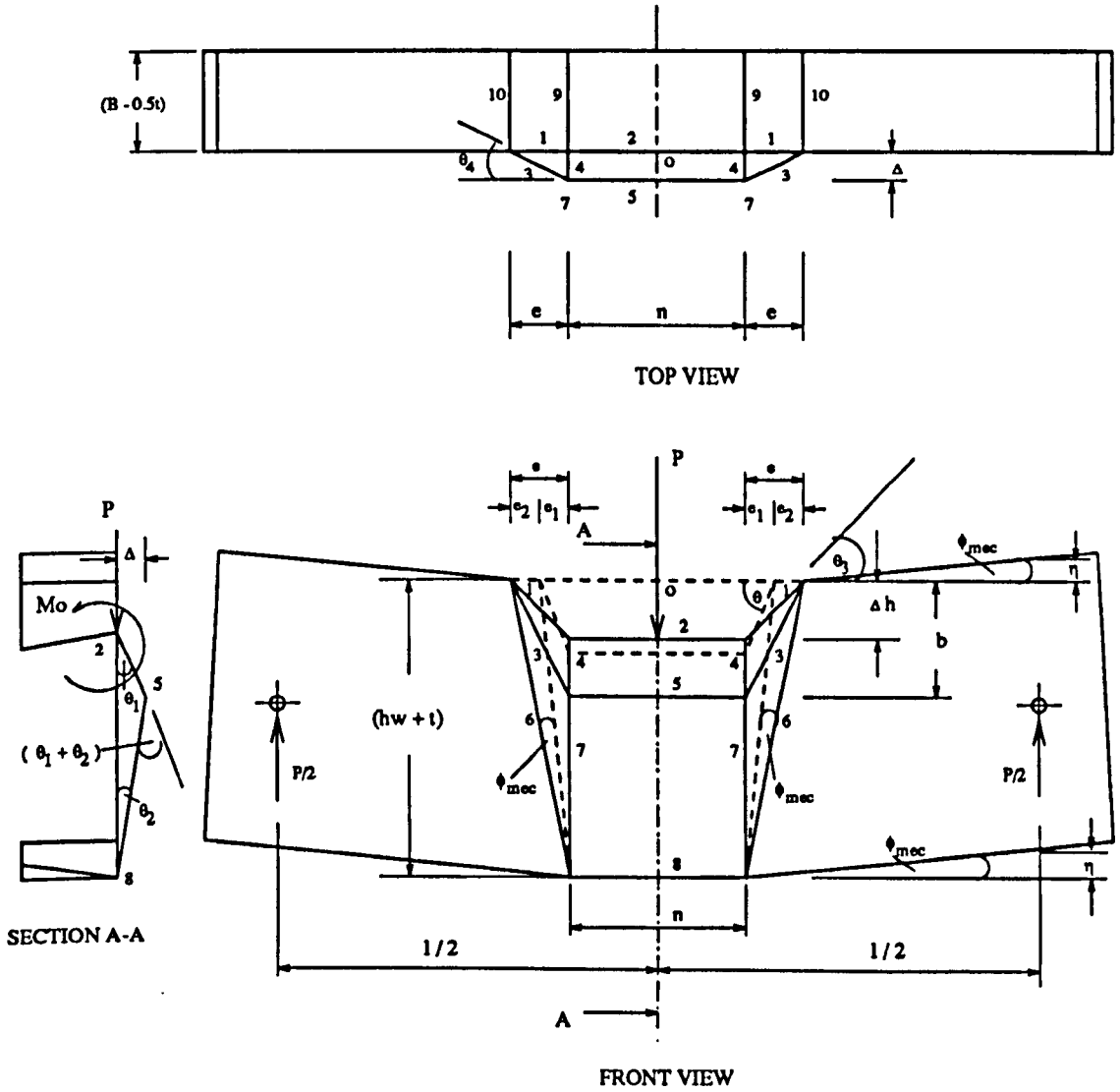
FRONT VIEW

Figure 7.4. Plastic hinge mechanisms.

225

7.3.1. WEB MECHANISM ANALYSIS.

Figure 7.4 (Front view) indicates that the web mechanisms consist of 13 plastic hinge lines. The energy dissipation at the plastic hinge lines 2,5 and 8 (W1) can be derived from the following equation.

$$W1 = \sum_{i=1}^{i=n} (M_p)_i . \theta_i . l_i$$

$$W1 = (M_p)_2 . \theta_1 . l_2 + (M_p)_5 . (\theta_1 + \theta_2) . l_5 + (M_p)_8 . \theta_2 . l_8$$

$$W1 = \frac{\sigma_y n t^2}{4} \theta_1 + \frac{\sigma_y n t^2}{4} (\theta_1 + \theta_2) + \frac{\sigma_y n t^2}{4} \theta_2$$

$$W1 = \frac{\sigma_y n t^2}{2} (\theta_1 + \theta_2) \quad \ldots \ldots \ldots (7.3.4)$$

θ_1 and θ_2 can be obtained from the geometrical analysis of the web deformation shown in section A-A of Figure 7.4, where this analysis is based on the small deflection theory (Δh and Δ are assumed to be very small).

$$\theta_1 = \frac{\Delta}{b} \quad ; \quad \theta_2 = \frac{\Delta}{(hw+t-b)} \quad ; \quad \theta_1 + \theta_2 = \frac{\Delta(hw+t)}{b(hw+t-b)}$$

From these relationships and equation (7.3.4), the energy dissipation at the plastic hinge lines 2,5 and 8 can be expressed as follows :

$$W1 = \frac{\sigma_y \, n \, t^2 \, \Delta \, (hw+t)}{2 \, b \, (hw+t-b)} \quad \ldots \ldots \ldots \ldots (7.3.5)$$

In the case of the energy dissipation at the plastic hinge lines 1,3 and 6, the rotation of these plastic hinge lines is determined by examining the web deformation shown

in Figure 7.5. On the basis of the geometry in Figure 7.5 and the approximation of small deflection theory, the rotation of the plastic hinge lines 1,3 and 6 are similar to that of the plastic hinge lines 2,5 and 8.
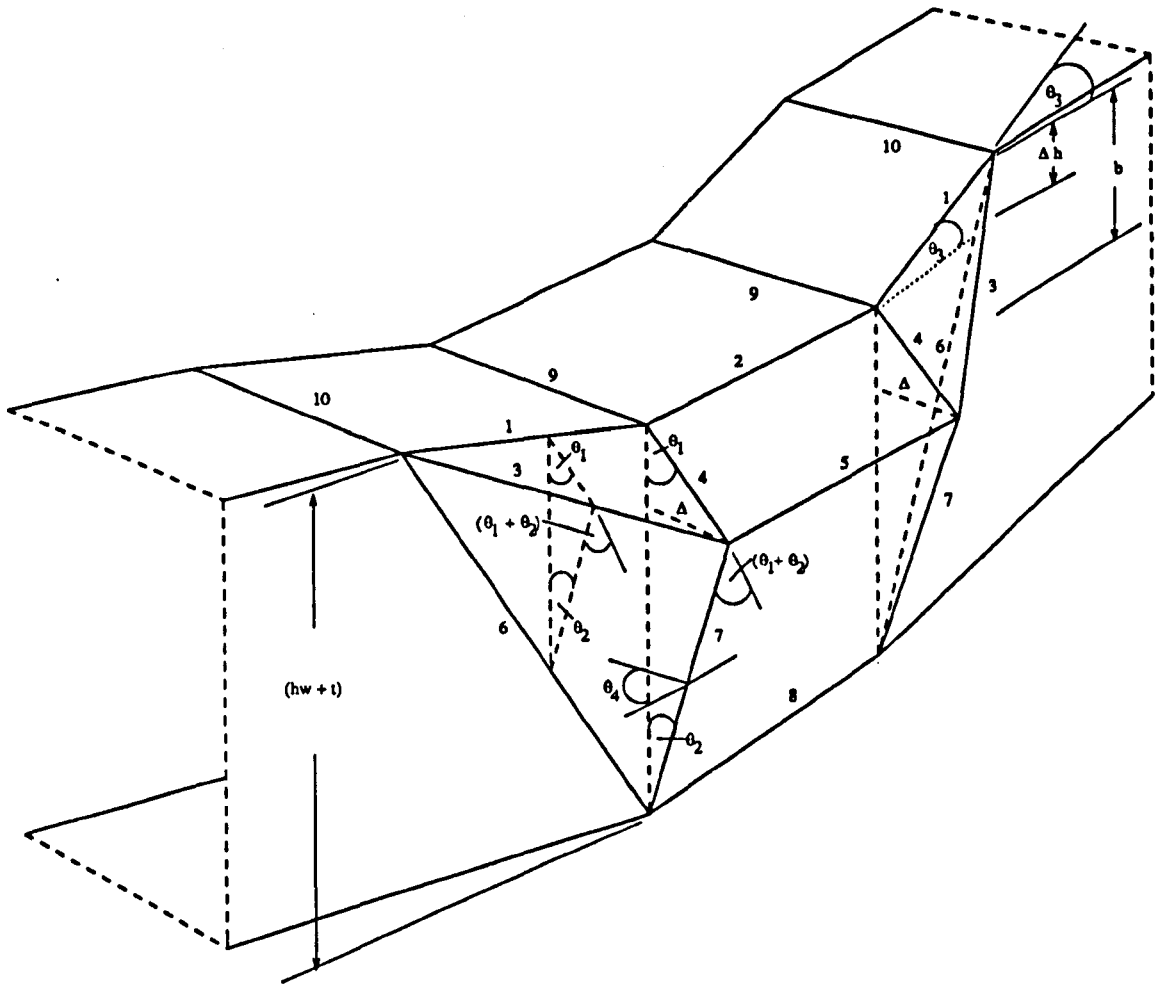
Figure 7.5. Web and flange deformation.

The energy dissipation at these hinge lines (W2) can therefore be obtained from :

$$W2 = 2 \ [(M_p)_1 . \theta_1 . l_1 \ + \ (M_p)_3 . (\theta_1 + \theta_2) . l_3 \ + \ (M_p)_6 . \theta_2 . l_6]$$

227

Because the analysis is based on the small deflection theory, the lengths of plastic

hinge lines 1 and 3 may be taken as follows :

$$l_1 = e \quad ; \quad l_3 = \sqrt{b^2 + e^2}$$

$$W2 = 2 \; \frac{\sigma_y t^2}{4} \; [\frac{\Delta e}{b} + \frac{\Delta (hw+t)\sqrt{b^2+e^2}}{b \; (hw+t-b)} + \frac{\Delta \sqrt{(hw+t)^2 + e^2}}{(hw+t-b)}]$$

$$W2 = \frac{\sigma_y t^2 \Delta \; [e(hw+t-b) + (hw+t)\sqrt{b^2 + e^2} + b\sqrt{(hw+t)^2 + e^2}]}{2 \; b \; (hw+t-b)}$$

$$\dots\dots\dots\dots\dots\dots\dots\dots (7.3.6)$$

Figure 7.5 also shows that the plastic hinge lines 4 and 7 are rotated through the

angles of θ_3 and θ_4 respectively. These angles can be determined using Figure 7.4,

i.e. :

$$\theta_3 = \frac{\Delta h}{e} \quad ; \quad \theta_4 = \frac{\Delta}{e}$$

The energy dissipation at the plastic hinge lines 4 and 7 (W3) is formulated as

follows :

$$W3 = 2 \; [(M_p)_4 . \theta_3 . l_4 + (M_p)_7 . \theta_4 . l_7]$$

$$W3 = 2 \; [\frac{\sigma_y t^2 b \Delta h}{4e} + \frac{\sigma_y t^2 (hw+t-b) \Delta}{4e}]$$

$$W3 = \frac{\sigma_y t^2}{2} \; \frac{[b \Delta h + (hw+t-b) \Delta]}{e}$$

$$\dots\dots\dots\dots\dots\dots (7.3.7)$$

Hence, the total energy dissipation at the plastic hinge lines in the web (Ww) can be

derived as follows :

$$Ww = W1 + W2 + W3$$

$$Ww = \frac{\sigma_y t^2 [n\Delta e(hw+t) + \Delta e[e(hw+t-b) + (hw+t)\sqrt{b^2+e^2}]]}{2\ b\ e\ (hw+t-b)} +$$

$$\frac{\sigma_y t^2 \Delta eb\sqrt{(hw+t)^2+e^2}}{2\ b\ e\ (hw+t-b)} + \frac{\sigma_y t^2 (hw+t-b)[b\Delta h + (hw+t-b)\Delta]}{2\ b\ e\ (hw+t-b)}$$

$$Ww = \frac{\sigma_y t^2 [C3\Delta + \Delta e(eC4+C5+C6) + b^2 C4\Delta h + bC4^2\Delta]}{2\ b\ e\ C4}$$

$$\dots\dots\dots\dots\dots\dots (7.3.8)$$

7.3.2. TOP FLANGE MECHANISM ANALYSIS.

In this analysis, the rotation of plastic hinge lines 9 and 10 can be seen from Figure 7.4, where the figure shows that the plastic hinge line 9 is rotated through the angle θ_3 and the plastic hinge line 10 is rotated through the angle $(\theta_3 - \phi_{mec})$. The energy dissipation at these hinge lines (Wfl) is

$$Wfl = 2\ [(M_p)_9 . \theta_3 . l_9 + (M_p)_{10} . (\theta_3 - \phi_{mec}) . l_{10}]$$

$$W_{fl} = \frac{2\ \sigma_y\ t^2\ (B-0.5t)}{4}\ (2\theta_3 - \phi_{mec})$$

$$Wfl = \sigma_y\ t^2\ (B-0.5t)\ (\frac{2\Delta h}{e} - \frac{\Delta h^2}{2e\sqrt{(hw+t)^2+e^2}})$$

$$Wfl = \frac{\sigma_y\ t^2\ \Delta h\ (B-0.5t)\ (4C1-\Delta h)}{4\ e\ C1}\ \dots\dots\dots\dots\dots (7.3.9)$$

On the basis of energy equations (7.3.1), (7.3.3), (7.3.8) and (7.3.9), the external energy is equated to the energy dissipation at all plastic hinge lines in order to derive the expression of ultimate web crippling load.

229

$$W_{ext} = Ww + Wfl$$

$$\frac{P[4beC1\Delta h + 2bC2\Delta h^2 + 4C1(r+0.5t)\Delta]}{4\ b\ e\ C1} =$$

$$\frac{\sigma_y t^2[C3\Delta + \Delta e(eC4+C5+C6) + b^2C4\Delta h + bC4^2\Delta]}{2\ b\ e\ C4} +$$

$$\frac{\sigma_y t^2\Delta h(B-0.5t)(4C1-\Delta h)}{4\ e\ C1}$$

$$P = \frac{\sigma_y t^2[2C1C3\Delta + 2C1\Delta e(eC4+C5+C6) + 2C1C4b^2\Delta h]}{C4[4beC1\Delta h + 2bC2\Delta h^2 + 4C1\Delta(r+0.5t)]}$$

$$+ \frac{\sigma_y t^2[2C1C4^2b\Delta + bC4\Delta h(B-0.5t)(4C1-\Delta h)]}{C4[4beC1\Delta h + 2bC2\Delta h^2 + 4C1\Delta(r+0.5t)]}$$

$$\dots\dots\dots\dots\dots\dots\dots (7.3.11)$$

Where: $C1 = \sqrt{(hw+t)^2 + e^2}$; $C2 = 1 - n$; $C3 = ne(hw + t)$

$C4 = hw+t-b$; $C5 = (hw+t)\sqrt{b^2 + e^2}$; $C6 = b\sqrt{(hw+t)^2 + e^2}$

The above equation gives the load P corresponding to deflections Δ and Δh in terms of the geometry of the mechanisms. By repeatedly varying e and b the lowest value of P for a given deflection condition can be found, and this minimisation process was incorporated in a computer program set up to evaluate the load deflection-behaviours. It was found that direct application of this equation, even with the minimisation procedure, resulted in non-conservative predictions, and gave loads more than 20% in excess of those measured in the tests. In order to overcome this, two additional procedures were incorporated, i.e. :

- The first procedure :

To take into account, in an approximate manner, the effect of axial load on bending capacity of the hinge lines. In reality the axial load effect is different for all hinges,

and even varies along some hinges, but for simplicity a single reduction factor can be used as follows :

The reduction factor $[1 - (P_p/P_s)^2]$ can be introduced to operate on P derived from equation (7.3.11), i.e.:

$$P_p = P[1 - (\frac{P_p}{P_s})^2] = \frac{P(P_p^2 - P_p^2)}{P_s^2}$$

$$PP_p^2 + P_s^2 P_p - PP_s^2 = 0$$

$$P_p = \frac{-P_s^2 + \sqrt{P_s^4 + 4P^2 P_s^2}}{2P} = \frac{-P_s^2 + P_s^2\sqrt{1 + 4(\frac{P}{P_s})^2}}{2P}$$

$$P_p = \frac{P_s^2}{2P}[\sqrt{1 + 4(\frac{P}{P_s})^2} - 1] \quad \ldots\ldots\ldots\ldots\ldots \quad (7.3.12)$$

where :

P_p : Reduced load carrying capacity.

P_s : σ_y n t (the squash load for the web load area).

- The second procedure :

The same reduction factor is still introduced to operate on P from equation (7.3.11).

In addition, to take some account of the fact that the full plastic moment is not attained at all hinges because of incomplete bending, the energy dissipation at the plastic hinge lines 4 and 7 is discounted. Thus, the value of P in equation (7.3.12) is calculated from equation (7.3.11) with the terms of $2 C_1 C_4 b^2 \Delta h$ and $2 C_1 C_4^2 b \Delta$ are equated to zero. This is a very approximate way to take account of reduction in energy dissipation, but may be at least justified by an increase in accuracy of the predicted values.

231

Two of the three web crippling parameters such as Δ and Δh are variables and their values depend on the magnitude of the applied load P. These two parameters can be correlated one to each other using the geometrical analysis shown in the following figure and this analysis is also based on the small deflection theory.
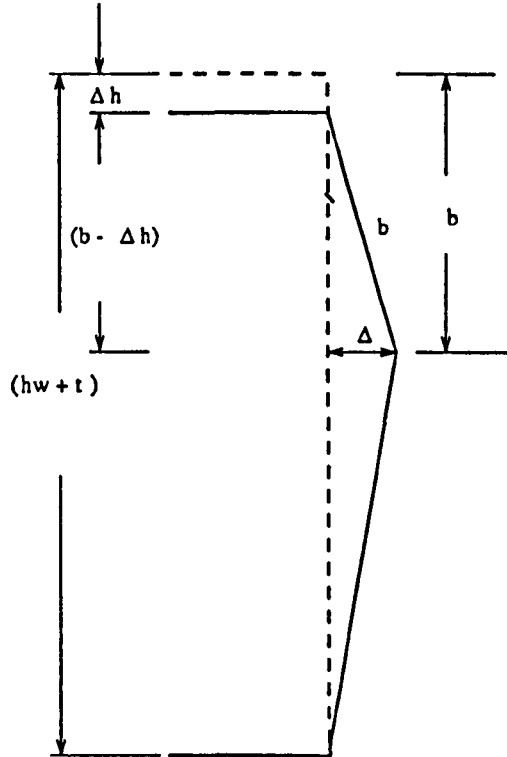
Figure 7.6. Lateral deflection of web.

$$b = \sqrt{(b - \Delta h)^2 + \Delta^2} \quad ; \quad b^2 = b^2 + \Delta h^2 - 2b\Delta h + \Delta^2$$

$$\Delta h^2 - 2b\Delta h + \Delta^2 = 0 \quad ; \quad \Delta h = \frac{2b - \sqrt{4b^2 - 4\Delta^2}}{2}$$

$$\Delta h = b - \sqrt{b^2 - \Delta^2} \quad \dots\dots\dots\dots \quad (7.3.13)$$

7.4. ELASTIC ANALYSIS OF THE BEAM.

As can be seen in equation (7.3.11) that from the plastic mechanism analysis, the load carrying capacity of the beam can be expressed in terms of lateral (Δ) and vertical (Δh) deflection of the web. The elastic analysis of the beam is aimed at establishing the other expression of load carrying capacity vs. vertical deflection (Δh) of the beam. This can be obtained by analysing the deflection of beam (η) using an elastic theory. In the elastic analysis, the effect of local buckling on the compression elements of the specimens is also taken into account by means of an effective width approach.

7.4.1. ELASTIC BEAM DEFLECTION.

The analysis of beam deflection caused by global bending moment is carried out according to Figure 7.7. From an elastic analysis, the elastic deflection of beam (η) is :

$$\eta = \frac{P \, l^3}{48 \, E \, I} \quad \dots \dots \dots \dots (7.4.1)$$

Where :

E   : modulus of elasticity

I   : the second moment of area and this is determined according to the effective cross-section of the beam, i.e. :

233

$$I = t \ [b_{eff} \ Y_c^2 + \frac{1}{3} (Y_c^3 + Y_t^3) + b_p \ Y_t^2] \ \ldots\ldots\ldots\ldots \ (7.4.2)$$
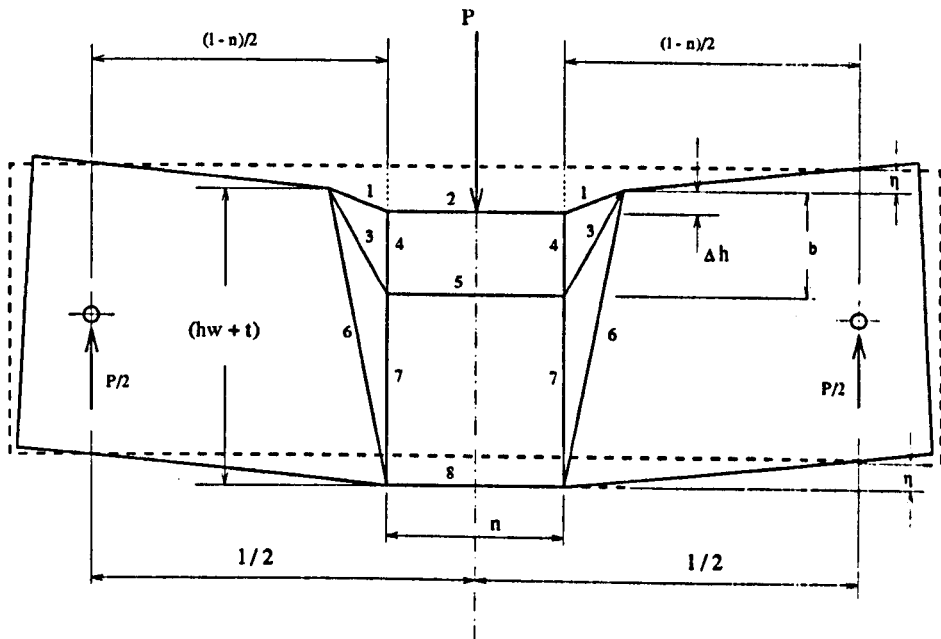
Figure 7.7. Beam deflection.

In equation (7.4.2), b_{eff} is the effective width of compression element while Y_c and Y_t are the position of neutral axis of the effective cross-section of the beam. The determination of b_{eff} will involve the analysis of maximum and critical buckling stresses of the compression element.

7.4.2. ELASTIC STRESSES IN THE BEAM.

Figure 7.8 shows the elastic stress distribution in the beam caused by the global bending moment. The compressive stress σ_c is uniformly distributed along the effective width (b_{eff}) of the top flange and non-uniformly distributed in the web. This stress is calculated from :

$$\sigma_c = \frac{P\ (1-n)}{4\ \dfrac{I_x}{Y_c}} \quad \ldots\ldots\ldots\ldots\ldots \quad (7.4.3)$$

I_x is the second moment of the effective cross-section of the beam about the neutral axis X-X and it is calulated using the following equation.

$$I_x = t\ [b_{eff}\ Y_c^2 + \frac{1}{3}\ (Y_c^3 + Y_t^3) + b_p\ Y_t^2] \quad \ldots\ldots\ldots\ldots \quad (7.4.4)$$
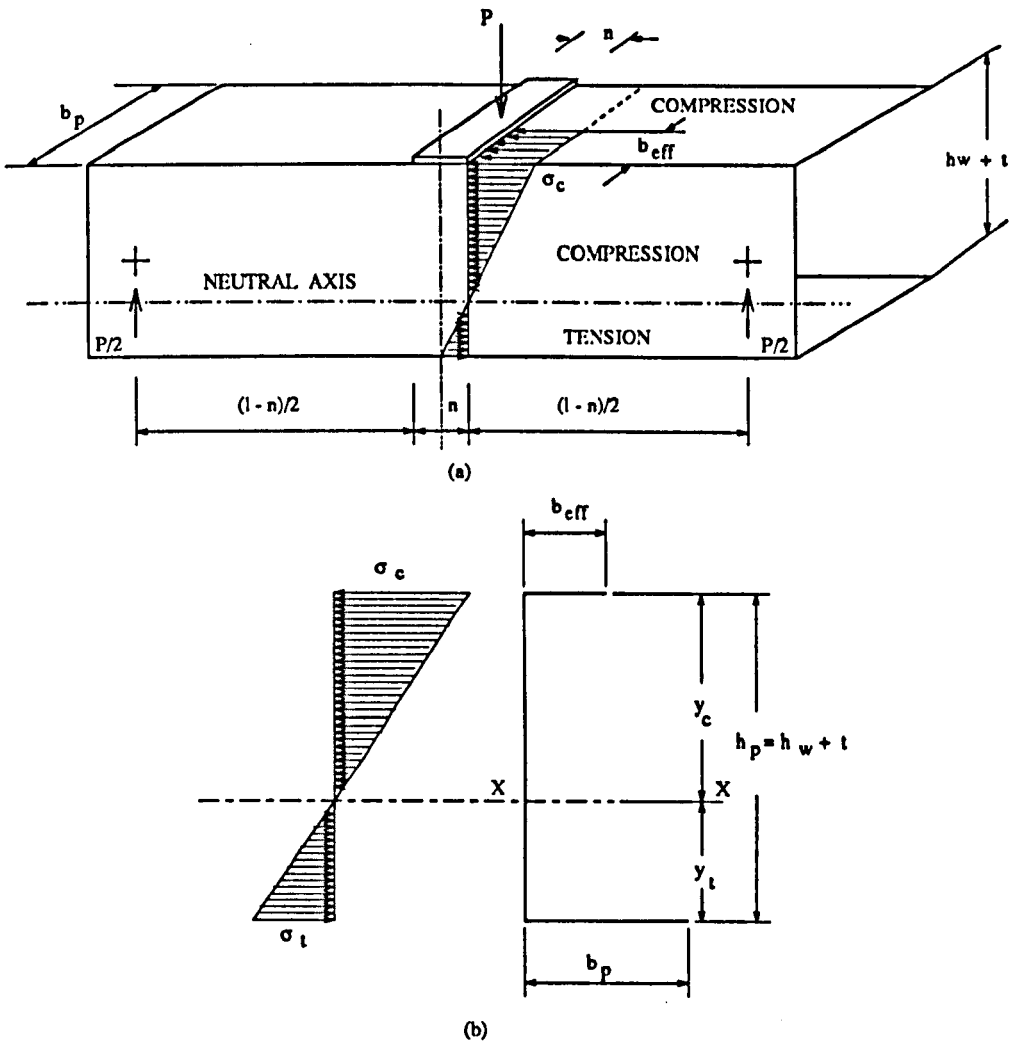
Figure 7.8. Elastic stresses due to global bending moment.

235

In equation (7.4.4), the effective width of the top flange (b_{eff}) is determined according to the following basic concept.

$$If \quad \frac{\sigma_{max}}{\sigma_{cr}} < 0.123 \quad ; \quad \frac{b_{eff}}{b} = 1 \quad \ldots\ldots\ldots\ldots \quad (7.4.5)$$

$$If \quad \frac{\sigma_{max}}{\sigma_{cr}} > 0.123 \quad ; \quad \frac{b_{eff}}{b} = [1 + 14 \ (\sqrt{\frac{\sigma_{max}}{\sigma_{cr}}} - 0.35 \ )^4]^{-0.2}$$

$$\ldots\ldots\ldots\ldots\ldots\ldots\ldots\ldots \quad (7.4.6)$$

where :

b_{eff}: effective width of compression element ; b : full width of compression element.

σ_{max}: maximum compressive stress ; σ_{cr}: the buckling stress.

The buckling stress is calculated from :

$$\sigma_{cr} = \frac{K \ \pi^2 \ E}{12 \ (1 - v^2)} \ (\frac{t}{b})^2 \quad \ldots\ldots\ldots\ldots \quad (7.4.7)$$

where :

K : coefficient of buckling ; E : modulus of elasticity.

v : Poisson's ratio ; t : thickness.

The maximum compressive stress acting on the top flange is taken to be equal to the yield strength of the basic material ($\sigma_{max} = \sigma_y$). From reference [54], Poisson's ratio for steel v = 0.3 and K is taken as 0.425 (the top flange is an unstiffened element). According to Figure 4.1, the full width of the compression element (b) as stated in the formulae (7.4.5) - (7.4.7) is certainly equal to b_p so that the value of b_{eff} of the

236

top flange can be calculated by replacing b_p for b in the above formulae. The position

of neutral axis (Y_c and Y_t) is determined from :

$$y_t = \frac{\sum A_i\, y_i}{\sum A_i}$$

y_i is measured from the bottom flange

$$y_t = \frac{b_{eff}\cdot(h_w+t) + \dfrac{(h_w+t)^2}{2}}{b_{eff} + (h_w+t) + b_p} = \frac{(h_w+t)\,[b_{eff} + 0.5(h_w+t)]}{b_{eff} + (h_w+t) + (B-0.5t)}$$

$$y_t = \frac{(h_w+t)\,(b_{eff} + 0.5\,h_w + 0.5\,t)}{(b_{eff} + h_w + B + 0.5\,t)} \quad \dots\dots\dots\dots\dots \quad (7.4.8)$$

$$y_c = h_p - y_t = h_w + t - \frac{(h_w+t)\,(b_{eff} + 0.5\,h_w + 0.5\,t)}{(b_{eff} + h_w + B + 0.5\,t)}$$

$$y_c = \frac{(h_w+t)\,(B+0.5\,h_w)}{(b_{eff} + h_w + B + 0.5\,t)} \quad \dots\dots\dots\dots\dots\dots \quad (7.4.9)$$

From equations (7.4.3) - (7.4.9), the second moment of the effective cross-section of

the beam about its neutral axis can be expressed as follows :

$$I_x = \frac{(hw+t)^2\,[3b_{eff}f_1 f_3^2 + f_3^3\,(hw+t)]}{12\,f_1^3} +$$

$$\frac{(hw+t)^2\,[f_2^3\,(hw+t) + 3f_1 f_2^2\,(B-0.5t)]}{12\,f_1^3}$$

$$\dots\dots\dots\dots\dots\dots\dots\dots\dots\dots\dots \quad (7.4.10)$$

Where :

$f_1 : b_{eff} + hw + B + 0.5t$; $f_2 : b_{eff} + 0.5hw + 0.5t$; $f_3 : B + 0.5hw$

In calculating the elastic deflection of the beam (η), this above equation is substituted

for I in equation (7.4.1). Thus, it can be summarized that the deflection of beam (η)

may be expressed as follows :

From the plastic mechanism analysis :

$$\eta = \frac{\Delta h^2 \ (1-n)}{4 \ e \ \sqrt{(hw+t)^2 + e^2}} \quad ; \quad \Delta h^2 = (b - \sqrt{b - \Delta^2})^2$$

From the elastic beam analysis :

$$\eta = \frac{P \ l^3}{48 \ E \ I} \quad ; \quad I = I_x$$

These above relationships are used as the basis of establishing the load-deflection

equation corresponding to the elastic analysis and expressing this in terms of the

plastic deformation. This equation is as follows :

$$P = \frac{12 \ E \ I \ (1-n) \ (b - \sqrt{b-\Delta^2})^2}{e \ l^3 \ \sqrt{(hw+t)^2 + e^2}} \quad \dots\dots\dots\dots\dots \quad (7.4.11)$$

Basically, the application of the plastic mechanism approach in determining the

ultimate web crippling load in this thesis follows the procedure shown in Figure 7.9.

The figure shows that the failure load (P_f) is obtained from the intersection of elastic

and plastic mechanism curves. These two theoretical curves can be predicted using

equations (7.3.12) and (7.4.11). From these equations, the ultimate web crippling load

can be obtained using an iteration method. In this method, the parameters which

govern these equations such as e, and Δ are initially set to zero and subsequently

increased with increments of 0.025 and 0.015 mm respectively until the following

condition is satisfied.

$$\frac{P_{el}}{P_p} \geq 0.9995$$

P_{el} is the load obtained from the elastic theory, i.e. equation (7.4.11), while P_p is

obtained from the plastic mechanism theory, i.e. equation (7.3.12) and this is based

on the two different procedures as suggested in the previous subchapter.
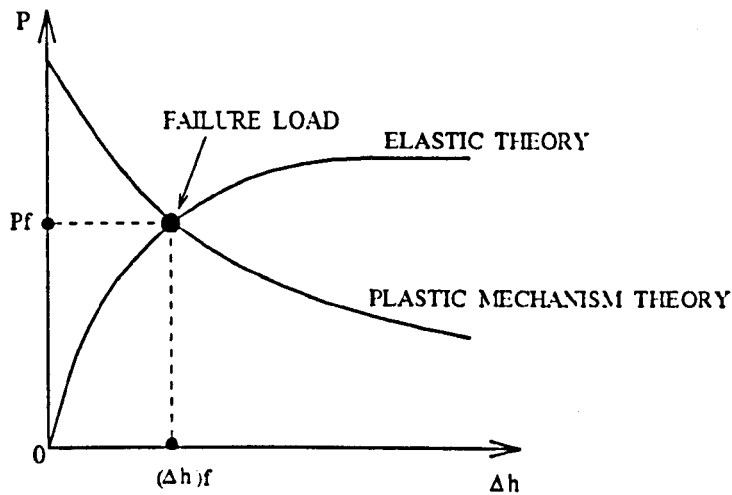
Figure 7.9. Determination of failure load.

The value of b was kept constant during the iteration and in order to obtain the

minimum value of theoretical ultimate load, the iteration was carried out step by step

with the value of b varied from (r+0.5t) to 0.25(hw+t). The minimum value of P_p

obtained was taken as the ultimate web crippling load (F_{CB}) and a computer program

for carrying out this iteration can be seen in appendix E. There are two different

values of F_{CB} presented in the following subchapter, i.e. $F_{CB}1$ which is based on the

application of the reduction factor only and $F_{CB}2$ which is based on the application

of the reduction factor and neglected energy dissipation at the plastic hinge lines 4

and 7.

7.5. RESULTS.

7.5.1. SERIES 1.

Table 7.1.

No.	Specimen	n/t	hw/t	r/t	l (mm)	$F_{CB}1$ (KN)	$F_{CB}2$ (KN)
1	H60-2	27.27	53.42	2.05	300	4.75	4.23
2	H60-4	27.27	53.42	2.05	300	4.77	4.26
3	H60-7	27.27	54.25	2.05	300	4.80	4.28
4	H60-9	27.27	54.23	2.05	300	4.77	4.24
5	H60-10	27.27	54.00	2.05	300	4.79	4.28
6	H60-18	31.53	54.86	2.03	300	5.19	4.66
7	H60-19	31.53	54.06	2.03	300	5.21	4.73
8	H60-20	31.53	54.52	2.03	300	5.19	4.66
9	H60-21	31.53	53.65	2.03	300	5.16	4.65
10	H60-22	31.53	53.95	2.03	300	5.18	4.67
11	H60-23	36.04	54.06	2.03	300	5.44	5.00

Table 7.1.

No.	Specimen	n/t	hw/t	r/t	l (mm)	$F_{CB}1$ (KN)	$F_{CB}2$ (KN)
12	H60-24	36.04	54.06	2.03	300	5.44	5.00
13	H60-25	36.04	54.41	2.03	300	5.46	5.00
14	H60-26	36.04	54.77	2.03	300	5.47	5.01
15	H60-27	36.04	54.06	2.03	300	5.45	5.01
16	H60-28	40.54	55.09	2.03	300	5.72	5.35
17	H60-29	40.54	54.54	2.03	300	5.70	5.35
18	H60-30	40.54	54.64	2.03	300	5.71	5.36
19	H60-31	40.54	54.36	2.03	300	5.70	5.35
20	H60-32	40.54	53.74	2.03	300	5.69	5.35
21	H60-33	44.64	54.71	2.01	304	5.91	5.69
22	H60-34	45.05	53.26	2.03	302	5.89	5.71
23	H60-35	45.05	55.71	2.03	302	5.94	5.70
24	H60-36	45.05	55.67	2.03	300	5.95	5.71
25	H60-37	45.05	55.21	2.03	300	5.94	5.71

Table 7.1.

No.	Specimen	n/t	hw/t	r/t	l (mm)	$F_{CB}1$ (KN)	$F_{CB}2$ (KN)
26	H70-6	27.03	62.35	2.03	350	4.72	4.12
27	H70-7	27.27	62.46	2.05	350	4.72	4.11
28	H70-8	27.27	62.46	2.05	350	4.70	4.11
29	H70-11	31.53	63.42	2.03	351	5.12	4.49
30	H70-12	31.53	63.22	2.03	351	5.11	4.48
31	H70-13	31.53	63.14	2.03	351	5.09	4.48
32	H70-14	31.53	63.79	2.03	350	5.13	4.50
33	H70-15	31.53	62.95	2.03	351	5.10	4.49
34	H70-18	36.04	63.68	2.03	352	5.38	4.78
35	H70-19	36.04	63.33	2.03	352	5.37	4.78
36	H70-20	36.04	63.47	2.03	351	5.37	4.77
37	H70-21	40.54	63.51	2.03	350	5.82	5.24
38	H70-23	40.54	63.90	2.03	350	5.62	5.09
39	H70-24	40.54	63.51	2.03	350	5.61	5.09

Table 7.1.

No.	Specimen	n/t	hw/t	r/t	l (mm)	$F_{CB}1$ (KN)	$F_{CB}2$ (KN)
40	H70-30	40.54	63.22	2.03	350	5.61	5.09
41	H70-25	45.05	63.13	2.03	350	5.81	5.39
42	H70-26	45.05	63.22	2.03	350	5.83	5.40
43	H70-27	45.05	62.76	2.03	350	5.80	5.39
44	H70-28	45.05	63.13	2.03	350	5.81	5.39
45	H70-29	45.05	63.56	2.03	350	5.82	5.39
46	H80-9	27.27	72.30	2.05	398	4.82	4.24
47	H80-10	27.27	72.51	2.05	398	4.83	4.25
48	H80-11	27.03	72.55	2.03	402	4.89	4.29
49	H80-12	27.03	72.67	2.03	402	4.89	4.29
50	H80-13	27.03	73.26	2.03	402	4.89	4.28
51	H80-14	31.53	72.00	2.03	402	5.18	4.59
52	H80-15	31.53	72.12	2.03	402	5.18	4.58
53	H80-16	31.53	71.94	2.03	402	5.16	4.57

Table 7.1.

No.	Specimen	n/t	hw/t	r/t	l (mm)	$F_{CB}1$ (KN)	$F_{CB}2$ (KN)
54	H80-17	36.04	72.23	2.03	402	5.45	4.85
55	H80-18	36.04	71.82	2.03	402	5.43	4.85
56	H80-19	36.04	72.44	2.03	402	5.54	4.93
57	H80-30	36.04	72.28	2.03	402	5.45	4.85
58	H80-31	36.04	71.89	2.03	402	5.44	4.85
59	H80-20	40.54	72.16	2.03	402	5.44	4.85
60	H80-21	40.54	73.04	2.03	402	5.69	5.12
61	H80-22	40.54	71.68	2.03	402	5.66	5.10
62	H80-23	40.54	72.96	2.03	403	5.68	5.10
63	H80-24	40.54	72.71	2.03	402	5.69	5.11
64	H80-25	45.05	72.85	2.03	402	5.88	5.36
65	H80-26	44.64	71.82	2.01	402	5.98	5.46
66	H80-27	45.05	72.10	2.03	402	5.87	5.36
67	H80-28	45.05	71.00	2.03	402	5.84	5.35

Table 7.1.

No.	Specimen	n/t	hw/t	r/t	l (mm)	$F_{CB}1$ (KN)	$F_{CB}2$ (KN)
68	H80-29	45.05	72.59	2.03	402	5.89	5.37
69	H90-10	27.27	80.78	2.05	453	4.78	4.15
70	H90-11	27.27	80.69	2.05	453	4.77	4.13
71	H90-12	27.27	81.59	2.05	450	4.80	4.15
72	H90-13	27.03	81.64	2.03	450	4.88	4.22
73	H90-14	30.00	88.98	2.25	451	4.10	3.54
74	H90-15	35.00	88.98	2.25	451	4.33	3.77
75	H90-16	31.53	82.25	2.03	451	5.18	4.51
76	H90-17	31.53	81.00	2.03	451	5.15	4.48
77	H90-18	36.04	81.52	2.03	451	5.40	4.72
78	H90-19	35.71	80.10	2.01	451	5.47	4.80
79	H90-20	36.36	81.82	2.05	451	5.32	4.66
80	H90-21	40.54	81.32	2.03	451	5.63	4.96
81	H90-22	40.18	80.09	2.01	451	5.63	4.96

Table 7.1.

No.	Specimen	n/t	hw/t	r/t	l (mm)	$F_{CB}1$ (KN)	$F_{CB}2$ (KN)
82	H90-23	40.54	81.32	2.03	450	5.64	4.97
83	H90-24	45.45	89.57	2.27	451	4.62	4.08
84	H90-25	40.54	81.18	2.03	451	5.63	4.97
85	H90-26	45.45	81.77	2.05	451	5.73	5.12
86	H90-27	45.05	81.45	2.03	451	5.83	5.21
87	H90-28	45.05	81.27	2.03	451	5.83	5.20
88	H90-29	44.64	79.96	2.01	451	5.89	5.27
89	H90-30	45.05	81.43	2.03	451	5.83	5.20
90	H100-1	30.00	99.35	2.25	500	4.16	3.53
91	H100-2	30.00	99.96	2.25	501	4.16	3.53
92	H100-3	30.00	98.97	2.25	502	4.14	3.51
93	H100-4	30.30	102.09	2.27	501	4.09	3.47
94	H100-5	30.30	101.29	2.27	502	4.10	3.47
95	H100-6	35.35	101.53	2.27	501	4.31	3.66

Table 7.1.

No.	Specimen	n/t	hw/t	r/t	l (mm)	$F_{CB}1$ (KN)	$F_{CB}2$ (KN)
96	H100-7	35.71	102.58	2.30	501	4.24	3.60
97	H100-8	35.00	99.90	2.25	501	4.38	3.73
98	H100-9	35.00	99.60	2.25	502	4.36	3.72
99	H100-10	35.00	99.90	2.25	501	4.37	3.73
100	H100-11	40.00	99.60	2.25	502	4.55	3.91
101	H100-12	40.00	98.51	2.25	502	4.52	3.89
102	H100-13	40.00	99.75	2.25	502	4.56	3.92
103	H100-14	40.00	99.60	2.25	502	4.55	3.91
104	H100-15	40.82	101.81	2.30	502	4.40	3.78
105	H100-16	45.00	98.77	2.25	502	4.71	4.08
106	H100-17	45.00	100.08	2.25	502	4.72	4.09
107	H100-18	45.00	100.26	2.25	502	4.73	4.09
108	H100-19	45.45	102.32	2.27	501	4.66	4.02
109	H100-20	45.45	100.39	2.27	503	4.63	4.02

Table 7.1.

No.	Specimen	n/t	hw/t	r/t	l (mm)	$F_{CB}1$ (KN)	$F_{CB}2$ (KN)
110	H100-21	50.00	99.52	2.25	503	4.86	4.26
111	H100-22	50.51	101.39	2.27	502	4.81	4.20
112	H100-23	50.00	100.11	2.25	502	4.88	4.26
113	H100-24	51.02	102.48	2.30	502	4.72	4.12
114	H100-25	50.00	100.24	2.25	502	4.88	4.26
115	H100-52	30.00	101.33	2.25	500	4.37	3.70
116	H100-53	30.61	104.89	2.30	500	4.25	3.60
117	H100-54	30.00	100.52	3.25	500	4.36	3.66
118	H100-55	30.00	99.39	3.25	500	4.34	3.64
119	H100-56	30.61	100.82	4.34	500	4.21	3.49
120	H100-57	30.93	101.87	4.38	500	4.14	3.42
121	H100-58	40.40	103.56	2.27	500	4.76	4.06
122	H100-59	40.82	105.44	2.30	500	4.68	3.99
123	H100-60	40.40	100.61	3.28	500	4.71	4.02

Table 7.1.

No.	Specimen	n/t	hw/t	r/t	l (mm)	$F_{CB}1$ (KN)	$F_{CB}2$ (KN)
124	H100-61	41.67	104.04	3.39	500	4.48	3.82
125	H100-62	40.00	99.36	4.25	500	4.78	4.04
126	H100-63	40.40	99.01	4.29	500	4.68	3.97
127	H100-64	50.51	103.29	2.27	500	5.08	4.42
128	H100-65	51.55	106.25	2.32	500	4.92	4.30
129	H100-66	49.50	98.95	2.23	500	5.14	4.50
130	H100-67	50.51	100.42	3.28	500	5.04	4.40
131	H100-68	49.50	97.40	4.21	500	5.20	4.54
132	H100-69	50.00	98.00	4.25	500	5.11	4.47

7.5.2. SERIES 2.

Table 7.2.

No.	Specimen	n/t	hw/t	r/t	l (mm)	$F_{CB}1$ (KN)	$F_{CB}2$ (KN)
1	H60-6	40.40	60.59	3.79	175	5.44	5.30
2	H60-8	40.00	59.62	3.50	176	5.53	5.30
3	H60-11	40.00	60.26	3.25	176	5.54	5.30
4	H60-12	51.02	60.33	3.32	177	5.83	5.52
5	H60-38	50.00	61.12	3.75	177	6.07	5.52
6	H60-39	50.00	59.40	3.50	175	6.02	5.52
7	H80-35	40.40	80.61	3.79	230	5.39	4.95
8	H80-36	40.00	80.20	3.75	230	5.49	5.03
9	H80-37	40.00	79.48	3.75	230	5.48	4.94
10	H80-32	30.00	80.52	3.50	230	4.87	4.19
11	H80-33	30.00	79.00	3.75	230	4.86	4.19
12	H80-34	30.00	80.00	3.75	230	4.86	4.18
13	H100-28	30.30	101.01	4.04	300	4.73	3.86

Table 7.2.

No.	Specimen	n/t	hw/t	r/t	l (mm)	$F_{CB}1$ (KN)	$F_{CB}2$ (KN)
14	H100-29	40.00	99.58	4.00	300	5.37	4.59
15	H100-30	40.00	99.98	4.00	300	5.38	4.60
16	H100-31	40.00	101.94	4.00	300	5.41	4.60
17	H100-32	50.51	101.94	4.04	300	5.73	5.15
18	H100-33	50.00	99.78	4.00	300	5.80	5.23
19	H100-34	50.00	99.80	4.00	300	5.82	5.26
20	H100-36	30.00	101.88	2.25	300	4.85	4.03
21	H100-37	30.30	99.41	3.28	300	4.95	4.12
22	H100-41	39.60	100.97	2.23	300	5.51	4.77
23	H100-42	40.40	103.05	2.27	300	5.61	4.84
24	H100-44	39.60	98.63	3.22	300	5.47	4.69
25	H100-47	50.51	102.40	2.27	300	6.04	5.49
26	H100-49	50.50	100.83	3.28	300	6.02	5.43
27	H100-50	50.00	98.00	4.25	300	6.08	5.53

CHAPTER 8

COMPARISONS OF DESIGN SPECIFICATIONS

AND

EXPERIMENTS

8.1. GENERAL.

The values of ultimate web crippling load predicted by BS 5950 Part 5 1987 and

European Recommendations 1987 are compared with those obtained from the

experiments in this chapter. In the comparisons, the experimental ultimate web

crippling loads (F_e) are divided by the theoretical ones (F_{CB} or F_C) and their ratios

are presented in the tables and plotted against the parameters studied in this research

programs. The accuracy of the theoretical results indicated by the various values of

F_e/F_{CB} and F_e/F_C is evaluated according to statistical methods, where this is employed

by calculating the mean, the standard deviation and the coefficient of variation.

The statistical measures of accuracy in this chapter were calculated from the

following formulae. [60]

The mean :

$$\overline{X} = \frac{\sum\limits_{i=1}^{N} X_i}{N} \quad \ldots\ldots\ldots\ldots \quad (8.1.1)$$

The standard deviation :

$$S = \sqrt{\frac{\sum\limits_{i=1}^{N} (X_i - \overline{X})^2}{(N-1)}} \quad \ldots\ldots\ldots\ldots\ldots \quad (8.1.2)$$

The coefficient of variation :

$$CV_x = \frac{s}{\overline{X}} \quad \ldots\ldots\ldots\ldots\ldots \quad (8.1.3)$$

In using the above formulae, the value of X_i was equated to an individual value of

F_e/F_{CB} or F_e/F_C and N was the total number of data of both ratios. The accuracy of

the theoretical results are also shown in diagrams of the ratios of F_e/F_{CB} or F_e/F_C

against the parameters studied. In the diagrams, the scatter data of F_e/F_{CB} and F_e/F_C

are limited to the values of $\pm$ 20% where these are based on the acceptable scatter

limits normally used in the web crippling tests. The experimental ultimate loads (F_e)

are also plotted against the theoretical ultimate loads (F_{CB} or F_C) and the scatter data

representing the difference of theoretical and experimental values of the ultimate

loads are limited to $\pm$ 20%. Finally, this chapter is closed with discussions concerning

the results of comparing the theoretical and experimental values of ultimate web

crippling load.

8.2. SPECIMENS TESTED UNDER IOF.

Table 8.1. SERIES 1 (M/M$_c$ $\geq$ 0.3)

No.	Speci-men	n/t	hw/t	r/t	F_e (KN)	F_{CB} (KN)		F_e / F_{CB}	
						BS	ER	BS	ER
1	H60-2	27.27	53.42	2.05	4.09	4.58	3.03	0.89	1.35

BS : BS 5950 Part 5 1987 and ER : EUROPEAN RECOMMENDATIONS 1987

Table 8.1. SERIES 1 (M/M$_c$ $\geq$ 0.3)

No.	Speci-men	n/t	hw/t	r/t	F$_e$ (KN)	F$_{CB}$ (KN)		F$_e$ / F$_{CB}$	
						BS	ER	BS	ER
2	H60-4	27.27	53.42	2.05	4.14	4.59	3.04	0.90	1.36
3	H60-7	27.27	54.25	2.05	4.18	4.61	3.06	0.91	1.36
4	H60-9	27.27	54.23	2.05	4.14	4.60	3.05	0.90	1.35
5	H60-10	27.27	54.00	2.05	4.09	4.61	3.06	0.89	1.34
6	H60-18	31.53	54.86	2.03	4.37	4.80	3.24	0.91	1.35
7	H60-19	31.53	54.06	2.03	4.37	4.80	3.22	0.91	1.35
8	H60-20	31.53	54.52	2.03	4.35	4.81	3.23	0.91	1.35
9	H60-21	31.53	53.65	2.03	4.39	4.79	3.21	0.92	1.37
10	H60-22	31.53	53.95	2.03	4.41	4.80	3.22	0.92	1.37
11	H60-23	36.04	54.06	2.03	4.57	4.91	3.33	0.93	1.37
12	H60-24	36.04	54.06	2.03	4.61	4.91	3.33	0.94	1.39
13	H60-25	36.04	54.41	2.03	4.53	4.92	3.34	0.92	1.36

BS : BS 5950 Part 5 1987 and ER : EUROPEAN RECOMMENDATIONS 1987

Table 8.1. SERIES 1 ($M/M_c \geq 0.3$)

No.	Speci-men	n/t	hw/t	r/t	F_e (KN)	F_{CB} (KN)		F_e / F_{CB}	
						BS	ER	BS	ER
14	H60-26	36.04	54.77	2.03	4.54	4.93	3.36	0.92	1.36
15	H60-27	36.04	54.07	2.03	4.57	4.92	3.33	0.93	1.37
16	H60-28	40.54	55.09	2.03	4.76	5.05	3.46	0.94	1.37
17	H60-29	40.54	54.54	2.03	4.86	5.04	3.45	0.96	1.41
18	H60-30	40.54	54.64	2.03	4.78	5.04	3.45	0.95	1.39
19	H60-31	40.54	54.36	2.03	4.81	5.03	3.44	0.96	1.40
20	H60-32	40.54	53.74	2.03	4.85	5.02	3.43	0.97	1.42
21	H100-60	44.64	54.71	2.01	4.89	5.24	3.62	0.93	1.35
22	H60-34	45.05	53.26	2.03	4.96	5.12	3.51	0.97	1.41
23	H60-35	45.05	55.71	2.03	4.88	5.18	3.58	0.94	1.36
24	H60-36	45.05	55.67	2.03	4.91	5.19	3.58	0.95	1.37
25	H60-37	45.05	55.21	2.03	4.91	5.17	3.57	0.95	1.38

BS : BS 5950 Part 5 1987 and ER : EUROPEAN RECOMMENDATIONS 1987

Table 8.1. SERIES 1 (M/M$_c$ ≥ 0.3)

No.	Speci-men	n/t	hw/t	r/t	F$_e$ (KN)	F$_{CB}$ (KN)		F$_e$ / F$_{CB}$	
						BS	ER	BS	ER
26	H70-6	27.27	62.88	2.05	3.97	4.58	3.14	0.87	1.26
27	H70-7	27.27	62.43	2.05	3.81	4.57	3.08	0.83	1.24
28	H70-8	27.27	62.03	2.05	3.91	4.56	3.08	0.86	1.24
29	H70-11	31.53	63.42	2.03	4.25	4.78	3.27	0.89	1.30
30	H70-12	31.53	63.22	2.03	4.27	4.77	3.26	0.89	1.31
31	H70-13	31.53	63.14	2.03	4.47	4.77	3.26	0.94	1.37
32	H70-14	31.53	63.79	2.03	4.40	4.79	3.28	0.92	1.34
33	H70-15	31.53	62.95	2.03	4.42	4.77	3.26	0.93	1.36
34	H70-18	36.04	63.68	2.03	4.39	4.89	3.38	0.90	1.30
35	H70-19	36.04	63.33	2.03	4.48	4.88	3.37	0.92	1.33
36	H70-20	36.04	63.47	2.03	4.40	4.89	3.37	0.90	1.30
37	H70-21	40.54	63.51	2.03	4.72	5.00	3.48	0.94	1.35

BS : BS 5950 Part 5 1987 and ER : EUROPEAN RECOMMENDATIONS 1987

256

Table 8.1. SERIES 1 ($M/M_c \geq 0.3$)

No.	Speci-men	n/t	hw/t	r/t	F_e (KN)	F_{CB} (KN)		F_e / F_{CB}	
						BS	ER	BS	ER
38	H70-23	40.54	63.90	2.03	4.65	5.01	3.49	0.93	1.33
39	H70-24	40.54	63.51	2.03	4.81	5.01	3.48	0.96	1.38
40	H70-30	40.54	63.22	2.03	4.77	4.99	3.48	0.95	1.37
41	H70-25	45.05	63.13	2.03	4.98	5.11	3.57	0.97	1.39
42	H70-26	45.05	63.22	2.03	4.82	5.12	3.58	0.94	1.35
43	H70-27	45.05	62.76	2.03	4.85	5.10	3.56	0.95	1.36
44	H70-28	45.05	63.13	2.03	4.89	5.11	3.57	0.96	1.37
45	H70-29	45.05	63.56	2.03	4.83	5.12	3.58	0.94	1.35
46	H80-9	27.27	72.26	2.05	4.07	4.64	3.18	0.86	1.29
47	H80-10	27.27	72.47	2.05	4.11	4.64	3.19	0.89	1.30
48	H80-11	27.03	72.55	2.03	4.24	4.72	3.24	0.90	1.31
49	H80-12	27.03	72.67	2.03	4.31	4.72	3.24	0.91	1.33

BS : BS 5950 Part 5 1987 and ER : EUROPEAN RECOMMENDATIONS 1987

257

Table 8.1. SERIES 1 ($M/M_c \geq 0.3$)

No.	Speci-men	n/t	hw/t	r/t	F_e (KN)	F_{CB} (KN)		F_e / F_{CB}	
						BS	ER	BS	ER
50	H80-13	27.03	73.26	2.03	4.20	4.73	3.25	0.89	1.29
51	H80-14	31.53	72.00	2.03	4.41	4.82	3.34	0.92	1.32
52	H80-15	31.53	72.12	2.03	4.59	4.82	3.34	0.95	1.37
53	H80-16	31.53	71.94	2.03	4.46	4.82	3.34	0.93	1.33
54	H80-17	36.04	72.23	2.03	4.56	4.93	3.46	0.92	1.32
55	H80-18	36.04	71.81	2.03	4.65	4.92	3.44	0.94	1.35
56	H80-19	36.04	72.44	2.03	4.60	5.02	3.46	0.92	1.33
57	H80-30	36.04	72.28	2.03	4.49	4.93	3.46	0.91	1.30
58	H80-31	36.04	71.89	2.03	4.56	4.93	3.45	0.92	1.32
59	H80-20	40.54	72.16	2.03	4.77	5.04	3.55	0.95	1.34
60	H80-21	40.54	73.04	2.03	4.68	5.05	3.58	0.93	1.31
61	H80-22	40.54	71.68	2.03	4.94	5.03	3.54	0.98	1.39

BS : BS 5950 Part 5 1987 and ER : EUROPEAN RECOMMENDATIONS 1987

Table 8.1. SERIES 1 ($M/M_c \geq 0.3$)

No.	Speci-men	n/t	hw/t	r/t	F_e (KN)	F_{CB} (KN)		F_e / F_{CB}	
						BS	ER	BS	ER
62	H80-23	40.54	72.96	2.03	4.82	5.05	3.57	0.95	1.35
63	H80-24	40.54	72.71	2.03	4.79	5.05	3.57	0.95	1.34
64	H80-25	45.05	72.85	2.03	5.16	5.16	3.67	1.00	1.41
65	H80-26	44.64	71.82	2.01	4.88	5.24	3.71	0.93	1.31
66	H80-27	45.05	72.10	2.03	5.07	5.15	3.65	0.99	1.39
67	H80-28	45.05	71.10	2.03	5.04	5.12	3.62	0.98	1.39
68	H80-29	45.05	72.59	2.03	5.04	5.16	3.66	0.98	1.38
69	H90-10	27.27	80.78	2.05	4.15	4.60	3.20	0.90	1.30
70	H90-11	27.27	80.69	2.05	4.13	4.59	3.20	0.90	1.29
71	H90-12	27.27	81.59	2.05	4.21	4.61	3.22	0.91	1.31
72	H90-13	27.03	81.64	2.03	4.16	4.70	3.28	0.89	1.27
73	H90-14	30.00	88.98	2.25	3.25	3.81	2.73	0.85	1.19

BS : BS 5950 Part 5 1987 and ER : EUROPEAN RECOMMENDATIONS 1987

259

Table 8.1. SERIES 1 ($M/M_c \geq 0.3$)

No.	Speci-men	n/t	hw/t	r/t	F_e (KN)	F_{CB} (KN)		F_e / F_{CB}	
						BS	ER	BS	ER
74	H90-15	35.00	88.98	2.25	3.35	3.91	2.83	0.86	1.18
75	H90-16	31.53	82.25	2.03	4.25	4.82	3.41	0.88	1.25
76	H90-17	31.53	81.00	2.03	4.39	4.80	3.39	0.91	1.30
77	H90-18	36.04	81.52	2.03	4.51	4.91	3.50	0.92	1.29
78	H90-19	35.71	80.10	2.01	4.53	4.99	3.54	0.91	1.28
79	H90-20	36.36	81.82	2.05	4.69	4.82	3.45	0.97	1.36
80	H90-21	40.54	81.32	2.03	4.64	5.01	3.60	0.93	1.29
81	H90-22	40.18	80.09	2.01	4.67	5.10	3.65	0.92	1.28
82	H90-23	40.54	81.32	2.03	4.63	5.02	3.61	0.92	1.28
83	H90-24	45.45	89.57	2.27	3.55	4.02	2.96	0.88	1.20
84	H90-25	40.54	81.18	2.03	4.83	5.02	3.60	0.96	1.34
85	H90-26	45.45	81.77	2.05	4.82	5.03	3.64	0.96	1.33

BS : BS 5950 Part 5 1987 and ER : EUROPEAN RECOMMENDATIONS 1987

Table 8.1. SERIES 1 $(M/M_c \geq 0.3)$

No.	Speci-men	n/t	hw/t	r/t	F_e (KN)	F_{CB} (KN)		F_e / F_{CB}	
						BS	ER	BS	ER
86	H90-27	45.05	81.45	2.03	5.07	5.13	3.70	0.99	1.37
87	H90-28	45.05	81.27	2.03	4.78	5.12	3.70	0.93	1.29
88	H90-29	44.64	79.96	2.01	5.12	5.20	3.74	0.99	1.37
89	H90-30	45.05	81.43	2.03	4.74	5.12	3.70	0.92	1.28
90	H100-1	30.00	99.35	2.25	3.41	3.83	2.79	0.89	1.22
91	H100-2	30.00	99.96	2.25	3.41	3.83	2.79	0.89	1.22
92	H100-3	30.00	98.97	2.25	3.42	3.82	2.78	0.89	1.23
93	H100-4	30.30	102.09	2.27	3.29	3.76	2.76	0.87	1.19
94	H100-5	30.30	101.29	2.27	3.29	3.75	2.75	0.88	1.20
95	H100-6	35.35	101.53	2.27	3.27	3.85	2.85	0.85	1.14
96	H100-7	35.71	102.58	2.30	3.31	3.77	2.81	0.88	1.18
97	H100-8	35.00	99.90	2.25	3.53	3.92	2.90	0.90	1.22

BS : BS 5950 Part 5 1987 and ER : EUROPEAN RECOMMENDATIONS 1987

Table 8.1. SERIES 1 (M/M$_c$ ≥ 0.3)

No.	Speci-men	n/t	hw/t	r/t	F$_e$ (KN)	F$_{CB}$ (KN)		F$_e$ / F$_{CB}$	
						BS	ER	BS	ER
98	H100-9	35.00	99.60	2.25	3.47	3.92	2.89	0.89	1.20
99	H100-10	35.00	99.90	2.25	3.43	3.92	2.90	0.87	1.18
100	H100-11	40.00	99.60	2.25	3.74	4.01	2.98	0.93	1.25
101	H100-12	40.00	98.51	2.25	3.49	4.00	2.97	0.87	1.18
102	H100-13	40.00	99.75	2.25	3.67	4.02	2.99	0.91	1.23
103	H100-14	40.00	99.60	2.25	3.51	4.01	2.98	0.87	1.17
104	H100-15	40.82	101.81	2.30	3.53	3.86	2.89	0.92	1.22
105	H100-16	45.00	98.97	2.25	3.72	4.10	3.06	0.91	1.22
106	H100-17	45.00	100.08	2.25	3.81	4.11	3.08	0.93	1.24
107	H100-18	45.00	100.26	2.25	3.82	4.11	3.08	0.93	1.24
108	H100-19	45.45	102.32	2.27	3.64	4.04	3.04	0.90	1.20
109	H100-20	45.45	100.39	2.27	3.66	4.02	3.02	0.91	1.21

BS : BS 5950 Part 5 1987 and ER : EUROPEAN RECOMMENDATIONS 1987

Table 8.1. SERIES 1 (M/M$_c$ ≥ 0.3)

No.	Speci-men	n/t	hw/t	r/t	F$_e$ (KN)	F$_{CB}$ (KN)		F$_e$ / F$_{CB}$	
						BS	ER	BS	ER
110	H100-21	50.00	99.52	2.27	3.81	4.13	3.12	0.92	1.22
111	H100-22	50.51	101.39	2.27	3.81	4.13	3.12	0.92	1.22
112	H100-23	50.00	100.11	2.25	3.83	4.20	3.16	0.91	1.21
113	H100-24	51.02	102.48	2.30	3.87	4.04	3.06	0.96	1.26
114	H100-25	50.00	100.24	2.25	3.90	4.20	3.16	0.93	1.23
115	H100-52	30.00	101.33	2.25	3.25	3.95	2.98	0.82	1.09
116	H100-53	30.61	104.89	2.30	3.16	3.80	2.90	0.83	1.09
117	H100-54	30.00	100.52	3.25	3.11	3.75	2.90	0.83	1.07
118	H100-55	30.00	99.39	3.25	3.11	3.74	2.89	0.83	1.08
119	H100-56	30.61	100.82	4.34	2.89	3.39	2.72	0.87	1.06
120	H100-57	30.93	101.87	4.38	2.89	3.32	2.68	0.87	1.10
121	H100-58	40.40	103.56	2.27	4.10	4.07	3.16	1.01	1.30

BS : BS 5950 Part 5 1987 and ER : EUROPEAN RECOMMENDATIONS 1987

Table 8.1. SERIES 1 (M/M$_c$ ≥ 0.3)

No.	Speci-men	n/t	hw/t	r/t	F$_e$ (KN)	F$_{CB}$ (KN)		F$_e$ / F$_{CB}$	
						BS	ER	BS	ER
122	H100-59	40.82	105.44	2.30	4.10	3.99	3.11	1.03	1.31
123	H100-60	40.40	100.61	3.28	4.07	3.85	3.04	1.06	1.29
124	H100-61	41.67	104.04	3.39	3.87	3.62	2.90	1.07	1.34
125	H100-62	40.00	99.36	4.25	3.96	3.72	3.03	1.07	1.31
126	H100-63	40.40	99.01	4.29	3.83	3.63	2.96	1.05	1.29
127	H100-64	50.51	103.29	2.27	4.09	4.25	3.33	0.96	1.23
128	H100-65	51.55	106.25	2.32	4.25	4.10	3.24	1.04	1.31
129	H100-66	49.50	98.95	2.23	4.16	4.41	3.41	0.94	1.22
130	H100-67	50.51	100.42	3.28	3.94	4.03	3.22	0.98	1.22
131	H100-68	49.50	97.40	4.21	3.96	3.97	3.24	1.00	1.22
132	H100-69	50.00	98.00	4.25	4.00	3.89	3.18	1.03	1.26

BS : BS 5950 Part 5 1987 and ER : EUROPEAN RECOMMENDATIONS 1987

Table 8.1. SERIES 1 (M/M$_c$ ≥ 0.3)

Statistical measures of accuracy of F$_e$/F$_{CB}$	BS 5950 Part 5 1987	EUROPEAN RECOMMENDATIONS 1987
Mean	0.932	1.294
Standard deviation	0.065	0.080
Coeff. of variation	0.070	0.062
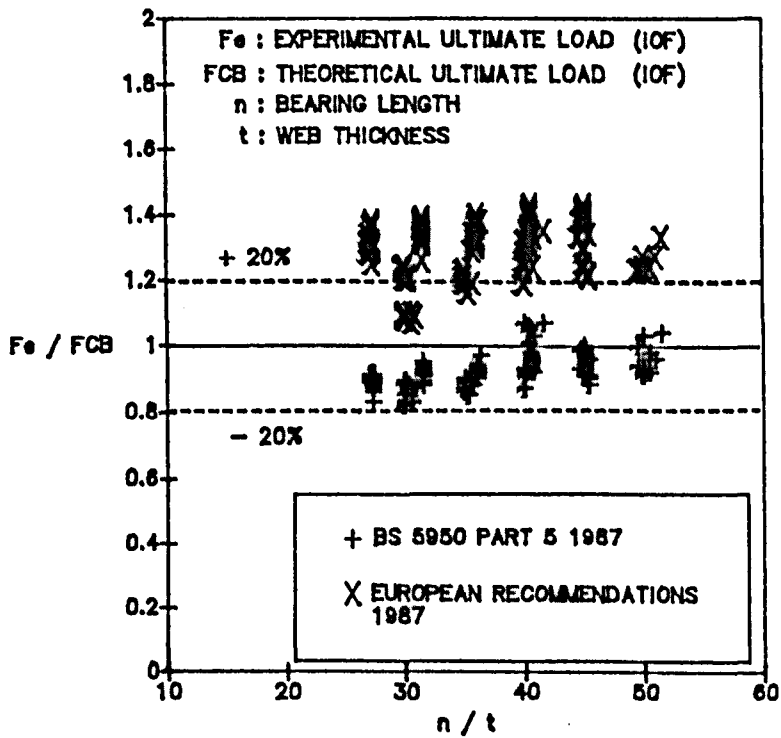
Figure 8.1. F$_e$/F$_{CB}$ vs. bearing length ratio, for M/M$_c$ ≥ 0.3.
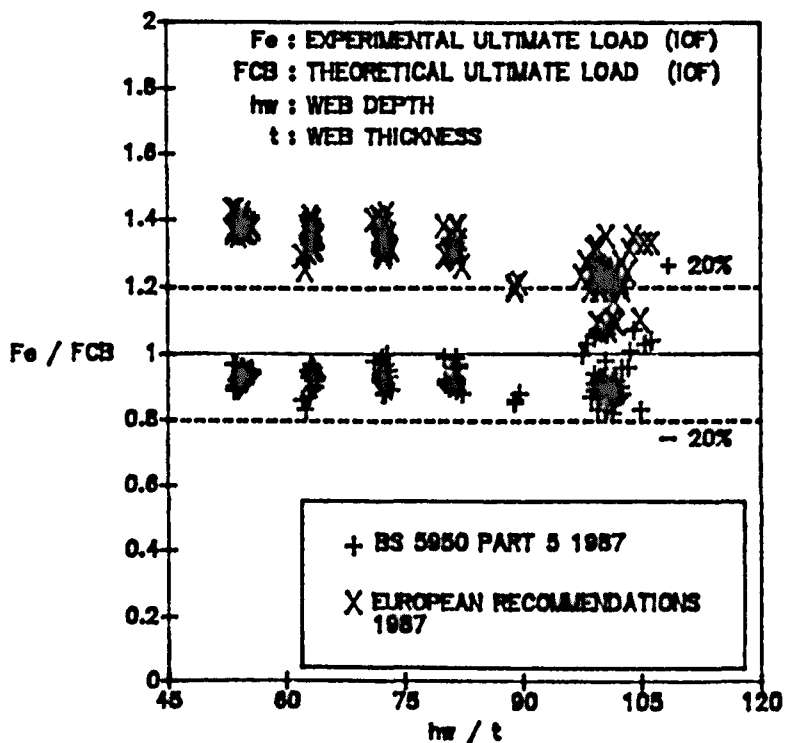
Figure 8.2. F_e/F_{CB} vs. web slenderness ratio, for $M/M_c \geq 0.3$.
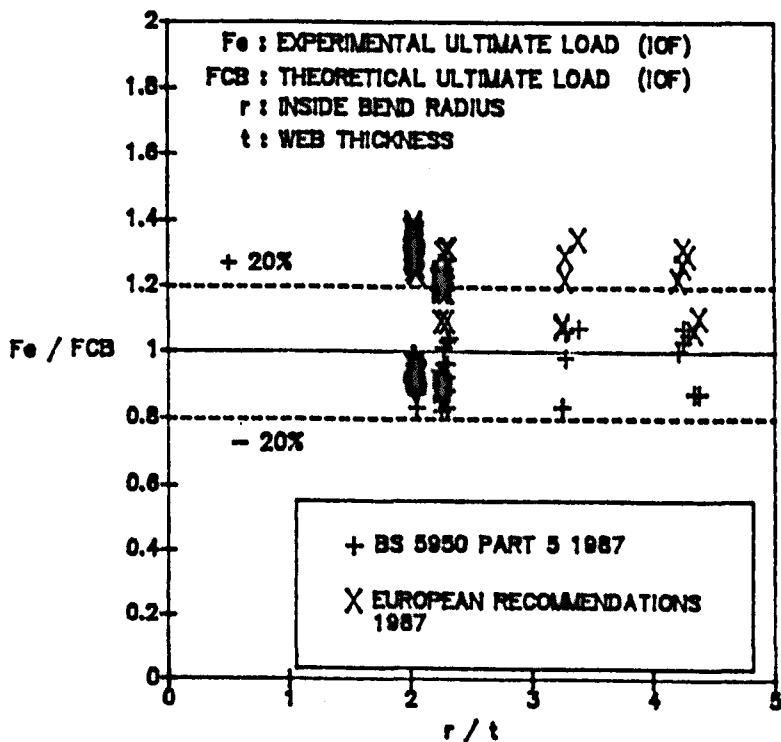
Figure 8.3. F_e/F_{CB} vs. inside bend radius ratio, for $M/M_c \geq 0.3$.

266
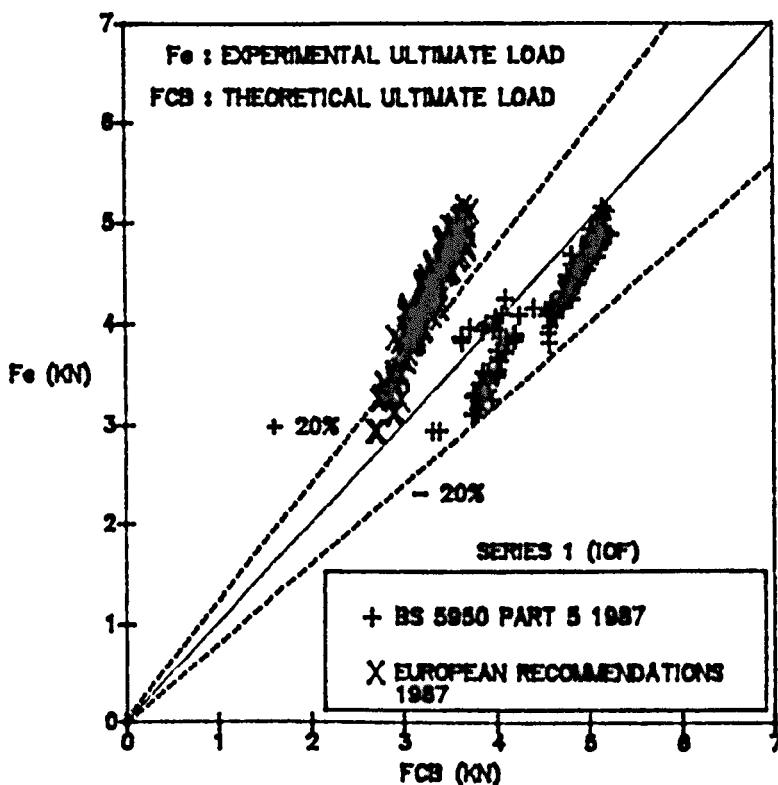
Figure 8.4. Theoretical load F_{CB} vs. experimental load F_e, for $M/M_c \geq 0.3$.

Table 8.2. SERIES 2 ($M/M_c < 0.3$)

No.	Speci- men	n/t	hw/t	r/t	F_e (KN)	F_{CB} (KN)		F_e / F_{CB}	
						BS	ER	BS	ER
1	H60-6	40.40	60.59	3.79	4.36	4.23	3.22	1.03	1.35
2	H60-8	40.00	59.62	3.50	4.27	4.38	3.29	0.97	1.30
3	H60-11	40.00	60.26	3.25	4.45	4.45	3.32	1.00	1.34

BS : BS 5950 Part 5 1987 and ER : EUROPEAN RECOMMENDATIONS 1987

267

Table 8.2. SERIES 2 (M/M$_c$ < 0.3)

No.	Speci-men	n/t	hw/t	r/t	F$_e$ (KN)	F$_{CB}$ (KN)		F$_e$ / F$_{CB}$	
						BS	ER	BS	ER
4	H60-12	51.02	60.33	3.32	4.67	4.51	3.43	1.04	1.36
5	H60-38	50.00	61.12	3.75	4.89	4.57	3.55	1.07	1.38
6	H60-39	50.00	59.40	3.50	4.76	4.64	3.54	1.03	1.34
7	H80-35	40.40	80.61	3.79	4.38	4.13	3.26	1.06	1.34
8	H80-36	40.00	80.20	3.75	4.36	4.22	3.32	1.03	1.31
9	H80-37	40.00	79.48	3.75	4.36	4.22	3.31	1.03	1.32
10	H80-38	50.51	80.55	3.79	4.89	4.36	3.49	1.12	1.40
11	H80-39	50.51	80.61	3.79	4.89	4.36	3.49	1.12	1.40
12	H80-40	50.00	79.38	3.75	5.07	4.45	3.55	1.14	1.43
13	H100-28	30.30	101.01	4.04	3.76	3.74	2.99	1.01	1.26
14	H100-29	40.00	99.58	4.00	4.45	4.03	3.29	1.10	1.35
15	H100-30	40.00	99.98	4.00	4.45	4.03	3.30	1.10	1.35

BS : BS 5950 Part 5 1987 and ER : EUROPEAN RECOMMENDATIONS 1987

Table 8.2. SERIES 2 ($M/M_c < 0.3$)

No.	Speci-men	n/t	hw/t	r/t	F_e (KN)	F_{CB} (KN)		F_e / F_{CB}	
						BS	ER	BS	ER
16	H100-31	40.00	101.94	4.00	4.47	4.03	3.31	1.11	1.35
17	H100-32	50.51	101.94	4.04	4.53	4.15	3.47	1.09	1.31
18	H100-33	50.00	99.78	4.00	4.71	4.24	3.52	1.11	1.34
19	H100-34	50.00	99.80	4.00	4.53	4.24	3.52	1.07	1.29
20	H100-36	30.00	101.88	2.25	4.27	4.35	3.41	0.98	1.25
21	H100-37	30.30	99.41	3.28	4.27	4.02	3.23	1.06	1.32
22	H100-41	39.60	100.97	2.23	4.58	4.68	3.75	0.98	1.22
23	H100-42	40.40	103.05	2.27	4.71	4.49	3.63	1.05	1.30
24	H100-44	39.60	98.63	3.22	4.89	4.42	3.63	1.11	1.35
25	H100-47	50.51	102.40	2.27	5.20	4.73	3.87	1.10	1.35
26	H100-49	50.50	100.83	3.28	5.18	4.47	3.75	1.16	1.38
27	H100-50	50.00	98.00	4.25	5.18	4.29	3.70	1.21	1.40

BS : BS 5950 Part 5 1987 and ER : EUROPEAN RECOMMENDATIONS 1987

Table 8.2. SERIES 2 (M/M$_c$ < 0.3)

Statistical measures of accuracy of F$_e$/F$_{CB}$	BS 5950 Part 5 1987	EUROPEAN RECOMMENDATIONS 1987
Mean	1.070	1.337
Standard deviation	0.058	0.048
Coeff. of variation	0.054	0.036
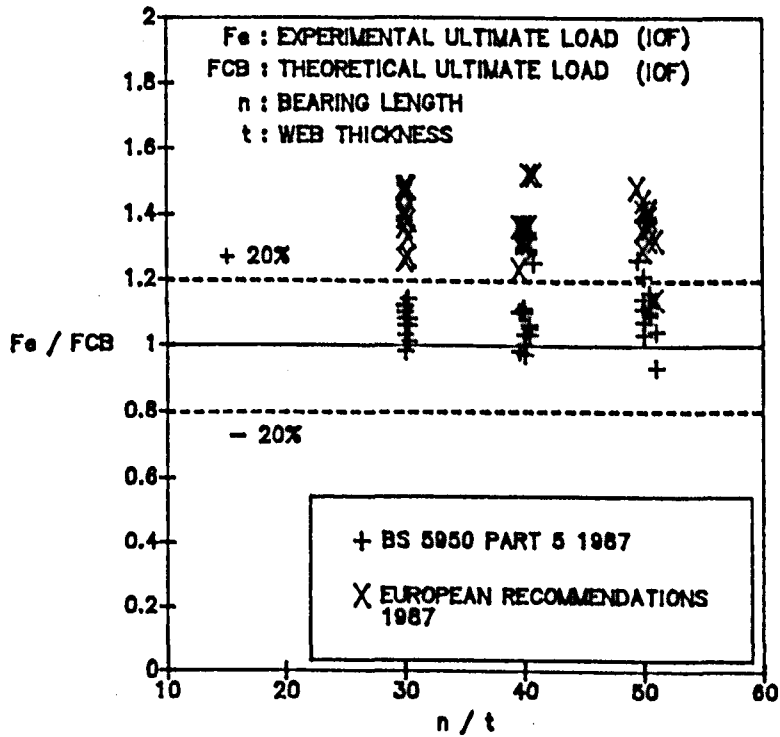
Figure 8.5. F$_e$/F$_{CB}$ vs. bearing length ratio, for M/M$_c$ < 0.3.
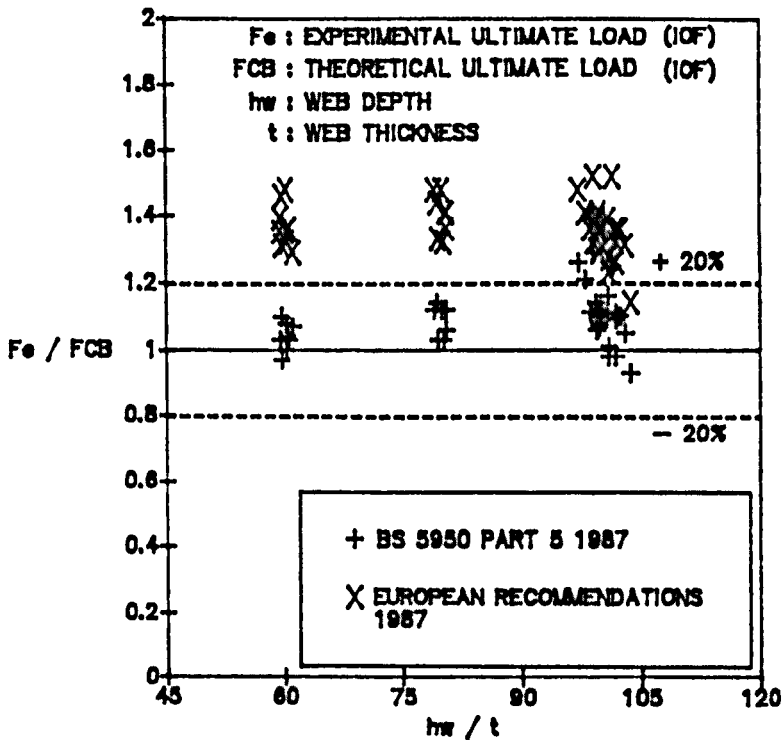
Figure 8.6. F_e/F_{CB} vs. web slenderness ratio, $M/M_c < 0.3$.
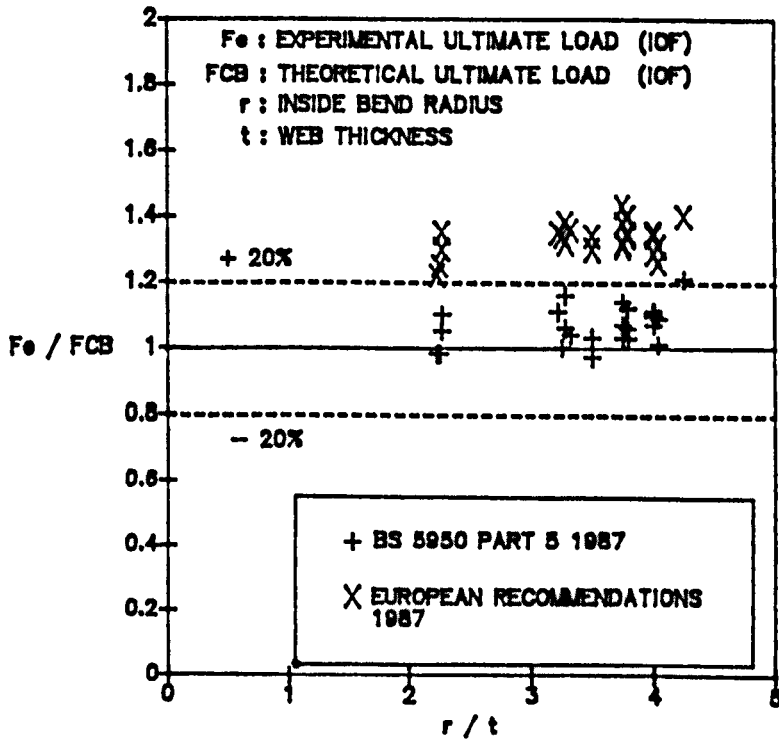
Figure 8.7. F_e/F_{CB} vs. inside bend radius ratio, for $M/M_c < 0.3$.

271
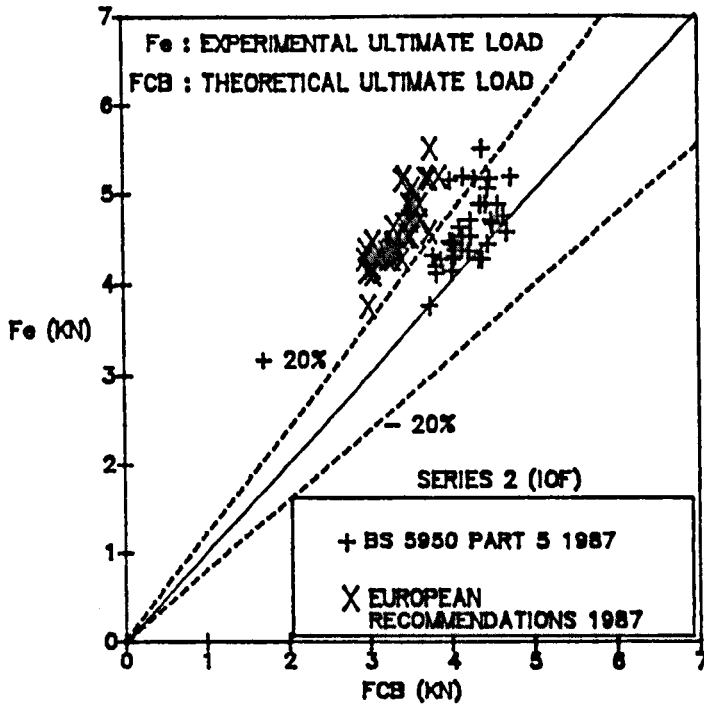
Figure 8.8. Theoretical load F_{CB} vs. experimental load F_e, for $M/M_c < 0.3$.

8.3. SPECIMENS TESTED UNDER EOF.

Table 8.3. SERIES 3

No.	Speci- men	n/t	hw/t	r/t	F_e (KN)	F_C (KN)		F_e / F_C	
						BS	ER	BS	ER
1	S100-1	30.00	99.36	4.00	1.73	1.00	1.53	1.72	1.13
2	S100-2	30.30	100.93	4.04	1.65	0.97	1.50	1.70	1.10
3	S100-3	30.30	101.03	4.04	1.68	0.97	1.50	1.73	1.12

BS : BS 5950 Part 5 1987 and ER : EUROPEAN RECOMMENDATIONS 1987

Table 8.3. SERIES 3

No.	Speci-men	n/t	hw/t	r/t	F_e (KN)	F_C (KN)		F_e / F_C	
						BS	ER	BS	ER
16	S80-7	50.00	79.00	3.75	2.38	1.28	1.82	1.87	1.31
17	S80-8	50.00	79.50	3.75	2.60	1.27	1.82	2.04	1.43
18	S80-9	50.00	79.50	3.75	2.37	1.27	1.82	1.86	1.30
19	S60-1	30.30	60.40	3.54	2.15	1.18	1.53	1.83	1.41
20	S60-2	30.30	60.00	3.54	2.08	1.18	1.53	1.77	1.36
21	S60-3	30.00	59.68	3.50	2.08	1.21	1.56	1.72	1.34
22	S60-4	40.00	59.78	3.50	2.54	1.30	1.70	1.96	1.49
23	S60-5	40.00	59.70	3.50	2.59	1.30	1.70	1.99	1.52
24	S60-6	40.00	59.38	3.50	2.58	1.30	1.70	1.98	1.52
25	S60-7	50.00	60.00	3.50	3.11	1.39	1.83	2.23	1.70
26	S60-8	50.00	59.50	3.50	2.94	1.39	1.83	2.11	1.60

BS : BS 5950 Part 5 1987 and ER : EUROPEAN RECOMMENDATIONS 1987

Table 8.3. SERIES 3

Statistical measures of accuracy of F_e/F_C	BS 5950 Part 5 1987	EUROPEAN RECOMMENDATIONS 1987
Mean	1.793	1.290
Standard deviation	0.268	0.168
Coeff. of variation	0.149	0.130
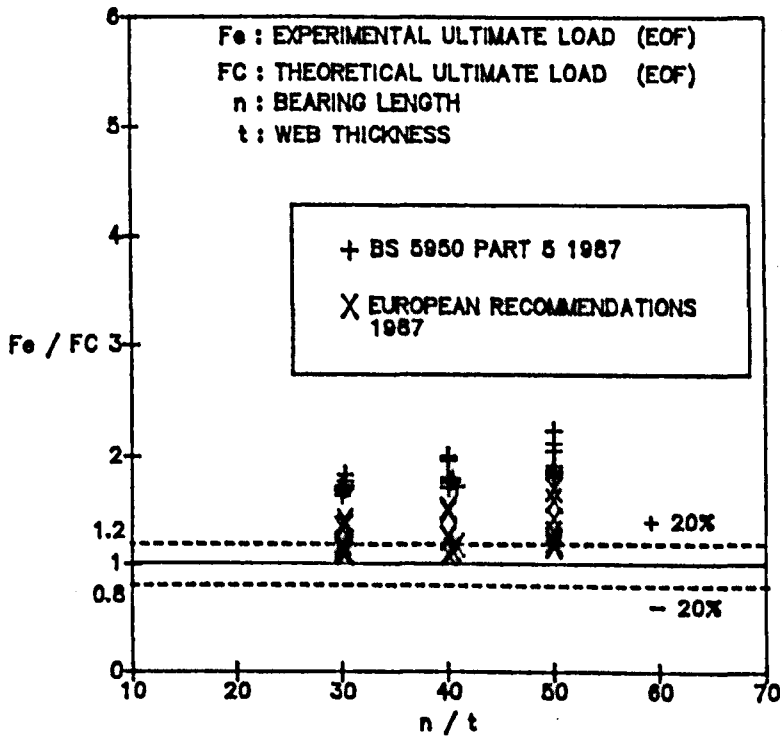
Figure 8.9. F_e/F_C vs. bearing length ratio (EOF).

Figure 8.10. F_e/F_C vs. web slenderness ratio (EOF).
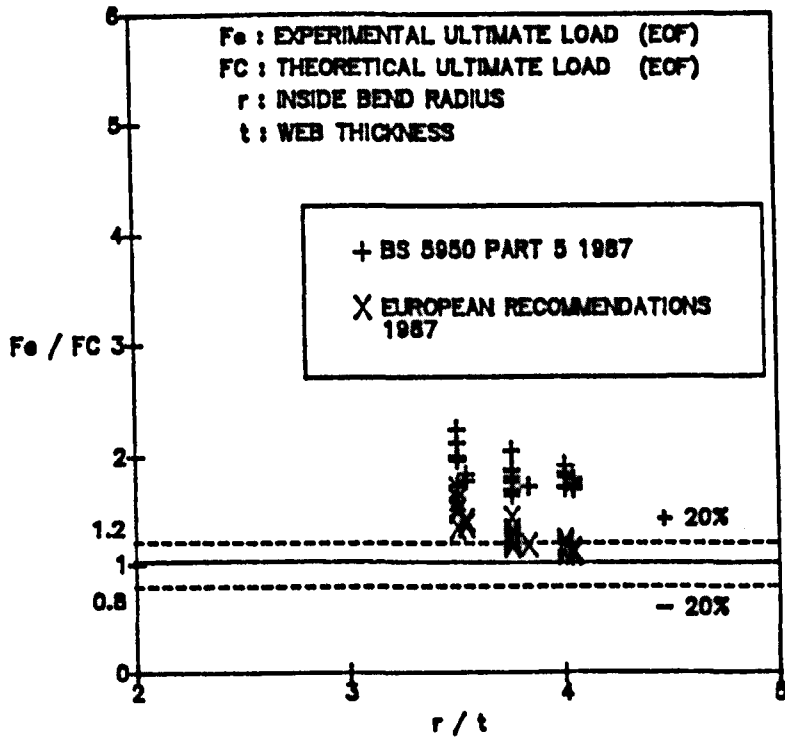
Figure 8.11. F_e/F_C vs. inside bend radius ratio (EOF).

276
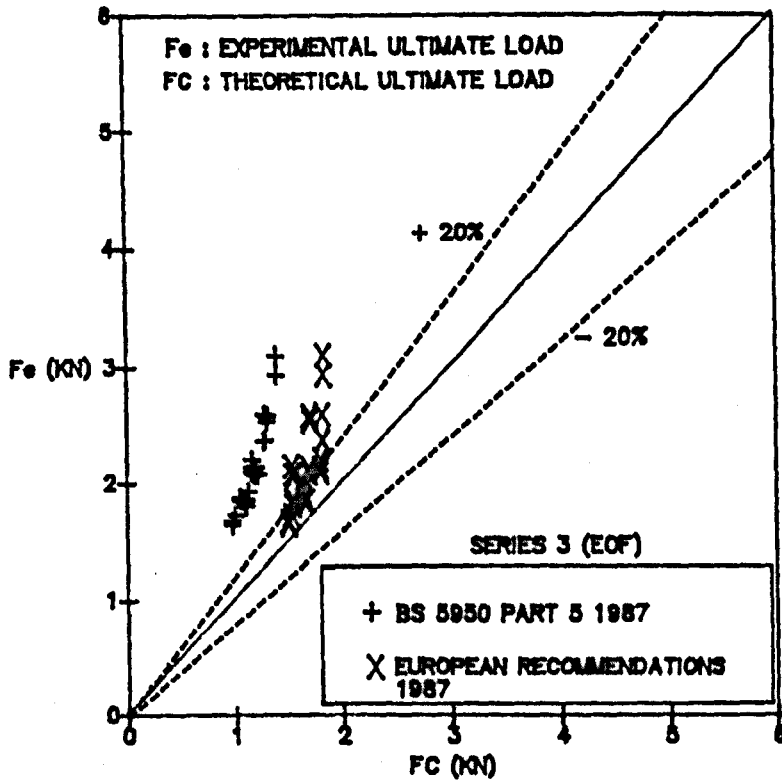
Figure 8.12. Theoretical load F_C vs. experimental load F_e, for (EOF).

8.4. SPECIMENS TESTED UNDER ETF.

Table 8.4. SERIES 4

No.	Speci -men	n/t	hw/t	r/t	F_e (KN)	F_C (KN)		F_e / F_C	
						BS	ER	BS	ER
1	H4-1	27.03	64.29	1.80	1.89	2.19	2.16	0.87	0.88
2	H4-2	27.27	65.09	2.05	1.78	2.06	2.10	0.86	0.85

BS : BS 5950 Part 5 1987 and ER : EUROPEAN RECOMMENDATIONS 1987

277

Table 8.4. SERIES 4

No.	Speci -men	n/t	hw/t	r/t	F_e (KN)	F_C (KN)		F_e / F_C	
						BS	ER	BS	ER
3	H4-3	27.03	64.94	1.80	1.81	2.18	2.16	0.83	0.84
4	H4-4	36.36	65.56	1.82	2.00	2.29	2.32	0.87	0.86
5	H4-5	36.04	65.21	1.80	2.03	2.34	2.35	0.87	0.86
6	H4-6	36.70	66.29	1.83	1.87	2.24	2.28	0.83	0.82
7	H4-7	45.87	66.09	2.06	2.16	2.30	2.43	0.94	0.89
8	H4-8	45.87	66.26	2.06	2.20	2.30	2.43	0.96	0.91
9	H4-9	45.87	65.39	2.06	2.25	2.31	2.43	0.98	0.93
10	H5-1	27.27	93.64	2.05	1.64	1.89	2.10	0.86	0.78
11	H5-2	27.27	92.62	2.05	1.84	1.90	2.10	0.97	0.88
12	H5-3	27.03	91.73	2.03	1.64	1.94	2.14	0.84	0.77
13	H5-4	36.04	91.50	2.03	2.05	2.08	2.33	0.98	0.88
14	H5-5	36.04	91.68	2.03	1.98	2.08	2.33	0.95	0.85

BS : BS 5950 Part 5 1987 and ER : EUROPEAN RECOMMENDATIONS 1987

Table 8.4. SERIES 4

No.	Speci-men	n/t	hw/t	r/t	F_e (KN)	F_C (KN)		F_e / F_C	
						BS	ER	BS	ER
15	H5-6	36.36	92.56	2.05	1.99	2.04	2.30	0.98	0.87
16	H5-7	45.45	93.55	2.05	2.19	2.17	2.47	1.01	0.89
17	H5-8	45.45	93.18	2.05	2.32	2.17	2.47	1.07	0.94
18	H5-9	45.05	92.07	2.03	2.22	2.22	2.51	1.00	0.88

BS : BS 5950 Part 5 1987 and ER : EUROPEAN RECOMMENDATIONS 1987

Table 8.4. SERIES 4

| Statistical measures of accuracy of F_e/F_C	BS 5950 Part 5 1987	EUROPEAN RECOMMENDATIONS 1987
Mean	0.926	0.866
Standard deviation	0.073	0.044
Coeff. of variation	0.079	0.051

279
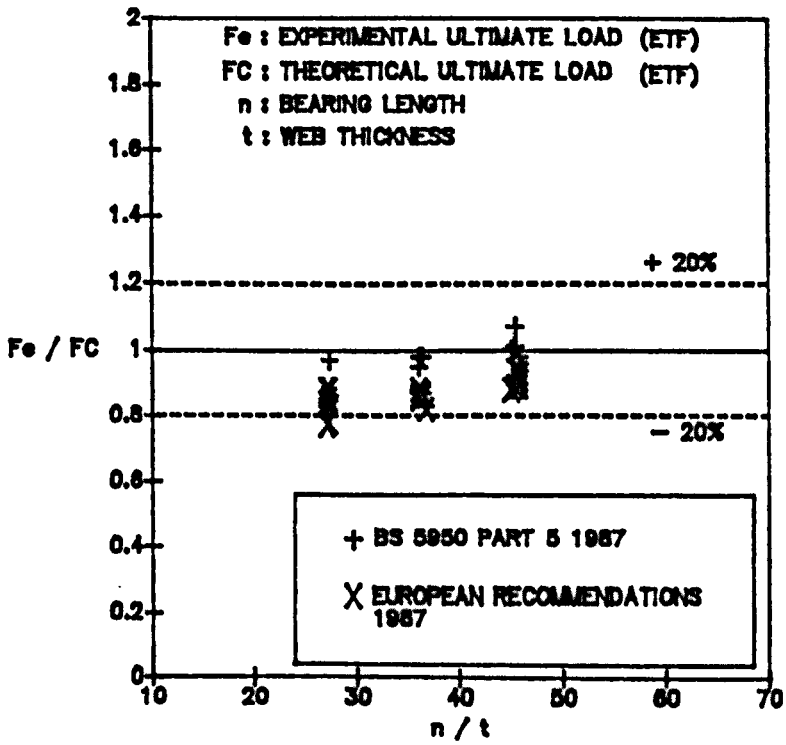
Figure 8.13. F_e/F_C vs. bearing length ratio (ETF).
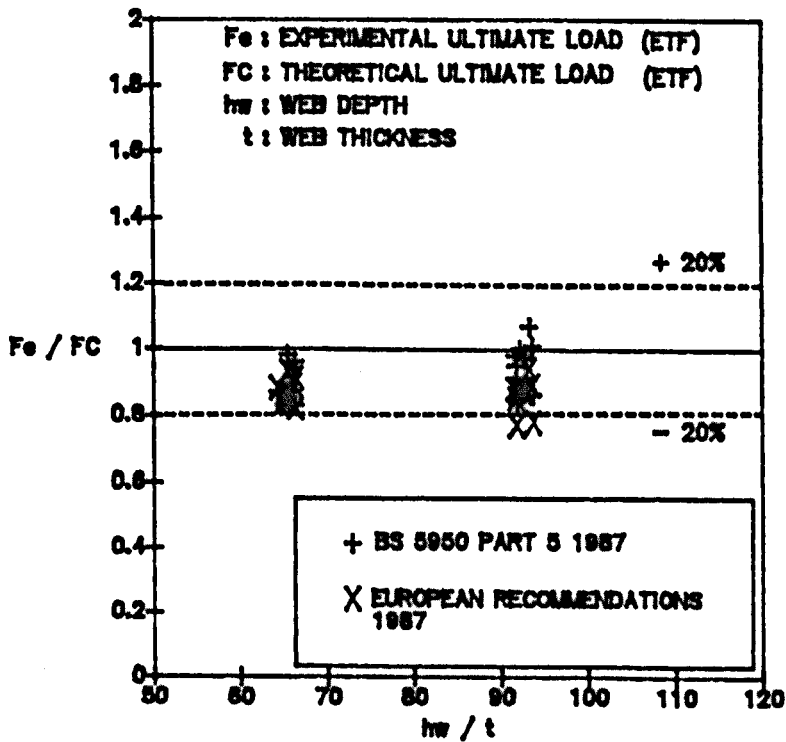
Figure 8.14. F_e/F_C vs. web slenderness ratio (ETF).

280
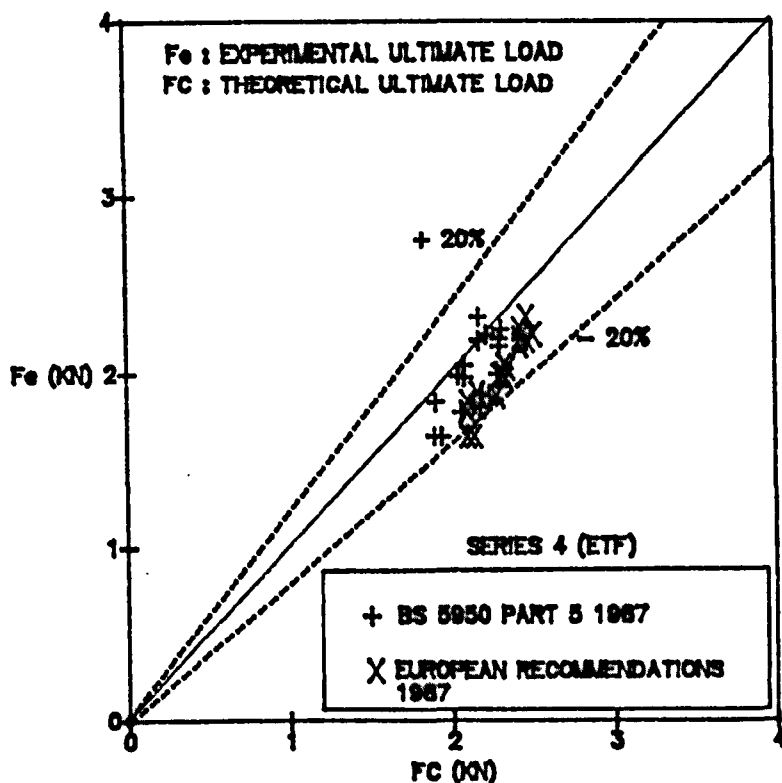
Figure 8.15. Theoretical load F_C vs. experimental load F_e, for ETF.

8.5. SPECIMENS TESTED UNDER ITF.

Table 8.5. SERIES 5

No.	Speci-men	n/t	hw/t	r/t	F_e (KN)	F_C (KN)		F_e / F_C	
						BS	ER	BS	ER
1	H6-1	27.03	64.34	1.80	4.53	6.15	4.31	0.74	1.05
2	H6-2	27.03	64.14	1.80	4.75	6.16	4.31	0.77	1.10

BS : BS 5950 Part 5 1987 and ER : EUROPEAN RECOMMENDATIONS 1987

Table 8.5. SERIES 5

No.	Speci-men	n/t	hw/t	r/t	F_e (KN)	F_C (KN)		F_e / F_C	
						BS	ER	BS	ER
3	H6-3	26.79	63.02	1.79	4.53	6.30	4.38	0.72	1.03
4	H6-4	36.04	64.07	1.80	4.87	6.23	4.71	0.78	1.03
5	H6-5	36.04	64.16	1.80	5.14	6.23	4.71	0.83	1.09
6	H6-6	36.04	63.68	1.80	5.05	6.24	4.71	0.81	1.07
7	H6-7	44.64	63.48	1.79	5.26	6.43	5.14	0.82	1.02
8	H6-8	45.05	64.25	1.80	5.17	6.29	5.06	0.82	1.02
9	H6-9	45.05	65.93	1.80	5.18	6.30	5.06	0.82	1.02
10	H7-1	27.27	92.40	1.82	4.58	5.43	4.24	0.84	1.08
11	H7-2	27.03	91.82	1.79	4.56	5.55	4.31	0.82	1.06
12	H7-3	27.03	92.41	1.80	4.63	5.53	4.31	0.84	1.07
13	H7-4	35.71	90.63	1.79	4.85	5.74	4.78	0.84	1.01
14	H7-5	36.04	91.51	1.80	4.88	5.62	4.71	0.87	1.04

BS : BS 5950 Part 5 1987 and ER : EUROPEAN RECOMMENDATIONS 1987

Table 8.5. SERIES 5

No.	Speci-men	n/t	hw/t	r/t	F_e (KN)	F_C (KN) BS	F_C (KN) ER	F_e / F_C BS	F_e / F_C ER
15	H7-6	36.36	92.24	1.82	4.88	5.50	4.63	0.89	1.05
16	H7-7	45.05	91.98	1.80	4.88	5.67	5.06	0.86	0.96
17	H7-8	45.45	92.75	1.82	5.28	5.55	4.98	0.95	1.06
18	H7-9	45.45	92.58	1.82	4.68	5.55	4.98	0.84	0.94

BS : BS 5950 Part 5 1987 and ER : EUROPEAN RECOMMENDATIONS 1987

Table 8.5. SERIES 5

Statistical measures of accuracy of F_e/F_C	BS 5950 Part 5 1987	EUROPEAN RECOMMENDATIONS 1987
Mean	0.826	1.039
Standard deviation	0.053	0.041
Coeff. of variation	0.064	0.039
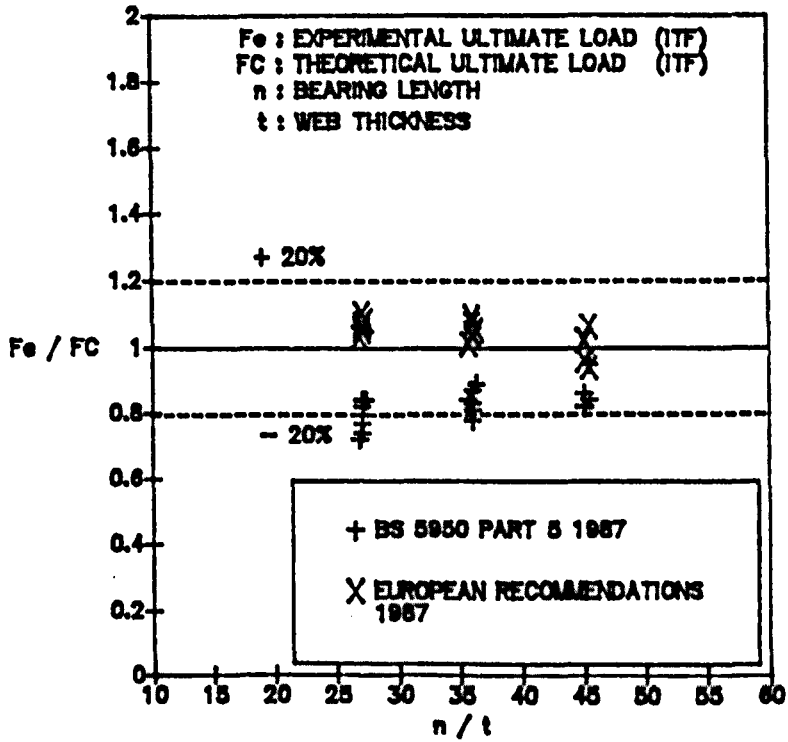
Figure 8.16. F_e/F_C vs. bearing length ratio (ITF).
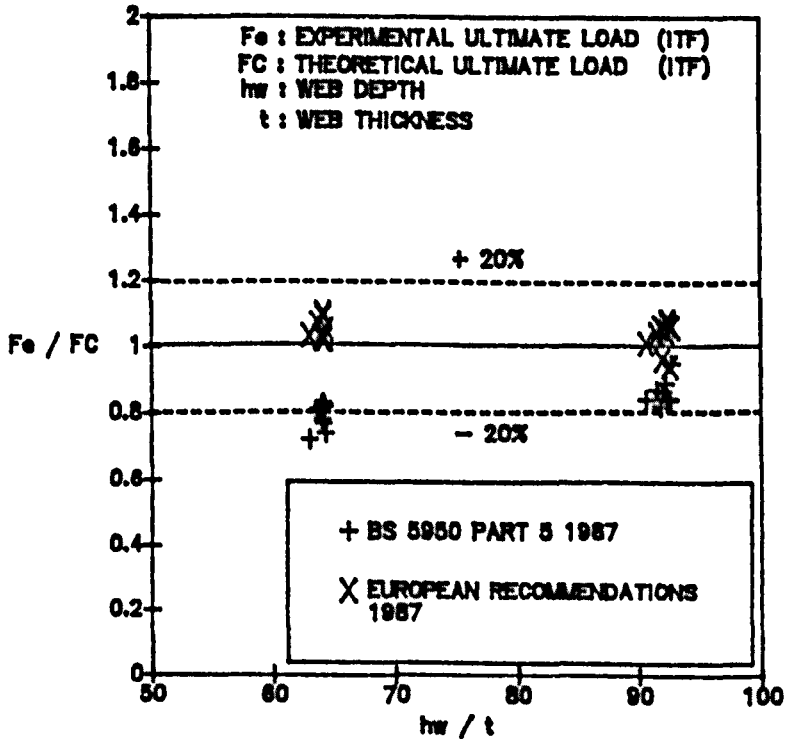
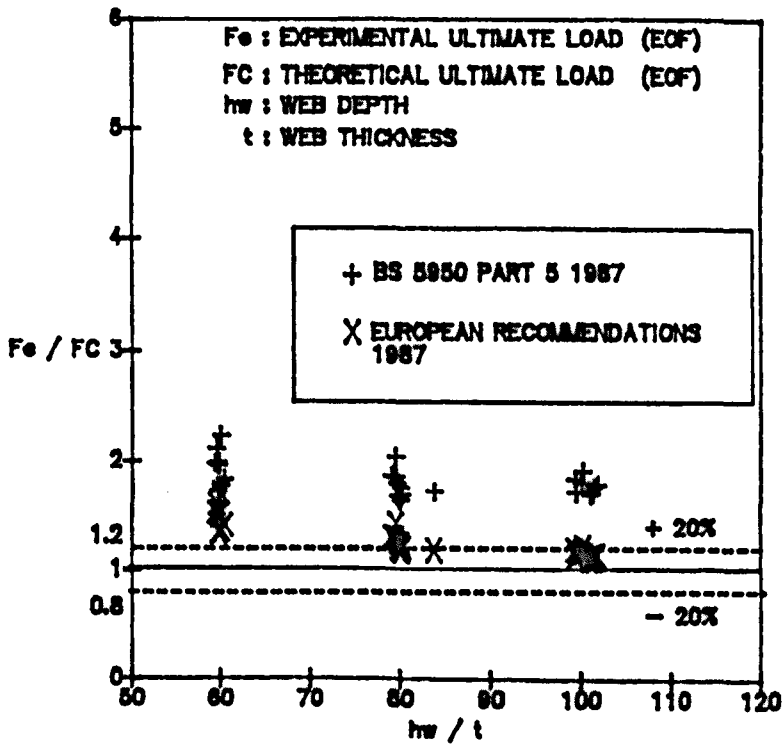Figure 8.17. F_e/F_C vs. web slenderness ratio (ITF).

284
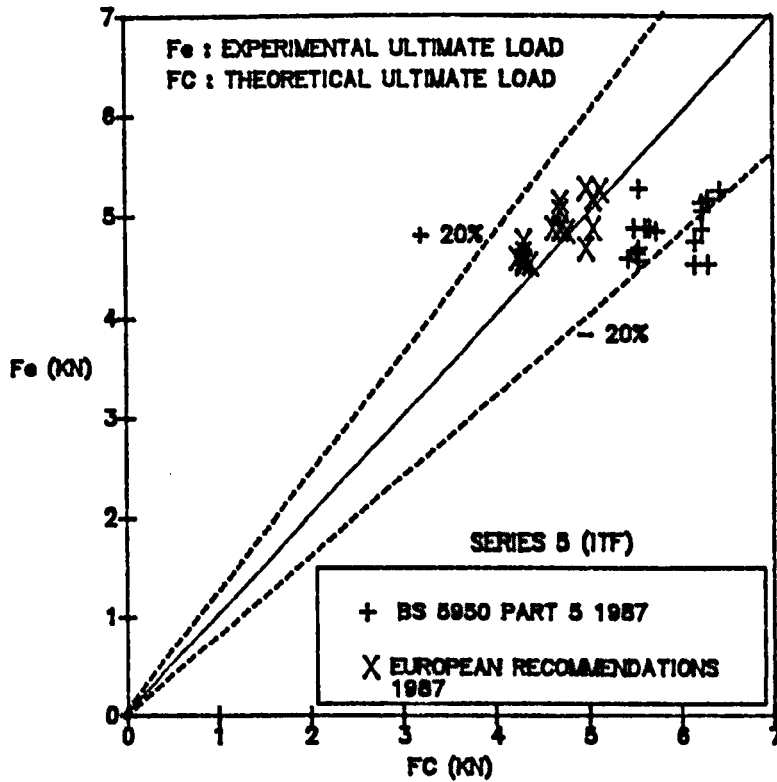
Figure 8.18. Theoretical load F_C vs. experimental load F_e, for ITF.

8.6. DISCUSSION.

Figures 8.1 - 8.18 have shown the accuracy of using the two different design specifications, namely BS 5950 Part 5 1987 and European Recommendations 1987 in predicting the ultimate web crippling loads of the specimens which were subjected to the four different loading conditions. It can be interpreted from the figures that the scatter data representing the deviation of theoretical results from the actual results obtained from experiments should lie within the area which is bounded by the dashed lines ± 20%. The accuracy of both design specifications indicated in the figures

depends on the types of loading condition and this can also be seen from the results of statistical analysis presented in the tables 8.1 - 8.5.

In the case of specimens tested under IOF, the accuracy of the theoretical results predicted by BS 5950 Part 5 1987 is affected by the magnitude of bending moment applied to the specimens. This is indicated in table 8.1 and Figures 8.1 - 8.4 where if the applied bending moment is equal or greater than 30% of the moment capacity of specimen, most of the theoretical values tend to overestimate the experimental values. On the other hand, as shown in table 8.2 and Figure 8.5 - 8.8, the experimental values tend to be underestimated by most of the theoretical values of BS 5950 Part 5 1987 when the applied bending moment is less than 30% of the moment capacity. Nevertheless, the accuracy of the theoretical results predicted by BS 5950 Part 5 1987 for this type of loading condition is mostly still within the acceptable scatter limits ± 20%.

In contrast to this, as shown in table 8.1 - 8.2 as well as Figures 8.1 - 8.8, most of the theoretical results calculated using the European Recommendations 1987 for this type of loading condition underestimate the experimental results. Although these results are safer than those predicted by BS 5950 Part 5 1987, the accuracy of most of them is not very good. This is clearly shown in Figures 8.1 - 8.8, where most of the scatter data of European Recommendations 1987 lie beyond the acceptable scatter limits ± 20%. Thus, it can be said that BS 5950 Part 5 1987 is more accurate than

European Recommendations 1987 in predicting the ultimate loads of the specimens subjected to combined web crippling and bending, but is not conservative.

The accuracy of theoretical results presented in table 8.3 and Figures 8.9 - 8.12 shows the similarity between BS 5950 Part 5 1987 and the European Recommendations 1987 in estimating the ultimate web crippling loads of the specimens tested under EOF. Both of these design specifications result in conservative values of ultimate web crippling loads. It can be seen from the figures that all experimental web crippling capacities exceed those predicted by BS 5950 Part 5 1987 by more than 20%. In the case of the European Recommendations 1987, Figures 8.10 - 8.11 show that for the specimens with larger web depths and inside bend radii, the accuracy of most of the estimated values still lies within the acceptable scatter limits ± 20%. The figures also show that the smaller the values of web depth and inside bend radius, the more inaccurate the values of ultimate web crippling load predicted by the Recommendations. On the basis of these results, it can be concluded that BS 5950 Part 5 1987 tend to be inaccurate in estimating the ultimate web crippling loads of the specimens tested under EOF, whereas the accuracy obtained using European Recommendations 1987 seems to be more affected by the dimensions of the specimens.

If the specimens are subjected to the loading on both flanges near or at the end (ETF), both design specifications seem to result in unconservative predictions of

287

ultimate web crippling load. This is clearly shown in Figures 8.13 - 8.15 and in table

8.4. However, the accuracy of the theoretical results for this type of end loading can

still be accepted because most of the scatter data are in the area between ± 20%. If

this two-flange loading is located far from free ends of the specimen (ITF), the

theoretical results predicted by the European Recommendations 1987 are more

accurate than those predicted by BS 5950 Part 5 1987. This can be seen in table 5

and Figures 8.16 - 8.18, where the scatter data of the European Recommendations

1987 are mostly closer to the ideal values. Thus, in this case, the European

Recommendations 1987 are better than BS 5950 Part 5 1987 in estimating the

ultimate web crippling loads of the specimens tested under ITF. Finally, in order to

achieve the necessary accuracy in using BS 5950 Part 5 1987 and the European

Recommendations 1987 for predicting the ultimate web crippling loads of the

specimens whose webs are eccentric to the directions of applied load, it is advisable

first to consider the type of loading condition which will be applied to the specimens

before deciding to choose which one of these design specifications is the best to be

used.

CHAPTER 9

COMPARISONS OF

PLASTIC MECHANISM APPROACH

AND

EXPERIMENTS

9.1. GENERAL.

In this chapter, the accuracy of theoretical results estimated using the plastic mechanism approach is assessed in a similar way as in the case of assessing the accuracy of both design specifications used in this research program. Because the plastic mechanism approach in this research program is only developed for analysing the strength of the specimens subjected to combined web crippling and bending, it is therefore necessary to use the experimental results of specimens tested under IOF only for verifying estimated results obtained from the plastic mechanism approach. The relative accuracy of the plastic mechanism approach presented herein corresponds to the verification of all estimated values of ultimate web crippling load for specimens tested under IOF with $M/M_c \geq 0.3$ and $M/M_c < 0.3$. From the results presented in the following tables, F_e still represents experimental ultimate web crippling loads and theoretical ultimate web crippling loads estimated using the plastic mechanism approach are represented by $F_{CB}1$ (The first procedure) and $F_{CB}2$ (The second procedure).

Besides the accuracy of plastic mechanism approach in predicting the ultimate web crippling loads, typical examples of comparing theoretical collapse curves and experimental ones are also presented in the form of load vs. web crippling deformation. These examples are illustrated by comparing the theoretical collapse curves of two specimens, namely H80-25 and H70-23 with their experimental load-

289

deflection curves. Discussions concerning the results of the plastic mechanism approach for analysing the web crippling strength of the specimens tested under IOF are presented in the last subchapter.

9.2. SPECIMENS IN TEST SERIES 1 (M/M$_c$ ≥ 0.3).

Table 9.1. SERIES 1 (M/M$_c$ ≥ 0.3) - A1 : Fe/F$_{CB}$1 and A2 : Fe/F$_{CB}$2

No.	Specimen	n/t	hw/t	r/t	F$_e$ (KN)	F$_{CB}$1 (KN)	F$_{CB}$2 (KN)	A1	A2
1	H60-2	27.27	53.42	2.05	4.09	4.75	4.23	0.86	0.97
2	H60-4	27.27	53.42	2.05	4.14	4.77	4.26	0.87	0.97
3	H60-7	27.27	54.25	2.05	4.18	4.80	4.28	0.87	0.98
4	H60-9	27.27	54.23	2.05	4.14	4.77	4.24	0.87	0.97
5	H60-10	27.27	54.00	2.05	4.09	4.79	4.28	0.85	0.96
6	H60-18	31.53	54.86	2.03	4.37	5.19	4.66	0.84	0.94
7	H60-19	31.53	54.06	2.03	4.37	5.21	4.73	0.84	0.92
8	H60-20	31.53	54.52	2.03	4.35	5.19	4.66	0.84	0.94

Table 9.1. SERIES 1 (M/M$_c$ ≥ 0.3) - A1 : Fe/F$_{CB}$1 and A2 : Fe/F$_{CB}$2

No.	Specimen	n/t	hw/t	r/t	F$_e$ (KN)	F$_{CB}$1 (KN)	F$_{CB}$2 (KN)	A1	A2
9	H60-21	31.53	53.65	2.03	4.39	5.16	4.65	0.85	0.94
10	H60-22	31.53	53.95	2.03	4.41	5.18	4.67	0.85	0.95
11	H60-23	36.04	54.06	2.03	4.57	5.44	5.00	0.84	0.91
12	H60-24	36.04	54.06	2.03	4.61	5.44	5.00	0.85	0.92
13	H60-25	36.04	54.41	2.03	4.53	5.46	5.00	0.83	0.90
14	H60-26	36.04	54.77	2.03	4.54	5.47	5.01	0.83	0.91
15	H60-27	36.04	54.07	2.03	4.57	5.45	5.01	0.84	0.91
16	H60-28	40.54	55.09	2.03	4.76	5.72	5.35	0.83	0.89
17	H60-29	40.54	54.54	2.03	4.86	5.70	5.35	0.85	0.91
18	H60-30	40.54	54.64	2.03	4.78	5.71	5.36	0.84	0.89
19	H60-31	40.54	54.36	2.03	4.81	5.70	5.35	0.84	0.90
20	H60-32	40.54	53.74	2.03	4.85	5.69	5.35	0.85	0.91
21	H60-33	44.64	54.71	2.01	4.89	5.91	5.69	0.83	0.86

Table 9.1. SERIES 1 (M/M$_c$ ≥ 0.3) - A1 : Fe/F$_{CB}$1 and A2 : Fe/F$_{CB}$2

No.	Specimen	n/t	hw/t	r/t	F$_e$ (KN)	F$_{CB}$1 (KN)	F$_{CB}$2 (KN)	A1	A2
22	H60-34	45.05	53.26	2.03	4.96	5.89	5.71	0.84	0.87
23	H60-35	45.05	55.71	2.03	4.88	5.94	5.70	0.82	0.86
24	H60-36	45.05	55.67	2.03	4.91	5.95	5.71	0.82	0.86
25	H60-37	45.05	55.21	2.03	4.91	5.94	5.71	0.83	0.86
26	H70-6	27.27	62.88	2.05	3.97	4.72	4.12	0.84	0.96
27	H70-7	27.27	62.43	2.05	3.81	4.72	4.11	0.81	0.93
28	H70-8	27.27	62.03	2.05	3.91	4.70	4.11	0.83	0.95
29	H70-11	31.53	63.42	2.03	4.25	5.12	4.49	0.83	0.95
30	H70-12	31.53	63.22	2.03	4.27	5.11	4.48	0.84	0.95
31	H70-13	31.53	63.14	2.03	4.47	5.09	4.48	0.88	1.00
32	H70-14	31.53	63.79	2.03	4.40	5.13	4.50	0.86	0.98
33	H70-15	31.53	62.95	2.03	4.42	5.10	4.49	0.87	0.98
34	H70-18	36.04	63.68	2.03	4.39	5.38	4.78	0.82	0.92

Table 9.1. SERIES 1 $(M/M_c \geq 0.3)$ - A1 : $Fe/F_{CB}1$ and A2 : $Fe/F_{CB}2$

No.	Specimen	n/t	hw/t	r/t	F_e (KN)	$F_{CB}1$ (KN)	$F_{CB}2$ (KN)	A1	A2
35	H70-19	36.04	63.33	2.03	4.48	5.37	4.78	0.83	0.94
36	H70-20	36.04	63.47	2.03	4.40	5.37	4.77	0.82	0.92
37	H70-21	40.54	63.51	2.03	4.72	5.82	5.24	0.81	0.90
38	H70-23	40.54	63.90	2.03	4.65	5.62	5.09	0.83	0.91
39	H70-24	40.54	63.51	2.03	4.81	5.61	5.09	0.86	0.94
40	H70-30	40.54	63.22	2.03	4.77	5.61	5.09	0.85	0.94
41	H70-25	45.05	63.13	2.03	4.98	5.81	5.39	0.86	0.92
42	H70-26	45.05	63.22	2.03	4.82	5.83	5.40	0.83	0.89
43	H70-27	45.05	62.76	2.03	4.85	5.80	5.39	0.84	0.90
44	H70-28	45.05	63.13	2.03	4.89	5.81	5.39	0.84	0.91
45	H70-29	45.05	63.56	2.03	4.83	5.82	5.39	0.83	0.90
46	H80-9	27.27	72.26	2.05	4.07	4.82	4.24	0.84	0.96
47	H80-10	27.27	72.47	2.05	4.11	4.83	4.25	0.85	0.97

Table 9.1. SERIES 1 (M/M$_c$ $\geq$ 0.3) - A1 : Fe/F$_{CB}$1 and A2 : Fe/F$_{CB}$2

No.	Specimen	n/t	hw/t	r/t	F$_e$ (KN)	F$_{CB}$1 (KN)	F$_{CB}$2 (KN)	A1	A2
48	H80-11	27.03	72.55	2.03	4.24	4.89	4.29	0.87	0.99
49	H80-12	27.03	72.67	2.03	4.31	4.89	4.29	0.88	1.01
50	H80-13	27.03	73.26	2.03	4.20	4.89	4.28	0.86	0.98
51	H80-14	31.53	72.00	2.03	4.41	5.18	4.59	0.85	0.96
52	H80-15	31.53	72.12	2.03	4.59	5.18	4.58	0.89	1.00
53	H80-16	31.53	71.94	2.03	4.46	5.16	4.57	0.86	0.98
54	H80-17	36.04	72.23	2.03	4.56	5.45	4.85	0.84	0.94
55	H80-18	36.04	71.81	2.03	4.65	5.43	4.85	0.86	0.96
56	H80-19	36.04	72.44	2.03	4.60	5.54	4.93	0.83	0.93
57	H80-30	36.04	72.28	2.03	4.49	5.45	4.85	0.82	0.93
58	H80-31	36.04	71.89	2.03	4.56	5.44	4.85	0.84	0.94
59	H80-20	40.54	72.16	2.03	4.77	5.44	4.85	0.84	0.94
60	H80-21	40.54	73.04	2.03	4.68	5.69	5.12	0.82	0.91

Table 9.1. SERIES 1 (M/M$_c$ ≥ 0.3) - A1 : Fe/F$_{CB}$1 and A2 : Fe/F$_{CB}$2

No.	Specimen	n/t	hw/t	r/t	F$_e$ (KN)	F$_{CB}$1 (KN)	F$_{CB}$2 (KN)	A1	A2
61	H80-22	40.54	71.68	2.03	4.94	5.66	5.10	0.87	0.97
62	H80-23	40.54	72.96	2.03	4.82	5.68	5.10	0.85	0.94
63	H80-24	40.54	72.71	2.03	4.79	5.69	5.11	0.84	0.94
64	H80-25	45.05	72.85	2.03	5.16	5.88	5.36	0.88	0.96
65	H80-26	44.64	71.82	2.01	4.88	5.98	5.46	0.82	0.89
66	H80-27	45.05	72.10	2.03	5.07	5.87	5.36	0.86	0.95
67	H80-28	45.05	71.00	2.03	5.04	5.84	5.35	0.86	0.94
68	H80-29	45.05	72.59	2.03	5.04	5.89	5.37	0.86	0.94
69	H90-10	27.27	80.78	2.05	4.15	4.78	4.15	0.87	1.00
70	H90-11	27.27	80.69	2.05	4.13	4.77	4.13	0.87	1.00
71	H90-12	27.27	81.59	2.05	4.21	4.80	4.15	0.88	1.02
72	H90-13	27.03	81.64	2.03	4.16	4.88	4.22	0.85	0.99
73	H90-14	30.00	88.98	2.25	3.25	4.10	3.54	0.79	0.92

Table 9.1. SERIES 1 (M/M$_c$ $\geq$ 0.3) - A1 : Fe/F$_{CB}$1 and A2 : Fe/F$_{CB}$2

No.	Specimen	n/t	hw/t	r/t	F$_e$ (KN)	F$_{CB}$1 (KN)	F$_{CB}$2 (KN)	A1	A2
74	H90-15	35.00	88.98	2.25	3.35	4.33	3.77	0.77	0.89
75	H90-16	31.53	82.25	2.03	4.25	5.18	4.51	0.82	0.94
76	H90-17	31.53	81.00	2.03	4.39	5.15	4.48	0.85	0.98
77	H90-18	36.04	81.52	2.03	4.51	5.40	4.72	0.84	0.96
78	H90-19	35.71	80.10	2.01	4.53	5.47	4.80	0.83	0.94
79	H90-20	36.36	81.82	2.05	4.69	5.32	4.66	0.88	1.01
80	H90-21	40.54	81.32	2.03	4.64	5.63	4.96	0.83	0.94
81	H90-22	40.18	80.09	2.01	4.67	5.63	4.96	0.83	0.94
82	H90-23	40.54	81.32	2.03	4.63	5.64	4.97	0.82	0.93
83	H90-24	45.45	89.57	2.27	3.55	4.62	4.08	0.77	0.87
84	H90-25	40.54	81.18	2.03	4.83	5.63	4.97	0.86	0.97
85	H90-26	45.45	81.77	2.05	4.82	5.73	5.12	0.84	0.94
86	H90-27	45.05	81.45	2.03	5.07	5.83	5.21	0.87	0.97

Table 9.1. SERIES 1 ($M/M_c \geq 0.3$) - A1 : $Fe/F_{CB}1$ and A2 : $Fe/F_{CB}2$

No.	Specimen	n/t	hw/t	r/t	F_e (KN)	$F_{CB}1$ (KN)	$F_{CB}2$ (KN)	A1	A2
87	H90-28	45.05	81.27	2.03	4.78	5.83	5.20	0.82	0.92
88	H90-29	44.64	79.96	2.01	5.12	5.89	5.27	0.87	0.97
89	H90-30	45.05	81.43	2.03	4.74	5.83	5.20	0.81	0.91
90	H100-1	30.00	99.35	2.25	3.41	4.16	3.53	0.82	0.97
91	H100-2	30.00	99.96	2.25	3.41	4.16	3.53	0.82	0.97
92	H100-3	30.00	98.97	2.25	3.42	4.14	3.51	0.82	0.97
93	H100-4	30.30	102.09	2.27	3.29	4.09	3.47	0.80	0.95
94	H100-5	30.30	101.29	2.27	3.29	4.10	3.47	0.80	0.95
95	H100-6	35.35	101.53	2.27	3.27	4.31	3.66	0.76	0.89
96	H100-7	35.71	102.58	2.30	3.31	4.24	3.60	0.78	0.92
97	H100-8	35.00	99.90	2.25	3.53	4.38	3.73	0.81	0.95
98	H100-9	35.00	99.60	2.25	3.47	4.36	3.72	0.80	0.93
99	H100-10	35.00	99.90	2.25	3.43	4.37	3.73	0.78	0.92

Table 9.1. SERIES 1 (M/M$_c$ ≥ 0.3) - A1 : Fe/F$_{CB}$1 and A2 : Fe/F$_{CB}$2

No.	Specimen	n/t	hw/t	r/t	F$_e$ (KN)	F$_{CB}$1 (KN)	F$_{CB}$2 (KN)	A1	A2
100	H100-11	40.00	99.60	2.25	3.74	4.55	3.91	0.82	0.96
101	H100-12	40.00	98.51	2.25	3.49	4.52	3.89	0.77	0.90
102	H100-13	40.00	99.75	2.25	3.67	4.56	3.92	0.81	0.94
103	H100-14	40.00	99.60	2.25	3.51	4.55	3.91	0.77	0.90
104	H100-15	40.82	101.81	2.30	3.53	4.40	3.78	0.80	0.93
105	H100-16	45.00	98.97	2.25	3.72	4.71	4.08	0.79	0.91
106	H100-17	45.00	100.08	2.25	3.81	4.72	4.09	0.81	0.93
107	H100-18	45.00	100.26	2.25	3.82	4.73	4.09	0.81	0.93
108	H100-19	45.45	102.32	2.27	3.64	4.66	4.02	0.78	0.91
109	H100-20	45.45	100.39	2.27	3.66	4.63	4.02	0.79	0.91
110	H100-21	50.00	99.52	2.25	3.88	4.86	4.26	0.80	0.91
111	H100-22	50.51	101.39	2.27	3.81	4.81	4.20	0.79	0.91
112	H100-23	50.00	100.11	2.25	3.83	4.88	4.26	0.79	0.90

Table 9.1. SERIES 1 ($M/M_c \geq 0.3$) - A1 : $Fe/F_{CB}1$ and A2 : $Fe/F_{CB}2$

No.	Specimen	n/t	hw/t	r/t	F_e (KN)	$F_{CB}1$ (KN)	$F_{CB}2$ (KN)	A1	A2
113	H100-24	51.02	102.48	2.30	3.87	4.72	4.12	0.82	0.94
114	H100-25	50.00	100.24	2.25	3.90	4.88	4.26	0.80	0.91
115	H100-52	30.00	101.33	2.25	3.25	4.37	3.70	0.74	0.88
116	H100-53	30.61	104.89	2.30	3.16	4.25	3.60	0.74	0.88
117	H100-54	30.00	100.52	3.25	3.11	4.36	3.66	0.71	0.85
118	H100-55	30.00	99.39	3.25	3.11	4.34	3.64	0.72	0.86
119	H100-56	30.61	100.82	4.34	2.89	4.21	3.49	0.70	0.84
120	H100-57	30.93	101.87	4.38	2.89	4.14	3.42	0.70	0.84
121	H100-58	40.40	103.56	2.27	4.10	4.76	4.06	0.86	1.01
122	H100-59	40.82	105.44	2.30	4.10	4.68	3.99	0.88	1.03
123	H100-60	40.40	100.61	3.28	4.07	4.71	4.02	0.86	1.01
124	H100-61	41.67	104.04	3.39	3.87	4.48	3.82	0.86	1.01
125	H100-62	40.00	99.36	4.25	3.96	4.78	4.04	0.83	0.98

Table 9.1. SERIES 1 ($M/M_c \geq 0.3$) - A1 : $Fe/F_{CB}1$ and A2 : $Fe/F_{CB}2$

No.	Specimen	n/t	hw/t	r/t	F_e (KN)	$F_{CB}1$ (KN)	$F_{CB}2$ (KN)	A1	A2
126	H100-63	40.40	99.01	4.29	3.83	4.68	3.97	0.82	0.96
127	H100-64	50.51	103.29	2.27	4.09	5.08	4.42	0.80	0.93
128	H100-65	51.55	106.25	2.32	4.25	4.92	4.30	0.86	0.99
129	H100-66	49.50	98.95	2.23	4.16	5.14	4.50	0.81	0.92
130	H100-67	50.51	100.42	3.28	3.94	5.04	4.40	0.78	0.89
131	H100-68	49.50	97.40	4.21	3.96	5.20	4.54	0.76	0.87
132	H100-69	50.00	98.00	4.25	4.00	5.11	4.47	0.78	0.90

Table 9.1. SERIES 1 ($M/M_c \geq 0.3$)

Statistical measures of accuracy of A1 and A2	A1	A2
Mean	0.827	0.935
Standard deviation	0.038	0.041
Coeff. of variation	0.046	0.044
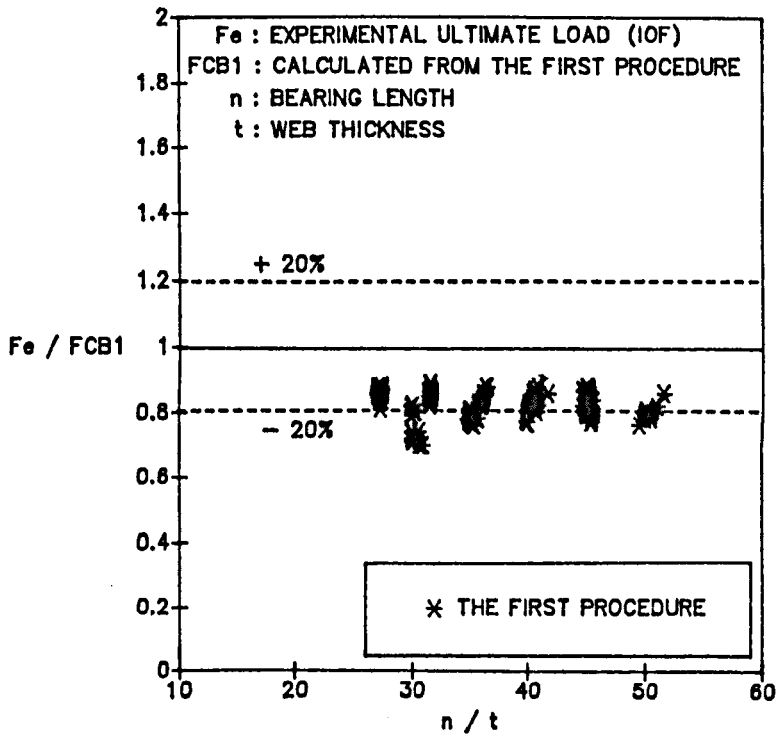
Figure 9.1. $F_e/F_{CB}1$ vs. bearing length ratio, for $M/M_c \geq 0.3$.
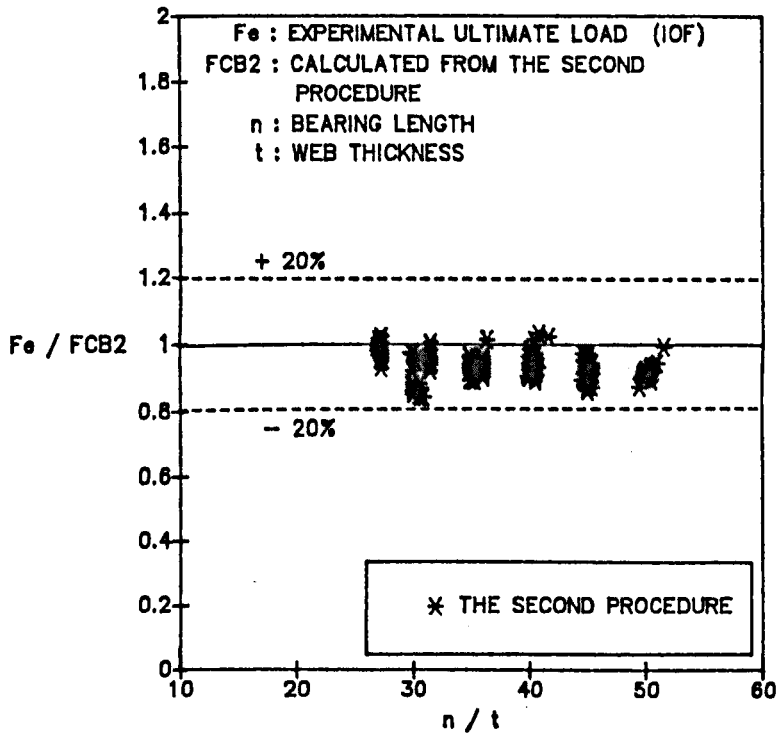
Figure 9.2. $F_e/F_{CB}2$ vs. bearing length ratio, for $M/M_c \geq 0.3$.

301
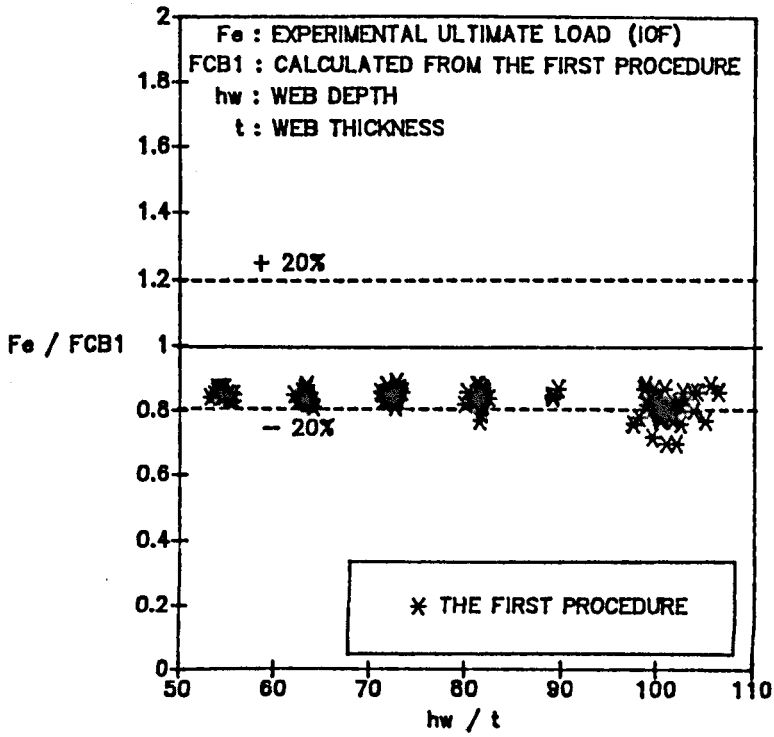
Figure 9.3. $F_e/F_{CB}1$ vs. web slenderness ratio, for $M/M_c \geq 0.3$.
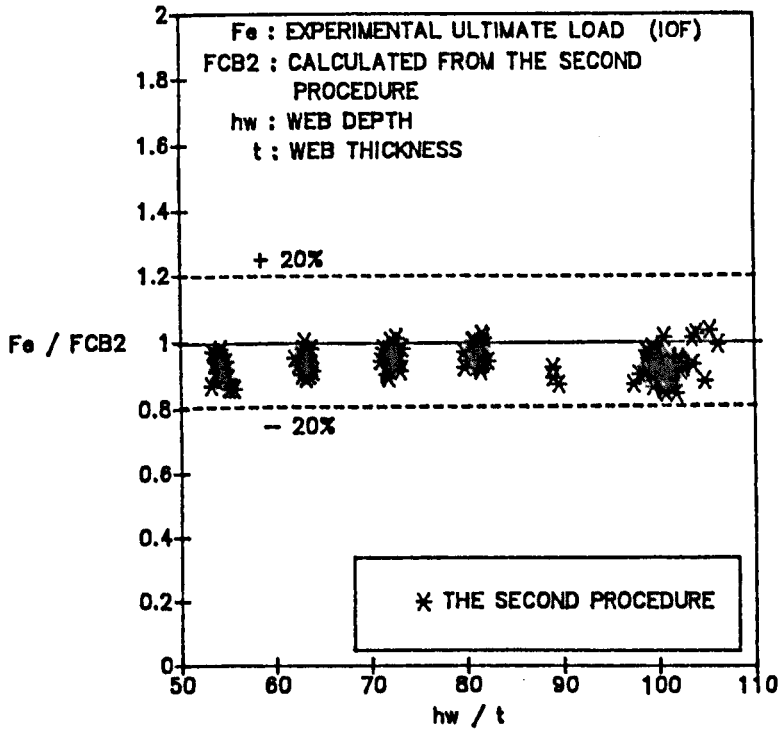
Figure 9.4. $F_e/F_{CB}2$ vs. web slenderness ratio, for $M/M_c \geq 0.3$.

302
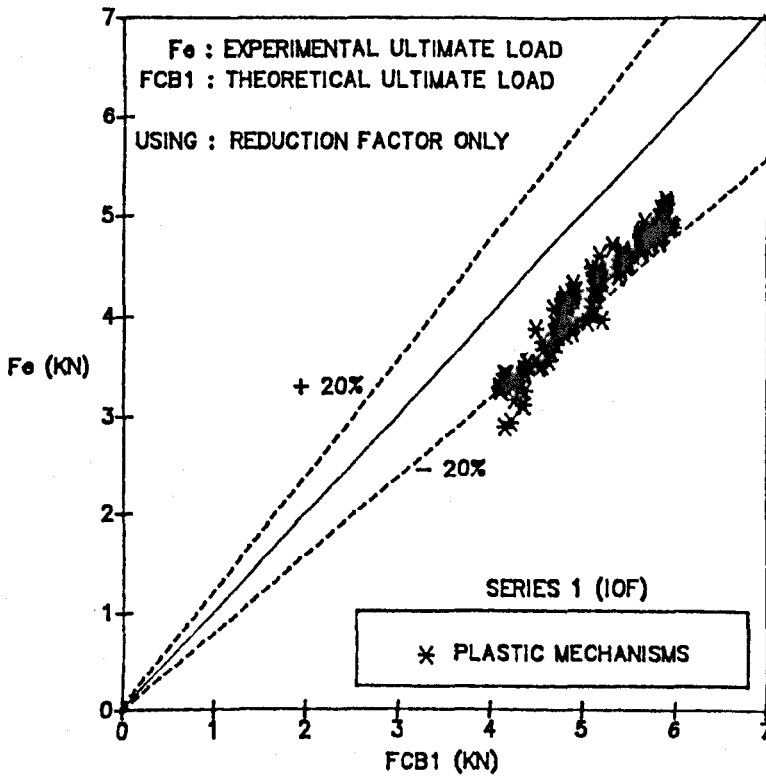
Figure 9.5. Theoretical load $F_{CB}1$ vs. experimental load F_e, for $M/M_c \geq 0.3$.
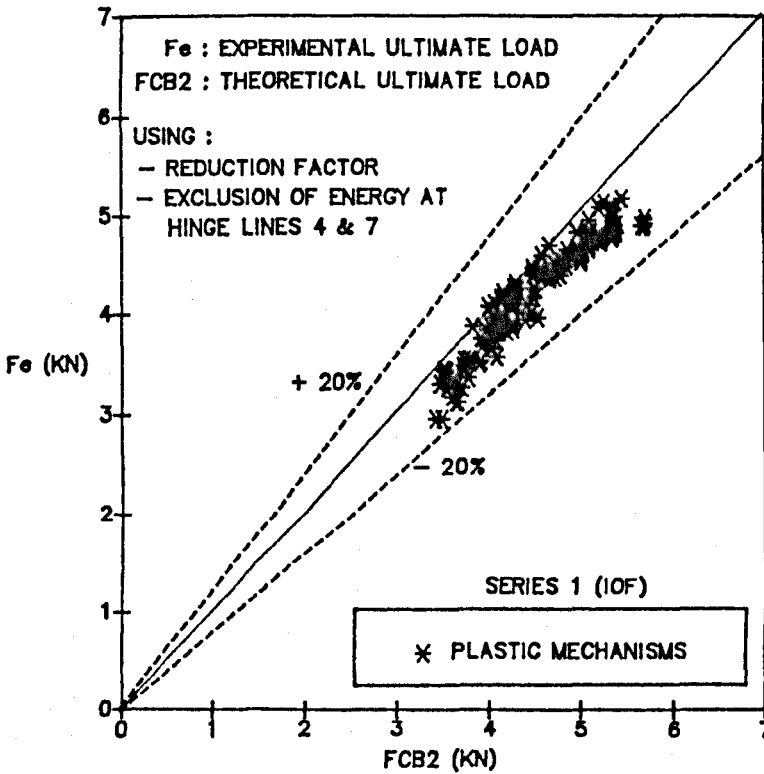
Figure 9.6. Theoretical load $F_{CB}2$ vs. experimental load F_e, for $M/M_c \geq 0.3$.

303

9.3. SPECIMENS IN TEST SERIES 2 (M/M$_c$ < 0.3).

Table 9.2. SERIES 2 (M/M$_c$ < 0.3) - A1 : Fe/F$_{CB}$1 and A2 : Fe/F$_{CB}$2

No.	Specimen	n/t	hw/t	r/t	F$_e$ (KN)	F$_{CB}$1 (KN)	F$_{CB}$2 (KN)	A1	A2
1	H60-6	40.40	60.59	3.79	4.36	5.44	5.30	0.80	0.82
2	H60-8	40.00	59.62	3.50	4.27	5.53	5.30	0.77	0.81
3	H60-11	40.00	60.26	3.25	4.45	5.54	5.30	0.80	0.84
4	H60-12	51.02	60.33	3.32	4.67	5.83	5.52	0.80	0.85
5	H60-38	50.00	61.12	3.75	4.89	6.07	5.52	0.81	0.89
6	H60-39	50.00	59.40	3.50	4.76	6.02	5.52	0.79	0.86
7	H80-35	40.40	80.61	3.79	4.38	5.39	4.95	0.81	0.88
8	H80-36	40.00	80.20	3.75	4.36	5.49	5.03	0.79	0.87
9	H80-37	40.00	79.48	3.75	4.36	5.48	4.94	0.80	0.88
10	H80-38	50.51	80.55	3.79	4.89	4.87	4.19	0.88	1.03
11	H80-39	50.51	80.61	3.79	4.89	4.86	4.19	0.92	1.07
12	H80-40	50.00	79.38	3.75	5.07	4.86	4.18	0.92	1.07
13	H100-28	30.30	101.01	4.04	3.76	4.73	3.86	0.79	0.97

Table 9.2. SERIES 2 ($M/M_c < 0.3$) - A1 : $Fe/F_{CB}1$ and A2 : $Fe/F_{CB}2$

No.	Specimen	n/t	hw/t	r/t	F_e (KN)	$F_{CB}1$ (KN)	$F_{CB}2$ (KN)	A1	A2
14	H100-29	40.00	99.58	4.00	4.45	5.37	4.59	0.83	0.97
15	H100-30	40.00	99.98	4.00	4.45	5.38	4.60	0.83	0.97
16	H100-31	40.00	101.94	4.00	4.47	5.41	4.60	0.83	0.97
17	H100-32	50.51	101.94	4.04	4.53	5.73	5.15	0.79	0.88
18	H100-33	50.00	99.78	4.00	4.71	5.80	5.23	0.81	0.90
19	H100-34	50.00	99.80	4.00	4.53	5.82	5.26	0.78	0.86
20	H100-36	30.00	101.88	2.25	4.27	4.85	4.03	0.88	1.06
21	H100-37	30.30	99.41	3.28	4.27	4.95	4.12	0.86	1.04
22	H100-41	39.60	100.97	2.23	4.58	5.51	4.77	0.83	0.96
23	H100-42	40.40	103.05	2.27	4.71	5.61	4.84	0.84	0.97
24	H100-44	39.60	98.63	3.22	4.89	5.47	4.69	0.89	1.04
25	H100-47	50.51	102.40	2.27	5.20	6.04	5.49	0.86	0.95
26	H100-49	50.50	100.83	3.28	5.18	6.02	5.43	0.86	0.95
27	H100-50	50.00	98.00	4.25	5.18	6.08	5.53	0.85	0.94

Table 9.2. SERIES 2 (M/M$_c$ < 0.3)

Statistical measures of accuracy of A1 and A2	A1	A2
Mean	0.830	0.937
Standard deviation	0.042	0.079
Coeff. of variation	0.051	0.084
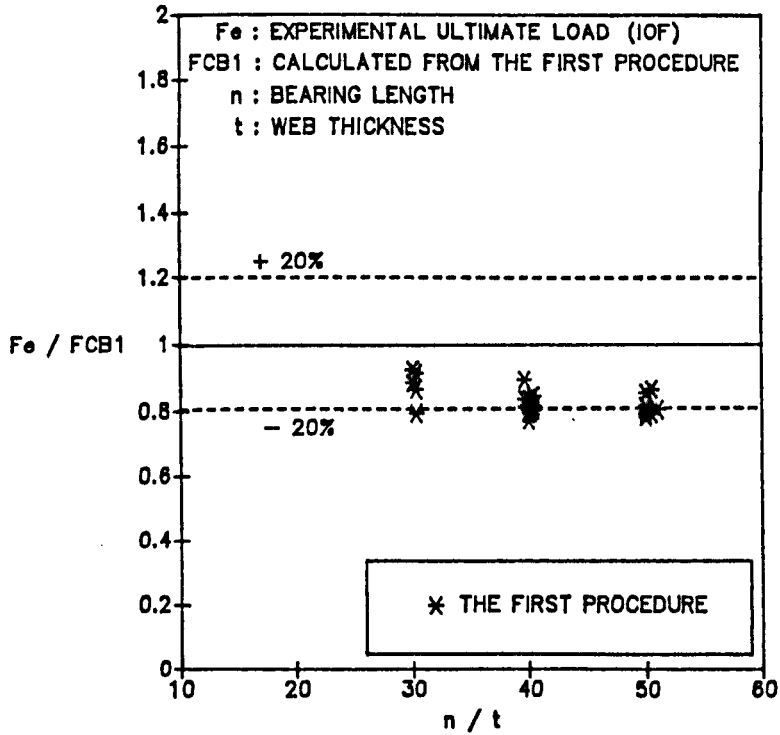
Figure 9.7. F$_e$/F$_{CB}$1 vs. bearing length ratio, for M/M$_c$ < 0.3.
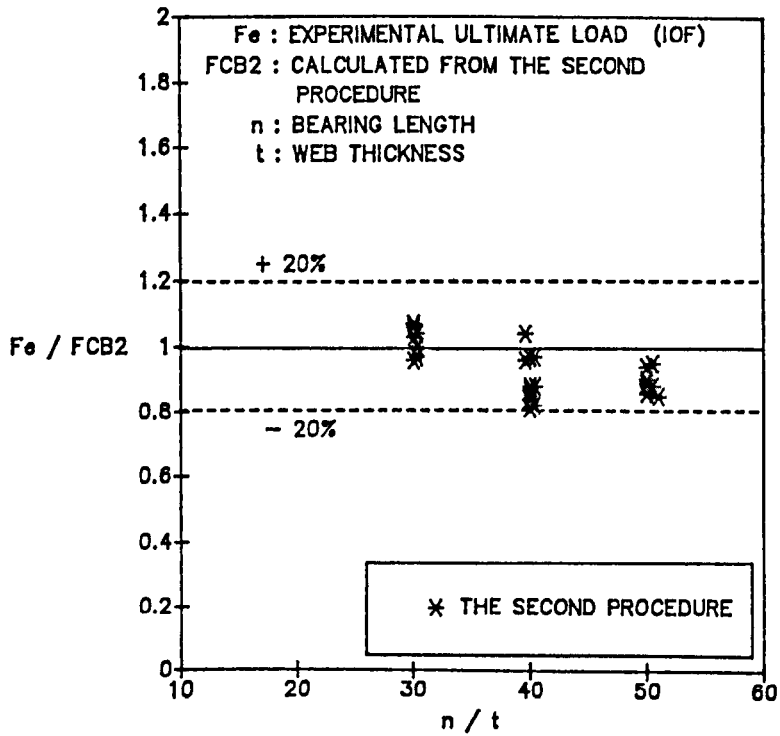
Figure 9.8. $F_e/F_{CB}2$ vs. bearing length ratio, for $M/M_c < 0.3$.
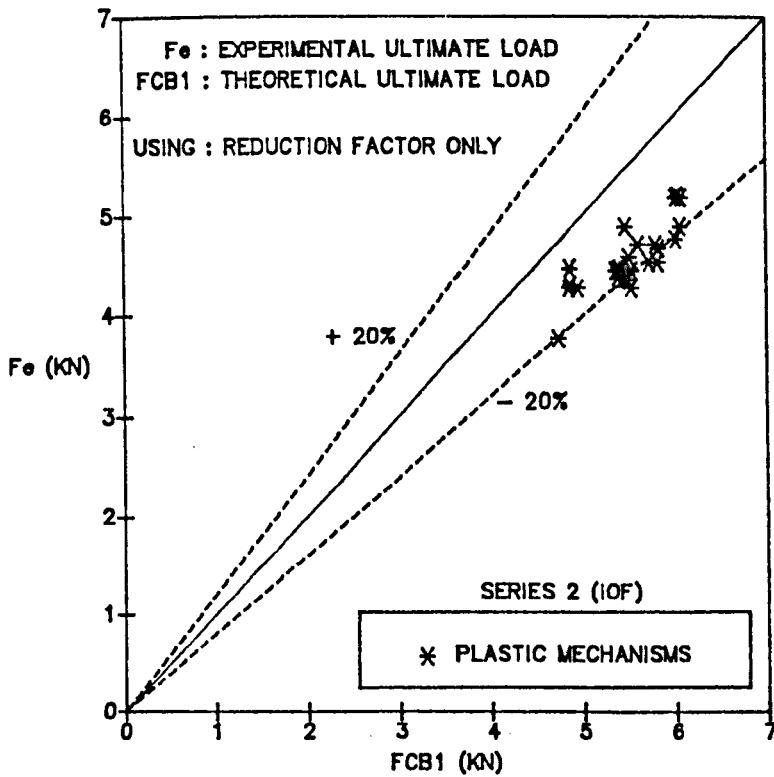
Figure 9.9. Theoretical load $F_{CB}1$ vs. experimental load F_e, for $M/M_c < 0.3$.

307
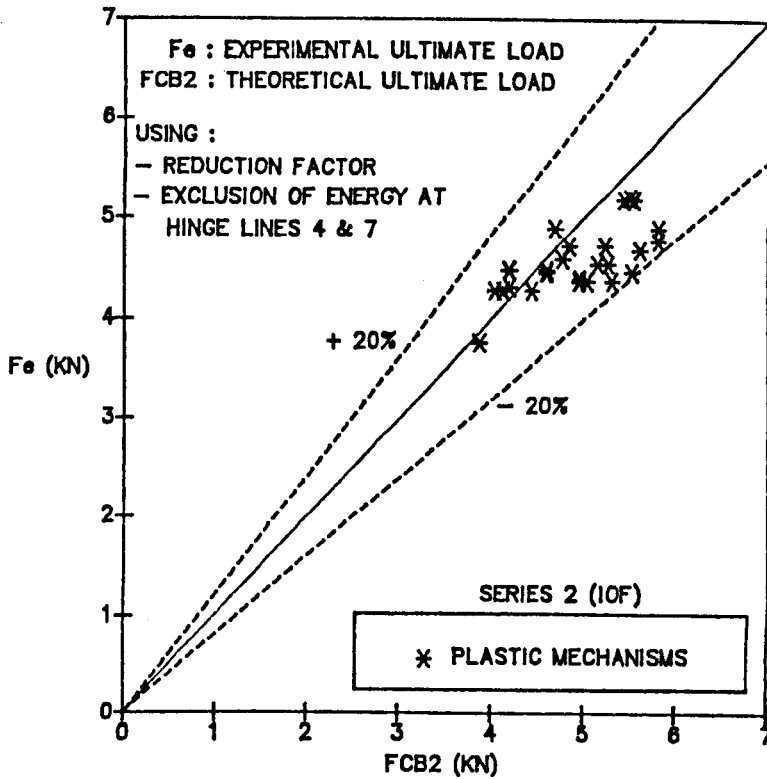
Figure 9.10. Theoretical load $F_{CB}2$ vs. experimental load F_e, for $M/M_c < 0.3$.

9.4. THEORETICAL COLLAPSE AND EXPERIMENTAL CURVES.
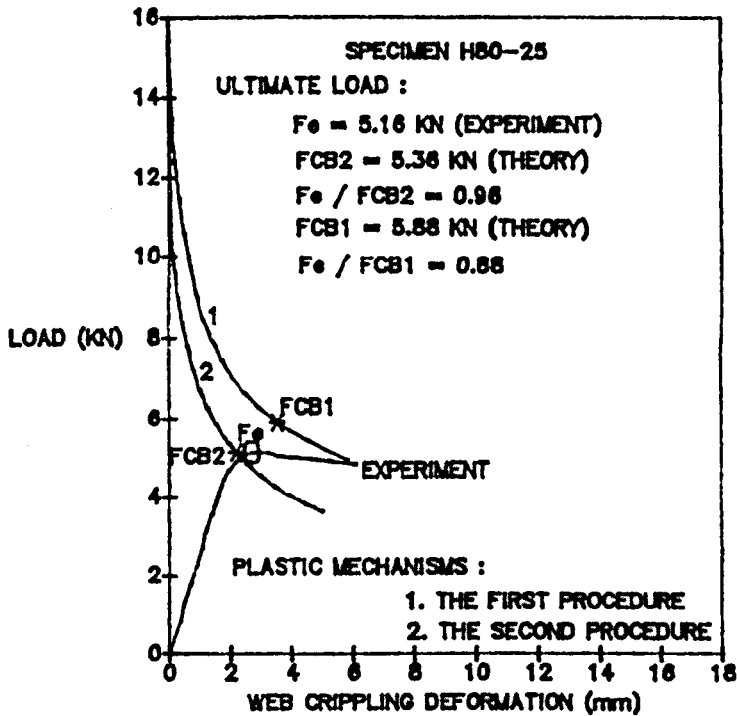
Figure 9.11. Collapse curve of specimen H80-25.

308
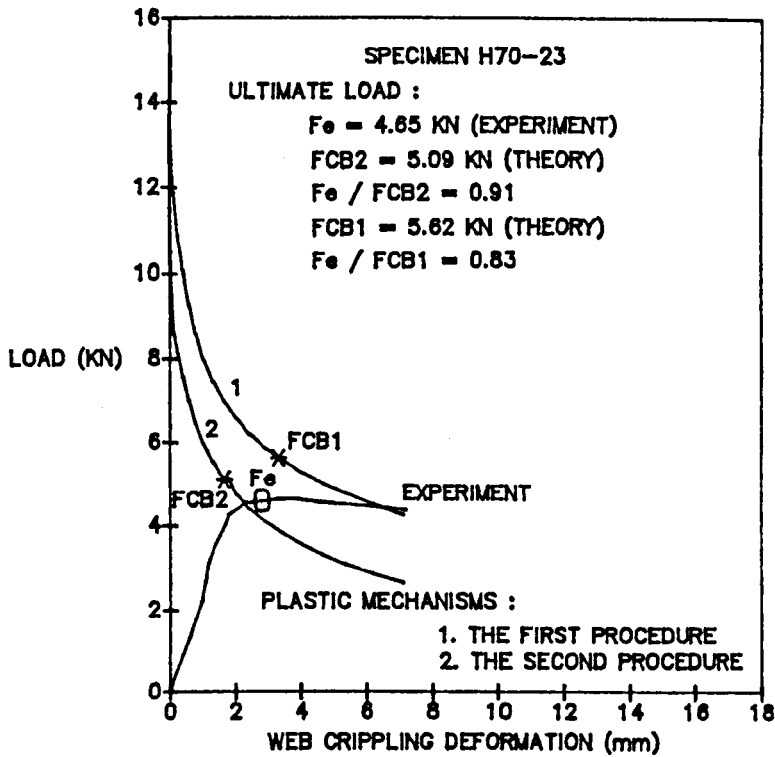
Figure 9.12. Collapse curve of specimen H70-23.

9.5. DISCUSSION.

Figures 9.1 - 9.10 (see also appendix F) show the accuracy of using the idealized

plastic mechanism model of web crippling failure (Figure 7.3) for analysing ultimate

web crippling loads of the specimens subjected to combined actions of web crippling

and bending (IOF). It can be seen in the figures that the theoretical results estimated

using this model mostly tend to overestimate the experimental results. However, the

accuracy of the theoretical values obtained from the first and the second procedures

is mostly still scattered within the acceptable limits $\pm 20\%$. In reducing the over-

predicted results, a reduction factor only (the first procedure) is actually not enough

309

to be used in the analysis, but if its application is complemented by the reduced total

energy dissipation at the plastic hinge lines (the second procedure), the improvement

of the over-predicted results can be achieved. This can be seen from the statistical

analyses that the results of the second procedure, on average, deviate only 6.3% -

6.5% from the experimental values, while the average accuracy of the first procedure

reaches 17.0% - 17.3%. It can also be found out from the figures that the accuracy

of the theoretical values is not affected by variations of applied bending moment and

parameters such as n/t and hw/t.

Figures 9.11 and 9.12 show the comparisons of theoretical collapse curves and the

actual load-deflection curves of specimens H80-25 and H70-23. The theoretical

collapse behaviour of both specimens estimated using the second procedure tends to

underestimate their actual load carrying capacities during collapse. The figures also

show the difference of actual and theoretical collapse behaviour of the specimens,

where the decrease of load carrying capacity in the actual behaviour is more gradual

than that in both theoretical curves. Although the actual collapse behaviour of the

specimens has not yet been properly predicted, but from the accuracy point of view,

the application of the idealized plastic mechanism model developed in this research

program can result in variations of the theoretical values which are mostly still

scattered within the acceptable limits. Nevertheless, most of the theoretical results are

non-conservative and this means that the method used to analyse the idealized plastic

mechanism model in this research program is actually an upper bound method.

CHAPTER 10

CONCLUSIONS

10. CONCLUSIONS.

The web crippling strength of cold-formed plain channel steel section beams has been investigated through this research program and this chapter presents the research findings. The investigations were carried out theoretically and experimentally, and also involved the application of two different design specifications, namely BS 5950 Part 5 1987 and European Recommendations 1987. In the theoretical investigations, an idealized plastic mechanism model of web crippling failure was developed and this model is used to analyse the web crippling strength of cold-formed plain channel steel section beams subjected to combined actions of web crippling and bending.

Experimental investigations of web crippling have been conducted for many plain channel beams with various dimensions and loading conditions as specified by AISI 1986. The results of the experiments are used for comparison with the results obtained from the analytical theory and both design specifications, so that their relative accuracy in predicting the web crippling strength of cold-formed plain channel steel section beams can be evaluated. The experimental results reveal that the web crippling strength of the plain channel beams is affected by various factors. From the three parameters studied, the bearing length ratio (n/t) and the inside bend radius ratio (r/t) have a significant influence on the web crippling strength of the plain channel beams while the web slenderness ratio (hw/t) only significantly affects the web crippling strength of the plain channel beams subjected to end one-flange

loading conditions.

With regard to the plain channel beams subjected to combined actions of web crippling and bending, the magnitude of bending moment has a significant role in influencing their ultimate web crippling loads. Figure 3.12 shows the influence of applied bending moment on the web crippling strength of the plain channel beams under IOF loading conditions, where the larger the values of applied bending moment, the lower the values of concentrated load which can be carried by the plain channel beams. These types of beam will be stronger to carry the concentrated loads if the bending moment applied on them is relatively small. The web crippling strength of the plain channel beams depends also on the types of loading condition, where irrespective of whether the loads are applied on one side or on both sides of their flanges the beams are generally able to carry substantially greater concentrated loads applied far from their free ends than applied exactly at their free ends.

The verification of both design specifications used in this research program indicates that the consistency of theoretical results estimated by BS 5950 Part 5 1987 and European Recommendations 1987 depends also on the types of loading condition. In the case of plain channel beams subjected to combined actions of web crippling and bending, the application of BS 5950 Part 5 1987 tends to be unsafe if the applied bending moment is relatively large. But if the applied bending moment is relatively small, BS 5950 Part 5 1987 can result in safer predictions. On the other hand, in all

cases of the applied bending moment the European Recommendations 1987 can give

extremely safe results although their accuracy is mostly beyond the expected one. The

large or small values of applied bending moment are measured with respect to the

moment capacity of the plain channel beams. In this research program, the applied

bending moment is considered to be relatively large if its ratio to the moment

capacity (M/M_c) is equal or greater than 0.3. Conversely, if the ratio of applied

bending moment to the moment capacity is less than 0.3, the applied bending moment

is therefore considered to be relatively small.

Basically, the criteria of determining the moment capacity required by BS 5950 Part

5 1987 and European Recommendations 1987 are similar, that is, the moment

capacity should be determined according to the maximum compressive stress in the

web and the effective width of compression elements. The difference of both design

specifications in determining the moment capacity is in the implementation of the

criteria where this can be summerized as follows :

- BS 5950 Part 5 1987 uses the limiting compressive stress as expressed in

  equation (4.2.1) for calculating the maximum compressive stress in the web,

  while European Recommendations 1987 use the yield strength of basic

  material for it.

- The calculation of effective width in BS 5950 Part 5 1987 is applied to the

  compression elements only, whereas in European Recommendations 1987 it

  is applied to the compression elements as well as compression parts of

313

bending elements.

- The effect of shear lag is not considered by BS 5950 Part 5 1987 in calculating the effective width, but it is considered by European Recommendations 1987 in calculating the effective width of compression elements of flexural members with short spans.

As a result of these above differences, the moment capacity of the plain channel beams calculated using BS 5950 Part 5 1987 is also different compared with that calculated using European Recommendations 1987. The moment capacity obtained from BS 5950 Part 5 1987 is generally higher than that obtained from the European Recommendations 1987. In this thesis, measures of the large or small bending moment are based on the moment capacity obtained from BS 5950 Part 5 1987.

Both of the design specifications have the same tendency if they are used to predict the web crippling strength of the plain channel beams subjected to end loadings. The design specifications tend to underestimate the actual web crippling strength of the plain channel beams under end one-flange loadings and they will tend to overestimate it if the beams are subjected to end two-flange loadings. The formula of BS 5950 Part 5 1987 expressed in the second row of table 2 is actually not quite accurate to estimate the web crippling strength of the plain channel beams under these types of loading. As can be seen in Figures 8.9 - 8.12, the accuracy of the theoretical values calculated using this formula deviates very far from the expected one. The results of statistical analysis also show that the average theoretical values are 79% lower than

314

the actual ones. These estimated values are of course very safe but the application of

the formula for this type of section beam is actually inefficient and it is advisable to

revise the formula before using it in calculations. In the case of estimating the web

crippling strength of the plain channel beams under interior two-flange loadings,

European Recommendations 1987 are better than BS 5950 Part 5 1987 because their

estimated results are mostly safe and closer to the actual ones.

In the plastic mechanism approach, the idealized plastic mechanism model of web

crippling failure has been analysed using the method of yield line analysis. The

analysis is carried out according to an energy method. This method is based on the

equilibrium of external energy caused by the applied loads and the total energy

dissipation at the plastic hinge lines. The model is also analysed using an elastic

theory and load-deflection expressions obtained from the plastic mechanism and

elastic analyses are used to determine the ultimate web crippling loads, where this is

accomplished by means of iteration methods. In order to minimize the over-predicted

results of ultimate web crippling load, two different procedures of the plastic

mechanism analysis have been performed, i.e. the first procedure is based on the

application of a reduction factor only, while the second procedure is based on the

application of the reduction factor and reduced total energy dissipation at the plastic

hinge lines.

The accuracy of the theoretical results estimated by both procedures has also been

315

verified and it can be seen that the results of the second procedure are quite better than those of the first procedure. Most of the theoretical values estimated by these procedures are consistently scattered within the non-conservative region and it is evident that the energy method applied in this plastic mechanism analysis is actually an upper bound method. From the statistical analysis, the average accuracy of using the mechanism model and the design specifications for the same loading conditions is as follows :

- Loading condition	IOF	IOF
- M/M_c	≥ 0.3	< 0.3
- Plastic mechanism model :		
- the first procedure	- 17.3%	- 17.0%
- the second procedure	- 6.5%	- 6.3%
- BS 5950 Part 5 1987	- 6.8%	7.0%
- European Recommendations 1987	29.4%	33.7%

Further investigations on the application of the idealized plastic mechanism model are still needed and it is suggested that the application of this model is extended for analysing the web crippling strength of the plain channel beams with larger dimensions and longer spans. The beam should be made of various materials instead of using Galvanized Steel BS 2989 Sheet Z 28 only and the thickness of the beams should also be varied. In order to minimize the theoretical values estimated using the energy method in the plastic mechanism analysis, it is also advisable to try to use the

reduced moment resisting capacity of the plastic hinge in determining the energy

dissipation at the plastic hinge lines. The reduced moment resisting capacity should

be taken into account especially in the determination of the energy dissipation at the

plastic hinge lines which are directly affected by uniformly axial loads only, while

the fully plastic moment can still be used for determining the energy dissipation at

the other hinge lines. By combining the energy dissipation determined in this way

and equating it to the external energy due to applied loads, it is expected the reduced

load carrying capacity can be obtained without introducing a reduction factor and

reducing the total energy dissipation at the plastic hinge lines. This proposed method

should also be compared with the first and the second procedures of the plastic

mechanism analysis established in this thesis in order to see which one of these

methods is actually the best to be used for obtaining the theoretical values which are

closer to the actual ones.

REFERENCES

REFERENCES.

1. W.W. Yu," Cold-formed steel structures - design analysis - construction ", McGraw-hill Book Company, 1973.

2. Winter, G. and Pian, R.H.J.," Crushing strength of thin steel webs ", Engineering Experiment Station, Bulletin No.35, Cornell University, New York, April 1946.

3. L. Zetlin," Elastic instability of flat plates subjected to partial edge loads ", Proceedings - American Society of Civil Engineers, Engineering Mechanics Division, Vol.81, September, 1955.

4. Winter, G.," Commentary on the 1968 Edition of the Specification for the design of cold-formed steel structural members ", American Iron and Steel Institute, 1970 ed.

5. American Iron and Steel Institute," Specification for the design of cold-formed steel structural members ", 1968 Edition.

6. George D. Ratliff, Jr.," Interaction of concentrated loads and bending in C-shaped beams ", The third Specialty Conference on Cold-Formed Steel Structures, University of Missouri-Rolla, November 24-25, 1975.

7. N. Hetrakul and W.W. Yu," Cold-formed steel I-beams subjected to combined bending and web crippling ", International Conference At The University of Strathclyde, Glasgow, April 3-6, 1979, pp. 413-426.

8. N. Hetrakul and W.W. Yu," Structural behavior of beam webs subjected to web crippling and a combination of web crippling and bending ", Final

Report, Civil Engineering Study 78-4, University of Missouri-Rolla, June 1978.

9. B.A. Wing and R.M. Schuster," Web crippling of decks subjected to two-flange loading ",Sixth International Specialty Conference On Cold-Formed Steel Structures, November 16-17,1982,pp. 157-178.

10. B.A. Wing and R.M. Schuster," Web crippling of multi-web deck sections subjected to interior one-flange loading ",Eight International Specialty Conference On Cold-Formed Steel Structures, St.Louis, Missouri, U.S.A., November 11-12,1986,pp. 371-402.

11. C. Santaputra, M.B. Parks and W.W. Yu," Web crippling of high strength steel beams ",Eight International Specialty Conference On Cold-Formed Steel Structures,St. Louis, Missouri,U.S.A.,November 11-12,1986,pp. 111-139.

12. J. Studnička," Web crippling of multi-web deck sections ",Thin-Walled Structures 11(1991),pp. 219-231.

13. K.S. Sivakumaran and K.M. Zielonka," Web crippling strength of thin-walled steel members with web opening ",Thin-Walled Structures 8(1989),pp. 295-319.

14. S.P. Timoshenko and J.M. Gere," Theory of Elastic Stability ",2nd ed. McGraw-Hill,1961.

15. M.Z. Khan and A.C. Walker," Buckling of plates subjected to localized edge loading ",The Structural Engineer, No.6, Vol.50,June 1972,pp. 225-232.

16. A.C. Walker," Design and Analysis of Cold-Formed Sections ", International Textbook Company Limited, 1975.

17. Kenneth C. Rockey, Mohamed A. El-gaaly and Debal K. Bagchi," Failure of thin-walled members under patch loading ", Journal of the Structural Division, ASCE, Vol.98, ST12, December, 1972.

18. Archibald N. Sherbourne and Robert M. Korol," Post-buckling of axially compressed plates ", Journal of the Structural Division, ASCE, Vol.98, ST10, October, 1972.

19. Robert M. Korol and Archibald N. Sherbourne," Strength predictions of plates in uniaxial compression ", Journal of the Structural Division, ASCE, Vol.98, ST9, September, 1972.

20. N.W. Murray," Buckling of stiffened panels loaded axially and in bending ", The Structural Engineer, Vol.51, 8, August, 1973.

21. Walker, A.C. and Murray, N.W.," A plastic collapse mechanism for compressed plates ", International Association For Brigde And Structural Engineering (IABSE), Vol.35, 1975, pp. 217-236.

22. P. Davies, K.O. Kemp and A.C. Walker," An analysis of the failure mechanism of axially-loaded simply-supported steel plates ", Proc. Inst. Civil Engineers, Part2, Vol.59, December 1975, pp. 645-658.

23. N.W. Murray and P.S. Khoo," Some basic plastic mechanisms in the local buckling of thin-walled steel structures ",International Journal of Mechanical Sciences, Vol.23, No.12, 1981, pp. 703-713.

24. M.C.M. Bakker," Web crippling of cold-formed steel members ",Doctor Thesis,Eindhoven University of Technology ,1992, pp. 28-252.

25. British Standard Institution," Structural use of steelwork in building ", Part 5.

Code of practice for design of cold-formed sections, BS 5950, 1987.

26. C. Santaputra and W.W. Yu," Web Crippling of cold-formed steel beams ", Civil Engineering Study 86-1, Eight Progress Report, Design of Automotive Structural Components Using High Strength Sheet Steels, University of Missouri-Rolla, U.S.A., August 1986.

27. American Iron and Steel Institute," Specification for the design of cold-formed steel structural members ",1980 Edition.

28. American Iron and Steel Institute," Specification for the design of cold-formed steel structural members ",1986 Edition.

29. European Recommendations for the design of light gauge steel members,1987.

30. Noel W. Murray," Introduction to the Theory of Thin-Walled Structures ", Oxford Engineering Sciences Series 13, 1986, pp. 312-313.

31. Theodore Baumeister and Lionel S. Marks," Standard handbook for mechanical engineers ", McGraw-Hill book company, Seventh Edition.

32. Charles G. Schilling," Web crippling tests on hybrid beams ", Journal of the Structural Division - ASCE, Vol.93, ST1, February, 1967.

33. Jeffrey A. Packer," Web crippling on rectangular hollow sections ", Journal of Structural Engineering, Vol.110, No.10, October, 1984.

34. J. Studnička," Web crippling of wide deck sections ", Tenth International Specialty Conference On Cold Formed Steel Structures, St. Louis, Missouri, U.S.A., October 23-24, 1990, pp. 317-334.

35. J. Rhodes," Design of cold formed steel members ", Elsevier Science Publishers Ltd., 1991

36. Roger L. Brockenbrough," Cold-formed steel members - Design Approaches in the United States ", Thin-Walled Structures 16, 1993, pp. 307-317.

37. Rolf Baehre," Cold-formed steel design and research in Germany ", Thin-Walled Structures 16, 1993, pp. 293-305.

38. A. Toma," European design methods for cold-formed steel ", Thin-Walled Structures 16, 1993, pp. 275-291.

39. M.R. Horne, " Plastic theory of structures ", Thomas Nelson and Sons Ltd., 1971.

40. J. Rhodes, " Some thoughts on future cold formed steel design rules ", Behaviour of Thin-Walled Structures - Edited by J. Rhodes and J. Spence,Elsevier Applied Science Publishers Ltd., 1984, pp. 125-142.

41. D.M. Currie," The use of light-gauge cold-formed steelwork in construction : developments in research and design ", Building Research Establishment Report, 1989, pp.106.

42. Dusan Kecman," Bending collapse of rectengular and square section tubes ", International Journal of Mechanical Science, Vol.25, 9-10, 1983.

43. V. Enjily," The inelastic post-buckling behaviour of cold-formed sections ", PhD Thesis, Department of Civil, Building and Cartography, Oxford Polytechnic, September 1985.

44. K.W. Sin," The collapse behaviour of thin-walled sections ", PhD Thesis, University of Strathclyde, August 1985.

45. N.W. Murray," The behaviour of thin stiffened steel plates ", International Association For Brigde And Structural Engineering (IABSE), Vol.33-I, 1973,

pp. 191-202.

46. Monique Bakker, Teoman Pekoz and Jan Stark," A model for the behavior of thin-walled flexural members under concentrated loads ", Tenth International Specialty Conference on Cold-formed Steel Structures, St. Louis, Missouri, U.S.A., October 23-24, 1990, pp. 299-316.

47. Xiao-Ling Zhao and Gregory J. Hancock," A Theoretical analysis of the plastic-moment capacity of an inclined yield line under axial force ", Thin-Walled Structures 15, 1993, pp. 185-207.

48. Xiao-Ling Zhao and Gregory J. Hancock," Experimental verification of the theory of plastic-moment capacity of an inclined yield line under axial force ", Thin-Walled Structures 15, 1993, pp. 209-233.

49. N.W. Murray," Analysis and design of stiffened plates for collapse load ", The Structural Engineer, Vol.53, No.3, March 1975, pp. 153-158.

50. N.W. Murray," The static approach to plastic collapse and energy dissipation in some thin-walled steel structures ", Structural Crashworthiness, Editors - N. Jones and T. Wierzbicki, Publisher - Butterworths, 1989, pp. 44-65.

51. Glenn A. Morris and Jeffrey A. Packer," Yield line analysis of cropped-web warren truss joints ", Journal of Structural Engineering, Vol.114, No.10, October 1988, pp. 2210-2224.

52. J.M.M. Out," Yield surface for bending moment, shear force and normal force ", Heron, Vol.30, No.4, 1985, pp. 30-58.

53. M.C.M. Bakker," Yield line analysis of post-collapse behaviour of thin-walled steel members ", Heron, Vol.35, No.3, 1990, pp. 3-50.

323

54. A.J. Munday and R.A. Farrar," An engineering data book ", The MacMillan Press Ltd, 1992, pp. 41.

55. Noel W. Murray," The elastic buckling & collapse behaviour of thin-walled structures ", International Conference on Steel and Aluminium Structures (ICSAS 91), Singapore, 22-24 May 1991, pp. 44-59.

56. M. Mahendran and N.W. Murray," Effect of initial imperfections on local plastic mechanisms in thin steel plates with in-plane compression ", International Conference on Steel and Aluminium Structures (ICSAS 91), Singapore, 22-24 May 1991, pp. 491-500.

57. H.G. Allen and P.S. Bulson," Background to buckling ", McGraw-Hill Book Company (UK) Limited, 1980.

58. British Standard Institution," Methods for tensile testing of metals ", BS 18, Part 3, 1971.

59. British Standard Institution," British standard specification for continuously hot-dip zinc coated and iron-zinc alloy coated steel : wide strip, sheet/plate and slit wide strip ", BS 2989, 1982.

60. John Mandell," The statistical analysis of experimental data ", Interscience publishers, 1964.

61. G.H. Little, " Collapse behaviour of aluminium plates ", Int. J. Mech. Sci., Vol. 24, No. 1, 1982, pp. 17-45.

APPENDICES

APPENDIX A

SPECIMEN DIMENSIONS AND BEARING LENGTHS

Table A1. Specimens for IOF ($M/M_c \geq 0.3$)

No.	Specimen	hw (mm)	B (mm)	r (mm)	t (mm)	l (mm)	L (mm)	n (mm)
1	H60-2	8.76	31.93	2.25	1.10	300	360	30
2	H60-4	58.76	33.40	2.25	1.10	300	360	30
3	H60-7	59.67	34.04	2.25	1.10	300	360	30
4	H60-9	59.65	32.29	2.25	1.10	300	360	30
5	H60-10	59.40	34.06	2.25	1.10	300	360	30
6	H60-18	60.90	31.50	2.25	1.11	300	360	35
7	H60-19	60.01	31.75	2.25	1.11	300	360	35
8	H60-20	60.52	31.70	2.25	1.11	300	360	35
9	H60-21	59.55	31.75	2.25	1.11	300	360	35
10	H60-22	59.88	32.51	2.25	1.11	300	360	35
11	H60-23	60.01	31.75	2.25	1.11	300	360	40

n : bearing length and the other symbols are defined in Figure 3.3.

325

Table A1. Specimens for IOF (M/M$_c$ ≥ 0.3)

No.	Specimen	hw (mm)	B (mm)	r (mm)	t (mm)	l (mm)	L (mm)	n (mm)
12	H60-24	60.01	31.75	2.25	1.11	300	360	40
13	H60-25	60.39	31.75	2.25	1.11	300	360	40
14	H60-26	60.80	31.75	2.25	1.11	300	360	40
15	H60-27	60.01	32.08	2.25	1.11	300	360	40
16	H60-28	61.15	31.50	2.25	1.11	300	360	45
17	H60-29	60.54	31.75	2.25	1.11	300	360	45
18	H60-30	60.65	31.75	2.25	1.11	300	360	45
19	H60-31	60.34	31.62	2.25	1.11	300	360	45
20	H60-32	59.65	32.00	2.25	1.11	300	360	45
21	H60-33	61.28	31.75	2.25	1.11	304	362	50
22	H60-34	59.12	32.51	2.25	1.11	302	362	50
23	H60-35	61.84	31.50	2.25	1.11	302	360	50
24	H60-36	61.79	31.37	2.25	1.11	300	360	50
25	H60-37	61.28	31.37	2.25	1.11	300	360	50

n : bearing length and the other symbols are defined in Figure 3.3.

Table A1. Specimens for IOF (M/M$_c \geq 0.3$)

No.	Specimen	hw (mm)	B (mm)	r (mm)	t (mm)	l (mm)	L (mm)	n (mm)
26	H70-6	69.17	32.77	2.25	1.10	350	410	30
27	H70-7	68.67	32.69	2.25	1.10	350	410	30
28	H70-8	68.23	32.78	2.25	1.10	350	410	30
29	H70-11	70.40	31.95	2.25	1.11	351	411	35
30	H70-12	70.17	31.72	2.25	1.11	351	411	35
31	H70-13	70.09	31.65	2.25	1.11	351	412	35
32	H70-14	70.81	31.88	2.25	1.11	350	411	35
33	H70-15	69.87	32.26	2.25	1.11	351	411	35
34	H70-18	70.68	31.65	2.25	1.11	352	411	40
35	H70-19	70.30	31.90	2.25	1.11	352	411	40
36	H70-20	70.45	31.29	2.25	1.11	351	411	40
37	H70-21	70.50	31.50	2.25	1.11	350	410	45
38	H70-23	70.93	31.39	2.25	1.11	352	410	45
39	H70-24	70.50	31.70	2.25	1.11	350	410	45

n : bearing length and the other symbols are defined in Figure 3.3.

Table A1. Specimens for IOF (M/M$_c$ ≥ 0.3)

No.	Specimen	hw (mm)	B (mm)	r (mm)	t (mm)	l (mm)	L (mm)	n (mm)
40	H70-30	70.17	31.75	2.25	1.11	350	400	45
41	H70-25	70.07	31.75	2.25	1.11	350	410	50
42	H70-26	70.17	32.26	2.25	1.11	350	410	50
43	H70-27	69.66	32.08	2.25	1.11	350	410	50
44	H70-28	70.07	32.08	2.25	1.11	350	410	50
45	H70-29	70.55	31.75	2.25	1.11	350	410	50
46	H80-9	79.49	42.34	2.25	1.10	398	459	30
47	H80-10	79.72	42.67	2.25	1.10	398	460	30
48	H80-11	80.53	41.96	2.25	1.11	402	463	30
49	H80-12	80.66	41.66	2.25	1.11	402	463	30
50	H80-13	81.32	41.12	2.25	1.11	402	461	30
51	H80-14	79.92	42.34	2.25	1.11	402	463	35
52	H80-15	80.05	41.76	2.25	1.11	402	463	35
53	H80-16	79.85	42.09	2.25	1.11	402	462	35

n : bearing length and the other symbols are defined in Figure 3.3.

Table A1. Specimens for IOF (M/M$_c \geq 0.3$)

No.	Specimen	hw (mm)	B (mm)	r (mm)	t (mm)	l (mm)	L (mm)	n (mm)
54	H80-17	80.18	42.09	2.25	1.11	402	463	40
55	H80-18	79.72	41.91	2.25	1.11	402	463	40
56	H80-19	80.41	41.91	2.25	1.12	402	462	40
57	H80-30	80.23	41.91	2.25	1.11	402	463	40
58	H80-31	79.80	42.14	2.25	1.11	402	462	40
59	H80-20	80.10	41.88	2.25	1.11	402	463	45
60	H80-21	81.07	41.78	2.25	1.11	402	463	45
61	H80-22	79.57	41.78	2.25	1.11	402	462	45
62	H80-23	80.99	41.25	2.25	1.11	403	463	45
63	H80-24	80.71	41.71	2.25	1.11	402	463	45
64	H80-25	80.66	41.10	2.25	1.11	402	463	50
65	H80-26	80.44	41.91	2.25	1.12	402	462	50
66	H80-27	80.03	41.61	2.25	1.11	402	462	50
67	H80-28	78.81	41.63	2.25	1.11	402	463	50

n : bearing length and the other symbols are defined in Figure 3.3.

329

Table A1. Specimens for IOF ($M/M_c \geq 0.3$)

No.	Specimen	hw (mm)	B (mm)	r (mm)	t (mm)	l (mm)	L (mm)	n (mm)
68	H80-29	80.58	41.83	2.25	1.11	402	462	50
69	H90-10	88.86	42.80	2.25	1.10	453	510	30
70	H90-11	88.76	42.34	2.25	1.10	453	510	30
71	H90-12	89.75	42.16	2.25	1.10	450	512	30
72	H90-13	90.62	41.86	2.25	1.11	450	513	30
73	H90-14	88.98	42.04	2.25	1.00	451	512	30
74	H90-15	88.98	42.04	2.25	1.00	451	513	35
75	H90-16	91.30	42.34	2.25	1.11	451	513	35
76	H90-17	89.91	41.83	2.25	1.11	451	513	35
77	H90-18	90.49	41.25	2.25	1.11	451	513	40
78	H90-19	89.71	42.09	2.25	1.12	451	513	40
79	H90-20	90.00	42.14	2.25	1.10	451	513	40
80	H90-21	90.26	41.50	2.25	1.11	451	513	45
81	H90-22	89.70	42.39	2.25	1.12	451	513	45

n : bearing length and the other symbols are defined in Figure 3.3.

330

Table A1. Specimens for IOF (M/M_c ≥ 0.3)

No.	Specimen	hw (mm)	B (mm)	r (mm)	t (mm)	l (mm)	L (mm)	n (mm)
82	H90-23	90.26	41.63	2.25	1.11	450	512	45
83	H90-24	88.67	42.19	2.25	0.99	451	512	45
84	H90-25	90.11	42.14	2.25	1.11	451	512	45
85	H90-26	89.95	42.14	2.25	1.10	451	512	50
86	H90-27	90.41	42.24	2.25	1.11	451	513	50
87	H90-28	90.21	42.09	2.25	1.11	451	512	50
88	H90-29	89.55	41.96	2.25	1.12	451	512	50
89	H90-30	90.39	41.68	2.25	1.11	451	512	50
90	H100-1	99.35	41.91	2.25	1.00	500	562	30
91	H100-2	99.96	41.91	2.25	1.00	501	562	30
92	H100-3	98.97	42.01	2.25	1.00	502	563	30
93	H100-4	101.07	41.28	2.25	0.99	501	562	30
94	H100-5	100.28	41.91	2.25	0.99	502	562	30
95	H100-6	100.51	41.15	2.25	0.99	501	562	35

n : bearing length and the other symbols are defined in Figure 3.3.

331

Table A1. Specimens for IOF (M/M$_c$ ≥ 0.3)

No.	Specimen	hw (mm)	B (mm)	r (mm)	t (mm)	l (mm)	L (mm)	n (mm)
96	H100-7	100.53	41.15	2.25	0.98	501	562	35
97	H100-8	99.90	41.91	2.25	1.00	501	562	35
98	H100-9	99.60	41.91	2.25	1.00	502	563	35
99	H100-10	99.90	41.91	2.25	1.00	501	562	35
100	H100-11	99.60	42.14	2.25	1.00	502	562	40
101	H100-12	98.51	41.14	2.25	1.00	502	563	40
102	H100-13	99.75	42.24	2.25	1.00	502	563	40
103	H100-14	99.60	42.24	2.25	1.00	502	563	40
104	H100-15	99.77	41.93	2.25	0.98	502	563	40
105	H100-16	98.97	42.24	2.25	1.00	502	563	45
106	H100-17	100.08	41.63	2.25	1.00	502	562	45
107	H100-18	100.26	41.78	2.25	1.00	502	562	45
108	H100-19	101.30	40.89	2.25	0.99	501	562	45
109	H100-20	99.39	42.11	2.25	0.99	503	562	45

n : bearing length and the other symbols are defined in Figure 3.3.

Table A1. Specimens for IOF (M/M$_c$ ≥ 0.3)

No.	Specimen	hw (mm)	B (mm)	r (mm)	t (mm)	l (mm)	L (mm)	n (mm)
110	H100-21	99.52	42.04	2.25	1.00	503	562	50
111	H100-22	100.38	42.11	2.25	0.99	502	563	50
112	H100-23	100.11	41.91	2.25	1.00	502	562	50
113	H100-24	100.43	41.73	2.25	0.98	502	562	50
114	H100-25	100.25	41.78	2.25	1.00	502	563	50
115	H100-52	101.33	40.80	2.25	1.00	500	560	30
116	H100-53	102.79	40.80	2.25	0.98	500	560	30
117	H100-54	100.52	42.36	3.25	1.00	500	560	30
118	H100-55	99.39	41.88	3.25	1.00	500	560	30
119	H100-56	98.80	43.76	4.25	0.98	500	560	30
120	H100-57	98.81	43.49	4.25	0.97	500	560	30
121	H100-58	102.52	40.90	2.25	0.99	500	560	40
122	H100-59	103.33	40.42	2.25	0.98	500	560	40
123	H100-60	99.60	42.50	3.25	0.99	500	560	40

n : bearing length and the other symbols are defined in Figure 3.3.

Table A1. Specimens for IOF ($M/M_c \geq 0.3$)

No.	Specimen	hw (mm)	B (mm)	r (mm)	t (mm)	l (mm)	L (mm)	n (mm)
124	H100-61	99.88	42.80	3.25	0.96	500	560	40
125	H100-62	99.36	42.86	4.25	1.00	500	560	40
126	H100-63	98.02	43.22	4.25	0.99	500	560	40
127	H100-64	102.25	40.58	2.25	0.99	500	560	50
128	H100-65	103.06	40.88	2.25	0.97	500	560	50
129	H100-66	99.94	42.30	3.25	1.01	500	560	50
130	H100-67	99.42	42.62	3.25	0.99	500	560	50
131	H100-68	98.37	43.31	4.25	1.01	500	560	50
132	H100-69	98.00	43.53	4.25	1.00	500	560	50

n : bearing length and the other symbols are defined in Figure 3.3.

Table A2. Specimens for IOF ($M/M_c < 0.3$)

No.	Specimen	hw (mm)	B (mm)	r (mm)	t (mm)	l (mm)	L (mm)	n (mm)
1	H60-6	59.98	32.26	3.75	0.99	175	235	40
2	H60-8	59.62	32.78	3.50	1.00	176	237	40
3	H60-11	60.26	31.40	3.25	1.00	175	235	40
4	H60-12	59.12	33.26	3.25	0.98	177	237	50
5	H60-38	61.12	31.98	3.75	1.00	174	235	50
6	H60-39	59.40	32.10	3.50	1.00	175	235	50
7	H80-35	79.80	32.00	3.75	0.99	230	290	40
8	H80-36	80.20	32.16	3.75	1.00	230	290	40
9	H80-37	79.48	32.50	3.75	1.00	230	290	40
10	H80-38	79.74	32.80	3.75	0.99	230	290	50
11	H80-39	79.80	32.00	3.75	0.99	230	290	50
12	H80-40	79.38	32.42	3.75	1.00	230	290	50
13	H100-28	100.00	32.46	4.00	0.99	300	360	30
14	H100-29	99.58	32.16	4.00	1.00	300	359	40

n : bearing length and the other symbols are defined in Figure 3.3.

Table A2. Specimens for IOF ($M/M_c < 0.3$)

No.	Specimen	hw (mm)	B (mm)	r (mm)	t (mm)	l (mm)	L (mm)	n (mm)
15	H100-30	99.98	32.20	4.00	1.00	300	360	40
16	H100-31	101.94	31.68	4.00	1.00	300	360	40
17	H100-32	100.92	32.00	4.00	0.99	300	360	50
18	H100-33	99.78	32.00	4.00	1.00	300	360	50
19	H100-34	99.80	33.50	4.00	1.00	300	360	50
20	H100-36	101.88	30.50	2.25	1.00	300	360	30
21	H100-37	98.42	32.11	3.25	0.99	300	360	30
22	H100-41	101.98	30.70	2.25	1.01	300	360	40
23	H100-42	102.02	30.60	2.25	0.99	300	360	40
24	H100-44	99.62	32.00	3.25	1.01	300	360	40
25	H100-47	101.38	30.90	2.25	0.99	300	360	50
26	H100-49	98.82	32.50	3.25	0.99	300	360	50
27	H100-50	98.00	33.50	4.25	1.00	300	360	50

n : bearing length and the other symbols are defined in Figure 3.3.

Table A3. Specimens for EOF

No.	Specimen	hw (mm)	B (mm)	r (mm)	t (mm)	L (mm)	n (mm)
1	S100-1	99.36	32.00	4.00	1.00	360	30
2	S100-2	99.92	32.00	4.00	0.99	360	30
3	S100-3	100.02	31.58	4.00	0.99	360	30
4	S100-4	100.82	31.90	4.00	0.99	360	40
5	S100-5	100.38	31.88	4.00	0.99	360	40
6	S100-6	101.14	31.84	4.00	1.00	360	40
7	S100-7	100.00	31.68	4.00	1.00	360	50
8	S100-8	100.16	32.56	4.00	1.00	360	50
9	S100-9	99.28	32.36	4.00	1.00	360	50
10	S80-1	79.68	33.20	3.75	1.00	290	30
11	S80-2	80.00	31.90	3.75	1.00	289	30
12	S80-3	80.20	32.66	3.75	1.00	290	30
13	S80-4	79.58	32.00	3.75	1.00	290	40
14	S80-5	80.00	31.90	3.75	1.00	290	40

n : bearing length and the other symbols are defined in Figure 3.3.

337

Table A3. Specimens for EOF

No.	Specimen	hw (mm)	B (mm)	r (mm)	t (mm)	L (mm)	n (mm)
15	S80-6	81.98	31.58	3.75	0.98	290	40
16	S80-7	79.00	32.46	3.75	1.00	290	50
17	S80-8	79.50	33.00	3.75	1.00	290	50
18	S80-9	79.50	33.00	3.75	1.00	290	50
19	S60-1	59.80	32.26	3.50	0.99	235	30
20	S60-2	59.40	32.40	3.50	0.99	235	30
21	S60-3	59.68	32.00	3.50	1.00	235	30
22	S60-4	59.78	32.58	3.50	1.00	235	40
23	S60-5	59.70	32.00	3.50	1.00	235	40
24	S60-6	59.38	32.68	3.50	1.00	235	40
25	S60-7	60.00	31.60	3.50	1.00	235	50
26	S60-8	59.50	32.20	3.50	1.00	235	50

n : bearing length and the other symbols are defined in Figure 3.3.

Table A4. Specimens for ETF

No.	Specimen	hw (mm)	B (mm)	r (mm)	t (mm)	L (mm)	n (mm)
1	H4-1	71.36	30.48	2.00	1.11	199	30
2	H4-2	71.60	30.64	2.25	1.10	200	30
3	H4-3	72.08	30.76	2.00	1.11	200	30
4	H4-4	72.12	30.72	2.00	1.10	200	40
5	H4-5	72.38	30.80	2.00	1.11	200	40
6	H4-6	72.26	30.44	2.00	1.09	200	40
7	H4-7	72.04	30.78	2.25	1.09	200	50
8	H4-8	72.22	30.80	2.25	1.09	199	50
9	H4-9	71.28	30.80	2.25	1.09	200	50
10	H5-1	103.00	30.98	2.25	1.10	200	30
11	H5-2	101.88	30.90	2.25	1.10	200	30
12	H5-3	101.82	30.88	2.25	1.11	200	30
13	H5-4	101.56	30.72	2.25	1.11	200	40
14	H5-5	101.76	30.80	2.25	1.11	200	40

n : bearing length and the other symbols are defined in Figure 3.3.

Table A4. Specimens for ETF

No.	Specimen	hw (mm)	B (mm)	r (mm)	t (mm)	L (mm)	n (mm)
15	H5-6	101.82	30.90	2.25	1.10	200	40
16	H5-7	102.90	30.62	2.25	1.10	200	50
17	H5-8	102.50	30.90	2.25	1.10	200	50
18	H5-9	102.20	30.90	2.25	1.11	200	50

n : bearing length and the other symbols are defined in Figure 3.3.

Table A5. Specimens for ITF

No.	Specimen	hw (mm)	B (mm)	r (mm)	t (mm)	L (mm)	n (mm)
1	H6-1	71.42	30.52	2.00	1.11	299	30
2	H6-2	71.20	30.68	2.00	1.11	300	30
3	H6-3	70.58	30.86	2.00	1.12	300	30
4	H6-4	71.12	30.70	2.00	1.11	300	40
5	H6-5	71.22	30.68	2.00	1.11	300	40

n : bearing length and the other symbols are defined in Figure 3.3.

Table A5. Specimens for ITF

No.	Specimen	hw (mm)	B (mm)	r (mm)	t (mm)	L (mm)	n (mm)
6	H6-6	70.68	30.80	2.00	1.11	300	40
7	H6-7	71.10	30.72	2.00	1.12	300	50
8	H6-8	71.32	30.56	2.00	1.11	300	50
9	H6-9	71.18	30.60	2.00	1.11	300	50
10	H7-1	101.64	30.62	2.00	1.10	360	30
11	H7-2	101.92	30.64	2.00	1.11	360	30
12	H7-3	102.58	30.72	2.00	1.11	360	30
13	H7-4	101.50	30.66	2.00	1.12	360	40
14	H7-5	101.58	30.54	2.00	1.11	360	40
15	H7-6	101.46	30.64	2.00	1.10	360	40
16	H7-7	102.10	30.60	2.00	1.11	360	50
17	H7-8	102.02	30.50	2.00	1.10	360	50
18	H7-9	101.84	30.80	2.00	1.10	360	50

n : bearing length and the other symbols are defined in Figure 3.3.

APPENDIX B

DERIVATION OF FORMULAE FOR

THE SECOND MOMENT OF AREA AND THE POSITION OF

NEUTRAL AXIS

This appendix is divided into 3 parts, i.e. B-1, B-2 and B-3 where each of these parts will discuss the derivation of the formulae as expressed in equations (4.2.11), (5.2.18) and (5.2.20).

B-1 : The second moment of area of the effective cross section of the specimen about the neutral axis according to BS 5950 Part 5 1987, i.e. equation (4.2.11).
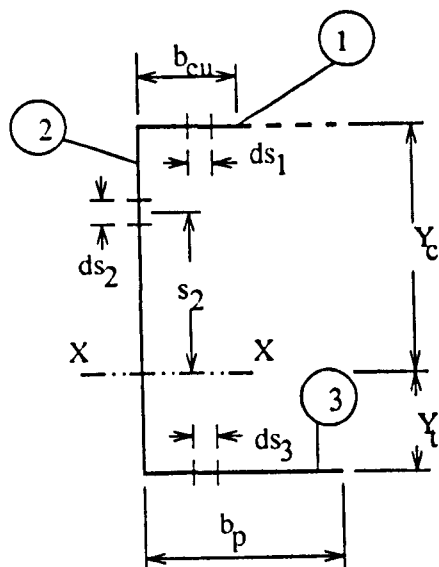
Figure B-1. Effective cross section according to

BS 5950 Part 5 1987.

The second moment of area of the above effective cross section about the neutral axis

X-X (I_x) can be derived from :

$$I_x = \sum_{i=1}^{i=3} I_{xi} \quad \ldots \ldots \ldots \ldots \ldots \quad (B-1.1)$$

Where :

I_{xi} is the second moment of elements 1, 2 and 3 about the neutral axis X-X. By

considering the strips ds_1, ds_2 and ds_3 the second moment of each element about X-X

can be derived as follows :

$$I_{x1} = t \int_{0}^{b_{eu}} y_c^2 \, ds_1 = t \, y_c^2 \, b_{eu} \quad \ldots \ldots \ldots \ldots \quad (B-1.2)$$

$$I_{x2} = t \int_{-y_t}^{+y_c} s_2^2 \, ds_2 = \frac{t}{3} (y_c^3 + y_t^3) \quad \ldots \ldots \ldots \ldots \quad (B-1.3)$$

$$I_{x3} = t \int_{0}^{b_p} y_t^2 \, ds_3 = t \, y_t^2 \, b_p \quad \ldots \ldots \ldots \ldots \ldots \quad (B-1.4)$$

Thus, the second moment of area of the effective cross section of the specimen about

the neutral axis X-X according to BS 5950 Part 5 1987 is

$$I_x = I_{x1} + I_{x2} + I_{x3} = t [b_{eu} y_c^2 + \frac{1}{3} (y_c^3 + y_t^3) + b_p y_t^2] \quad \ldots \quad (B-1.5)$$

t is the thickness of the specimen.

B-2 :   The position of neutral axis of the effective cross section of the specimen

according to European Recommendations 1987, i.e. equation (5.2.18).

The position of the neutral axis X-X in Figure B-2 is derived from the following

relationship.

$$y_t = \frac{\sum\limits_{i=1}^{n} A_i\, y_i}{\sum\limits_{i=1}^{n} A_i} \quad \ldots \ldots \ldots \ldots \ (B\text{-}2.1)$$
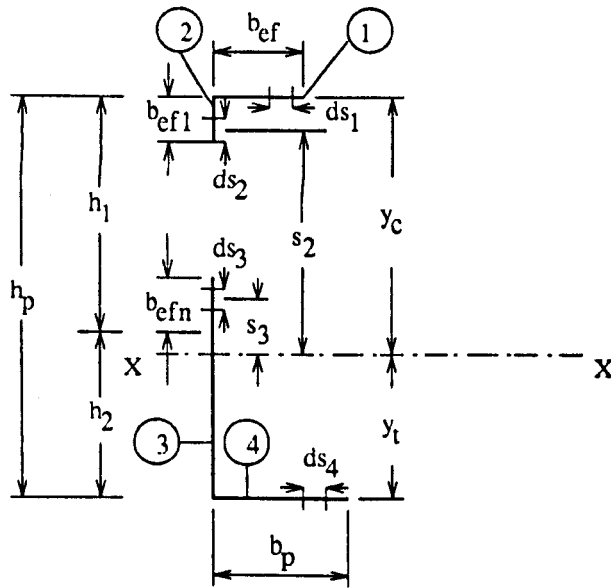
Figure B-2. Effective cross section according to

European Recommendations 1987.

In the formula (B-2.1), all static moments are taken about the bottom flange so that

y_t can be expressed as follows :

$$y_t = \frac{t\,[b_{ef}h_p + b_{ef1}(h_p - 0.5b_{ef1}) + b_{efn}(h_2 + 0.5b_{efn}) + 0.5h_2^2]}{t\,(b_{ef} + b_{ef1} + b_{efn} + h_2 + b_p)}$$

$$y_t = \frac{b_{ef}h_p + b_{ef1}h_p - 0.5b_{ef1}^2 + b_{efn}h_2 + 0.5b_{efn}^2 + 0.5h_2^2}{b_{ef} + b_{ef1} + b_{efn} + h_2 + b_p}$$

$$\ldots \ldots \ldots \ldots \ldots \ (B\text{-}2.2)$$

$$y_c = h_p - y_t \quad \ldots \ldots \ldots \ldots \ (B\text{-}2.3)$$

$$b_{ef1} = 0.4\,\rho\,h_1 \quad ; \quad b_{efn} = 0.6\,\rho\,h_1$$

Where :

ρ : Reduction coefficient accounting for local buckling.

344

B-3 : The second moment of area of the effective cross section of the specimen

according to European Recommendations 1987, i.e. equation (5.2.20).

On the basis of Figure B-2, the second moment of area about the neutral axis X-X

according to the European Recommendations 1987 is obtained from :

$$I_x = I_{x1} + I_{x2} + I_{x3} + I_{x4} \quad \ldots\ldots\ldots \quad (B\text{-}3.1)$$

The second moment of area of each element about the neutral axis X-X is

$$I_{x1} = t \int_0^{b_{ef}} y_c^2 \, ds_1 = t \cdot y_c^2 \, b_{ef} \quad \ldots\ldots\ldots \quad (B\text{-}3.2)$$

$$I_{x2} = t \int_0^{b_{ef1}} s_2^2 \, ds_2 = \frac{t}{3} \, b_{ef1}^3 \quad \ldots\ldots\ldots\ldots \quad (B\text{-}3.3)$$

$$I_{x3} = t \int_{-y_t}^{+(b_{efn}+h_2-y_t)} s_3^2 \, ds_3 = \frac{t}{3} [\, (b_{efn} + h_2 - y_t)^3 + y_t^3 \,] \quad \ldots \quad (B\text{-}3.4)$$

$$I_{x4} = t \int_0^{b_p} y_t^2 \, ds_4 = t \, y_t^2 \, b_p \quad \ldots\ldots\ldots\ldots \quad (B\text{-}3.5)$$

Hence, the second moment of area of the effective cross section of the specimen

about the neutral axis X-X according to the European Recommendations 1987 is as

follows :

$$I_x = t y_c^2 b_{ef} + \frac{t}{3} b_{ef1}^3 + \frac{t}{3} [\, (b_{efn} + h_2 - y_t)^3 + y_t^3 \,] + t y_t^2 b_p$$

or

$$I_x = t \, [y_c^2 \, b_{ef} + \frac{b_{ef1}^3 + (b_{efn} + h_2 - y_t)^3 + y_t^3}{3} + y_t^2 \, b_p]$$

$$\ldots\ldots\ldots\ldots\ldots\ldots\ldots\ldots\ldots\ldots \quad (B\text{-}3.6)$$

t is also the thickness of the specimen.

COMPUTER PROGRAMS FOR BS 5950 PART 5 1987

```
REM  **********************************************
REM  *          PROGRAMS FOR CALCULATING          *
REM  *         ULTIMATE WEB CRIPPLING LOADS OF     *
REM  * COLD-FORMED PLAIN CHANNEL STEEL SECTION BEAMS *
REM  *          USING BS 5950 PART 5 1987          *
REM  *          WRITTEN BY : HARKALI SETIYONO      *
REM  **********************************************
```

```
1  INPUT" SPECIMEN NUMBER :";No$
   INPUT" THE OVERALL WEB DEPTH (D in mm) =";D
   INPUT" THE INSIDE BEND RADIUS (r in mm) =";r
   INPUT" THE ACTUAL LENGTH OF BEARING (n in mm) =";n
   PRINT" THE ANGLE BETWEEN PLANES OF WEB AND BEARING
          SURFACE"
   INPUT" (Θ in degrees) =";A
   INPUT" THE FLANGE WIDTH (W in mm) =";W
   INPUT" THE DESIGN STRENGTH (py in MPa) =";py
   INPUT" THE EXPERIMENTAL ULTIMATE LOAD (Fe in N) =";Fe
   PRINT
   PRINT" D=";D;"mm";TAB(15);"t=";t;"mm";TAB(30);"r=";r;"mm";TAB(45);
   PRINT" W=";W;"mm"
   PRINT" n=";n;"mm";TAB(15);"Θ=";A;"degrees";TAB(30);
          "py=";py;"MPa";TAB(45);
   PRINT" Fe=";Fe;"N"
   PRINT
   PRINT" ARE THESE ABOVE DATA ALREADY CORRECT ?"
2  INPUT" TYPE YES OR NO !";TY$
   IF (TY$="YES" OR TY$="Y") THEN 3
   IF (TY$="NO" OR TY$="N") THEN 6
   IF (TY$ <> "YES" OR TY$ <> "Y" OR TY$ <> "NO" OR TY$ <> "N") THEN
   PRINT" INCORRECT INPUT, REPEAT AGAIN !"
   G0T0 2
3  LET K = py/228 : C1 = 1.22 - 0.22*K
   LET C2 = 1.06 - 0.06*r/t  :  C3 = 1.33 - 0.33*K
   LET C4 = 1.15 - 0.15*r/t  :  C5 = 1.49 - 0.53*K
   LET C6 = 0.88 - 0.12*t/1.9
   IF (D/t) < 150 THEN 4
   LET C7 = 1.2
4  LET C7 = 1 + (D/t)/750
   IF (D/t) < 66.5 THEN 5
   LET C8 = (1.1 - (D/t)/665)/K
```

```
5   LET C8 = 1/K
    LET C9 = 0.82 + 0.15*(t/1.9) :  C10 = (0.98 - (D/t)/865)/K
    LET C11 = 0.64 + 0.31*(t/1.9) :  C12 = 0.7 + 0.3*(A/90)^2
    GOTO 7
6   PRINT" INPUT THE CORRECT DATA AGAIN !"
    GOTO 1
7   PRINT" TYPE AND POSITION OF LOADING :"
    PRINT
    PRINT" 1. SINGLE LOAD OR REACTION NEAR OR AT FREE END"
    PRINT" 2. SINGLE LOAD OR REACTION FAR FROM FREE END"
    PRINT" 3. TWO OPPOSITE LOADS OR REACTIONS NEAR OR AT FREE
           END"
    PRINT" 4. TWO OPPOSITE LOADS OR REACTIONS FAR FROM FREE
           END"
    PRINT
    INPUT" SELECT THE TYPE AND POSITION OF LOADINGS !";TYPE
    ON ERROR GOTO 8
    ON TYPE GOTO 9,13,15,16
8   PRINT" INCORRECT INPUT, REPEAT AGAIN !"
    GOTO 7
9   INPUT" ENTER 1 FOR STIFFENED FLANGES OR 2 FOR UNSTIFFENED
           FLANGES!";F1
    ON ERROR GOTO 34
    ON F1 GOTO 10,11
34  PRINT" INCORRECT INPUT, REPEAT AGAIN!"
    GOTO 9
10  Fc = t^2*K*C3*C4*C12*(2060 - 3.8*(D/t))*(1 + 0.01*(n/t))
    GOTO 17
11  IF (n/t) > 60 THEN 12
    Fc = t^2*K*C3*C4*C12*(1350 - 1.73*(D/t))*(1 + 0.01*(n/t))
    GOTO 17
12  Fc = t^2*K*C3*C4*C12*(1350 - 1.73*(D/t))*(0.71 + 0.015*(n/t))
    GOTO 17
13  IF (n/t) > 60 THEN 14
    Fc = t^2*K*C1*C2*C12*(3350 - 4.6*(D/t))*(1 + 0.007*(n/t))
    GOTO 17
14  Fc = t^2*K*C1*C2*C12*(3350 - 4.6*(D/t))*(0.75 + 0.011*(n/t))
    GOTO 17
15  Fc = t^2*K*C3*C4*C12*(1520 - 3.57*(D/t))*(1 + 0.01*(n/t))
    GOTO 17
16  Fc = t^2*K*C1*C2*C12*(4800 - 14*(D/t))*(1 + 0.0013*(n/t))
17  Rt = Fe/Fc  :  B1 = n/t  :  B2 = D/t  :  B3 = r/t
32  PRINT" THE LOADING CONDITIONS :"
    PRINT"        1. WEB CRIPPLING ONLY "
    PRINT"        2. COMBINED ACTIONS OF WEB CRIPPLING AND
                  BENDING "
```

```
    INPUT" SELECT AND TYPE NO. 1 OR NO. 2 !";NUMBER
    ON ERROR GOTO 33
    ON NUMBER GOTO 18,22
33  PRINT" INCORRECT INPUT, REPEAT AGAIN !"
    GOTO 32
    PRINT" n/t =";B1;TAB(20);"D/t =";B2;TAB(38);"r/t =";B3
18  PRINT" WEB CRIPPLING RESISTANCE Pw (UNDER WEB CRIPPLING
            ONLY) :"
    PRINT"          (Pw)t = Fc =";Fc;" N (THEORY)"
    PRINT"          (Pw)e = Fe =";Fe;" N (EXPERIMENT)"
    PRINT"           Fe/Fc =";Rt
    PRINT" DO YOU WANT TO PRINT OUT THE RESULTS ?"
19  INPUT" TYPE YES OR NO !";TYP$
    IF (TYP$="YES" OR TYP$="Y") THEN 20
    IF (TYP$="NO" OR TYP$="N") THEN 27
    IF (TYP$ <> "YES" OR TYP$ <> "Y" OR TYP$ <> "NO" OR TYP$ <> "N")
        THEN
    PRINT" INCORRECT INPUT, REPEAT AGAIN !"
    GOTO 19
20  GOSUB RESULT
    LPRINT" n/t =";B1;TAB(20);"D/t =";B2;TAB(38);"r/t =";B3
    LPRINT" WEB CRIPPLING RESISTANCE Pw (UNDER WEB CRIPPLING
            ONLY) :"
    LPRINT"          (Pw)t = Fc =";Fc;" N (THEORY)"
    LPRINT"          (Pw)e = Fe =";Fe;" N (EXPERIMENT)"
    LPRINT"           Fe/Fc =";Rt
    GOTO 27
22  GOSUB MOMCAP
    INPUT" DISTANCE BETWEEN TWO SUPPORTS (SPAN LENGTH l in mm)
            =";l
    LET Z = (1.2/Fc) + (l-n)/(4*Mc) : FCB = 1.5/Z : Ma = FCB*(l-n)/4 : Mr =
            Ma/Mc
    LET Rs = Fe/FCB : Rst = FCB/Fc : Me = Fe*(l-n)/4 : Mre = Me/Mc
    PRINT" MOMENT CAPACITY Mc =";Mc;" Nmm"
    PRINT" THE SECOND MOMENT OF EFFECTIVE CROSS SECTION ABOUT
            THE NEUTRAL AXIS Ix =";Ix;" mm^4"
    PRINT" ELASTIC SECTION MODULUS IN COMPRESSION REGION Zc
            =";Zc;" mm^3"
    PRINT" ELASTIC SECTION MODULUS IN TENSION REGION Zt =";Zt;"
            mm^3"
    PRINT" APPLIED BENDING MOMENT :"
    PRINT"                    Mt =";Ma;" Nmm (THEORY)"
    PRINT"                    Me =";Me;" Nmm (EXPERIMENT)"
    PRINT" RATIO OF APPLIED BENDING MOMENT TO MOMENT CAPACITY
            :"
    PRINT"                    Mt/Mc =";Mr;" (THEORY)"
```

PRINT"   Me/Mc =";Mre;"(EXPERIMENT)"
PRINT" WEB CRIPPLING STRENGTH IN THE ABSENCE OF BENDING
        MOMENT Pw =";Fc;" N"
PRINT" RATIO OF APPLIED CONCENTRATED LOAD TO WEB CRIPPLING
        STRENGTH :"
PRINT"   FCB/Pw =";Rst;" (THEORY)"
PRINT"   Fe/Pw =";Rt;" (EXPERIMENT)"
PRINT" n/t =";B1;TAB(20);"D/t =";B2;TAB(38);"r/t =";B3
PRINT" THE ULTIMATE LOAD (UNDER COMBINED WEB CRIPPLING
        AND BENDING):"
PRINT"   FCB =";FCB;" N (THEORY)"
PRINT"   Fe =";Fe;" N (EXPERIMENT)"
PRINT" RATIO OF EXPERIMENTAL AND THEORETICAL ULTIMATE
        LOAD Fe/FCB =";Rs
PRINT" DO YOU WANT TO PRINT OUT THE RESULTS ?"
25 INPUT" TYPE YES OR NO !";TYPE$
IF (TYPE$="YES" OR TYPE$="Y") THEN 26
IF (TYPE$="NO" OR TYPE$="N") THEN 27
IF (TYPE$ <> "YES" OR TYPE$ <> "Y" OR TYPE$ <> "NO" OR TYPE$ <>
    "N") THEN
PRINT" INCORRECT INPUT, REPEAT AGAIN !"
GOTO 25
26 GOSUB RESULT
LPRINT" MOMENT CAPACITY OF THE SECTION Mc =";Mc;" mm"
LPRINT" THE SECOND MOMENT OF EFFECTIVE CROSS SECTION
        ABOUT THE NEUTRAL AXIS Ix =";Ix;" mm^4"
LPRINT" ELASTIC SECTION MODULUS IN COMPRESSION REGION Zc
        =";Zc;" mm^3"
LPRINT" ELASTIC SECTION MODULUS IN TENSION REGION Zt =";Zt;"
        mm^3"
LPRINT" SPAN LENGTH l =";l;" mm"
LPRINT" APPLIED BENDING MOMENT :"
LPRINT"   Mt =";Ma;" Nmm (THEORY)"
LPRINT"   Me =";Me;" Nmm (EXPERIMENT)"
LPRINT" RATIO OF APPLIED BENDING MOMENT TO MOMENT
        CAPACITY :"
LPRINT"   Mt/Mc =";Mr;" (THEORY)"
LPRINT"   Me/Mc =";Mre;"(EXPERIMENT)"
LPRINT" WEB CRIPPLING STRENGTH IN THE ABSENCE OF BENDING
        MOMENT Pw =";Fc;" N"
LPRINT" RATIO OF APPLIED CONCENTRATED LOAD TO WEB
        CRIPPLING STRENGTH :"
LPRINT"   FCB/Pw =";Rst;" (THEORY)"
LPRINT"   Fe/Pw =";Rt;"   (EXPERIMENT)"
LPRINT" n/t =";B1;TAB(20);"D/t =";B2;TAB(38);"r/t =";B3
LPRINT" THE ULTIMATE LOAD (UNDER COMBINED WEB CRIPPLING

```
          LPRINT"                    FCB =";FCB;" N (THEORY)"
          LPRINT"                    Fe  =";Fe;"  N (EXPERIMENT)"
          LPRINT" RATIO OF EXPERIMENTAL AND THEORETICAL ULTIMATE
                  LOAD Fe/FCB =";Rs
      27 END


   RESULT :

      REM ***********************************************
      REM * SUBROUTINE FOR THE PRINT OUT OF THE INPUT DATA *
      REM ***********************************************


      LPRINT"RESULTS OF CALCULATING ULTIMATE WEB CRIPPLING LOADS"
      LPRINT" ON COLD-FORMED PLAIN CHANNEL STEEL SECTION BEAMS "
      LPRINT"                      BY USING : "
      LPRINT"                 BS 5950 PART 5 1987 "
      LPRINT" ————————————————————————————————————————
      LPRINT"              SPECIMEN NUMBER :";No$
      LPRINT
      LPRINT" THE OVERALL WEB DEPTH D =";D;" mm"
      LPRINT" THE FLANGE WIDTH W =";W;" mm"
      LPRINT" THE WEB THICKNESS t =";t;" mm"
      LPRINT" THE INSIDE BEND RADIUS r =";r;" mm"
      LPRINT" THE ACTUAL LENGTH OF BEARING n =";n;" mm"
      LPRINT" THE ANGLE BETWEEN PLANE OF WEB AND PLANE OF
              BEARING SURFACE Θ =";A;"degrees"
      LPRINT" THE DESIGN STRENGTH py =";py;" MPa"
      RETURN


   MOMCAP :

      REM ***********************************************
      REM * SUBROUTINE FOR CALCULATING THE MOMENT CAPACITY *
      REM ***********************************************


        LET hp = D + t  :  bp = W - 0.5*t
        LET Fr = (py/280)^0.5  :  po = (1.13 - 0.0019*(D/t)*Fr)*py
        LET h = bp/hp
        LET K1 = 1.28 - ((0.8*h)/(2+h)) - 0.0025*h^2
        LET pcr = 185000*K1*(t/bp)^2  :  U = po/pcr
        IF U >= 0.123 THEN 23
        LET beff = bp
        GOTO 24
     23 LET beff = bp*(1 + 14*(U^0.5 - 0.35)^4)^-0.2
```

STRENGTH :

$$FCB/Pw = 0.9183757 \text{ (THEORY)}$$
$$Fe/Pw = 0.8794652 \text{ (EXPERIMENT)}$$

n/t = 45.45454   D/t = 81.77272   r/t = 2.045455

THE ULTIMATE LOAD (*UNDER COMBINED WEB CRIPPLING AND BENDING*) :

$$FCB = 5033.253 \text{ N (THEORY)}$$
$$Fe = 4824.050 \text{ N (EXPERIMENT)}$$

RATIO OF EXPERIMENTAL AND THEORETICAL ULTIMATE LOAD Fe/FCB = 0.9584358

COMPUTER PROGRAMS FOR EUROPEAN RECOMMENDATIONS 1987

```
REM ***************************************************
REM *            PROGRAMS  FOR  CALCULATING              *
REM *          ULTIMATE  WEB  CRIPPLING  LOADS  OF        *
REM * COLD-FORMED  PLAIN  CHANNEL  STEEL  SECTION  BEAMS  *
REM *                    BY  USING                        *
REM *   EUROPEAN  RECOMMENDATIONS  FOR  THE  DESIGN  OF   *
REM *        LIGHT  GAUGE  STEEL  MEMBERS  -  1987         *
REM *           WRITTEN  BY :  HARKALI  SETIYONO          *
REM ***************************************************
```

```
1    INPUT" SPECIMEN NUMBER :";No$
     INPUT" BEARING LENGTH (la in mm) =";la
     INPUT" WEB THICKNESS (t in mm) =";t
     INPUT" WEB INCLINATION (Θ in degrees) =";X
     INPUT" DESIGN YIELD STRESS (fty in MPa) =";Y
     INPUT" INNER RADIUS (r in mm) =";r
     INPUT" MODULUS OF ELASTICITY (E in MPa) =";E
     INPUT" DISTANCE BETWEEN THE POINTS OF INTERSECTION OF THE
              SYSTEM LINES OF THE WEB AND FLANGES (hw in mm) =";hw
     INPUT" THE FLANGE WIDTH (b in mm) =";b
     INPUT" EXPERIMENTAL ULTIMATE LOAD Fe =";Fe
     PRINT
     PRINT" r=";r;"mm";TAB(15);"la=";la;"mm";TAB(30);"t=";t;"mm";TAB(45);"b="
              ;b;"mm"
     PRINT" Θ=";X;"degrees";TAB(15);"fty=";Y;"MPa";TAB(30);"E=";E;"MPa";
              TAB(45);"hw=";hw;"mm"
     PRINT
     PRINT" ARE THE ABOVE DATA ALREADY CORRECT ?"
2    INPUT" TYPE YES OR NO !";TY$
     IF (TY$="YES" OR TY$="Y") THEN 3
     IF (TY$="NO" OR TY$="N") THEN 00
     IF (TY$ <> "YES" OR TY$ <> "Y" OR TY$ <> "NO" OR TY$ <> "N") THEN
     PRINT" INCORRECT INPUT, REPEAT AGAIN !"
     GOTO 2
00   PRINT" INPUT THE CORRECT DATA AGAIN !"
     GOTO 1
3    IF hw/t > 200 THEN GOTO 4
```

```
32  PRINT" SELECT ONE OF THE FOLLOWING CATAGORIES OF
            CONCENTRATED LOADS AND END REACTIONS !"
    PRINT" 1. FIRST CATAGORY AND 2. SECOND CATAGORY"
    INPUT" WHAT CATAGORY ?";CAT
    ON ERROR GOTO 31
    ON CAT GOTO 5,6
31  PRINT" INCORRECT INPUT, REPEAT AGAIN !"
    GOTO 32
5   LET RD = 0.057*t^2*(Y*E)^0.5*(1-0.1*(r/t)^0.5)*(0.5+(0.02*la/t)^0.5)*
            (2.4+(X/90)^2)
    LET Rt = Fe/RD  :  B1 = la/t  :  B2 = hw/t  :  B3 = r/t
    GOTO 7
6   LET RD = 0.114*t^2*(Y*E)^0.5*(1-0.1*(r/t)^0.5)*(0.5+(0.02*la/t)^0.5)*
            (2.4+(X/90)^2)
    LET Rt = Fe/RD  :. B1 = la/t  :  B2 = hw/t  :  B3 = r/t
7   PRINT" THE LOADING CONDITION :"
    PRINT
    PRINT" 1. WEB CRIPPLING ONLY OR 2. COMBINED WEB CRIPPLING
            AND BENDING"
    PRINT
    INPUT" TYPE THE NUMBER OF SELECTED LOADING CONDITION !";SEL
    ON ERROR GOTO 33
    ON SEL GOTO 8,11
33  PRINT" INCORRECT INPUT, REPEAT AGAIN !"
    GOTO 7
8   PRINT" THE DESIGN LOAD WITH RESPECT TO WEB CRIPPLING ONLY
            RD =";RD;"N"
    PRINT" EXPERIMENTAL ULTIMATE LOAD Fe =";Fe;" N"
    PRINT"           Fe/RD =";Rt
    PRINT
    PRINT" DO YOU WANT TO PRINT OUT THE RESULTS ?"
9   INPUT" TYPE YES OR NO !";TYP$
    IF (TYP$="YES" OR TYP$="Y") THEN 10
    IF (TYP$="NO" OR TYP$="N") THEN 30
    IF (TYP$ <> "YES" OR TYP$ <> "Y" OR TYP$ <> "NO" OR TYP$ <> "N")
        THEN
    PRINT" INCORRECT INPUT, REPEAT AGAIN !"
    GOTO 9
10  GOSUB RESULT
    LPRINT" la/t =";B1;TAB(20);"hw/t =";B2;TAB(38);"r/t=";B3
    LPRINT" THE DESIGN LOAD WITH RESPECT TO WEB CRIPPLING ONLY
            RD =";RD;"N"
    LPRINT" EXPERIMENTAL ULTIMATE LOAD Fe =";Fe;" N"
    LPRINT"              Fe/RD =";Rt
    GOTO 30
11  GOSUB DESMOM
```

```
        IF Md <= 0 THEN 28
        LET Z = (l-la)/(4*Md) + (1/RD)  :  FCB = 1.25/Z  :  Ma = FCB*(l-la)/4
        LET Mr = Ma/Md  :  Me = Fe*(l-n)/4  :  Mre = Me/Md
        LET Rs = Fe/FCB  :  Rst = FCB/RD
        PRINT" RATIO OF EXPERIMENTAL AND THEORETICAL LOADS Fe/FCB
                 =";Rs
        PRINT" DESIGN STRENGTH WITH RESPECT TO BENDING MOMENT Md
                 =";Md;"Nmm"
        PRINT" SECOND MOMENT OF EFFECTIVE CROSS SECTION ABOUT THE
                 NEUTRAL AXIS Ix =";Ix;" mm^4"
        PRINT" SECTION MODULUS IN COMPRESSION REGION (Wef)c =";Wefc;
                 "mm^3"
        PRINT" SECTION MODULUS IN TENSION REGION (Wef)t =";Weft;"mm^3"
        PRINT" APPLIED BENDING MOMENT :"
        PRINT"                         Mt =";Ma;" Nmm (THEORY)"
        PRINT"                         Me =";Me;" Nmm (EXPERIMENT)"
        PRINT" RATIO OF APPLIED BENDING MOMENT TO MOMENT
                 CAPACITY :"
        PRINT"                         Mt/Md =";Mr;" (THEORY)"
        PRINT"                         Me/Md =";Mre;"(EXPERIMENT)"
        PRINT" THE DESIGN LOAD WITH RESPECT TO WEB CRIPPLING ONLY
                 RD =";RD;"N"
        PRINT" THE ULTIMATE LOAD (UNDER COMBINED ACTIONS OF WEB
                 CRIPPLING AND BENDING) FCB =";FCB;" N"
        PRINT" Fe/FCB =";Rs  :  PRINT" FCB/RD =";Rst  :  PRINT" Fe/RD =";Rt
        PRINT
        PRINT" DO YOU WANT TO PRINT OUT THE RESULTS ?"
  34    INPUT" TYPE YES OR NO !";TYPE$
        IF (TYPE$="YES" OR TYPE$="Y") THEN 29
        IF (TYPE$="NO" OR TYPE$="N") THEN 30
        IF (TYPE$ <> "YES" OR TYPE$ <> "Y" OR TYPE$ <> "NO" OR TYPE$ <>
           "N") THEN
        PRINT" INCORRECT INPUT, REPEAT AGAIN !"
        GOTO 34
  29    GOSUB RESULT
        LPRINT" THE SPAN LENGTH l =";l;" mm"
        LPRINT" DESIGN STRENGTH WITH RESPECT TO BENDING MOMENT
                 Md =";Md;"Nmm"
        LPRINT" SECOND MOMENT OF EFFECTIVE CROSS SECTION ABOUT
                 THE NEUTRAL AXIS Ix =";Ix;" mm^4"
        LPRINT" SECTION MODULUS IN COMPRESSION REGION (Wef)c =";Wefc;
                 " mm^3"
        LPRINT" SECTION MODULUS IN TENSION REGION (Wef)t =";Weft;"
                 mm^3"
        LPRINT" APPLIED BENDING MOMENT :"
        LPRINT"                         Mt =";Ma;" Nmm (THEORY)"
```

355

```
      LPRINT"                      Me =";Me;" Nmm (EXPERIMENT)"
      LPRINT"                      Mt/Md =";Mr;"  (THEORY)"
      LPRINT"                      Me/Md =";Mre;" (EXPERIMENT)"
      LPRINT" la/t =";B1;TAB(20);"hw/t =";B2;TAB(38);"r/t =";B3
      LPRINT" THE DESIGN LOAD WITH RESPECT TO WEB CRIPPLING ONLY
              RD =";RD;" N"
      LPRINT" THE ULTIMATE LOAD (UNDER COMBINED ACTIONS OF WEB
              CRIPPLING AND BENDING) :"
      LPRINT"                      FCB =";FCB;" N (THEORY)"
      LPRINT"                      Fe =";Fe;" N (EXPERIMENT)"
      LPRINT"                      Fe/FCB =";Rs
      LPRINT"                      FCB/RD =";Rst;"(THEORY)"
      LPRINT"                      Fe/RD =";Rt;" (EXPERIMENT)"
      GOTO 30
4   PRINT" THE CALCULATION CAN NOT BE DONE, BECAUSE IT IS ONLY
              VALID FOR hw/t <= 200"
    PRINT" CHANGE THE VALUE OF EITHER t OR hw OR BOTH SO THAT
              THE RATIO OF hw/t <= 200 AND REPEAT FROM THE
              BEGINNING !"
    INPUT" ENTER 1 TO CONTINUE THE WORK OR ENTER 2 TO FINISH IT
              !";ENTER
    ON ERROR GOTO 35
    ON ENTER GOTO 1,30
35  PRINT" INCORRECT INPUT, REPEAT AGAIN !"
    GOTO 4
28  PRINT" YIELDING FIRST OCCURS AT THE TENSION EDGE OF THE
              WEB."
30  END


  DESMOM :

    REM ***********************************************
    REM * SUBROUTINE FOR CALCULATING THE DESIGN STRENGTH *
    REM *        WITH RESPECT TO BENDING MOMENT (Md)      *
    REM ***********************************************


    LET bp = b - 0.5*t  :  h = hw + t
    INPUT" THE SPAN LENGTH (l in mm) =";l
    IF (l/b) >= 20 THEN 12
    PRINT" l/b < 20 "  :  INPUT" REDUCTION COEFFICIENT ψs =";Ys
    LET F1 = (4*0.85*Ys*Y)/E   :   pl = (0.75*bp*F1^0.5)/t
    IF pl <= 0.673 THEN 13
    LET Rol = (1 - (0.22/pl))/pl
    GOTO 14
13  LET Rol = 1
```

REM * THE EFFECTIVE WIDTH OF THE TOP FLANGE bt1 *
14   LET bt1 = 0.85*Ys*Ro1*bp
     GOTO 15
12   LET F2 = (4*Y)/E : p2 = (0.75*bp*F2^0.5)/t
     IF p2 <= 0.673 THEN 17
     LET Ro2 = (1 - (0.22/p2))/p2
     GOTO 16
17   Ro2 = 1
     REM * THE EFFECTIVE WIDTH OF THE TOP FLANGE bt2 *
16   LET bt2 = Ro2 * bp
15   IF (l/b) >= 20 THEN 21
     LET h21 = (bt1*h + 0.5*h^2)/(bt1 + h + bp) : h11 = h - h21
     LET y1 = -h21/h11
     IF y1 <= -0.5 THEN 18
     IF (y1 > -0.5 OR y1 < 0) THEN kt1 = ((1-y1)/(0.362-0.103*y1))^2
     GOTO 19
18   kt1 = 5.85*(1-y1)^2
19   LET F3 = Y/(E*kt1) : p3 = (1.052*bp*F3^0.5)/t
     IF p3 <= 0.673 THEN 20
     Row1 = (1 - (0.22/p3))/p3
     GOTO 26
20   Row1 = 1
     GOTO 26
21   LET h22 = (bt2*h + 0.5*h^2)/(bt2 + h + bp) : h12 = h - h22
     LET y2 = -h22/h12
     IF y2 <= -0.5 THEN 22
     IF (y2 > -0.5 OR y2 < 0) THEN kt2 = ((1-y2)/(0.362-0.103*y2))^2
     GOTO 23
22   LET kt2 = 5.85*(1-y2)^2
23   LET F4 = Y/(E*kt2) : p4 = (1.052*bp*F4^0.5)/t
     IF p4 <= 0.673 THEN 24
     Row2 = (1 - (0.22/p4))/p4
     GOTO 25
24   Row2 = 1

     REM ***
     REM *   CALCULATION OF THE SECOND MOMENT OF   *
     REM * EFFECTIVE CROSS SECTION ABOUT THE NEUTRAL *
     REM *   AXIS (Ix)   *
     REM ***

25   LET A12 = 1.0625 + 0.1025*Row2^2 - 1.075*Row2
     LET A22 = bt2 + bp + 0.8*Row2*h + 0.2*Row2^2*h
     LET A32 = bt2*h + 0.4*Row2*h^2 + 0.1*Row2^2*h^2
     LET Y2t = (- A22 + (A22^2 + 4*A12*A32)^0.5)/(2*A12) : Y2c = h - Y2t
     REM * EFFECTIVE WIDTH OF THE COMPRESSED PORTION OF WEB *

357

```
REM *              (befl AND befn) WHEN l/b >= 10              *
LET befl = 0.4*Row2*Y2c  :  befn = 0.6*Row2*Y2c
LET I2 = t*(Y2c^2*bt2 + 0.33*(befl^3 + befn^3 + Y2t^3) + Y2t^2*bp)
LET Wefc2 = I2/Y2c  :  LET Weft2 = I2/Y2t
IF Wefc2 > Weft2 THEN RETURN
LET Wefc = Wefc2  :  Weft = Weft2  :  Ix = I2
LET Md = Y * Wefc
RETURN
26 LET A11 = 1.0625 + 0.1025*Row1^2 - 1.075*Row1
LET A21 = bt1 + bp + 0.8*Row1*h + 0.2*Row1^2*h
LET A31 = bt1*h + 0.4*Row1*h^2 + 0.1*Row1^2*h^2
LET Y1t = (- A21 + (A21^2 + 4*A11*A31)^0.5)/(2*A11)  :  Y1c = h - Y1t
REM * EFFECTIVE WIDTH OF THE COMPRESSED PORTION OF WEB *
REM *              (befl AND befn) WHEN l/b < 10              *
LET befl = 0.4*Row1*Y1c  :  befn = 0.6*Row1*Y1c
LET I1 = t*(Y1c^2*bt1 + 0.33*(befl^3 + befn^3 + Y1t^3) + Y1t^2*bp)
LET Wefc1 = I1/Y1c  :  Weft1 = I1/Y1t
IF Wefc1 > Weft1 THEN RETURN
LET Wefc = Wefc1  :  Weft = Weft1  :  Ix = I1
LET Md = Y * Wefc
RETURN

RESULT :

REM ************************************************************
REM * SUBROUTINE FOR THE PRINT OUT OF THE INPUT DATA *
REM ************************************************************


LPRINT"RESULTS OF CALCULATING ULTIMATE WEB CRIPPLING LOADS"
LPRINT" ON COLD-FORMED PLAIN CHANNEL STEEL SECTION BEAMS"
LPRINT"                    BY USING :"
LPRINT"EUROPEAN RECOMMENDATIONS FOR THE DESIGN OF LIGHT"
LPRINT"          GAUGE STEEL MEMBER - 1987"
LPRINT" ─────────────────────────────────────────────
LPRINT"              SPECIMEN NUMBER :";No$
LPRINT
LPRINT" INNER RADIUS r =";r;" mm"
LPRINT" BEARING LENGTH la =";la;" mm"
LPRINT" WEB THICKNESS t =";t;" mm"
LPRINT" WEB INCLINATION Θ =";X;" degrees"
LPRINT" DESIGN YIELD STRESS Y =";Y;" MPa"
LPRINT" MODULUS OF ELASTICITY E =";E;" MPa"
LPRINT" DISTANCE BETWEEN POINTS OF INTERSECTION OF SYSTEM
          LINES OF"
LPRINT" THE WEB AND THE FLANGES hw =";hw;" mm"
LPRINT" FLANGE WIDTH b =";b;" mm"
```

358

```
RETURN
END IF
END IF
END IF
```

Results of using these programs can be seen in the following print out.

RESULTS OF CALCULATING ULTIMATE WEB CRIPPLING LOADS ON COLD-FORMED PLAIN CHANNEL STEEL SECTION BEAMS BY USING : EUROPEAN RECOMMENDATIONS FOR THE DESIGN OF LIGHT GAUGE STEEL MEMBERS - 1987

SPECIMEN NUMBER : H90-26

INNER RADIUS r = 2.25 mm
BEARING LENGTH la = 50 mm
WEB THICKNESS t = 1.10 mm
WEB INCLINATION Θ = 90 degrees
DESIGN YIELD STRESS Y = 303 MPa
MODULUS OF ELASTICITY E = 196850 MPa
DISTANCE BETWEEN POINTS OF INTERSECTION OF SYSTEM LINES OF THE WEB AND THE FLANGES hw = 89.95 mm
THE SPAN LENGTH l = 451 mm
DESIGN STRENGTH WITH RESPECT TO BENDING MOMENT Md = 801340.40 Nmm
SECOND MOMENT OF EFFECTIVE CROSS SECTION ABOUT THE NEUTRAL AXIS Ix = 144231.50 mm^4
SECTION MODULUS IN COMPRESSION REGION (Wef)c = 2644.688 mm^3
SECTION MODULUS IN TENSION REGION (Wef)t = 3950.065 mm^3
APPLIED BENDING MOMENT :
                    Mt = 361388.90 Nmm (THEORY)
                    Me = 543911.60 Nmm (EXPERIMENT)
                    Mt/Md = 0.4509805 (THEORY)
                    Me/Md = 0.6787522 (EXPERIMENT)
la/t = 45.45454   hw/t = 81.77272   r/t = 2.045455
THE DESIGN LOAD WITH RESPECT TO WEB CRIPPLING ONLY RD = 4511.625 N
THE ULTIMATE LOAD (UNDER COMBINED ACTIONS OF WEB CRIPPLING AND BENDING) :
                    FCB = 3604.877 N (THEORY)
                    Fe = 4824.05 N (EXPERIMENT)
                    Fe/FCB = 1.338201
                    FCB/RD = 0.7990195 (THEORY)
                    Fe/RD = 1.069249 (EXPERIMENT)

359

COMPUTER PROGRAMS FOR PLASTIC MECHANISM APPROACH

```
REM *********************************************************
REM*               PROGRAMS  FOR  ESTIMATING                *
REM*             ULTIMATE WEB CRIPPLING LOADS               *
REM* OF COLD-FORMED PLAIN CHANNEL STEEL SECTION BEAMS*
REM*                         UNDER                          *
REM*  COMBINED ACTIONS OF WEB CRIPPLING AND BENDING  *
REM*            USING PLASTIC MECHANISM APPROACH            *
REM*             WRITTEN BY : HARKALI SETIYONO              *
REM* *******************************************************
```

1 INPUT" SPECIMEN NUMBER :";No$
   INPUT" THE OVERALL WEB DEPTH (hw in mm) :";hw
   INPUT" THE WEB THICKNESS (t in mm) :";t
   INPUT" THE INSIDE BEND RADIUS (r in mm) :";r
   INPUT" THE ACTUAL LENGTH OF BEARING (n in mm) :";n
   INPUT" THE FLANGE WIDTH (B in mm) :";F
   INPUT" THE SPAN LENGTH OF THE BEAM (l in mm) :";l
   INPUT" THE YIELD STRENGTH (Y in MPa) :";Y
   INPUT" MODULUS OF ELASTICITY (E in MPa) :";E
   INPUT" EXPERIMENTAL ULTIMATE LOADS (Fe in N) :";Pe
   INPUT" EXPERIMENTAL LATERAL DEFLECTION OF WEB (Δ_e in mm)
        =";de
   INPUT" EXPERIMENTAL WEB CRIPPLING DEFORMATION (Δh_e in mm)
        =";he
   INPUT" EXPERIMENTAL YIELD ARC DEPTH (b_e in mm) =";be
   PRINT" hw =";hw;" mm" : PRINT" t =";t;" mm" : PRINT" r =";r;" mm"
   PRINT" n =";n;" mm"   : PRINT" B =";F;" mm": PRINT" l =";l;" mm"
   PRINT" Y =";Y;" MPa"   : PRINT" E =";E;" MPa": PRINT" Fe =";Pe;" N"
   PRINT" Δe =";de;" mm" : PRINT" Δhe =";he;" mm" : PRINT" be =";be;" mm"
2 PRINT" ARE ALL THESE ABOVE INPUT DATA ALREADY CORRECT ?"
   INPUT" TYPE YES OR NO !";TY$
   IF (TY$ = "YES" OR TY$ = "Y") THEN 5
   IF (TY$ = "NO" OR TY$ = "N") THEN 3
   IF (TY$<>"YES" OR TY$<>"Y" OR TY$<>"NO" OR TY$<>"N") THEN 4
3 PRINT" INPUT THE CORRECT DATA AGAIN !"
   GOTO 1
4 PRINT" INCORRECT INPUT, REPEAT AGAIN !"
   GOTO 2

```
REM **********************************************************
REM *    CALCULATION OF THE EFFECTIVE WIDTH OF THE TOP     *
REM *                     FLANGE (beff)                     *
REM **********************************************************
5  LET Smax = Y  :  Scr = 0.38*E*(t^2/(F-0.5*t)^2)  :  U = Smax/Scr
   IF U >= 0.59 THEN 6
   LET beff = F - 0.5*t
   GOTO 7
6  LET Rs = ((F - 0.5*t)/t)*(Y/(0.38*E))^0.5
   LET beff = (F - 0.5*t)/(1 + 14*(Rs - 0.35)^4)^0.2
   REM **********************************************************
   REM * CALCULATION OF THE SECOND MOMENT OF EFFECTIVE *
   REM *     CROSS-SECTION ABOUT THE NEUTRAL AXIS (Ix)      *
   REM **********************************************************
7  INPUT" NUMBER OF ITERATION N =";J
   LET Yt = ((hw+t)*(beff+0.5*hw+0.5*t))/(beff+hw+F+0.5*t)
   LET Yc = ((hw+t)*(F+0.5*hw))/(beff+hw+F+0.5*t)
   LET Ix = t*(beff*Yc^2 + (Yc^3+Yt^3)/3 + (F-0.5*t)*Yt^2)
   REM *****************************************************
   REM * CALCULATION OF THE ULTIMATE WEB CRIPPLING *
   REM *                     LOAD FCB                      *
   REM *****************************************************
   DIM h(J) : DIM d(J) : DIM X(J) : DIM e1(J)
   LET a1 = r + 0.5*t  : a2 = 0.25 * (hw+t)        ' NOTE 1
   FOR b = a1 TO a2 STEP 2.5
   FOR I = 1 TO J
   IF I = 1 THEN 8
   K = I - 1
   e1(I) = e1(K) + 0.055                        ' NOTE 2
   LET C1 = ((hw+t)^2 + e1(I)^2)^0.5  :  C2 = 1 - n
   LET C3 = n*e1(I)*(hw+t)   :   C4 = hw + t - b
   LET C5 = (hw+t)*(b^2+e1(I)^2)^0.5  :  C6 = b*((hw+t)^2 + e1(I)^2)^0.5
   LET C7 = 1^3*e1(I)*((hw+t)^2+e1(I)^2)^0.5
   Ps = n*t*Y
   d(I) = d(K) + 0.015
   X(I) = ABS(b^2 - d(I)^2)
   h(I) = b - X(I)^0.5
   B1 = Y*t^2*(2*C1*C3*d(I)+2*C1*e1(I)*(e1(I)*C4+C5+C6)*d(I))
   B2 = Y*t^2*(2*C1*C4*b^2*h(I)+2*C1*C4^2*b*d(I))     ' NOTE 3
   B3 = Y*t^2*b*C4*(F-0.5*t)*(4*C1-h(I))*h(I)
   B4 = C4*(4*b*e1(I)*C1*h(I)+b*C2*h(I)^2+4*C1*(r+0.5*t)*d(I))
   P = (B1 + B2 + B3)/B4                        ' NOTE 4
   Pp = (Ps^2/(2*P))*(-1 + (1 + (4*P^2)/Ps^2)^0.5)
   B5 = 12*E*Ix*C2*h(I)^2
   Pel = B5/C7
   A = Pel/Pp  :  A1 = Pp - Pel
```

```
        IF A >= 0.9995 THEN 9
        GOTO 10
8    h(I) = 0  :  d(I) = 0  :  e1(I) = 0
     C1 = hw + t  :  C3 = 0  :  C4 = hw + t - b  :  C5 = b*(hw+t)  :  C6 = C5
     M1 = Y*t^2*(2*C1*C3+2*C1*e1(I)*(e1(I)*C4+C5+C6)+2*C1*C4^2*b)
     M2 = 4*C1*(r + 0.5*t)
     Pp1 = M1/M2
     Pel1 = 0
10   NEXT I
     IF I > J THEN 14
9    Pu = Pp  :  ht = h(I)  :  dt = d(I)  :  e1 = e1(I)
     LET G1 = Pe/Pu  :  G2 = n/t  :  G3 = hw/t  :  G4 = r/t  :  G5 = de/dt
     LET G6 = he/ht  :  G7 = be/b  :  G8 = ht/dt
     PRINT" FOR b =";b;" :"
     PRINT"Pu =";Pu;" N";"e =";e1;" mm";"Δh =";ht;" mm";"Δ =";dt;" mm"
     PRINT"Pe/Pu =";G1;"Pel =";Pel;" N";"Pu/Pel =";A;"Pu-Pel =";A1;" N"
     PRINT"I =";I
     IF (G1 >= 0.80 AND e1 >= n) THEN 11
     NEXT b
     GOTO 17
11   PRINT" DO YOU WANT TO PRINT OUT THE RESULTS ?"
12   INPUT" ENTER YES OR NO !";ENTER$
     IF (ENTER$="YES" OR ENTER$="Y") THEN 13
     IF (ENTER$="NO" OR ENTER$="N" ) THEN 18
     IF (ENTER$<>"YES" OR ENTER$<>"Y" OR ENTER$<>"NO" OR
        ENTER$<>"N") THEN
     PRINT" INCORRECT INPUT, REPEAT AGAIN !"
     GOTO 12
13   LPRINT"      RESULTS OF USING PLASTIC MECHANISM APPROACH"
     LPRINT"     FOR ESTIMATING ULTIMATE WEB CRIPPLING LOADS"
     LPRINT" OF COLD-FORMED PLAIN CHANNEL STEEL SECTION BEAMS"
     LPRINT"        UNDER COMBINED ACTIONS OF WEB CRIPPLING"
     LPRINT"                    AND BENDING"
     LPRINT" ─────────────────────────────────────────────
     LPRINT"           SPECIMEN NUMBER :";No$
     LPRINT
     LPRINT" THE OVERALL WEB DEPTH hw =";hw;" mm"
     LPRINT" THE WEB THICKNESS t =";t;" mm"
     LPRINT" THE INSIDE BEND RADIUS r =";r;" mm"
     LPRINT" THE ACTUAL LENGTH OF BEARING n =";n;" mm"
     LPRINT" THE FLANGE WIDTH B =";F;" mm"
     LPRINT" THE SPAN LENGTH OF THE BEAM l =";l;" mm"
     LPRINT" THE YIELD STRENGTH Y =";Y;" MPa"
     LPRINT" THE MODULUS OF ELASTICITY E =";E;" MPa"
     LPRINT" THE THEORETICAL WEB CRIPPLING DEFORMATION Δh_t =";ht;
            "mm"
     LPRINT" THE EXPERIMENTAL WEB CRIPPLING DEFORMATION Δh_e =";he;"
            mm"
     LPRINT" Δh_e/Δh_t = ";G6
     LPRINT" THE THEORETICAL YIELD ARC DEPTH b_t =";b;" mm"
```

362

```
          LPRINT" THE EXPERIMENTAL YIELD ARC DEPTH $b_e$ =";be;" mm"
          LPRINT" $b_e/b_t$ =";G7
          LPRINT" THE THEORETICAL MAXIMUM OVERALL LATERAL
                 DEFLECTION OF WEB $\Delta_t$ =";dt;" mm"
          LPRINT" THE EXPERIMENTAL MAXIMUM OVERALL LATERAL
                 DEFLECTION OF WEB $\Delta_e$ =";de;" mm"
          LPRINT" $\Delta_e/\Delta_t$ =";G5
          LPRINT" n/t =";G2
          LPRINT" hw/t =";G3
          LPRINT" r/t =";G4
          LPRINT" THE POSITION OF OUTER YIELD LINE ON THE TOP FLANGE e
                 =";e1(I);" mm"
          LPRINT" EFFECTIVE WIDTH OF THE TOP FLANGE beff =";beff;" mm"
          LPRINT" Pfp FROM PLASTIC ANALYSIS =";Pp;" N"
          LPRINT" Pfe FROM ELASTIC ANALYSIS =";Pel;" N"
          LPRINT" Pfp - Pfe =";A1;" N"  :  LPRINT" Pfe/Pfp =";A
          LPRINT" AFTER NUMBER OF ITERATION N =";I
          LPRINT" THE ULTIMATE WEB CRIPPLING LOAD :"
          LPRINT"          FCB =";Pu;" N (THEORY)"
          LPRINT"          Fe  =";Pe;" N (EXPERIMENT)"  :  LPRINT" Fe/FCB =";G1
          GOTO 18
14   PRINT" NUMBER OF ITERATION (N) IS NOT ENOUGH."
     PRINT" DO YOU WANT TO CONTINUE THE WORK ?"
15   INPUT" ENTER YES OR NO !";T$
     IF (T$="YES" OR T$="Y") THEN 16
     IF (T$="NO" OR T$="N") THEN 18
     IF (T$<>"YES" OR T$<>"Y" OR T$<>"NO" OR T$<>"N") THEN
     PRINT" INCORRECT INPUT, REPEAT AGAIN !"
     GOTO 15
16   ERASE h : ERASE d : ERASE X : ERASE e1
     GOTO 7
17   PRINT" ITERATION OF b EXCEEDS ITS MAXIMUM NUMBER."
     b = b - 2.5
     GOTO 11
18   END
     END IF
     END IF
```

** NOTE **

The above program is for the first procedure of the plastic mechanism analysis and if

this program is used for the second procedure, the line statements indicated by notes 1-4

have to be altered as follows :

Note 1 :   a2 = 0.5 * (hw+t)

Note 2 :   e1(I) = e1(K) + 0.025

Note 3 :   B2 = 0

Note 4 :   P = (B1 + B3)/B4

The following example is the results of using the above programs for analysing the specimen H90-26.

RESULTS OF USING PLASTIC MECHANISM APPROACH FOR ESTIMATING ULTIMATE WEB CRIPPLING LOADS OF COLD-FORMED PLAIN CHANNEL STEEL SECTION BEAMS UNDER COMBINED ACTIONS OF WEB CRIPPLING AND BENDING

SPECIMEN NUMBER : H90-26

THE OVERALL WEB DEPTH hw = 89.95 mm
THE WEB THICKNESS t = 1.10 mm
THE INSIDE BEND RADIUS r = 2.25 mm
THE ACTUAL LENGTH OF BEARING n = 50 mm
THE FLANGE WIDTH B = 42.14 mm
THE SPAN LENGTH OF THE BEAM l = 451 mm
THE YIELD STRENGTH Y = 303 MPa
THE MODULUS OF ELASTICITY E = 196850 MPa
THE THEORETICAL WEB CRIPPLING DEFORMATION Δh_t = 3.585387 mm (1.969565 mm)
THE EXPERIMENTAL WEB CRIPPLING DEFORMATION Δh_e = 2.78 mm
$\Delta h_e/\Delta h_t$ = 0.7753696 (1.411479)
THE THEORETICAL YIELD ARC DEPTH b_t = 20.3 mm (22.8 mm)
THE EXPERIMENTAL YIELD ARC DEPTH b_e = 17.4 mm
b_e/b_t = 0.9880553   (0.7631579)
THE THEORETICAL MAXIMUM OVERALL LATERAL DEFLECTION OF WEB
Δ_t = 11.52006 mm   (9.270005 mm)
THE EXPERIMENTAL MAXIMUM OVERALL LATERAL DEFLECTION OF WEB
Δ_e = 4.08000 mm
Δ_e/Δ_t = 0.3541649   (0.4401292)
n/t = 45.45454
hw/t = 81.77272
r/t = 2.045455

THE POSITION OF OUTER YIELD LINE ON THE TOP FLANGE e = 42.24018 mm
(15.44991 mm)
EFFECTIVE WIDTH OF THE TOP FLANGE beff = 13.7702 mm
Pfp FROM PLASTIC MECHANISMS = 5725.688 N   (5120.542 N)
Pfe FROM ELASTIC ANALYSIS = 5740.479 N   (5147.316 N)
Pfp - Pfe = - 14.7915 N   (-26.77441 N)
Pfe/Pp = 1.002583   (1.005229)
AFTER NUMBER OF ITERATION N = 769   (619)
THE ULTIMATE WEB CRIPPLING LOAD :
     FCB = 5725.688 N (THEORY)   (5120.542 N)
     Fe = 4824.05 N (EXPERIMENT)
Fe/FCB = 0.8425275   (0.9420975)

The values in the bracket are obtained from the second procedure of the plastic

mechanism analysis.

APPENDIX F

RATIOS OF EXPERIMENTAL AND THEORETICAL LOADS vs.
PARAMETERS STUDIED
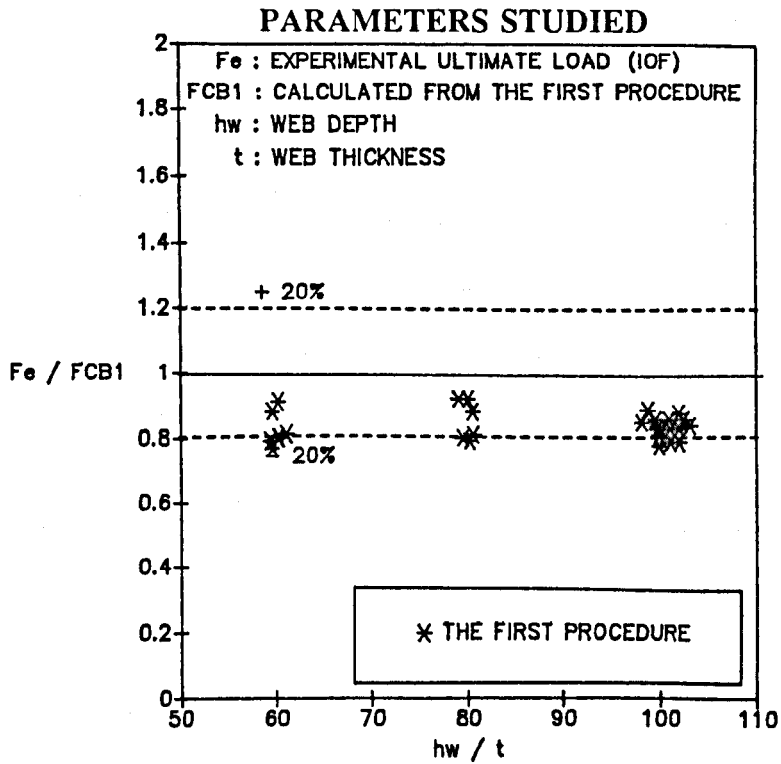
Figure F1. $F_e/F_{CB}1$ vs. web slenderness ratio, for $M/M_c < 0.3$.
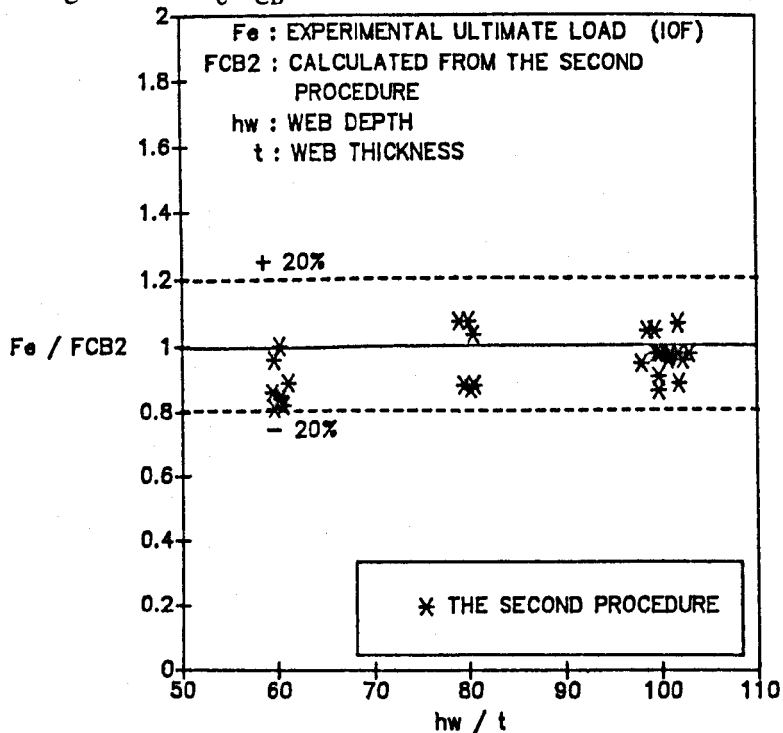
Figure F2. $F_e/F_{CB}2$ vs. web slenderness ratio, for $M/M_c < 0.3$.
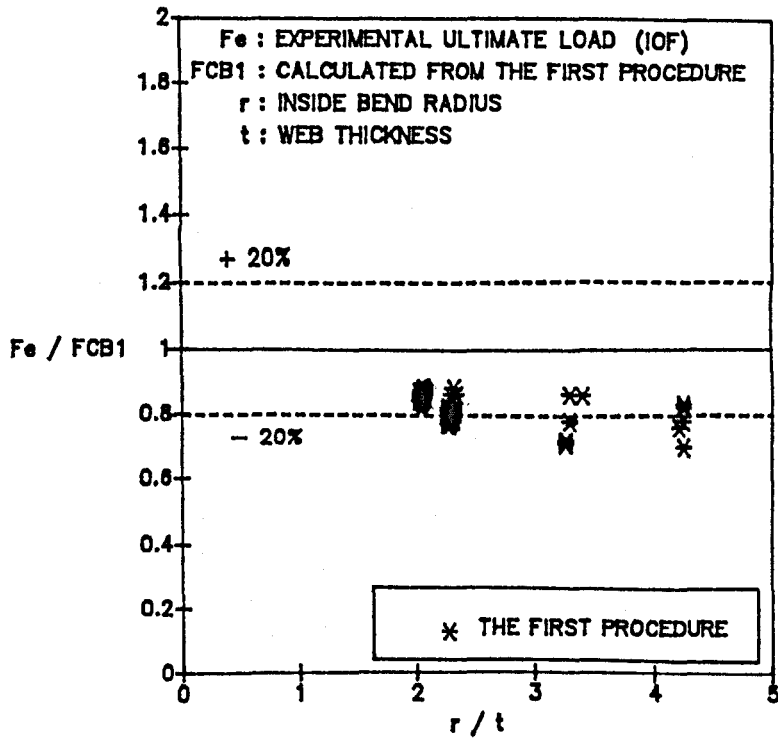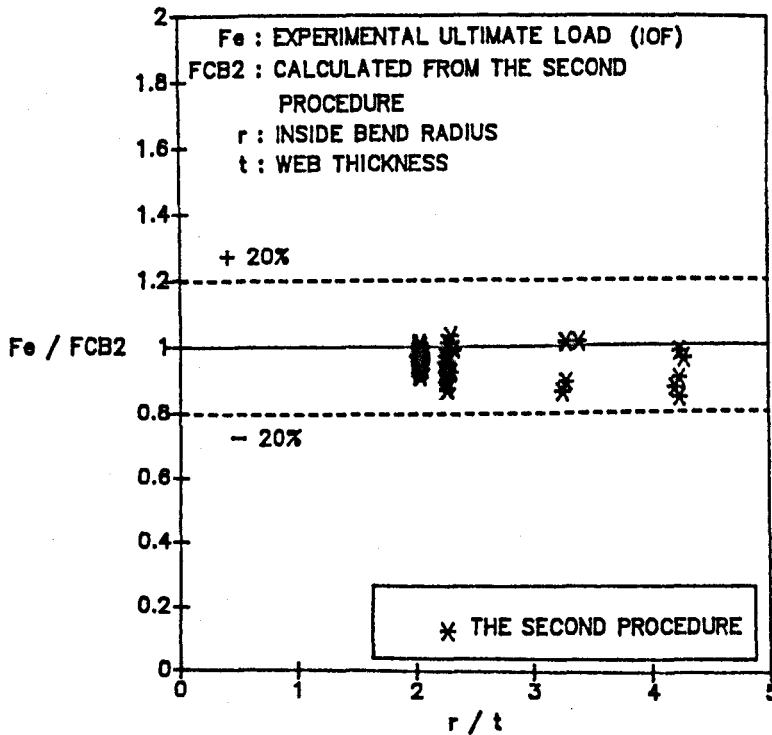
Figure F3. $F_e/F_{CB}1$ vs. inside bend radius ratio, for $M/M_c \geq 0.3$.

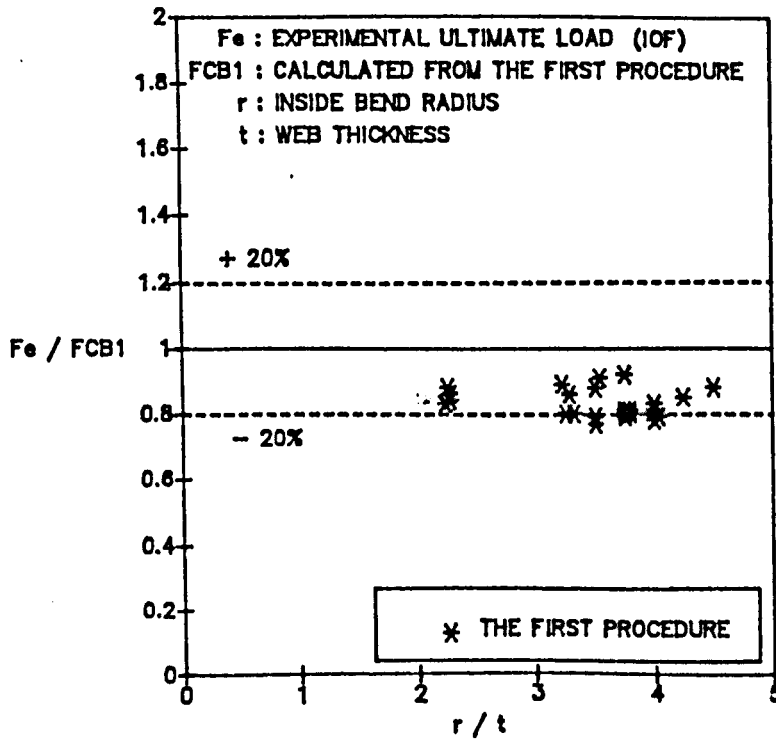Figure F4. $F_e/F_{CB}2$ vs. inside bend radius ratio, for $M/M_c \geq 0.3$.

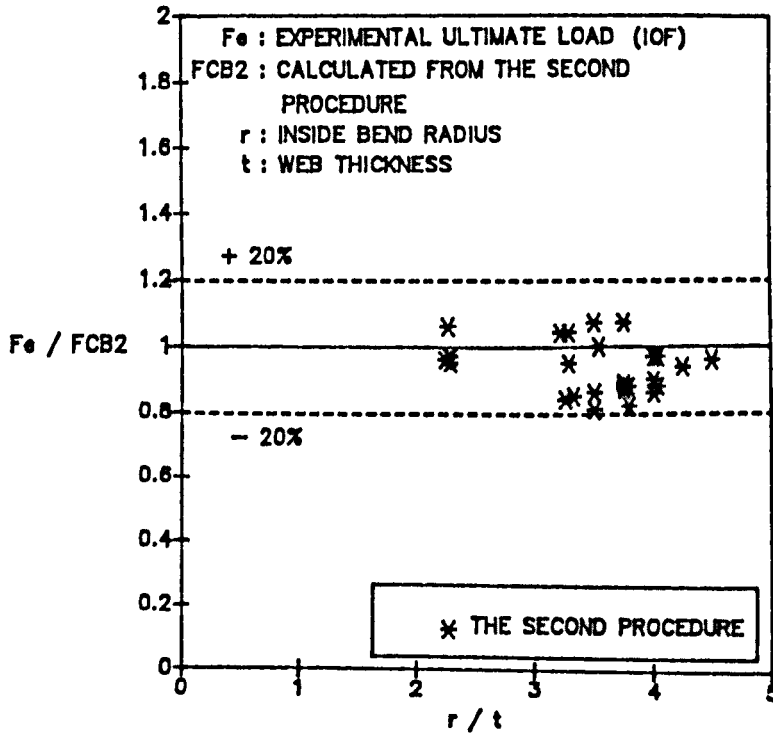Figure F5. $F_e/F_{CB}1$ vs. inside bend radius ratio, for $M/M_c < 0.3$.

Figure F6. $F_e/F_{CB}2$ vs. inside bend radius ratio, for $M/M_c < 0.3$.

368